

STEADY STATE AND TRANSIENT TWO DIMENSIONAL
HEAT TRANSFER IN A THICKENED-EDGE SLAB-ON-
GRADE FOUNDATION

BY

CINDY A. ARIAS

A Thesis
Presented to the Faculty of Graduate Studies
In Partial Fulfilment of the Requirements for the Degree of

MASTER OF SCIENCE

Department of Mechanical and Manufacturing Engineering
University of Manitoba
Winnipeg, Manitoba

© Cindy A. Arias, 2005



Library and
Archives Canada

Bibliothèque et
Archives Canada

Published Heritage
Branch

Direction du
Patrimoine de l'édition

395 Wellington Street
Ottawa ON K1A 0N4
Canada

395, rue Wellington
Ottawa ON K1A 0N4
Canada

Your file *Votre référence*

ISBN:

Our file *Notre référence*

ISBN:

NOTICE:

The author has granted a non-exclusive license allowing Library and Archives Canada to reproduce, publish, archive, preserve, conserve, communicate to the public by telecommunication or on the Internet, loan, distribute and sell theses worldwide, for commercial or non-commercial purposes, in microform, paper, electronic and/or any other formats.

The author retains copyright ownership and moral rights in this thesis. Neither the thesis nor substantial extracts from it may be printed or otherwise reproduced without the author's permission.

AVIS:

L'auteur a accordé une licence non exclusive permettant à la Bibliothèque et Archives Canada de reproduire, publier, archiver, sauvegarder, conserver, transmettre au public par télécommunication ou par l'Internet, prêter, distribuer et vendre des thèses partout dans le monde, à des fins commerciales ou autres, sur support microforme, papier, électronique et/ou autres formats.

L'auteur conserve la propriété du droit d'auteur et des droits moraux qui protègent cette thèse. Ni la thèse ni des extraits substantiels de celle-ci ne doivent être imprimés ou autrement reproduits sans son autorisation.

In compliance with the Canadian Privacy Act some supporting forms may have been removed from this thesis.

Conformément à la loi canadienne sur la protection de la vie privée, quelques formulaires secondaires ont été enlevés de cette thèse.

While these forms may be included in the document page count, their removal does not represent any loss of content from the thesis.

Bien que ces formulaires aient inclus dans la pagination, il n'y aura aucun contenu manquant.


Canada

THE UNIVERSITY OF MANITOBA
FACULTY OF GRADUATE STUDIES

COPYRIGHT PERMISSION

**STEADY STATE AND TRANSIENT TWO DIMENSIONAL
HEAT TRANSFER IN A THICKENED-EDGE SLAB-ON-GRADE
FOUNDATION**

BY

CINDY A. ARIAS

**A Thesis/Practicum submitted to the Faculty of Graduate Studies of The University of
Manitoba in partial fulfillment of the requirement of the degree**

Of

MASTER OF SCIENCE

Cindy A. Arias © 2005

Permission has been granted to the Library of the University of Manitoba to lend or sell copies of this thesis/practicum, to the National Library of Canada to microfilm this thesis and to lend or sell copies of the film, and to University Microfilms Inc. to publish an abstract of this thesis/practicum.

This reproduction or copy of this thesis has been made available by authority of the copyright owner solely for the purpose of private study and research, and may only be reproduced and copied as permitted by copyright laws or with express written authorization from the copyright owner.

ABSTRACT

The thickened-edge slab-on-grade (TES) foundation as its name implies is a shallow foundation of an integral casting of a flat slab with thickened footings. The foundation is placed to a maximum depth of 30.5 cm (12 in) under the soil grade. This foundation has been deemed a Power Smart application by Manitoba Hydro. It is cost effective as its construction, excavation, labour and material costs are much lower than traditional foundations. This research studies the optimal amount and location of insulation in order to minimize the amount of heat loss while effectively avoiding the threat of frost heave. Steady state and transient approximations were studied using a two dimensional domain of constant composite material properties.

The study of heat transfer between a building and its surrounding soil is a complex process. In reality the problem is three dimensional with various materials all with physical properties, some of which vary with different factors such as depth and humidity. In addition, complex climate processes are involved that change with time of day and time of year due to seasonal temperatures. In the present study a commercial Computational Fluid Dynamics code CFX-5 was used to simulate the problem. The energy governing equation was solved using a conservative finite element based control volume method of discretization.

To compare among different insulation configuration cases, the zero temperature isotherm line and heat loss values were calculated. The zero temperature isotherms are very important in determining the location and the amount of frost penetration. The overall heat loss was quantified as the heat loss from the house through the top horizontal edge of the foundation slab. The frost line can be raised and moved away from the foundation by the proper location of insulation, while reducing heat loss. The heat loss from TES foundation results primarily from convection to the outdoor air and conduction to the soil under layers. However, insulating the slab not only reduces the heat loss but it also allows for the heat to be directed strategically to raise the soil temperature.

The insulation configuration cases tested include variations of thickness and location placement. Insulation was placed in regions such as at the edge, under the slab, under the footing and skirt insulation. Insulation needs to be placed strategically around the outside of foundation. The purpose of insulation is to reduce heat loss and redirect the building's heat loss to the footing of the foundation. The edge insulation was found to be effective in significantly reducing the heat loss. The skirt insulation was found to raise and guide the zero isotherm line while conserving the Earth's natural geothermal heat. It was found that the footing was the most strategic area to raise the soil temperature as it is the location most prone to frost heave. Therefore leaving the foot without insulation redirects heat to the most needed area.

Affordable heat efficient applications can be obtained through the use of the TES foundation. Applications include heated building structures such as residential housing, strip malls, agricultural sheds, etc. Energy savings are expected when compared to the traditional full basement foundation as the heating of the additional air space is avoided. The TES foundation is a good alternative in cases when the considerable investment needed to make a basement a comfortable living space is absent.

ACKNOWLEDGEMENTS

I would like to thank Manitoba Hydro, the Natural Sciences and Engineering Research Council of Canada and the Department of Mechanical and Manufacturing Engineering at the University of Manitoba for the funding provided to carry through this research.

I would like to thank my co-advisors Dr. Ormiston and Dr. Soliman for their continued guidance and supervision, without which this research would have not been possible. Many thanks go to Mr. Eyolfson, who first acknowledged the need of this research and was the line advocate for Manitoba Hydro. His guidance and input have been very much appreciated. I would like to thank Professor Paul Bullock from the Department of Soil Science at the University of Manitoba, for his assistance in obtaining the soil data through Agriculture Manitoba.

Also I would like to thank my family, for their support and encouragement throughout my academic career. I would like thank my good friend, Oscar Ramirez for being there for me whenever I have needed his help. Last, but most important, I would like to thank my Lord and Saviour Jesus Christ for giving me the blessing of obtaining my Masters of Science degree and work in this research.

It is my hope and desire that this scientific research will broaden the understanding to construct and provide affordable housing to many Canadians.

TABLE OF CONTENTS

<u>Title</u>	<u>Page</u>
ABSTRACT.....	ii
ACKNOWLEDGEMENTS.....	iv
TABLE OF CONTENTS.....	v
LIST OF FIGURES	viii
LIST OF TABLES.....	xii
NOMENCLATURE	xiv
CHAPTER 1 - INTRODUCTION.....	1
1.1 Background.....	1
1.2 Domain Heat Flows	6
1.3 Frost Heave and Frost Penetration.....	8
1.3.1 Frost Heave	8
1.3.2 Frost Penetration	11
1.4 Overall Scope of the Thesis	11
CHAPTER 2 – LITERATURE REVIEW	13
2.1 Introduction.....	13
2.2 Deep Basements.....	13
2.3 Conventional Slab-on-Grade Foundations.....	16
2.4 Thickened-Edge Slab-on-Grade Foundations.....	22
2.5 Closing Remarks.....	28
CHAPTER 3 – STATEMENT OF THE PROBLEM.....	30
3.1 Problem Definition.....	30
3.1.1 Geometry.....	30
3.2 Mathematical Model	32
3.3 Boundary Conditions	33
3.3.1 Material Thermal Properties	36
3.4 Initial Conditions	37
3.5 Solution Approach	37

CHAPTER 4 – NUMERICAL SOLUTION METHOD	38
4.1 Introduction.....	38
4.2 Grid Generation	38
4.3 The Numerical Solution Approach.....	39
CHAPTER 5 – VALIDATION TESTS.....	42
5.1 Grid Independence Tests.....	42
5.1.1 Heat Loss Tests for Grid Independence.....	50
5.2 Validation Tests	52
5.2.1 Semi-Infinite Solid.....	52
5.2.1.1 Semi-Infinite Solid Subjected to a Step Change in Surface Temperature	53
5.2.1.2 Semi-Infinite Solid Subject to Periodic Surface Temperature Variation	54
5.2.2 Composite Material Interface Balance.....	62
5.2.3 Validation Tests Against the Work of Krarti (1993b)	64
5.2.4 Other Verification Tests.....	68
5.2.4.1 Steady Periodic Results.....	68
CHAPTER 6 – RESULTS AND DISCUSSION.....	69
6.1 Domain Definitions.....	69
6.1.1 Insulation Configurations.....	69
6.1.2 Geometries Studied.....	69
6.2 Steady State Results.....	73
6.2.1 Cases Studied.....	73
6.2.2 Heat loss and zero temperature isotherm results.....	74
6.2.3 Overall Trends	87
6.3 Transient Results.....	93
6.3.1 Cases Studied.....	93
6.3.2 Grade Level Temperature Boundary Conditions.....	93
6.3.3 Domain and Solution Approach.....	95
6.3.4 Zero Temperature Isotherms.....	95
6.3.5 Summary of Transient Analysis Heat Loss	104

6.3.6 Effect of Edge Insulation	107
6.3.7 Zero Temperature Isotherms for Thompson	111
6.3.8 Relative Benefit of Insulation Placement	120
6.3.9 Overall Trends for Isotherms	123
CHAPTER 7 - SUMMARY, CONCLUSIONS AND RECOMMENDATIONS	127
7.1 Summary	127
7.2 Conclusions Based on the Steady State Analyses	128
7.3 Conclusions Based on the Transient Analyses	129
7.4 Recommendations	131
REFERENCES	132
APPENDIX A – DETERMINATION OF GRADE LEVEL PERIODIC TEMPERATURE BOUNDARY CONDITION.....	140
A.1 Introduction	140
A.2 Assumed Behaviour of Soil	144
A.3 Curve Fitting Procedure	145
A3.1 Separate Method	146
A.3.2 Two-Dimensional Method	146
A.4 Soil Temperature Data	150
APPENDIX B – MATERIAL PROPERTIES.....	162
B.1 Soil	162
B.2 Insulation.....	164
B.3 Gravel	164
B.4 Concrete	165
APPENDIX C - GEOMETRY PARAMETERS IN ENGLISH UNITS	169

LIST OF FIGURES

Figure 1.1 Building foundation styles (a) thickened-edge slab-on-grade, (b) conventional slab with footing, (c) deep basement, (d) crawl space.....	2
Figure 1.2 Heat flows in the TES foundation solution domain	6
Figure 1.3 Insulation locations used in this work	7
Figure 2.1 Three insulation configurations covered in Krarti (1993a), for Steady-State heat transfer from horizontally insulated slabs	20
Figure 2.2 Insulation configuration covered in Krarti (1993b), for Steady-state heat transfer from slab-on-grade floors with vertical insulation	20
Figure 2.3 Temperature contour plot from CMHC, (2000b).....	24
Figure 3.1 Composite material domain regions.....	31
Figure 3.2 Problem definition geometry and parameters.....	31
Figure 3.3 Boundary conditions placed on the model domain	33
Figure 4.1 Subdomains composed of same material property regions	39
Figure 5.1 Sample grid cross section at $k = 2$ (The mid plane in the z direction)	43
Figure 5.2 Approximate location of cross-sections tested for grid independence tests....	44
Figure 5.3 (a) Case B1, temperature profile at $y = 2.98$ m, (b) detailed view of (a)	46
Figure 5.4 (a) Case B1, temperature profile at $x = 6.88$ m, (b) detailed view of (a)	47
Figure 5.5 (a) Case E1, temperature profile at $y = 2.98$ m, (b) detailed view of (a).....	48
Figure 5.6 (a) Case E1, temperature profile at $x = 6.88$ m, (b) detailed view of (a).....	49
Figure 5.7 Key energy flows in the domain.....	51
Figure 5.8 Step surface temperature change for a semi-infinite solid: (a) boundary conditions and (b) instantaneous temperature profile at (Mills, 1992, pg. 156).....	54
Figure 5.9 Comparison of numerical results to analytical solution for a semi-infinite solid subjected to a step change in temperature at its boundary.....	55
Figure 5.10 Periodic surface temperature variation for a semi-infinite solid: (a) boundary conditions and (b) instantaneous temperature profile at $t = t_1$. (Mills, 1992, pg. 161)	56

Figure 5.11 Numerical monitor point results comparison against analytical solution solution for $y = 1.005 \times 10^{-4}$ m	58
Figure 5.12 Numerical results comparison against analytical solution for $t = 0.5$ s.....	60
Figure 5.13 Numerical results comparison against analytical solution for $t = 2.0$ s.....	61
Figure 5.14 Example of thermal balance at a composite material interface.....	62
Figure 5.15 One-dimensional validation of a composite wall.....	63
Figure 5.16 Two-dimensional validation of a composite wall	64
Figure 5.17 Validation against Krarti, differential heat flux results.....	66
Figure 5.18 Validation of total slab heat loss results against Krarti	67
Figure 6.1 Diagrams of numerical cases studied	70
Figure 6.2 Steady state zero isotherm line results for Cases A, B1 and B2.....	77
Figure 6.3 Steady state zero isotherm line results for Cases C1, C2, C3 and C4.....	78
Figure 6.4 Steady state zero isotherm line results for Cases C1, C2, C5 and C6	80
Figure 6.5 Steady state zero isotherm line results for Cases C3, C4, C7 and C8	81
Figure 6.6 Steady state zero isotherm line results for Cases C1, C2, D1 and D2.....	82
Figure 6.7 Steady state zero isotherm line results for Cases C3, C4, D3 and D4.....	83
Figure 6.8 Steady state zero isotherm line results for Cases D1, D2, E1 and E2	85
Figure 6.9 Steady state zero isotherm line results for Cases D3, D4, E3 and E4	86
Figure 6.10 Steady state zero isotherm line results for Cases A, B1 and F1	90
Figure 6.11 Steady state zero isotherm line results for Cases A, B2 and F2	91
Figure 6.12 Steady state zero isotherm line results for Cases C1, D1, E1 and F1.....	92
Figure 6.13 Surface soil temperature results for Winnipeg and Thompson	94
Figure 6.14 Winnipeg zero temperature isotherms for Case A, (a) full domain (b) detailed view of foundation corner.....	98
Figure 6.15 Winnipeg zero temperature isotherm for Case B1, (a) full domain, (b) detailed view of foundation corner	99
Figure 6.16 Winnipeg zero temperature isotherm for Case C1, (a) full domain, (b) detailed view of foundation corner	100
Figure 6.17 Winnipeg zero temperature isotherm for Case D1, (a) full domain, (b) detailed view of foundation corner	101

Figure 6.18 Winnipeg zero temperature isotherm for Case E1, (a) full domain, (b) detailed view of foundation corner	102
Figure 6.19 Winnipeg zero temperature isotherm for Case F1, (a) full domain, (b) detailed view of foundation corner	103
Figure 6.20 Winnipeg zero temperature isotherm for Case B2, (a) full domain, (b) detailed view of foundation corner	108
Figure 6.21 Winnipeg zero temperature isotherm for Case C5, (a) full domain, (b) detailed view of foundation corner	109
Figure 6.22 Winnipeg zero temperature isotherm for Case F2, (a) full domain, (b) detailed view of foundation corner	110
Figure 6.23 Thompson zero temperature isotherm for Case A, (a) full domain, (b) detailed view of foundation corner	114
Figure 6.24 Thompson zero temperature isotherm for Case B1, (a) full domain, (b) detailed view of foundation corner	115
Figure 6.25 Thompson zero temperature isotherm for Case C1, (a) full domain, (b) detailed view of foundation corner	116
Figure 6.26 Thompson zero temperature isotherm for Case D1, (a) full domain, (b) detailed view of foundation corner	117
Figure 6.27 Thompson zero temperature isotherm for Case E1, (a) full domain, (b) detailed view of foundation corner	118
Figure 6.28 Thompson zero temperature isotherm for Case F1, (a) full domain, (b) detailed view of foundation corner	119
Figure 6.29 Summary of location of insulation Cases versus amount of insulation for Winnipeg and Thompson.....	120
Figure 6.30 Winnipeg zero temperature isotherm for the month of february (deepest frost penetration), Cases A, B1, C1, D1, E1 and F1 (a) full domain, (b) detailed view of foundation corner	125
Figure 6.31 Thompson zero temperature isotherm for the month of February (deepest frost penetration), Cases A, B1, C1, D1, E1 and F1 (a) full domain, (b) detailed view of foundation corner.....	126
Figure A.1 Assumption of convection coefficient equals infinity.....	142

Figure A.2 Temperature versus month for Winnipeg, 5 cm	155
Figure A.3 Temperature versus month for Winnipeg, 10 cm	155
Figure A.4 Temperature versus month for Winnipeg, 20 cm	156
Figure A.5 Temperature versus month for Winnipeg, 50 cm	156
Figure A.6 Temperature versus month for Winnipeg, 100 cm	157
Figure A.7 Temperature versus month for Winnipeg, 150 cm	157
Figure A.8 Temperature versus month for Winnipeg, 300 cm	158
Figure A.9 Temperature versus month for Thompson, 5 cm.....	159
Figure A.10 Temperature versus month for Thompson, 10 cm.....	159
Figure A.11 Temperature versus month for Thompson, 20 cm.....	160
Figure A.12 Temperature versus month for Thompson, 50 cm.....	160
Figure A.13 Temperature versus month for Thompson, 100 cm.....	161
Figure A.14 Temperature versus month for Thompson, 150 cm.....	161

LIST OF TABLES

Table 3.1 Concrete, insulation and gravel thermal properties	36
Table 3.2 Soil thermal properties.....	36
Table 5.1 Grid descriptions for grid independence tests.....	42
Table 5.2 Summary of Case B1 calculated percentage difference for grid independence tests	45
Table 5.3 Summary of Case E1 calculated percentage difference for grid independence tests	45
Table 5.4 Heat transfer values for Case B1	51
Table 5.5 Heat transfer values for Case E1.....	51
Table 5.6 Monitor point percentage difference comparison at $y = 1.005 \times 10^{-4}$ m.....	57
Table 5.7 Percentage difference comparison at $t = 0.5$ s	59
Table 5.8 Percentage difference comparison at $t = 2.0$ s	59
Table 5.9 Summary of differential heat flux results comparison against Krarti.....	65
Table 5.10 Summary of total slab heat loss results.....	67
Table 5.11 Steady periodic maximum percentage difference.....	68
Table 6.1 Horizontal, vertical and angular parameters fixed for all grids used (see Figure 3.2)	71
Table 6.2 Values of horizontal and vertical parameters varied in steady state simulation grids 1 to 8, in cm (see Figure 3.2)	72
Table 6.3 Values of horizontal and vertical parameters varied in steady state simulation grids 9 to 16, in cm (see Figure 3.2)	72
Table 6.4 Values of horizontal and vertical parameters varied in the transient simulation grids 17 to 20, in cm (see Figure 3.2)	73
Table 6.5 Steady state heat loss values for TES foundation cases.....	75
Table 6.6 Dimensions of skirt insulation	75
Table 6.7 Transient cases studied	93
Table 6.8 Surface soil temperature for Winnipeg and Thompson	94

Table 6.9 Monthly and annual heat loss for Winnipeg, Cases A, B1, C1, D1, E1 and F1	105
Table 6.10 Monthly and annual heat loss for Winnipeg, Cases B2, C5 and F2	105
Table 6.11 Monthly and annual heat loss for Thompson, Cases A, B1, C1, D1, E1 and F1	106
Table 6.12 Monthly and annual heat loss for Thompson, Cases B2, C5 and F2.....	106
Table 6.13 Quantitative summary of annual heat loss versus amount of insulation.....	122
Table A.1 Winnipeg coefficients for the separate method	151
Table A.2 Winnipeg coefficients for the two-dimensional method.....	152
Table A.3 Observed monthly average earth temperatures.....	152
Table A.4 Thompson coefficients for the separate method	152
Table A.5 Thompson coefficients for the two-dimensional method	153
Table A.6 Observed daily average earth temperatures for Thompson at different depths	154
Table B.1 Soil thermal properties found in literature	166
Table C.1 Horizontal, vertical and angular parameters fixed for all grids used (see Figure 3.2).....	169
Table C.2 Variable horizontal and vertical parameters varied in steady state simulation grids 1 to 8, in inches (see Figure 3.2).....	170
Table C.3 Values of horizontal and vertical parameters varied in steady state simulation grids 9 to 16, in inches (see Figure 3.2).....	170
Table C.4 Values of horizontal and vertical parameters varied in the transient simulations grid 17 to 20, in inches (see Figure 3.2)	171

NOMENCLATURE

C_p	Specific Heat [J/Kg·K]
Hv	Krarti ratio [1/m]
L1	half width of foundation [m]
L2	distance to boundary from the slab edge [m]
L3	height of domain at right boundary [m]
L4	total soil thickness below foundation [m]
L5	domain height at left boundary [m]
L6	nominal thickness of skirt insulation [m]
L7	skirt insulation nominal length [m]
Px1	half width of centre slab [m]
Px2	width of inclined section of footing [m]
Px3	width of footing base [m]
Px4	width of wall [m]
Px5	thickness of side insulation [m]
Px6	horizontal length of skirt insulation [m]
Px7	skirt edge to boundary distance [m]
Py1	lower soil region thickness [m]
Py2	upper soil thickness [m]
Py3	sub base thickness [m]
Py4	insulation thickness under footing [m]
Py5	footing height [m]
Py6	above grade foundation height [m]
Py7	depth below grade level of top of skirt [m]
Py8	sand layer thickness above skirt [m]
Py9	vertical thickness of skirt insulation [m]
Py10	thickness of insulation under slab centre [m]
Py11	slab thickness [m]
Q''	heat flux [W/m^2]

Q	heat transfer rate [W]
T	temperature [°C]
T*	maximum temperature [°C]
t	time [s]
ω	frequency [1/s]
n	number of time steps
NX	number of nodes in the x direction
NY	number of nodes in the y direction
NZ	number of nodes in the z direction
Δt	time step [s]
x, X	horizontal coordinate dimensional [m], dimensionless
y, Y	vertical coordinate dimensional [m], dimensionless
z, Z	depth coordinate dimensional [m], dimensionless

Greek Symbols

α	thermal diffusivity [m ² /s]
θ_1	slab angle [rad]
θ_2	skirt angle [rad]
k	thermal conductivity [W/m·K]
ρ	density [kg/m ³]

Subscripts

0	initial condition
annual	entire year
b	bottom boundary
bottom	bottom of domain
edge,a	outside air slab edge
edge,b	below grade slab edge
footing,1	slab inclined foot section
footing,2	slab horizontal foot section
G	gravel

i	inside surface of slab
inside	inside structure
o	soil grade level boundary
outside	outside structure
S	Soil
s	surface
underslab	slab bottom section

Acronyms

IE	vertical edge insulation
IS	skirt insulation
IC	centre slab insulation
IF	insulation under foundation footing

Chapter 1

INTRODUCTION

1.1 Background

Residential and commercial building foundations can be of different types such as full basement, crawl space, or slab-on-grade. The Thickened-Edge Slab-on-Grade (TES) foundation is a special type of slab-on-grade foundations that has a thickened-edge for structural support. Most of the structural load is carried by the thickened portion or integrally poured footing of the slab. Figure 1.1(a) shows a cross sectional diagram of the TES foundation. This type of foundation is also called a monolithic slab as its footings are cast integrally and poured at once with the rest of the slab. The traditional slab-on-grade foundation consists of a slab sustained by deep extending footings commonly in the shape of a reversed “T”. A cross section of this foundation is found in Figure 1.1(b).

Traditionally, in Canada and the United States, builders have mitigated the effects of frost heave by extending the foundation to depths below the freezing line. Constructions of deep foundation with perimeter footings below the frost line include full basements (Figure 1.1(c)), crawlspaces (Figure 1.1(d)) and conventional slabs (with deep footings).

According to the Canadian Mortgage and Housing Corporation (CMHC) which is the Canadian government national housing agency and one of the major Canadian research groups in housing development, “In Canada, tradition and concerns about frost heave have led to the mistaken impression that good design practice requires that foundations must be constructed on footings located below the frost line” (CMHC-SCHL, 2000a). Consequently, the TES foundation is not used in common practice in Canada. Excavating deep to below the frost penetration line makes basement foundations the most rational choice. Deep basement foundations are currently the most common foundation type in the majority of homes in Manitoba.

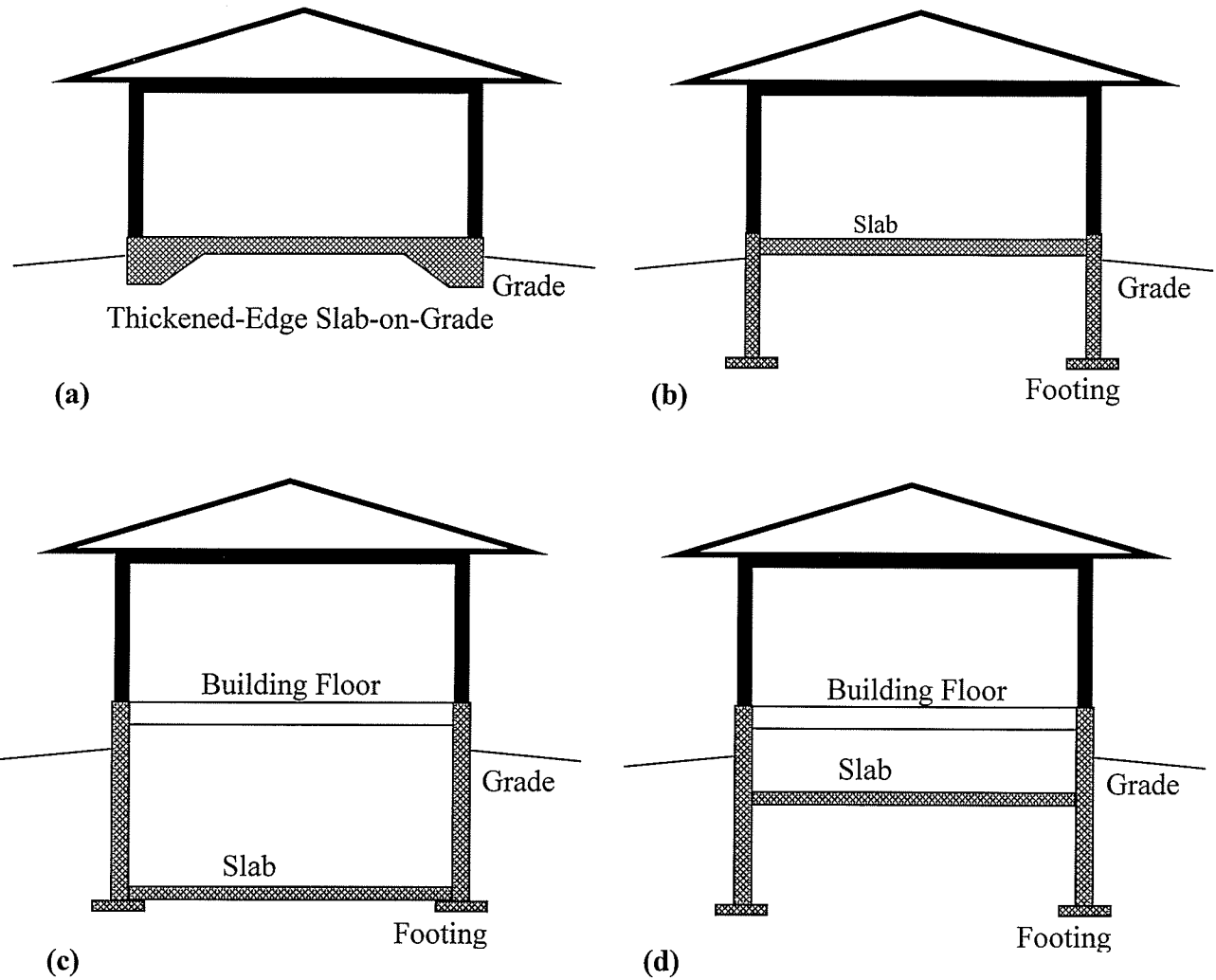


Figure 1.1 Building foundation styles (a) thickened-edge slab-on-grade, (b) conventional slab with footing, (c) deep basement, (d) crawl space

There are however, many problems related with deep basement foundations. Generally, it gets humid as one digs underground. Humidity is a big problem for deep basement foundations. According to a CMHC publication entitled "Home Care a Guide to Repair and Maintenance" (CMHC-SCHL, 1982), "The basement is the most likely place to find moisture and mould problems. Most foundation problems relate to either water vapour being transferred from the ground into the house through wall and floor or liquid water entering through cracks". Since a basement gives a greater surface area in contact with soil, and it lies between 1.5 to 2 meters underground, it increases the chance of a problem

with moisture. The problem is aggravated when a basement is not constructed, equipped or maintained against moisture. Then it becomes an unpleasant living environment that is cold in winter, damp in summer and prone to mould and mildew.

In brief, the most common basement problems are minor cracks and excessive mould growth. Also, it creates an additional space needed to be heated that many times is not used as a result of the above mentioned problems. Hence, the TES foundation may be preferred in situations where a basement is undesirable and a more energy efficient foundation where moisture problems need to be avoided.

In addition, construction of a foundation that goes below frost penetration creates a very expensive task. The costs are augmented for colder regions as the penetration of frost deepens. According to Robinsky and Bessflug (1973), the freezing depth penetration in Canada and the US is between 0.3 to 2.7 metres (1 to 9 feet). In Alaska, it is down to 3.7 m (12 ft) below the ground surface (Danyluk, 1997). With the TES foundation, the savings obtained from excluding excavation expenses are greater for colder climates (deeper frost depth). Winnipeg and Thompson, Manitoba have about 1.4 m (4½ feet) of frost depth, which can really benefit from using a TES foundation.

With the TES foundation, excavation costs are not only minimal but the construction process can also be expedited. Its construction results in overall lower construction costs as less labour and construction materials are used, such as concrete, concrete block, fill, etc. The soil bed is minimally disturbed, which provides for an environmental friendly construction, as tree roots may not be disturbed. Applications for the TES foundation include new construction of residential homes, in-fill retrofit of existing houses where basements are not a necessity, small commercial buildings and agricultural sheds.

According to researchers, there are some limitations to the TES foundation. These include the space need for mechanical system that usually take place in the basement will take place in the main level. Also, the pre-planning of the location of utility services needs to be carefully identified. However, a properly designed and insulated TES

foundation can provide a comfortable, trouble-free, cost and energy efficient construction for residential and non-residential buildings.

The major technical problem associated with the TES foundation construction in Canadian climate relates to the foundation's bottom lying above the ground frost line. For the most part, Canada's ground freezes during the winter season to depths varying from a few centimetres in mild areas to several metres in colder regions. This could allow for the potential of frost heave and pose significant threat to the building structure.

Frost heave results in strong forces exerted normal to the frost line due to the expansion of water during phase change. Generally, the forces are seen as upward movement of the ground that results from the growth of ice lenses in the soil mass beneath and around the foundation (Robinsky and Bessflug, 1973). These forces could make the foundation unstable and threaten the structural integrity of the building. Therefore, it is essential to ensure that frost heave will not occur underneath the TES foundation. One way of doing this is to let energy from the building warm the soil around the foundation.

In maintaining a constant indoor temperature, a house furnace provides a source of energy for heat conduction through the concrete into the soil. This energy transfer can warm up the soil underneath and next to the foundation to above freezing conditions. Raising the soil temperature ensures that frost heave will not endanger the foundation. While frost heave can also be avoided by eliminating frost susceptible soil and removing as much soil moisture as possible, raising the soil temperature above freezing provides the most readily and assured option against frost heave.

However, more energy than required to maintain the soil above freezing may be lost. These losses can be substantial and can increase the cost of heating the building. Insulating the foundation can reduce those heat losses.

The Builders Foundation Handbook by the American Oak Ridge National Laboratory states that "A foundation that is not insulated may represent up to 50% of the heat loss in

a tightly sealed house that is well insulated above grade”. Therefore, it is imperative to know the strategic placement and amount of insulation in order to impede unnecessary heat losses but allow the necessary heat transfer to prevent frost heave of the surrounding soil.

The optimal insulation system will reduce heat loss while allowing just the amount of heat transfer needed to eliminate frost heaving. Insulation can be placed anywhere around the TES perimeter to direct the heat transfer strategically. Consequently, the insulation will effectively direct the right amount of heat loss coming from the house around the foundation soil. Also the insulation may capitalize on heat from deep underground where the soil temperature remains nearly constant throughout the year. This may be achieved by extending insulation nearly horizontally outward from the slab edge. This extended insulation is commonly referred to as a skirt.

The TES foundation has been proposed by Manitoba Hydro as a “Power Smart” application for its potential cost effective benefits. In addition, in a report dealing with Insulated Slab-on-Grade Foundations, CMHC mentions that “Many Canadian authorities have concluded that slab-on-grade foundations provide one of the most effective ways of improving the affordability and quality of housing in northern climates” (CMHC-SCHL, 2000a).

At present in the Province of Manitoba, only rule of thumb guidelines from Manitoba Hydro exist regarding the placement of insulation around the TES foundation. In the long term it is desirable that this research will result in proven solid guidelines to be given to contractors in the hope of utilizing more cost and energy efficient construction in the Province of Manitoba. A methodological, scientifically based analysis is needed to develop better guidelines.

1.2 Domain Heat Flows

When using symmetry, a cross sectional view of the TES foundation can be considered to be the domain of interest. In this typical view, the foundation energy can be transferred through the foot edge above the grade, which is exposed to the outside air ($Q_{edge,a}$) and through the slab below the grade. That is, through the remaining vertical section of the foot edge ($Q_{edge,b}$) and through the bottom section of the foundation, these being the slab ($Q_{underslab}$) and footing inclined ($Q_{footing,1}$) and horizontal section ($Q_{footing,2}$). The area of sections through which heat is lost is indicated schematically in Figure 1.2.

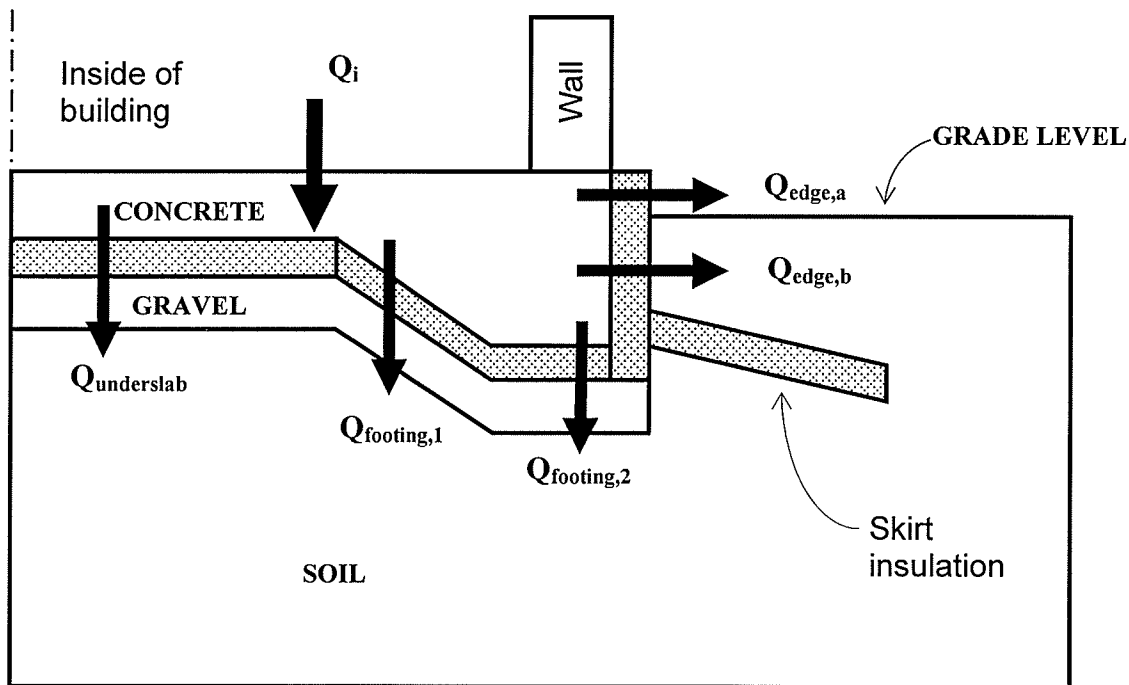


Figure 1.2 Heat flows in the TES foundation solution domain

According to CMHC, one concern with the slab-on-grade foundation is the displeasure of a sensation of a cold floor (slab). At the same time, in the CMHC Research Highlights on Slab-on-Grade publication (2000b), CMHC conveys that the use of insulation will help make the floor slab feel warmer to the occupants.

Large amounts of heat transferred from the house through the foundation or 'heat loss' warms the ground under and next to the slab and avoids frost heave. Adding insulation to the slab reduces the heat loss from the house. However, adding too much insulation will prevent this heat flow that is necessary to maintain above zero temperatures in the soil. Consequently, it is important to determine the most effective amount and location of insulation to maintain a balance between heat loss savings and allowing enough heat to escape and prevent frost heaving.

Figure 1.3 shows the different locations of insulation tested in this thesis. The tests performed are explained in detail in later chapters. The IE (Insulation, Edge location) insulation will prevent heat loss through the side of the foundation. This vertical insulation is important because significant amounts of heat can escape through the above section of the slab. The IS (Insulation, Skirt location) insulation extends from the edge of the slab throughout the perimeter of the slab forming a skirt. The IS insulation protects the slab from the outside frost penetration. Other insulation locations include IC (Insulation, Centre slab location) and IF (Insulation, under Footing location). The purpose of these insulation locations is to further reduce the heat loss into the ground.

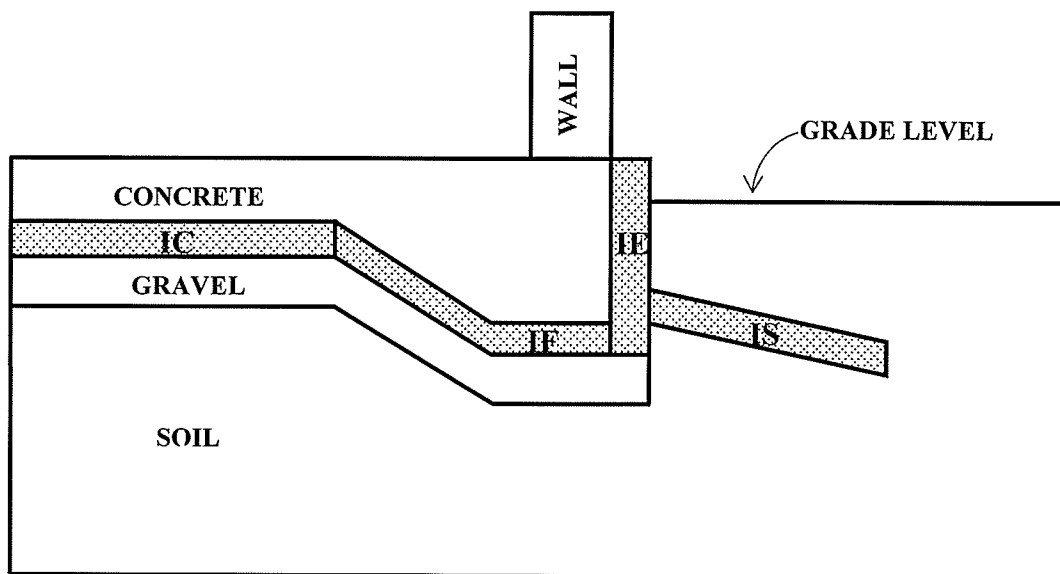


Figure 1.3 Insulation locations used in this work

The most energy efficient insulation configuration (indicated by its location and thickness) that maintains the freezing line away from the foundation corners is to be determined by the present study. It is for that reason that many cases were solved for steady and transient conditions in the present research.

According to the NAHB Research Centre (1999), in Norway, Sweden and Finland, 2-inch thick under slab insulation, either EPS Expanded Polystyrene or XPS Extruded Polystyrene, is used under concrete slabs to keep the concrete warm for thermal comfort. NAHB recommends the use of these two types of insulation for their Frost Protected Shallow Foundation design. For the purposes of this research, the insulation type used is Extruded Polystyrene Board (Incropera and DeWitt, 1996). Further details on the material properties used in this research will be given as needed later in the thesis.

1.3 Frost Heave and Frost Penetration

The ground freezes for the majority of the regions in Canada. The depth of the frost penetration varies from few centimetres to several metres in depth. The forces created by the expansion of the frozen ground can be very dangerous to the integrity of building structures. The nature of ground freezing is well known and has been amply discussed by many authors who arrive at the same facts and conclusions in this area. Since the main threat against the TES foundation is the probability of frost heave, it was deemed appropriate to include a section that summarizes the common theories found in the literature. The nature of ground freezing and frost heaving are discussed in detail in this section.

1.3.1 Frost Heave

Initially, the volume increase resulting from frost heave was thought to be the result of volume expansion of freezing water. Nowadays, researchers widely recognize that it is the result of a mechanism called 'ice segregation'. In this mechanism growing ice crystals in the soil area exposed to freezing temperatures, draw water from the

surrounding and unfrozen soil beneath, through capillary action. Developing ice lenses form layers of ice. The expansion of these layers of ice forces the soil particles apart and cause the soil surface to heave. According to Burn (1976), “Without physical restraint, there is no apparent limit to the amount of heaving that may occur. Movements in excess of 10.2 cm (4 in)., developing under basement floors in only three weeks, have been recorded”.

Although at times, there may not be a visual change in the frozen ground, the strength of the soil is increased. Other times, as the ground freezes there is significant pressure developed creating displacement of the ground surface. According to Penner (1962), “The actual vertical displacement is far in excess of the expansion that occurs when water freezes”. As explained by NAHB (1999), the pressure generated by the growing ice lenses is at right angles of the frost line. As the frost line nears the foundation of a heated building the frost line turns upward, creating a pressure that is horizontal outward and against the foundation wall or slab edge.

Penner (1962) explained that no heaving can take place unless the heaving pressure exceeded the load on the soil. These heaving pressures vary in range depending primarily on the soil type and its moisture content. For instance, maximum heaving pressure will develop in saturated soil. In terms of soil types, Penner explains that clay soils develop higher pressure than silts. A quote by Penner (1962) gives an interesting fact, “In a laboratory experiment a pressure of 213 psi was developed in a clay soil. Pressures of this order are much in excess of the pressures found under roadways or under the footings of most buildings, so that these structures can be heaved quite readily when conditions are appropriate for ice lens formation”.

It is generally accepted by many researchers including Robinsky and Bessflug (1973), that for frost heave to occur, three conditions must be present:

- a. Freezing temperatures in the ground
- b. Frost susceptible soils

c. Ground water

Frost susceptible soils are those with a fine grain through which moisture can move. For instance, NAHB (1999) explains that “Soil type affects the degree of frost heave. Well-drained sand and gravel (large soil particles) do not heave because they do not support capillary movement of water and because the spaces between the sand and gravel are too large to allow the growth of ice lenses. Clay (very fine soil particles) is not very frost-susceptible because it blocks the movement of water. This property allows use of clay in building earthen dams. Silt is most frost-susceptible because its particles are of moderate size and support both capillary action and frost lens growth”. NAHB also explains that moderate amount of water in soil will contribute to frost heave. In some part the report explains that frost can raise the ground up to two feet.

While heaving occurs when the right combination of fine grain soil, soil moisture and freezing soil temperature exists, researchers explain that eliminating anyone of these factors will eliminate frost heave for all practical purposes. They go on to explain that frost heaving is most readily prevented by replacing fine grain soil with a coarse granular material. In addition, soil moisture can also be controlled by careful attention to drainage in order to reduce the frost heaving probabilities. According to Robinsky and Besspflug (1973), this is the focal concept used, behind frost protection for highway pavement. The design concept reduces soil moisture by lowering the ground water table using ditches. That is the reason why the roadbed sits high over the water table. In addition, the roadbed soil is changed by highly frost non-susceptible material such as gravel. The concept of eliminating any one of the conditions that grant frost heaving, allows for lengthy kilometres of Trans Canada highway where freezing soil conditions are present for most of the winter season and where no heating of the soil takes place during this time.

The concept of eliminating any one of the above mentioned factors to avoid frost heave is applied in this research. Frost heaving is prevented by warming up the soil under the slab above freezing conditions.

1.3.2 Frost Penetration

When freezing air temperatures starts to take place with the winter season, the freezing plane slowly penetrates into the ground. The frozen soil mass physical characteristics change in that it hardens significantly. This high strength characteristic can be attributed to the binding together of soil particles with the ice. According to Penner (1962) “In a porous body like soil, water exists in a network of inter-connecting pores; when it freezes, this network becomes rigid and encloses the soil particles in a solid block”. He also explains that “The rate at which soil freezes is dependent upon its thermal properties, moisture content, and the ambient air temperature. The density, conductivity of the soil particles and water content all influence the over-all thermal conductivity of soil.”

Robinsky and Besspflug (1973) explain that the depth of frost penetration is determined by climate and the soil’s own insulating efficiency. This insulating efficiency depends on factors such as:

- a. Ground surface cover
- b. Soil gradation
- c. Grain size
- d. Density
- e. Ground water conditions
- f. Properties of the materials comprising the below-ground portion of the structure and foundations.

1.4 Overall Scope of the Thesis

Strategic insulation placement of the TES foundation will provide minimal heating requirements yet at the same time protect against frost heave potential. Therefore, preventing frost heave but minimizing heat loss is the main focus of this research. This is achieved by finding the optimal amount and placement of insulation. For this reason numerous insulation configurations are simulated.

This research work includes a two dimensional numerical analysis of a typical region below a building with a TES foundation. The domain to be studied entails a complex geometry that includes a concrete region formed by the TES foundation, a gravel region below the foundation, insulation regions and soil.

This research includes the development of a numerical model using a commercial software called "CFX-5". The code uses a finite element based control volume method of solution. The ground-coupled simulations model steady state and transient time varying temperature field predictions in two dimensions.

Chapter 2

LITERATURE REVIEW

2.1 Introduction

This chapter summarizes the previous work done by researchers in ground coupled building structure foundations. Considerable research has been done on other ground-coupled foundations such as deep basement, conventional slab-on-grade, and crawl space foundations. Much less research, however, has been done on thickened-edge slab-on-grade foundations. The subsections in this chapter discuss the relevant earlier work in the area of ground-coupled heat transfer for deep basements, conventional slab-on-grade foundations, and the thickened-edge slab-on-grade foundation.

2.2 Deep Basements

Much emphasis has been placed on the heat loss analysis of basement foundations. Efforts have been made to calculate basement heat loss. Latta and Boileau (1969) were one of the first groups of researchers to publish their work in basement heat loss. Up to then, basements were not used as living space and were generally not heated. However, basements were becoming a living space constructed in many houses. Latta and Boileau calculated the heat loss based on their experimental values as well as from published meteorological records. The authors explained that heat loss through the soil surrounding a house basement can be calculated on the basis of steady-state heat flow from round concentric circular paths centred on the intersection of the ground surface and the basement wall.

Wang (1979), in another pioneering work, addressed heat loss from below grade applications such as basements and slab-on-grade foundation as a two dimensional problem. A numerical analysis using a finite element method was used with transient boundary conditions. At that time there was no method to address a two-dimensional

problem in the ASHRAE handbook and this research was eventually incorporated into the ASHRAE recommendations for basement heat loss calculations.

Canadian researchers Swinton and Platts (1981) attempted to overcome the complexities of solving the heat loss from a basement to the atmosphere due to the multiple effects encountered in the domain, such as layers of insulation, concrete and adjacent backfill, which all have different heat conduction properties. The authors performed an experimental analysis to estimate annual basement heat loss and studied insulation performance. The authors placed 18 “mimic box” test programs in various basements, in a wide range of climates such as Saskatoon, Ottawa and Charlottetown. They presented some empirical relations, which resulted from the analysis, such as corner effects, wall height above grade and slab losses. Empirical relations of basement wall annual heat loss were developed as a function of insulation level, basement temperature and climate. The authors indicated the importance of insulation in deep basements, indicating that there are 40% savings when insulating all the way down to the floor instead of 60 cm below grade.

Mitalas (1983, 1987), another Canadian researcher, developed one of the earliest methods to calculate the heat loss of basements. Mitalas determined the maximum rate of heat loss from a basement and the total heat loss over the heating season. The procedure utilizes the combination of a two-dimensional heat conduction analysis using a finite element numerical method and experimental data to develop factors to predict the monthly heat loss for various insulation basement configurations. Mitalas concluded that this simplified method could predict both the total basement heat loss and the heat loss through sections of the basement within $\pm 10\%$ of measured values. The 1987 journal article is a revised and extended version of the 1983 article, which included slab-on-grade and shallow basement foundations.

MacDonald *et al.* (1985), summarized and compared the work of seven basement heat loss calculation methods. This was done in an attempt to measure the accuracy of these methods due to the lack of a standard against which to compare. Some of the methods were based on the variable base degree-day. The methods included were: two variations

of the work of Latta and Boileau (1968) and those of Akridge and Poulos (1983), Mitalas (1983), Shipp (1983), Swinton and Platts (1981), and Yard *et al.* (1984). The authors stated the advantages and disadvantages for using each method. The authors concluded that six of the seven methods show good agreement on the heat loss from insulated basement walls. However, poor agreement was found for uninsulated basement walls with deviations as much as 1000%, when comparing the methods of the above mentioned researchers. The work did not attempt to determine which method is most satisfactory. However, it provided a good summary of the methods discussed.

Ackerman and Dale (1987) performed a 16-months experimental study to measure heat losses from insulated and uninsulated concrete basement walls. The results were compared against computer predictions from a two-dimensional transient finite element program and the Mitalas (1983) method. The field measurements were within 20% of the values calculated from the two-dimensional program using the Mitalas method.

Shen and Ramsey (1988) performed a transient two-dimensional numerical simulation of heat loss from a full basement foundation. The authors investigated coupled heat and moisture flow surrounding a basement wall. Greater heat flow was observed when coupling moisture flow since more energy was transported by the moisture from the ground surface. The effect that moisture gradients had on the building heat flow was dependent on the soil type. The authors reported a 9% increase in heat flow from the wall during the winter season for sandy soil. However, for clay soil, which is a fine-grained soil, there was no difference in heat flow values between coupled and uncoupled results.

Krarti (1994a) developed a transient, two-dimensional analytical solution where the temperature distribution was assumed to be steady periodic. Krarti solved the governing heat conduction equation using a semi-analytical technique based on a Fourier series and the Gauss-Jordan elimination method. This procedure was called "Interzone Temperature Profile Estimation" or ITPE, which combined numerical and analytical techniques (Krarti *et al.*, 1988a and 1988b; Krarti and Claridge, 1990; Krarti *et al.*, 1990).

The effects looked at in this study include: basement depth, partial insulation length on basement wall, and the effect on total heat loss from the basement floor and walls. The work provided results of temperature contour lines in the domain and heat loss values.

Other more recent work focused on basement heat loss calculations from walls and the use of insulation. Examples of these cases are the works of Sobotka *et al.* (1994), Adjali *et al.* (1998, 1999), Khalifa (1999) and Maref *et al.* (2001). Finally, there has been a recent drive to include foundation energy loss prediction methods such as the methods discussed in this chapter and incorporate them into a package that predicts overall building energy losses. Among the articles found in this category are those by Krarti *et al.* (1994) and Deru *et al.* (2003).

2.3 Conventional Slab-on-Grade Foundations

More recently, a number of studies have been made that concentrated on the heat transfer loss from slab-on-grade foundations. Many of these studies simulate the domain of the slab-on-grade foundation as a simple, rectangular slab over the surface of the ground. Other authors simulate the domain as a slab with a stem wall and footing, sometimes referred to as T-shape foundation.

Christian and Strzepek (1987) determined the optimal insulation level for basements, crawl space and slab-on-grade foundations for many locations in the United States. The purpose of that work was to develop the recommended insulation levels for ASHRAE Standard 90.2P, "Energy Efficient Design of New, Low-Rise Residential Buildings". The use of some insulation was found to be cost effective for all foundation types and for most of the locations studied. This was inconsistent with the general building practices around that time. The authors recommended further investigation for the crawl space and slab-on-grade models. The foundation models were simply derived from the basement model and no independent validation was attempted for these foundation types in that study. Foundation energy loads were calculated using the Shipp model (1983), which was based on regression equations derived from finite difference computer runs that were

validated against twenty months of measured data from three basements located in Granville, Ohio. The thermal performance predictions of Shipp's model could be used to estimate crawl spaces and flat slab-on-grade foundations for all climates in the United States derived from the basement calculations. However, no independent validation of the crawl spaces and flat slab-on-grade foundations estimates was attempted.

Parker (1987) developed what he called F-Factor correlations for determining earth contact heat loads for full and shallow basement, crawl space and slab-on-grade foundation configurations. The method was based on the correlations of Shipp (1983). The objective of the work was to obtain simple correlations that will give simple calculations of annual space heating loads. The method used was, however, limited to heating loads on an annual basis as it tends to distort the variation of annual heat load when used in a monthly basis. Parker compared with the methods of Mitalas (1983) and Yard (1984) and found that the results were within 30% of each other. However, Parker stated that his method was not intended to replace more thorough methods of estimating floor heat loss, but, it can be used as a convenient rough estimate for initial design purposes.

Shen *et al.* (1988) calculated building foundation heat loss using superposition and numerical scaling. The authors performed these numerical simulations of foundation heat loss for a large variety of climates. The computational time was reduced by the superposition and scaling procedures. The study of the foundations was performed for 13 different cities in the United States that represented a variety of climates. The authors separated the governing heat conduction equation into steady state and periodic components. Superposition of the corresponding steady state components resulted in an accurate calculation of the foundation heat loss. Four foundation configurations were studied: full basement, shallow basement, crawl space and slab-on-grade. For the four foundation types, a range of insulation configurations and thicknesses were considered. The foundation heat flux data were obtained using a two-dimensional finite difference heat conduction code. This finite difference method was the same procedure used by Shipp (1979, 1983).

Bahnfleth and Pedersen (1990) performed a three-dimensional numerical study of a flat slab-on-grade foundation. They treated the ground surface heat transfer as involving an energy balance of conduction, convection, evaporation and radiation. In their study, the ground surface heat conduction was composed of solar and infrared radiation absorbed at the surface, sensible convective and evapotranspiration fluxes. The domain was solved using Cartesian coordinates in a FORTRAN program based on a finite difference method. The parameters that they considered in the study included: floor shape and size, climate, surface and deep ground boundary conditions, soil properties, insulation, and shadowing of the ground by the building. The authors mentioned that the existing method for estimating the heat loss from a slab-on-grade, the F_2 method found in ASHRAE documentation, was not correct. They concluded that floor heat transfer was dependent on both the shape and size of the slab. It was noted that heavily insulated floors showed the greatest deviation from the behaviour implicit in the F_2 method.

In studying the thermal properties and boundary condition effects, the results of Bahnfleth and Pedersen (1990) demonstrated that thermal conductivity of the soil and ground surface conditions exerted a strong influence on floor heat transfer rates, while thermal diffusivity, far-field boundaries and deep ground conditions do not. They concluded that for an accurate estimation, models should take into consideration the effects of soil conductivity and ground surface condition. According to their results, the effect of building ground shadow, which is a local surface boundary condition effect, had very little to almost negligible effects, except in climatic conditions of high evapotranspiration potential. In such conditions, changes of more than 20% could take place.

Krarti (1989) studied steady-state heat transfer beneath a partially insulated slab-on-grade floor. Krarti assumed a water table at a constant temperature for the bottom boundary condition at 8 metres underground. The water table was assumed to maintain a constant temperature of 11°C at all times. The outside air temperature and the soil surface temperature were fixed at 16°C. The above-slab air temperature was 21°C. Among the

results presented were temperature contour plots within the ground beneath and to the side of the slab-on-grade floor. Krarti concluded that the horizontal insulation placed from the slab edge inwards, followed the law of diminishing returns and that most heat loss reduction was provided by the first 0.5 metres of insulation. He mentioned that the two most important variables in the design of slab horizontal insulation are the insulation width and the U-value.

Other work by Krarti using the ITPE method included a study of steady-state heat transfer from horizontally insulated slabs, (Krarti, 1993a). That work included three insulation configurations. These were: (a) uniform insulation coverage under the flat slab, (b) partial insulation starting from the slab edge inward under the slab, and (c) insulation extending outward from the edge of the slab. These insulation configurations are shown in Figure 2.1. The results included temperature contour plots for the soil under and next to the slab for the different insulation configurations. Heat flux plots showing the effect of outer edge insulation and total heat loss plots showing the effect of outer and inner edge insulation and inner edge insulation with respect to insulation length were presented. Krarti concluded that the outer insulation was effective in reducing heat loss from the slab edges. He stated that it is also more effective for the outer edge insulation to extend its length than to increase the thermal resistance over a short distance from the slab edge.

In Krarti (1993b), the previous research was expanded to include steady-state heat transfer from slab-on-grade floors with vertical insulation. Krarti considered the effect of increasing the depth of the vertical insulation. The vertical insulation configuration is shown in Figure 2.2. The results included temperature contour plots for the soil under and next to the slab. Other results presented included a slab heat flux plot showing the effect of including vertical insulation and a total slab heat loss plot showing the effect of vertical insulation depth. Krarti concluded that the vertical edge insulation is effective in reducing the total heat losses from the building to the ground. For instance, as the depth and the thermal resistance of the vertical insulation was increased, the slab heat loss decreased following the law of diminishing returns. However, the depth of the vertical

insulation had more impact than its thermal resistance on the soil temperature field and total slab heat loss.

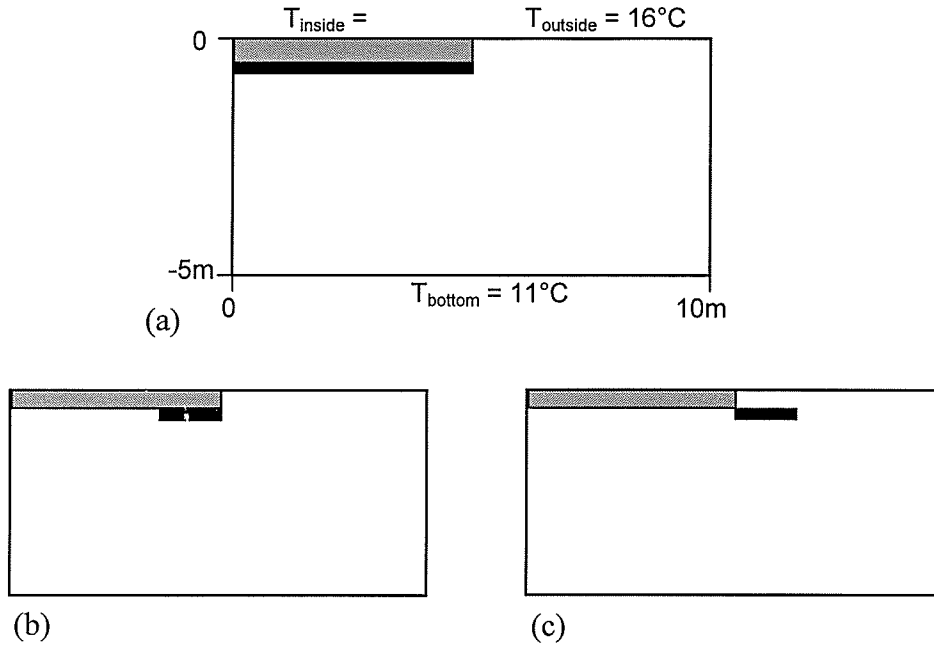


Figure 2.1 Three insulation configurations covered in Krarti (1993a), for “Steady-State heat transfer from horizontally insulated slabs”

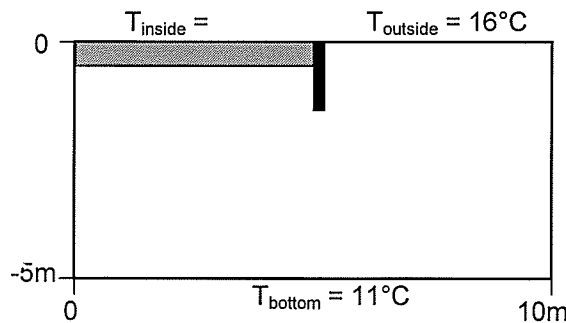


Figure 2.2 Insulation configuration covered in Krarti (1993b), for “Steady-state heat transfer from slab-on-grade floors with vertical insulation”

In Krarti (1994b), time varying heat transfer from horizontally insulated slab-on-grade floors was addressed. This study assumed a steady-periodic solution to the heat conduction problem. He concluded from this work that the annual mean and amplitude

of total slab heat losses can be reduced by increasing the insulation R-values or length. In addition, the time lag between soil surface temperature and slab heat losses increased with insulation R-value and length, except when using two or more metres of insulation width under the slab.

In addition to addressing the horizontal insulation, Krarti (1994c) addressed the effect of vertical insulation. The vertical insulation extended from the slab vertically downwards, up to 5 metres from the ground surface. In this study, Krarti concluded that the vertical insulation provided a shielding against the soil surface temperature fluctuations, which decreased the heat loss in winter. Also, a more pronounced shielding effect was obtained by increasing the R-value of the vertical insulation.

In Krarti and Piot (1995), the steady state heat transfer from adjacent slab-on-grade floors was addressed. In this study, Krarti concluded that foundation heat loss was reduced when neighbouring buildings were present. However, this was only applicable to buildings no more than 5 metres apart. Thermal interaction was reduced when the foundations were well insulated.

In Krarti and Choi (1998) the heat transfer for a slab-on-grade floor with a stepped ground surface was examined. The work involved studying the effect on foundation heat loss of various horizontal insulation configurations along the slab. Vertical insulation depth along the stepped ground surface and other effects such as the height of the lifted ground and distance between the slab and the stepped ground were also included. The authors found that the soil temperature field and the total foundation heat loss were not significantly affected by the existence of a stepped ground surface.

Recent work involving the ITPE method of solution developed by Krarti also included foundation heat loss from internally heated slab-on-grade floors (Chuangchid and Krarti, 2001a). In this work they performed a steady three-dimensional slab-on-grade foundation heat transfer analysis. Also, Chuangchid and Krarti (2001b) studied three-dimensional conduction in circular and rectangular slab-on-grade foundations.

2.4 Thickened-Edge Slab-on-Grade Foundations

In their pioneering work, Robinsky and Bessflug (1973) described the design of shallow foundations. The work concentrated mainly on the slab-on-grade foundation with stem wall and footing but also included some results for a thickened-edge slab-on-grade foundation. Twelve different structures were built using this technology near Timmins, Ontario, Canada. Four of the structures were instrumented with thermocouples and settlement gauges. The authors indicated that the results represented satisfactorily the expected behaviour of the foundation.

According to the authors, the computer program entitled "Finite Element Methods for Permafrost Temperature Analysis" was used as a solution to the heat conduction problem, which allowed for a two-dimensional transient heat flow and included the effect of latent heat of fusion. The external soil surface temperature was assumed equal to the air temperature. This assumption was made from a practical viewpoint, in light of the complexities of freezing soil-water systems and the many uncertainties involved.

One of the key limitations of the work by Robinsky and Bessflug (1973) was the assumption that phase change occur at $T = 0^{\circ}\text{C}$, which they explained was almost true for clean granular soil but not for fine-grained soils. In the latter, not all the water freezes or thaws at 0°C . Another limitation was that the model did not account for moisture migration, which would result in additional heat flow, but is not severe except in cases where freezing and the formation of ice lenses occurred.

Robinsky and Bessflug (1973) presented the design of shallow foundations for both heated and unheated structures. The values of insulation width and thickness were determined based on the severity of the 'Freezing Index' at the construction site location. The Freezing Index was defined as the summation of the degree-days below freezing of the mean daily air temperature during the winter season. The article discussed the effects of the shape of seasonal time-temperature curve. The air temperature variation with time

was changed to test the severity of winter (i.e., short severe freezing season vs. long mild winter). The results showed that frost penetration was not significant for unheated structures but it was significant for heated structures.

Robinsky and Bessflug (1973) concluded that, for design purposes, the severity of the winter temperature follows the shape of a sine curve which is a close approximation of actual winter conditions. Based on the authors' analysis, there was little change in the predictions for an isothermal bottom boundary placed at 4.9 metres or deeper. Although they did not include it in their model, the authors considered the effects of latent heat to be important in predicting frost penetration. Results were presented for a T foundation without insulation and with insulation skirts with lengths of 121.9 cm (48 in), 183.0 cm (72 in), and 243.8 cm (96 in) for clayed and silty/sandy soils. No results for a TES foundation were presented.

The Ontario First Nations Technical Service Corporation and the CMHC commissioned research into heat loss from thickened-edge slab-on-grade foundations and the result was a design Guide for Rural, Northern and First Nations Housing (CMHC-SCHL, 2000a). The aim of the work was to provide information that would remove barriers to the use of frost protected TES foundations. According to the report, "Slab-on-grade foundations are gaining increasing interest across Canada and hold considerable potential for rural, northern and First Nations housing as a means of constructing a lower cost, durable and energy-efficient foundations".

The report gave the amount and location of insulation guidelines for 23 cities and towns for the province of Ontario. Insulation is to be placed under the slab as well as at the slab edge of a minimum of R-10 (RSI-1.8). Horizontal skirt insulation is to be installed around the slab perimeter. The thickness and width amounts of the skirt were given in a table according to ranges of degree days for the selected city or town. The skirt may vary in width from two feet for warmer climate cities to six feet for colder climate cities. The report also gave construction procedures for the TES foundation. There was no reference

to any experimental, analytical or numerical work supporting the recommendations. In addition, the recommendations apply only to the given locations in Ontario.

The Canada Mortgage and Housing Corporation published a report that briefly summarized the most common problems encountered in slab-on-grade construction and gave solution guidelines to them (CMHC, 2000b). The aim of the report was to clarify the use of slab-on-grade foundations in Canada. The report did not give specific amounts of insulation required at any specific site. It mainly addressed the need to incorporate insulation on the slab to protect from frost heaving and make the floor slab feel warmer to the occupants. The report provided a temperature contour plot of a TES foundation with outside and indoor fixed temperature boundary condition of -10°C and $+20^{\circ}\text{C}$, respectively, as shown in Figure 2.3. No information was found on how this solution was obtained.

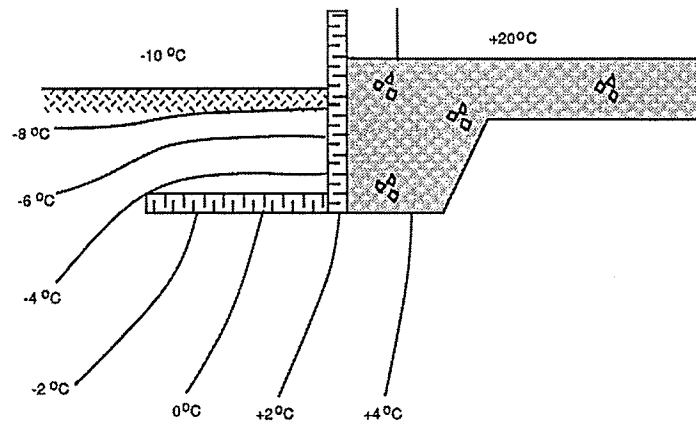


Figure 2.3 Temperature contour plot from CMHC (2000b)

The above report mentioned that slab-on-grade construction can provide an alternative to undesirable deep basement foundations, provided that the structure was well constructed. In addition, slab-on-grade structures can also be used where unstable and soil problems are encountered.

The handbook by Carmody *et al.* (1991) provided general background information and an introduction to foundation design issues for basements, crawl spaces and slab-on-grade foundations. The authors stated that following the recommended practices in their handbook will result in practical and economical advantages for the major issues treated. The handbook provided the reader with information in order to understand foundation design problems and solutions. It summarized the major recommendations and practices related to foundation design according to the U.S. Renewable Energy Office of Building and Community Systems. It showed typical recommended levels of insulation for five representative U.S. climates. The northern most city was Minneapolis, Minnesota. Design and construction practices covering the following areas were summarized: structural aspects, location of insulation, drainage, termite and wood decay control, and radon control. Check lists were also included for use during the design and construction of a slab-on-grade foundation. Insulation guidelines were given for slab-on-grade foundations with stem wall and footing. It is unclear if these guidelines can also be applicable to monolithic (i.e, TES) slabs. The recent work was based on an earlier work by Labs *et al.* (1988). The guidelines for insulation configuration for the foundations in the 1988 design handbook were composed from the works of Shen *et al.* (1988), Huang *et al.* (1988), and Parker and Carmody (1988).

National Association of Home Builders (NAHB) Research Centre published an article (NAHB, 1999) that introduced the benefits of Frost-Protected Shallow Foundations (FPSF) and the different foundation types that can be used under this technology. Among these foundations was the monolithic slab or thickened-edge slab-on-grade foundation. The work summarized the locations where these foundations were used in the United States and the success that contractors have had with this cost effective and energy efficient foundation. It indicated that according to contractors, there are savings in avoiding the construction of a basement with a premium of \$10,000 to \$15,000.

According to the report, construction of FPSF's has taken place all over the United States, including colder states such as North Dakota and Minnesota. In all cases, the contractors indicated having no problems with frost heave in these foundations when

using the proper amounts of insulation. According to the report, an estimated 3,000 FPSF's were built by the year 2000 including single family houses, townhouses, housing for the elderly and disabled, additions, apartments, stores and other commercial buildings.

The "Design Guide for Frost-Protected Shallow Foundations (FPSF), Second Edition" (NAHB, 1996) gave guidelines and recommendations to insulate shallow foundations, among which was the thickened-edge slab-on-grade. The report capitalized on the notable technological development of the use of FPSF in Europe, stating that "The most practical advancements in understanding and applying FPSF's have come from the Nordic countries, where these foundations have been constructed over the last 50 years and have gained wide acceptance". The report specified that Swedish and Norwegian researchers constructed the first experimental houses in the 1950s, using insulated shallow foundations, which provided practical experience and empirical data on which the FPSF technology was based. The design procedure specified the amount of insulation and foundation foot depth to ensure protection against frost heave damage for all types of soils. The design procedure assumed a conservative 100-year return winter, where the top ground surface was exposed to elements by eliminating insulation resulting from ground vegetation and snow cover.

Two design approaches were considered:

1. Simplified FPSF Design Method. Used only for heated buildings, based on the Air Freezing Index to distinguish between latitude locations in the United States. A table gave the appropriate insulation R-value and dimensions used along the foundation, as well as the depth of the footing.
2. Detailed FPSF Design Method; Used for a more precise and economical construction cost. This method must be followed for unheated building foundations.

The types of FPSF addressed included a monolithic slab-on-grade, an independent slab and stem wall, and crawl-space foundations for heated, unheated, and semi-heated indoor conditions. These conditions were based on expected average indoor monthly temperature range of $T > 17^{\circ}\text{C}$, $5^{\circ}\text{C} < T < 17^{\circ}\text{C}$ and $T < 5^{\circ}\text{C}$ for heated, semi-heated and unheated structures, respectively. Thereby, the design procedure included a wide range of structures such as homes, offices, agricultural structures, garages and exposed slabs.

Goldberg (1999) prepared a report for the Minnesota Housing Finance Agency (MHFA) on work that studied shallow foundations design specifications for the climate of the state of Minnesota. In Minnesota, the air freezing index varies from slightly less than 2500 to a little over 4250. The report provided detailed drawings for the thickened-edge slab-on-grade foundation. The figures provided the dimensions of the different geometric parameters of the foundation. The report contained some three-dimensional drawings showing the freezing temperature contour line for air freezing indexes of 2500, 3500, 4250 for heated and unheated structures. Incomplete information was given regarding the method of analysis.

Danyluk (1997) described a shallow frost protected foundation that was constructed for a building addition to the airport control tower at Galena, Alaska. Although the foundation consisted of a slab-on-grade with footings, the foundation was still very shallow with footing length of 0.661 metres (2.17 ft). The theoretical ideas that assisted the design came from the Norwegian Building Research Institute. To protect the shallow foundation from the extreme weather in Alaska, they used extruded polystyrene insulation under the slab (5.1 cm (2 in) thick), at the slab edge (10.2 cm (4 in) thick), and for skirt insulation (10.2 cm (4 in) thick). The skirt insulation extended outward six feet from the footing. Danyluk monitored the soil temperature under and next to the foundation for three years with the use of thermocouples. The three winters monitored were 5600, 6100 and 5500 degree Fahrenheit days. During the first winter, construction was still underway and the slab was only partially heated. Originally, 64 temperature sensors were installed. However, 16 additional sensors were installed after the first full winter of data acquisition

since the frost line was penetrating deeper than anticipated and more detailed temperature information was needed under the ground insulation. The report stated that the freezing front was never closer than approximately 15.2 to 30.5 cm (6 to 12 in) from the bottom corner of the footing regardless of the frost load, so that at no time during the monitoring period did the freezing isotherm threaten the bottom of the footing. It was noted that the maximum frost penetration next to the footing occurred in early to mid February. Danyluk concluded that the shallow insulated foundation was a cost effective alternative. Had a conventional foundation been built, it would have had to extend 12 ft underground where the freezing line does not penetrate.

2.5 Closing Remarks

The literature review discussed in this chapter summarizes the pertinent work done on ground-couple heat transfer in building foundations for basement, conventional slab-on-grade and the monolithic slab-on-grade or thickened-edge slab-on-grade. The following general observations can be made:

1. There has been a significant effort made in the study of heat transfer from basement foundations. Research in this area on different insulation configurations, however, has been mainly confined to full basements. There have been no detailed studies of insulation placement for TES foundations.
2. In recent years slab-on-grade have become a popular alternative to full basements. This popularity has led to studies of heat transfer from this foundation type. The research on slab-on-grade foundations, however, deals mainly with flat slabs placed on the ground surface. Other authors such as Mitalas (1997) used reverse “T” slab-on-grade as their domain geometry.
3. The accuracy of applicability of the conventional flat slab-on-grade or reverse “T” slab-on-grade to the thickened-edge slab-on-grade is uncertain. Because the geometry is different, an analysis of the TES geometry is needed.

4. Work on the thickened-edge slab-on-grade foundation was found mainly in reports for government agencies. Only a few reports gave some insulation guidelines with respect to climate differences. However, none of the studies show the effects on temperature contour plots and heat losses when introducing a variety of amount and location of insulation configurations. There are no scientific journal articles published on a thermal analysis of the thickened-edge slab-on-grade foundation. Furthermore, no scientific work has been found on the thickened-edge slab-on-grade foundation that uses different location and amount of insulation placement giving temperature contour plots and heat losses for soil temperature and conditions for climate and soil conditions in Canada.

Chapter 3

STATEMENT OF THE PROBLEM

3.1 Problem Definition

The problem domain modeled in this research is taken as half the region under a building structure with the thickened-edge slab-on-grade foundation, as seen in Figure 1.1 (a). The domain modelled also includes the soil regions directly under and next to the foundation as well as the regions of insulation and gravel under and around the slab. The modelled domain with its composite material regions is shown in the most general case in Figure 3.1. The following sections in this chapter deal with the geometrical description of the domain as well as the assumptions, governing equations, boundary conditions and thermal properties used to simulate the problem.

3.1.1 Geometry

The geometry can be described by a set of horizontal, vertical, angular and depth parameters. Figure 3.2 gives the nomenclature of the vertical and horizontal parameters that describe the problem. Some parameter values will be fixed while others will be varied according to the tests and cases discussed later. For example, in the case where the side edge was allowed to vary from 1.5 to 3.0 inches, parameter Px5 was changed. Other parameters remained fixed throughout the tests performed. Many of the fixed parameters were obtained from previous literature such as Labs *et al.* (1988), Robinsky and Bessflug (1973) and Goldberg (1999). These parameters were also confirmed with Manitoba Hydro (Eyolfson, 2002) to ensure that they fall within expected construction practice. The physical values of the parameters describing the geometry are discussed in more detail in Chapter 6. Table 6.1 through Table 6.4 summarize the SI unit values for these parameters. Also, Appendix C includes the same tables in English units.

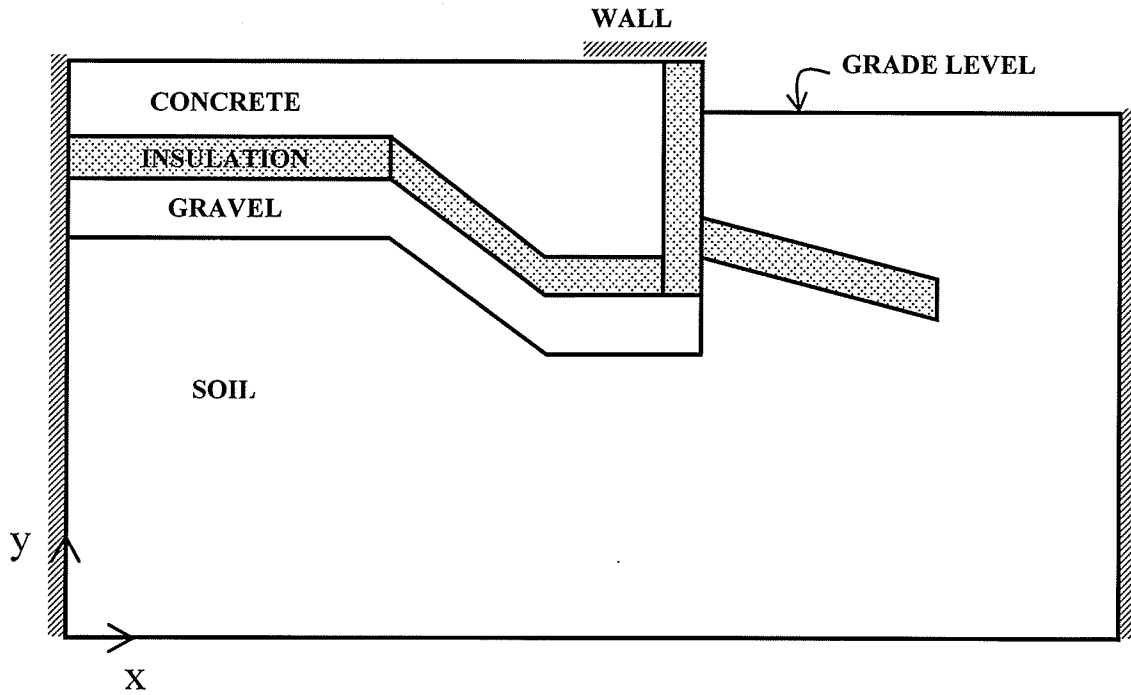


Figure 3.1 Composite material domain regions

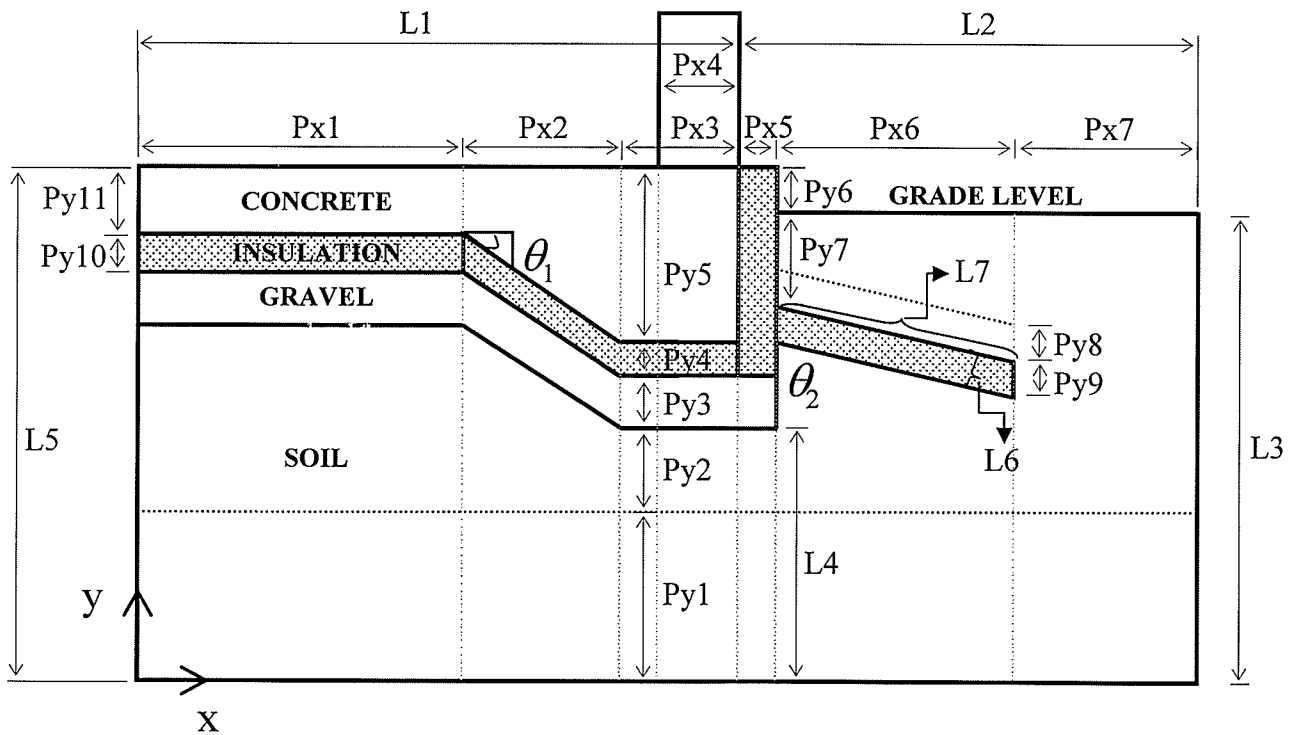


Figure 3.2 Problem definition geometry and parameters

3.2 Mathematical Model

The following assumptions were made in developing the model of the foundation and its surroundings:

- Symmetry at the centreline in the slab is assumed.
- The domain can be considered two dimensional. This is considered valid over a large area of the slab. Edge effects are neglected.
- Water in soil is assumed to freeze at 0°C.
- The indoor building air will be maintained at a constant temperature of 20°C.
- The building structure is assumed to be completed and heated before the freezing weather occurs.
- The insulation is assumed to be extruded polystyrene sheet. Insulation properties are assumed constant throughout the years simulated. Therefore, no insulation degradation was considered.
- All thermal properties are assumed constant.
- Soil latent heat effects are not as important as insulation placement and are neglected.
- The vertical boundary in the soil at the right-side of the domain is assumed to be far enough away that no energy transfer occurs across it.

The main governing equation is the conservation of energy in a solid. Equation (3.1) is the transient two-dimensional conduction equation in Cartesian coordinates. Equation (3.1) applies in all solid regions with their different properties. An initial condition is required and spatial boundary conditions can be either fixed or varying with time.

$$\rho C_p \frac{\partial T}{\partial t} = \left[\frac{\partial}{\partial x} \left(k \frac{\partial T}{\partial x} \right) + \frac{\partial}{\partial y} \left(k \frac{\partial T}{\partial y} \right) \right] \quad (3.1)$$

3.3 Boundary Conditions

Figure 3.3 gives a summary of where the boundary conditions are placed in the model domain.

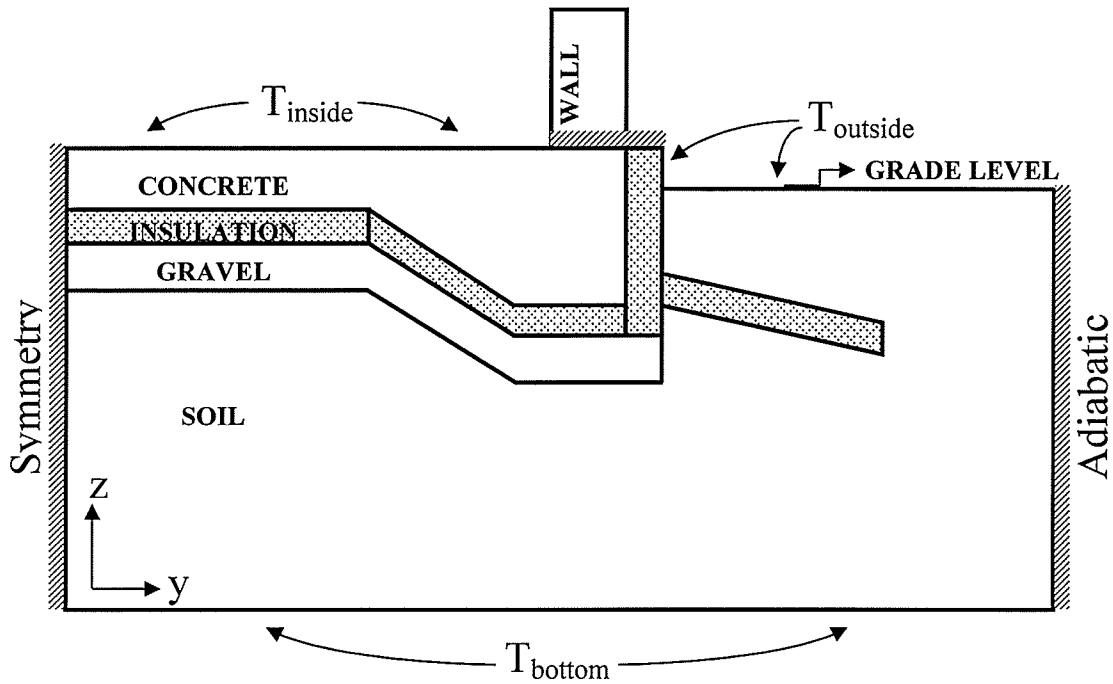


Figure 3.3 Boundary conditions placed on the model domain

- Boundary Condition: $T = T_{\text{inside}}$

$T = T_{\text{inside}}$ at:

$$0 \leq x \leq (L1 - Px4) \text{ and } y = L5$$

The top of the slab was assumed to be at a constant temperature. Therefore, the inside top boundary condition is at a fixed temperature of $T_{\text{inside}} = 20^{\circ}\text{C}$.

- Boundary Condition: Adiabatic

$$\frac{\partial T}{\partial x} = 0 \text{ at:}$$

$$(L1 - Px4) \leq x \leq (L1 + Px5) \text{ and } y = L5$$

No energy transfer is assumed through wall segment on the top surface.

- Boundary Condition: $T = T_{\text{outside}}$

$T = T_{\text{outside}}$ at:

$(L1 + Px5) \leq x \leq (L1 + L2)$ and $y = L3$ and

$L3 \leq y \leq L5$ and $x = L1$ or $x = (L1+Px5)$ depending on insulation IE

The outside top boundary condition is the determining factor between the steady state and transient cases. The values specified are:

- (a) Steady state outside top boundary condition is at a fixed temperature of

$$T_{\text{outside}} = -20^{\circ}\text{C}.$$

- (b) The outside top temperature boundary condition for the transient (variable with time) case

For Winnipeg:

$$T(t) = 5.58 - 11.86 \cos \left[\omega \left(t - \frac{1}{2} \Delta t \right) - 0.50 \right] \quad (3.2)$$

For Thompson:

$$T(t) = 2.36 - 8.95 \cos \left[\omega \left(t - \frac{1}{2} \Delta t \right) - 0.59 \right] \quad (3.3)$$

Where:

$$\omega = \frac{2\pi}{n \cdot \Delta t} \quad (3.4)$$

and

$$n = 12$$

$$\Delta t = 2.592\text{E}+06 \text{ sec (30 days)}$$

The transient case boundary condition equations were derived from a least-square fit of soil-temperature data at different depths. The temperature data for

Winnipeg were obtained from Environment Canada (Environment Canada, 2002), as monthly averages over many years. For Thompson the temperature data were obtained from Agriculture Manitoba (Bullock, 2003). The data were obtained as single daily non-sequential readings over a period of a few years. When working with these data, it showed constant trends that allowed suitable curve fit approximations. Appendix A explains in detail the procedure used to arrive at Equations (3.2) and (3.3).

- Boundary Condition: Symmetry

$$\frac{\partial T}{\partial x} = 0 \text{ at:}$$

$$x = 0 \text{ and } 0 \leq y \leq L5$$

Half of the slab is modelled as it is assumed to be perfectly symmetric. The symmetry boundary condition therefore passes exactly at the middle of the slab.

- Boundary Condition: Adiabatic

$$\frac{\partial T}{\partial x} = 0 \text{ at:}$$

$$x = (L1 + L2) \text{ and } 0 \leq y \leq L3$$

The adiabatic boundary condition at the right side of the domain shown in Figure 3.3 was placed far enough such that the effect of the heat flow from the building structure was insignificant. The domain size was changed and solutions were checked to ensure that they were consistent with these boundary conditions.

- Boundary Condition: $T = T_{\text{bottom}}$

$$T = T_{\text{bottom}} \text{ at:}$$

$$0 \leq x \leq (L1 + L2) \text{ and } y = 0$$

Bottom boundary condition was placed at 3 m below grade for the steady state Cases and at 6 m below grade for the transient Cases. At a depth of 6m (20ft) there is almost insignificant variation in ground temperature throughout the year. This is particularly important for the transient case, as the outside weather effects

do not reach at this depth. Consistent with Equations (3.2) and (3.3), $T_{\text{bottom}} = 5.58^{\circ}\text{C}$ for Winnipeg, and $T_{\text{bottom}} = 2.36^{\circ}\text{C}$ for Thompson.

3.3.1 Material Thermal Properties

Table 3.1 lists the material thermal property values for concrete, insulation, and granular regions in the solution domain. Appendix B provides details about the sources of these values. Table 3.2 lists the soil thermal properties as obtained from both scientific literature for the soil type for Winnipeg and Thompson, as well as from the thermal diffusivity calculated from underground temperature data at different depths for the two cities. The treatment of the underground temperature data is explained in detail in Appendix A.

Table 3.1 Concrete, insulation and gravel thermal properties

Symbol [Units]	Concrete	Insulation Extruded Polystyrene Board	Sand/Gravel Aggregate (dried)
k [W/m·K]	1.4	0.027	1.296
ρ [kg/m ³]	2300	55	2240
C_p [J/kg·K]	880	1210	920
α [m ² /s]	6.9170×10^{-7}	4.0571×10^{-7}	6.2888×10^{-7}

Table 3.2 Soil thermal properties

	Winnipeg Soil	Thompson Soil
k [W/m·K]	1.2	0.52
ρ [kg/m ³]	1800	2050
C_p [J/kg·K]	1666	1840
α [m ² /s]	4.0016×10^{-7}	1.3786×10^{-7}

3.4 Initial Conditions

At a time of $t = 0$ sec, $T(x,y) = 2.0^{\circ}\text{C}$. The choice of this value was completely arbitrary. This initial condition was set at all locations in the domain. The initial condition serves as a “start up” for the numerical code to approach the correct solution. However, the iterative solver proceeds through various iterations until the solution is independent of whichever value the initial condition was given. This is explained in more detail in Section 5.3.4.1.

3.5 Solution Approach

There is no analytical solution to the given governing equations for the non-Cartesian regions with the boundary conditions given. Therefore, a numerical solution of the governing equations is required.

Chapter 4

NUMERICAL SOLUTION METHOD

4.1 Introduction

Solving the governing equations by means of a numerical solution required the use of a numerical computational code. The computer code used to solve the governing equations is a commercial Computational Fluids Dynamics code called CFX-5, now distributed by ANSYS Ltd. The domain shown in Figure 3.2 was subdivided into small control volumes by creating a computational grid for which the governing equation was discretized. An iterative solution of the linearized algebraic equations was performed and the required energy scalars were solved at the nodal point of each control volume. The following sections give an explanation of the numerical solution method.

4.2 Grid Generation

The computational grid was generated with CFX-TASCgrid which is the structured grid generation component of CFX-TASCflow, also distributed by ANSYS Ltd. The grid was created in four steps: First, the geometry of the grid was described in a file called gdf. To define the grid regions they were specified by giving the vertex locations of each region. The regions were attached to one another, which tied the different regions into one continuous domain. In the second step, the nodes of the grid were read in as described in the cdf file. This file contains all the nodal description to create the grid. In this step, the distribution of nodes along lines joining vertices was defined. Next, surfaces were declared with particular names in the sdf file. The final step was to define the interior nodes which were named in the idf file. The output of TASCgrid results in a structured grid that was stored in the grd file.

Since the problem modeled consists of different materials, the grid was composed of 63 regions. Each region was assigned with a specific material property to create different

cases to study. Regions were gathered in subdomains of the same material properties. For example, the concrete was made up of 20 regions which were gathered in one subdomain of the same concrete properties. Figure 4.1 illustrates how the 63 regions were gathered into 12 subdomains. One of the subdomains (AIR69+AIR79) was blocked off in order to account for the step between the concrete foundation and the surface soil (grade level).

4.3 The Numerical Solution Approach

Considerable time was spent at the initial phase of the research to identify a numerical solver that was able to handle the correct solution of the interface between solids. The composite make up of the domain was found to be accurately modeled by CFX-5 as it was able to handle the interface between materials, enabling discontinuities in thermal conductivity to be modeled exactly thereby avoiding solution smearing at the interface between different solids. Initial tests with CFX-TASCflow indicated that it was not a suitable solver for this application.

CONC19	CONC29	CONC39	CONC49	INSU59	AIR69	AIR79
CONC18	CONC28	CONC38	CONC48	INSU58	SOIL68	SOIL78
CONC17	CONC27	CONC37	CONC47	INSU57	SOIL67	SOIL77
CONC16	CONC26	CONC36	CONC46	INSU56	INSU66	SOIL76
CONC15	CONC25	CONC35	CONC45	INSU55	SOIL65	SOIL75
INSU14	INSU24	INSU34	INSU44	INSU54	SOIL64	SOIL74
GRVL13	GRVL23	GRVL33	GRVL43	GRVL53	SOIL63	SOIL73
SOIL12	SOIL22	SOIL32	SOIL42	SOIL52	SOIL62	SOIL72
SOIL11	SOIL21	SOIL31	SOIL41	SOIL51	SOIL61	SOIL71

Figure 4.1 Subdomains composed of same material property regions

The numerical solver used in the study was CFX-5.5.1. CFX-5 is a robust computational fluids dynamic code that uses a conservative finite-element-based control-volume method of discretization (Patankar, 1980; Ferziger and Peric, 1999). CFX-5 was used in the present study due to its strong Conjugate Heat Transfer (CHT) capability. CFX-5's multidomain approach makes it possible to simulate different physical behaviour in different domains and couple the solution of variables across the interface between them. In addition, the thermal or total energy equation of the domain was solved while the equations representing the fluids were disabled.

CFX-5 solves the governing equations by integrating them over a control volume. The Gauss divergence theorem was applied to convert volume integrals into surface integrals. CFX-5 approximates the solution using discrete functions of surface fluxes at integration points located at the centre of each surface segment of a three-dimensional element surrounding the finite volume.

CFX-5 uses the first order backward euler scheme to approximate the transient term. In the case of solutions with a flow field, the advection term can be discretised and evaluated in CFX-5 by either using the first order upwind differencing scheme, the numerical advection correction scheme (specify blend), the high resolution scheme or the central difference scheme. For this model, the first order upwind differencing scheme was selected, but this choice of model does not affect the results because there is no flow solution in this case.

The solver used in CFX-5 was a coupled solver, which solves the velocity and pressure equations as a single system. This solution approach uses a fully implicit discretisation of the equations at any given time step. In the steady state approximation, the number of iterations to reach the convergence criteria was reduced as the time-step behaves like an 'acceleration parameter' to obtain the solution. Similarly, for a transient simulation, the number of iterations to converge within each physical time step was reduced (ANSYS CFX-5.7, 2004).

The iterative solver in CFX-5 uses Additive Correction Multigrid (ACM) acceleration with an Incomplete Lower Upper (ILU) factorization technique for solving the discrete system of linearised equations. The ACM technique greatly enhances the convergence behaviour of the matrix solver by using coarse mesh equations formed by merging the original finite volumes to create larger ones. The solver iterates on a cycle of meshes that go from fine to progressively coarser meshes and then back to the solution on the original fine mesh. The discretisation of equations was only done once for the finer mesh, resulting in a more efficient convergence.

The residuals resulting from the imbalance of the matrix solution of discrete equations were monitored to obtain a convergence criterion through the iterative process. For the present model, the converge criterion was specified as the RMS (Root Mean Square) normal residual to be equal to or less than 1×10^{-6} .

The general solution procedure used by the solver is as follows: in each iteration, the non-linear equations are linearised and assembled into a matrix and the linear equations were solved using the ACM method. The timestep iteration was controlled by the physical timestep (global) or local timestep factor (local) setting to advance the solution in time for a steady state simulation. In the transient analysis performed in this work, there was only one linearisation (coefficient) iteration per timestep.

CFX-5 is divided into three consecutive components. First of all, the description of parameters describing the problem were entered into CFX-PRE which resulted in the creation of the definition file. The definition file is the input for the CFX solver. The solver is a series of program subroutines that solve the governing equations and compute the results. The results from the solver were processed in CFX-POST using the Graphical User Interface (GUI). The results of post-processing are shown in the following chapters. The grd file created in TASCgrid containing the grid was read into CFX-PRE. The appropriate boundary conditions were created. CFX-5 command language allows for the direct entry of physical property data for the materials of the domain. Initial values to the variables were set to initialize the iterative process.

Chapter 5

VALIDATION TESTS

Validation tests were performed in order to confirm the accuracy of both the numerical code CFX-5 and ensure grid independence of the numerical solution. Section 5.1 presents tests done to achieve grid independence. Computations were performed using a variety of mesh refinements to ensure that solutions did not depend on the mesh used. Section 5.2 deals with the validation cases done against known analytical solutions and others reported in the literature.

5.1 Grid Independence Tests

In order to obtain reliable solutions from any numerical code, one must ensure that the solution is grid independent. Grid independence ensures that the results will not change significantly if the grid is further refined. The grid needs to be refined until a suitable measure is found to remain reasonably constant. The results presented for grid independence are for three grids described by the number of nodes in the x , y and z coordinates, as shown in Table 5.1. To simulate a two-dimensional problem in a three-dimensional numerical code, three nodes were placed in the z direction.

Table 5.1 Grid descriptions for grid independence tests

Grid Name	Nodal Dimension [NX,NY,NZ]	Total Number of Nodes
Coarse	[101, 64, 3]	19,392
Medium	[201, 127, 3]	76,581
Fine	[201, 201, 3]	121,203

The nodal distribution was uniform in each of the regions of the grid. These grid regions are shown in Figure 4.1. Regions with denser nodal concentration were placed in regions

of higher temperature gradients, such as the upper part of the domain and near the foundation corner. Figure 5.1 shows the nodal density of a typical coarse grid profile.

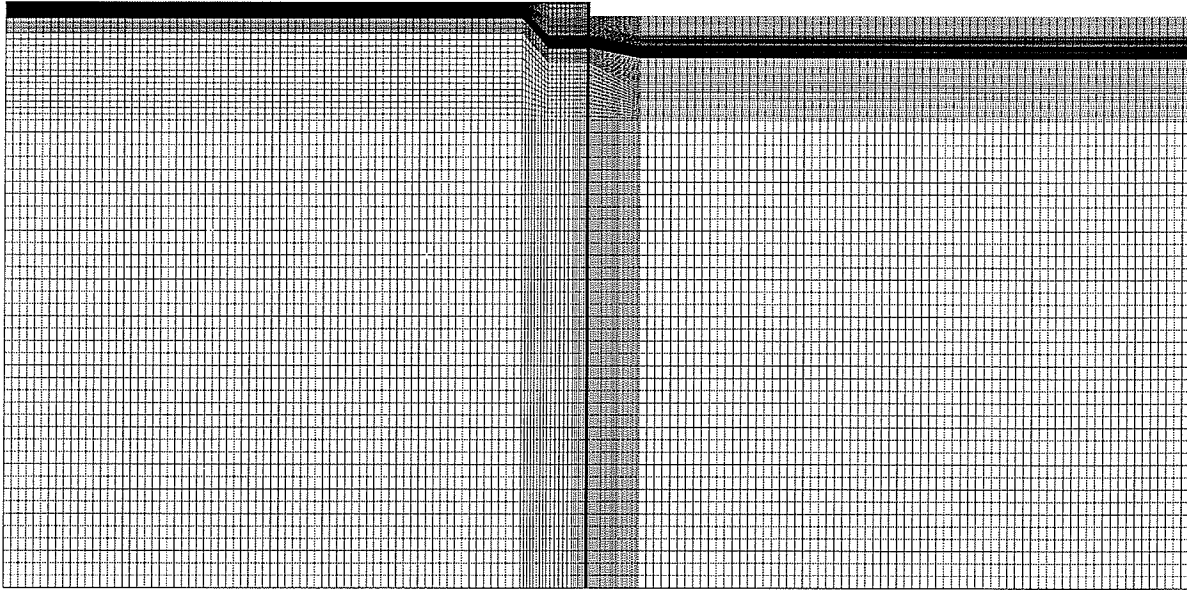


Figure 5.1 Sample coarse grid at $k = 2$ (The mid plane in the z direction)

To compare results among the three grids, temperature cross-sections were taken at different locations in the vertical and horizontal directions. The data for the different cross-sections were plotted and the percentage difference between them was calculated. The results were compared to see which location showed the greatest discrepancies in the vertical and horizontal directions. The horizontal cross-section with the largest discrepancies was found to be at a height of $y = 2.98\text{m}$, while the vertical cross-section with the largest discrepancies was found at $x = 6.88\text{m}$. Figure 5.2 shows the location of these lines with respect to the rest of the domain.

Numerous insulation configuration tests with different region sizes (for different thicknesses of insulation) led to the creation of many grids. For this reason, two cases were selected to perform grid independence tests as a representation of the rest of the grids. Tests were performed on the grids for Cases B1 and E1. These cases are

explained in detail in Section 6.1.2. In the mean time, note that Case B1 contains insulation only along the slab edge, while Case E1 contains insulation in all the insulation regions. These being the slab edge, skirt, under the centre slab, and under the foundation footing. The cases used for grid independence tests were done for steady state simulations.

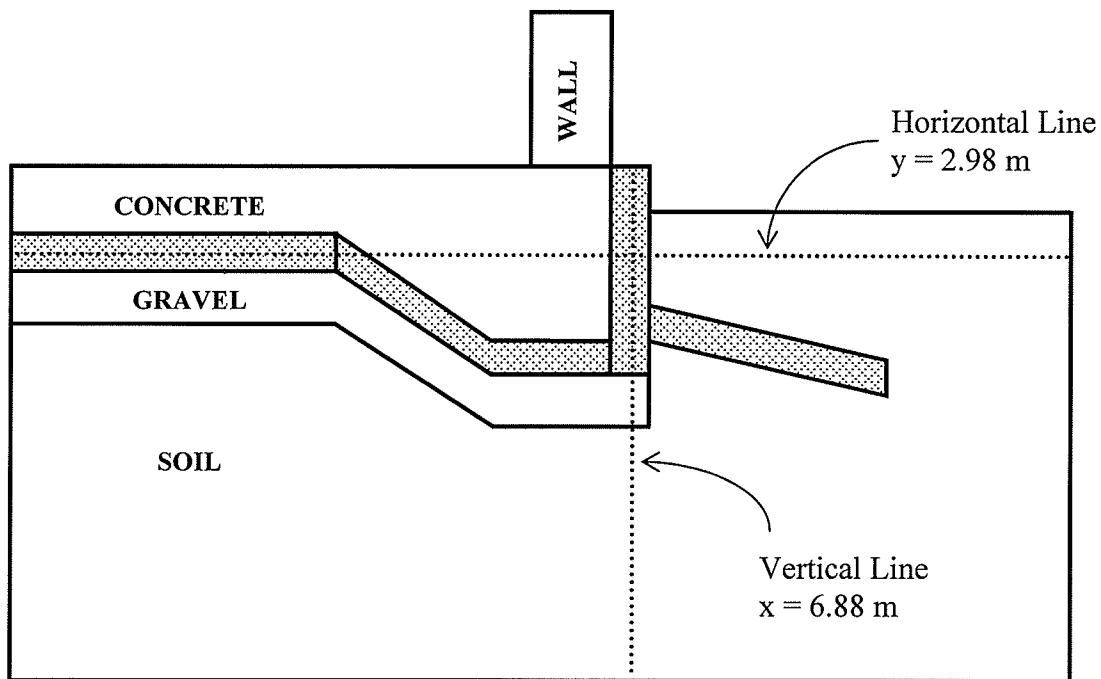


Figure 5.2 Approximate location of cross-sections tested for grid independence tests

Table 5.2 shows a summary of the results obtained for the temperature profile comparison for Case B1. Figure 5.3 (a) shows the temperature profile along $y = 2.98$ m. Table 5.2 shows that, for this profile, the maximum percentage difference between the coarse and medium grids is 49% and it occurs at $x = 6.9$ m. This is detailed in Figure 5.3 (b). The temperature profile for Case B1 at $x = 6.88$ m is shown in Figure 5.4. Table 5.2 shows that the largest percentage difference along this line is 2.98% at $y = 2.70$ m. Table 5.2 shows that the percentage difference between the medium and fine grids is less than one percent for both temperature profiles. The two curves for the medium and fine grids in Figure 5.3 and Figure 5.4 are also nearly indistinguishable from each other. These results indicate that the medium grid can achieve acceptable grid-independent results.

Table 5.2 Summary of Case B1 calculated percentage difference for grid independence tests for temperature along two lines

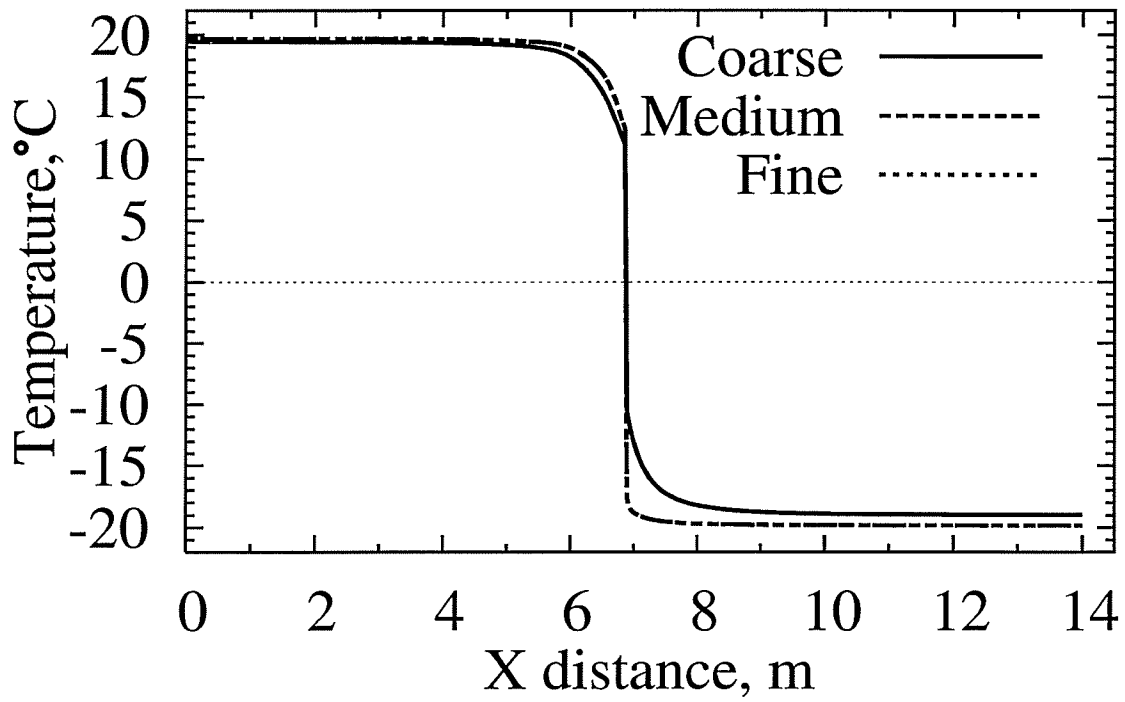
Profile	Difference Coarse to Medium Grid		Difference Medium to Fine Grid	
	Maximum Difference [%]	Location of Maximum Percentage Difference [m]	Maximum Difference [%]	Location of Maximum Percentage Difference [m]
Line y = 2.98 [m]	49.095	x = 6.896	-0.343	x = 6.807
Line x = 6.88 [m]	2.981	y = 2.695	0.231	y = 2.695

The same locations of temperature profiles as in Case B1 were compared for grid independence for Case E1. Figure 5.5 shows the plot for the temperature profile at y = 2.98m. Figure 5.6 shows the plot for the temperature profile at x = 6.88m. Both figures show a detailed view of where the greatest deviation occurred in each profile. Again, the medium and fine grid temperature profiles are very close to each other.

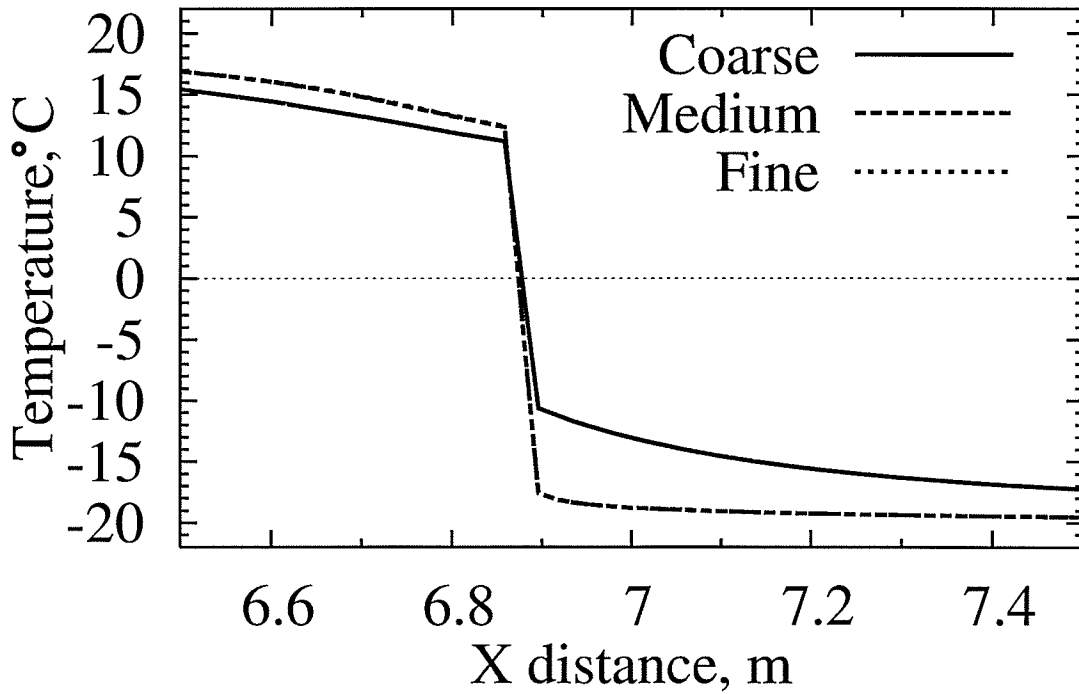
Table 5.3 gives a summary of the percentage differences calculated among the temperature profiles for Case E1. The percentage difference between the medium and fine grids is again around one percent. These results indicate that the medium grid will achieve acceptable grid-independent results. In addition to calculating the percentage difference of the temperature profiles, the heat transfer rate was also examined to assess grid independence of the results. This is explained in the following sub-section.

Table 5.3 Summary of Case E1 calculated percentage difference for grid independence tests for temperature along two lines

Profile	Difference Coarse to Medium Grid		Difference Medium to Fine Grid	
	Maximum Difference [%]	Location of Maximum Percentage Difference [m]	Maximum Difference [%]	Location of Maximum Percentage Difference [m]
Line y = 2.98 [m]	34.606	x = 6.896	1.155	x = 6.096
Line x = 6.88 [m]	-1.037	y = 2.725	-0.176	y = 3.0109

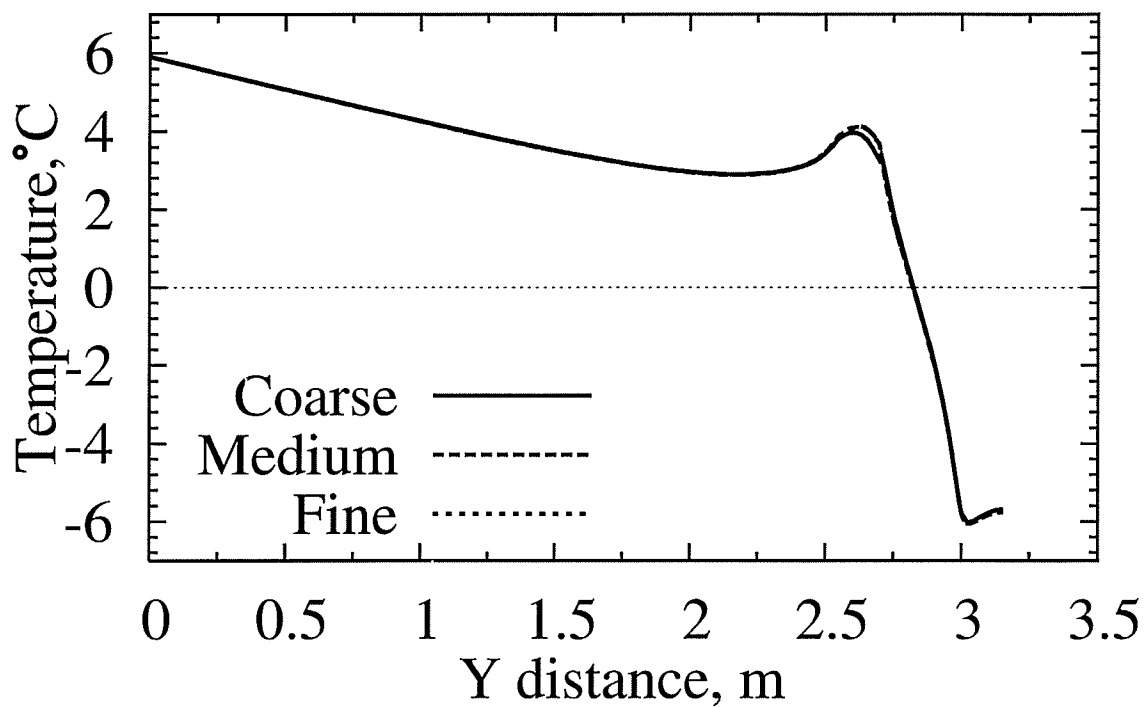


(a)

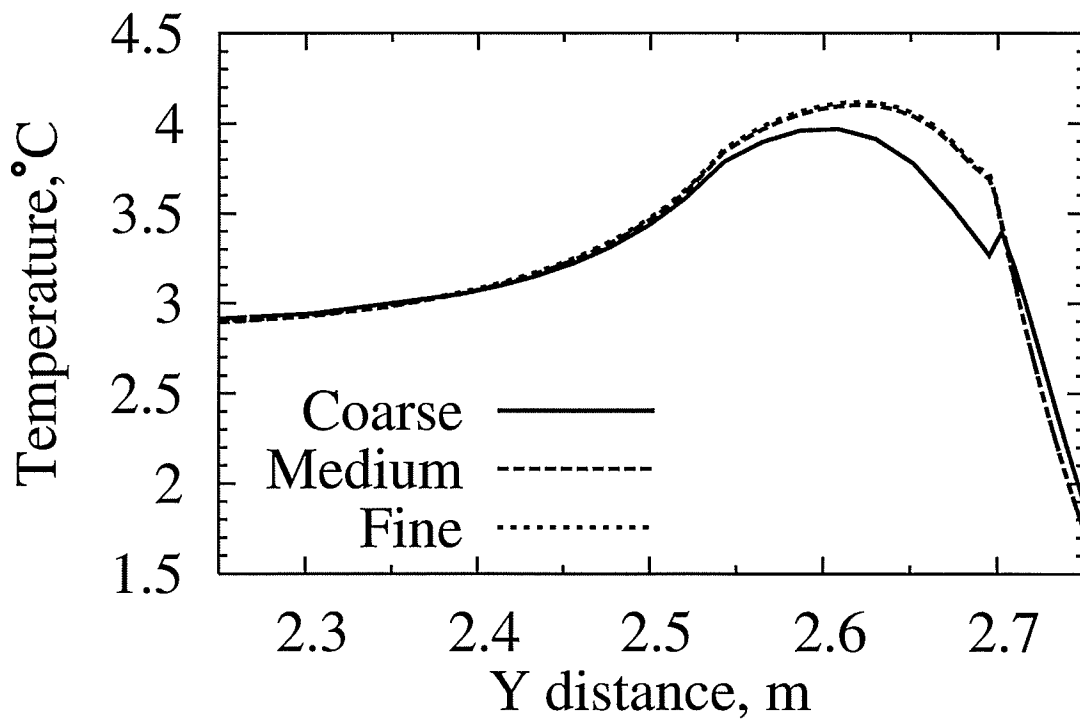


(b)

Figure 5.3 (a) Case B1, temperature profile at $y = 2.98$ m, (b) detailed view of (a)

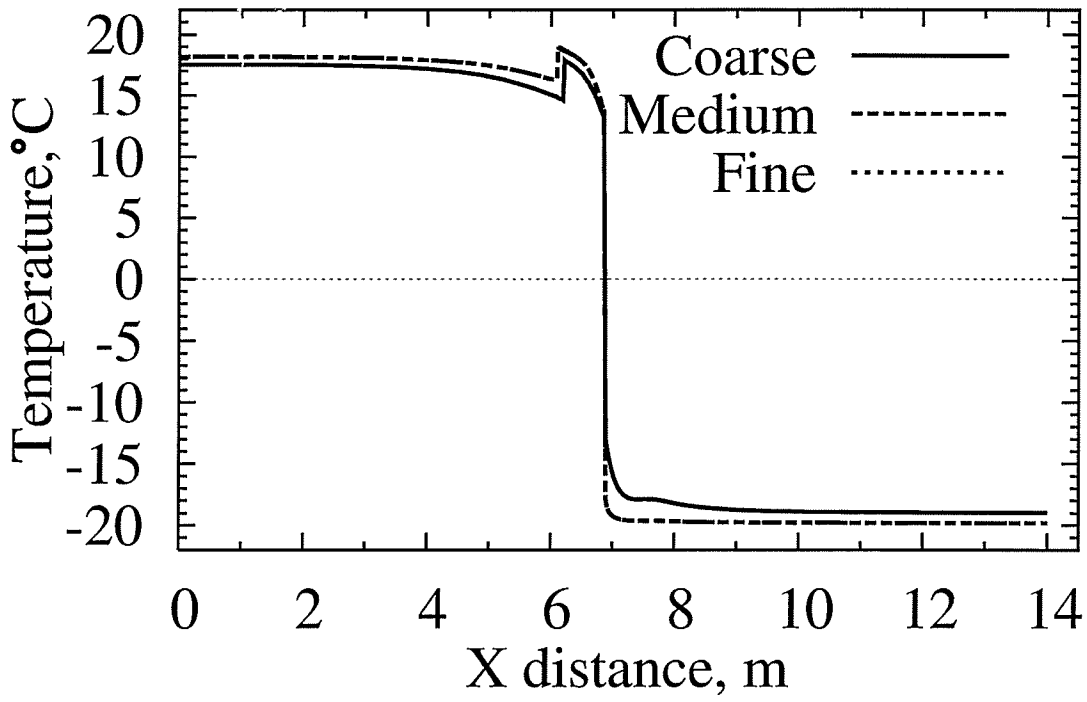


(a)

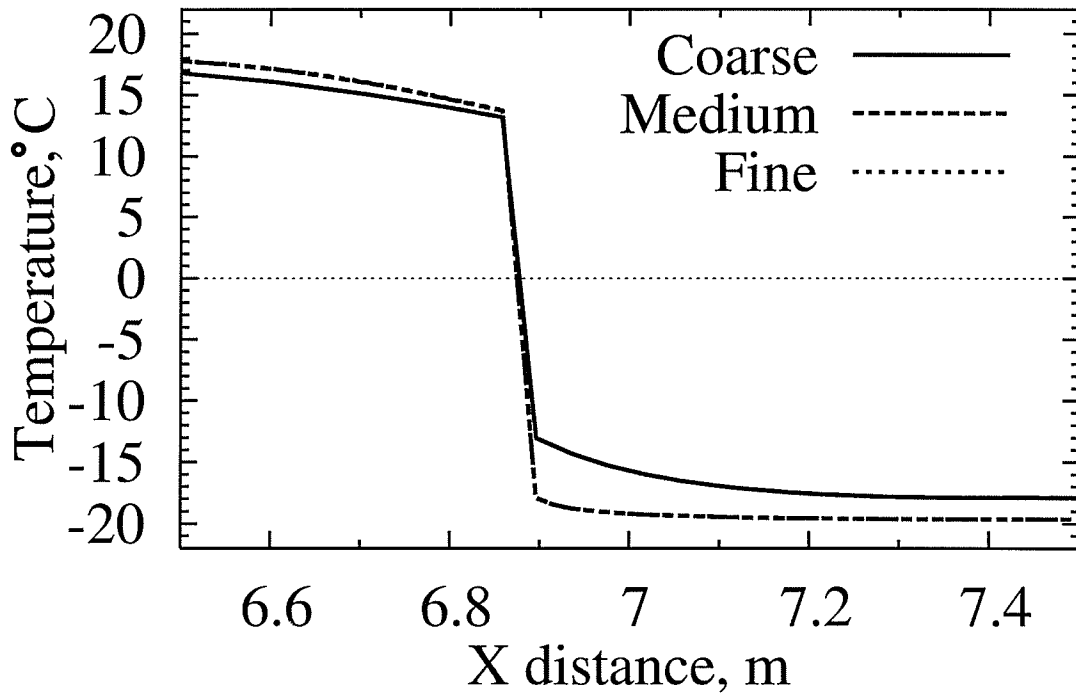


(b)

Figure 5.4 (a) Case B1, temperature profile at $x = 6.88$ m, (b) detailed view of (a)

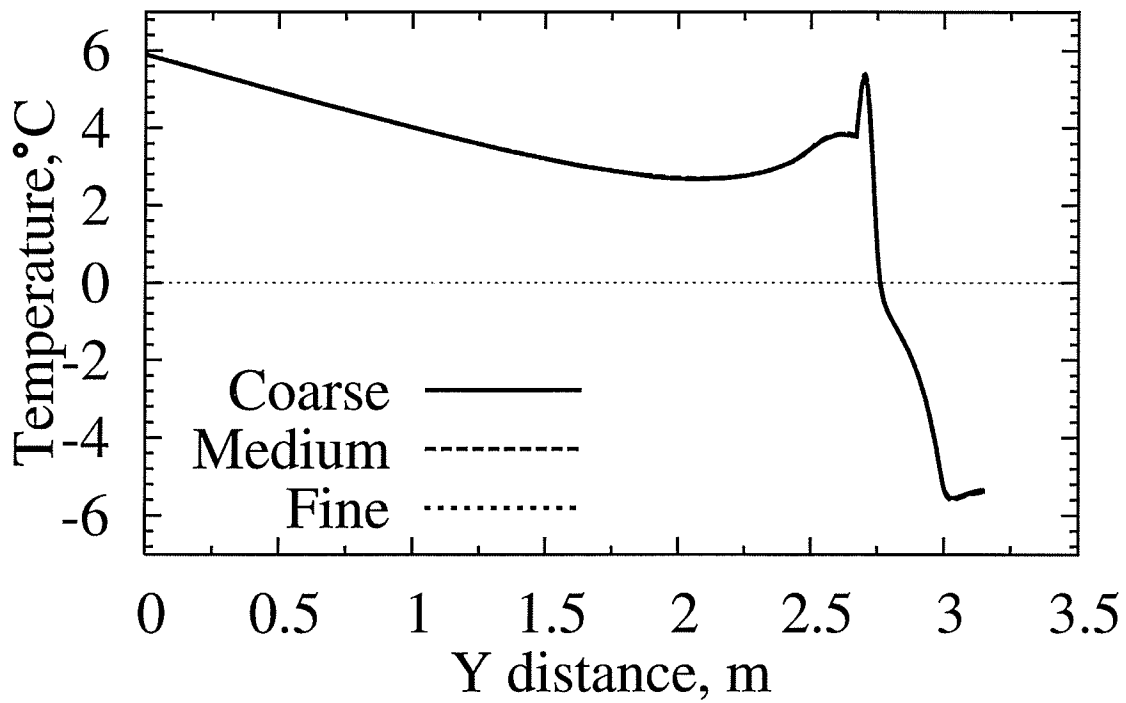


(a)

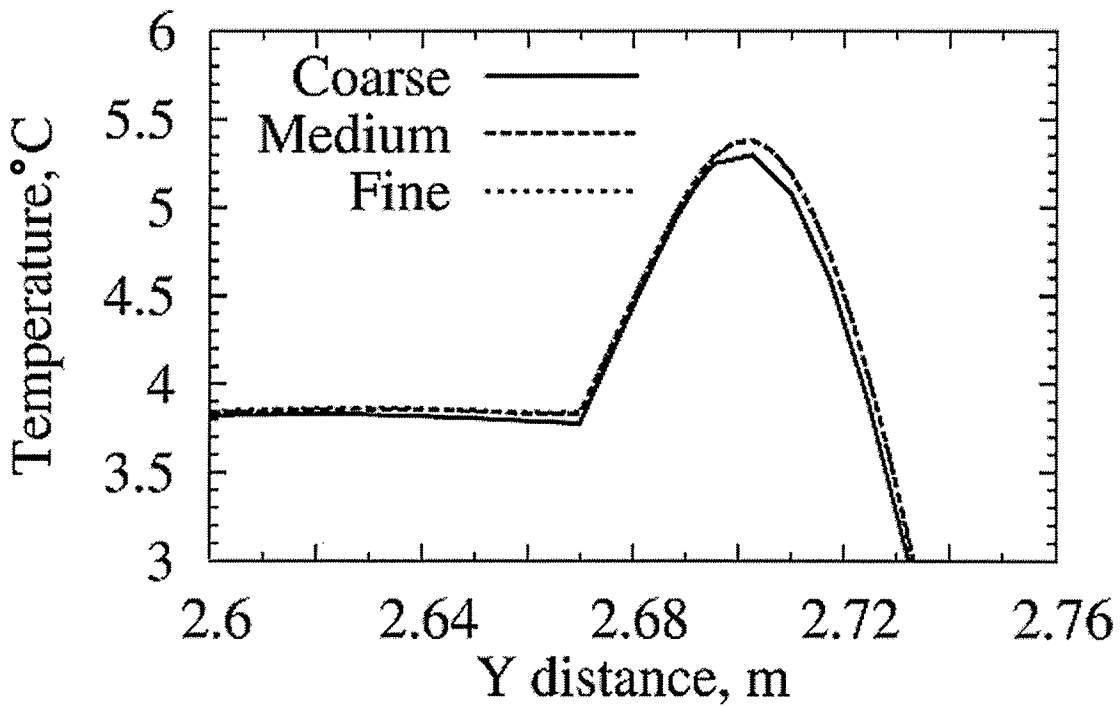


(b)

Figure 5.5 (a) Case E1, temperature profile at $y = 2.98$ m, (b) detailed view of (a)



(a)



(b)

Figure 5.6 (a) Case E1, temperature profile at $x = 6.88$ m, (b) detailed view of (a)

5.1.1 Heat Loss Tests for Grid Independence

Heat-transfer-rate results at each of the major boundaries were examined for Cases B1 and E1. Figure 5.7 illustrates the nomenclature used for these key heat flows. These include the top boundary or top of slab (Q_i), the outside boundary composed of the side edge of the foundation above grade ($Q_{edge,a}$) and the soil grade (Q_o), and the bottom boundary (Q_b).

Nodal heat transfer rates at each boundary were added to get the overall heat gain or loss. These values are summarized in Table 5.4 for Case B1 and in Table 5.5 for Case E1. All the comparisons show very small percentage differences between the results of the three grids. It is noted that all percentage difference values meet a target of less than one percent. Through the comparison of both temperature profiles and heat transfer results it is concluded that grid independent results can be achieved with the medium grid.

It is also important to note that the above results were obtained for steady state results, for which a 3-m height grid was used (from bottom boundary to grade level). When obtaining the transient results, the grids were extended to six metres in height, from the bottom boundary to grade level. The same control-volume size was maintained in the extended portion as in the 3-m grid. This means that additional control volumes were added at the bottom of the domain for the transient case. All transient computations were performed with a [201, 151, 3] grid subdivisions in the x, y, and z directions. It was noticed that in the steady state section, negligible temperature differences occurred at the bottom of the grid as most of the effects occur near the grade. As well, temperature gradients influenced by the outside temperature are dampened through the soil depth and are almost negligible by the bottom boundary of the 3-m height grid. It was then concluded, that these grid-independence results can be considered applicable to the transient analysis.

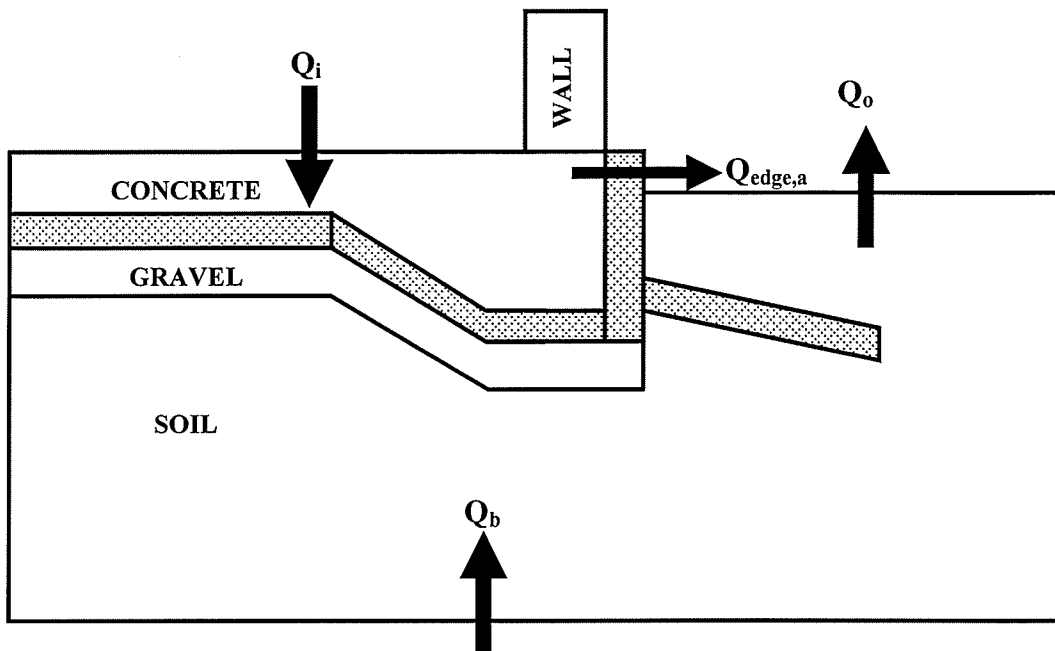


Figure 5.7 Key energy flows in the domain

Table 5.4 Heat transfer rates for Case B1

Boundary	Heat Rate [W/m]			Percentage Difference	
	Coarse	Medium	Fine	Coarse to Medium Grid	Medium to Fine Grid
Q_i	37.517	37.497	37.533	-0.053	0.098
$Q_{edge,a}$	-3.628	-3.616	-3.621	-0.332	0.138
Q_o	-48.393	-48.390	-48.393	-0.007	0.007
Q_b	14.508	14.518	14.516	0.071	-0.011

Table 5.5 Heat transfer rates for Case E1

Boundary	Heat Rate [W/m]			Percentage Difference	
	Coarse	Medium	Fine	Coarse to Medium Grid	Medium to Fine Grid
Q_i	30.050	29.978	29.837	-0.240	-0.473
$Q_{edge,a}$	-3.729	-3.721	-3.725	-0.224	0.107
Q_o	-43.223	-43.157	-43.177	-0.154	0.046
Q_b	16.894	16.893	16.882	-0.006	-0.067

5.2 Validation Tests

Three sets of validation tests are now presented. The first two are comparisons with analytical solutions, and the third is a comparison with a previous numerical study. The first validation test deals with the solution compared to a semi-infinite solid. Two surface boundary condition cases were examined. First, the surface was subjected to a step change in temperature. Second, a periodic surface temperature variation was applied. The second test gives a theoretical simulation of a sinusoidal temperature condition similar to that used in this research.

A second set of validation tests included in this section are the validation of the code in terms of composite material interface balance. These tests were of key importance in the early stages of the research. Finally, validation tests against a published work of Krarti (1993b) are presented.

5.2.1 The Semi-Infinite Solid

A semi-infinite solid is a region of material which has a surface with a known boundary condition and a very large extent in the direction away from the boundary. The condition of the material far away from the boundary is considered to be unchanged with time. As explained by Mills (1992), in the case of a semi-infinite solid, the conduction process is confined to a thin region near the surface into which temperature changes have penetrated. The time evolution of the temperature in the semi-infinite solid is determined subject to a given surface boundary condition applied at $t = 0$. The following assumptions are included in the semi-infinite solid solution:

- Transient
- One Dimensional
- No internal heat generation
- Constant thermal diffusivity, $\alpha = \frac{k}{\rho C_p}$

The governing energy equation is

$$\frac{\partial T}{\partial t} = \alpha \frac{\partial^2 T}{\partial y^2} \quad (5.1)$$

The boundary and initial conditions are as follows:

- The initial condition at time zero

$$T = T_0 \quad \text{at } t = 0 \quad (5.2)$$

- Boundary condition deep into the Semi-Infinite solid

$$T = T_0 \quad \text{as } y \rightarrow \infty \quad (5.3)$$

The third and last boundary condition describing the semi-infinite solid is the boundary condition at the surface ($y = 0$). The following subsections detail the two conditions studied at this boundary. In general, this boundary condition can be a constant temperature change, a constant surface heat flux, a convective heat transfer to the surface, a surface energy pulse and or a periodic surface temperature variation.

5.2.1.1 Semi-Infinite Solid Subjected to a Step Change in Surface Temperature

- Boundary condition at the surface

$$T = T_s \quad \text{at } y = 0 \quad (5.4)$$

The boundary condition at the surface is a constant temperature represented by T_s . The analytical solution to this problem, found in Mills (1992), gives the general solution equation as given in Equation (5.5). Figure 5.8 is a sketch of the analytical solution to this equation.

$$\frac{T - T_0}{T_s - T_0} = \text{erfc} \left[\frac{y}{(4\alpha t)^{1/2}} \right] \quad (5.5)$$

The following properties and temperatures were used for this test:

$$k = 0.52 \text{ W/m}\cdot\text{K}$$

$$\rho = 2050 \text{ kg/m}^3$$

$$C_p = 1840 \text{ J/kg}\cdot\text{K}$$

$$\alpha = 1.3786 \times 10^{-7} \text{ m}^2/\text{s}$$

$$T_o = 20^\circ \text{ C}$$

$$T_s = 50^\circ \text{ C}$$

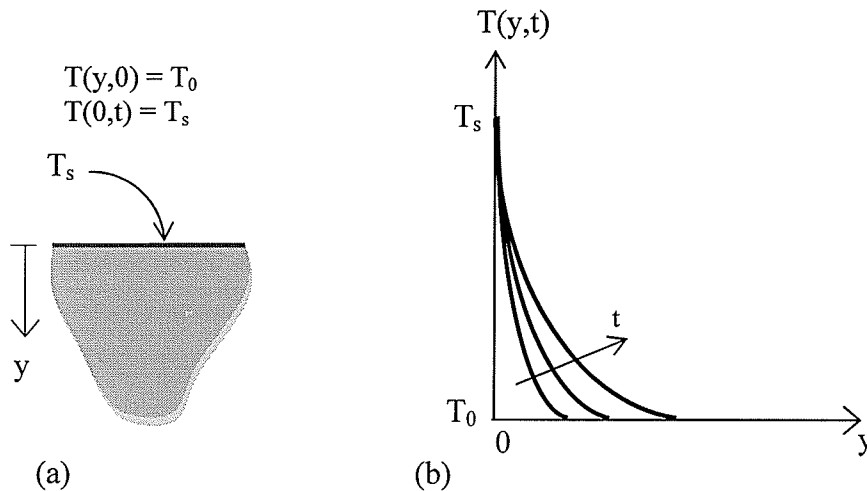


Figure 5.8 Step surface temperature change for a semi-infinite solid: (a) boundary conditions and (b) instantaneous temperature profile (Mills, 1992, pg. 156)

Figure 5.9 shows a comparison of the numerical results against the analytical results. The results were taken over a distance of 0.1 m from the surface, in which the effects of the surface boundary step change took place. Several time intervals were plotted. In all cases, the numerical results agreed closely with the analytical solution.

5.2.1.2 Semi-Infinite Solid Subjected to Periodic Surface Temperature Variation

- Boundary condition at the surface

$$T = T_s = T_o + (T_s^* - T_o) \sin(\omega t) \quad \text{at } y = 0 \quad (5.6)$$

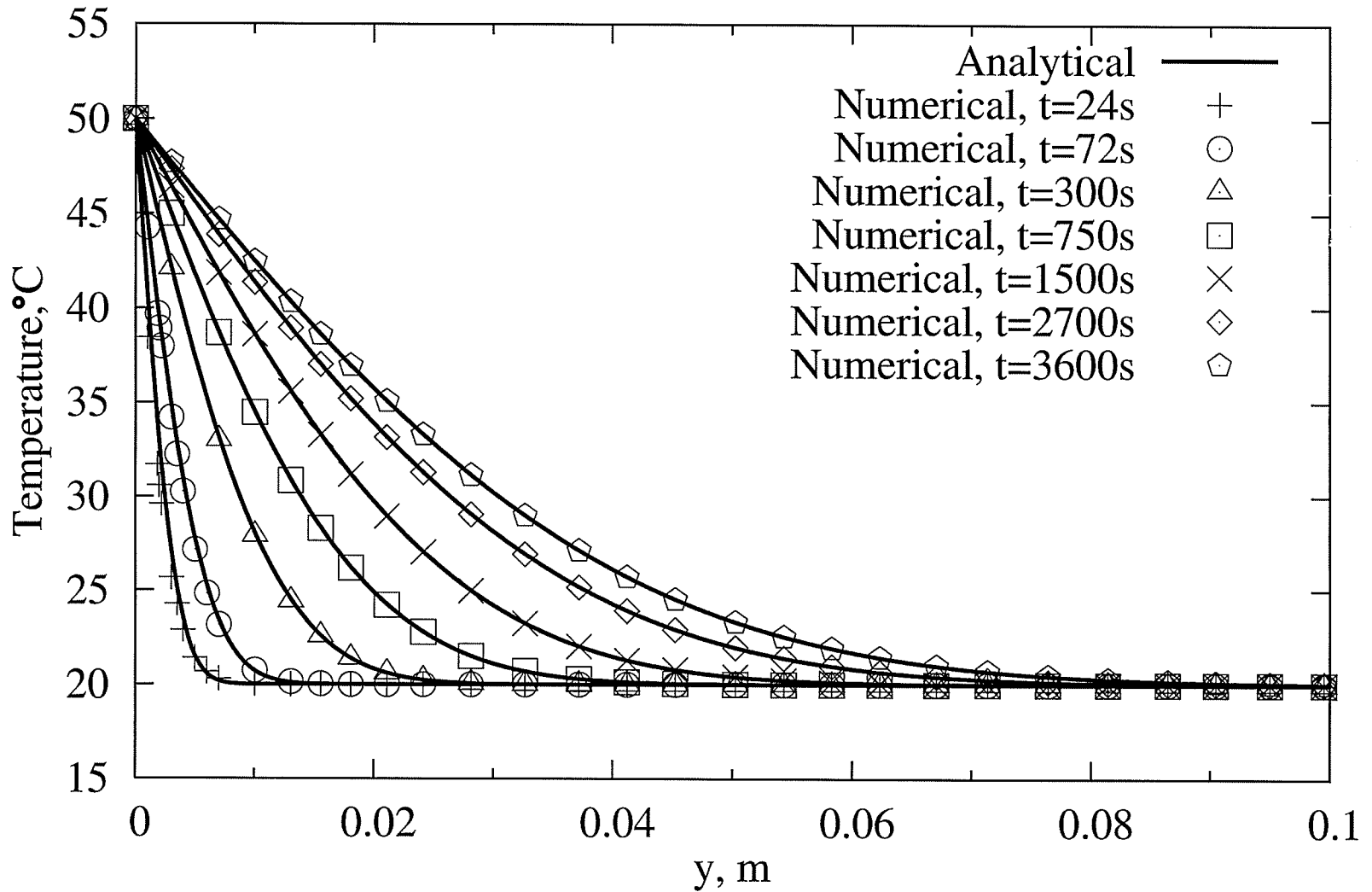


Figure 5.9 Comparison of numerical results to analytical solution for a semi-infinite solid subjected to a step change in temperature at its boundary

In this case the boundary condition at the surface is a periodic temperature represented by a sinusoidal function, as described by Equation (5.6). The analytical solution for this case is given by Equation (5.7). The surface temperature function is given in Equation (5.8). A sketch of the analytical solution to these equations is illustrated in Figure 5.10.

$$T(y,t) = T_0 + (T_s^* - T_0) e^{-y \left(\frac{\omega}{2\alpha}\right)^{1/2}} \sin \left[\omega t - y \left(\frac{\omega}{2\alpha}\right)^{1/2} \right] \quad (5.7)$$

$$T_s = T_0 + (T_s^* - T_0) \sin[\omega t] \quad (5.8)$$

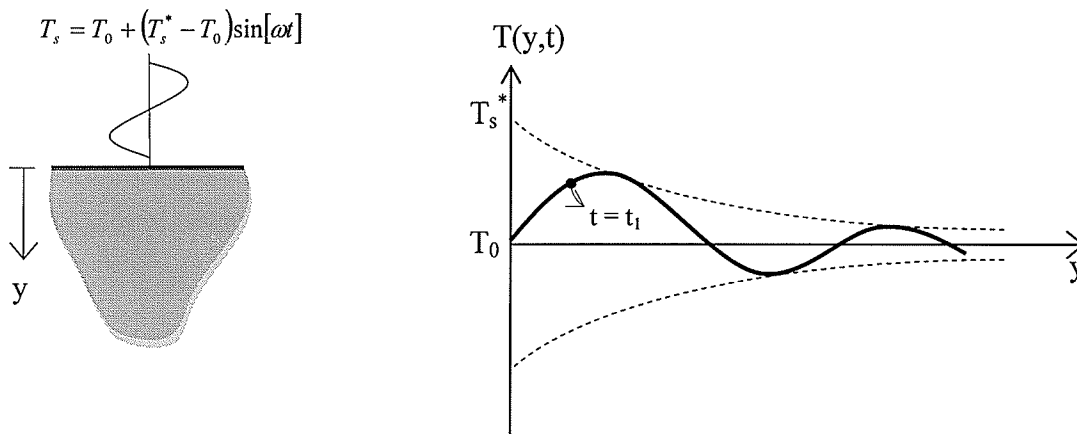


Figure 5.10 Periodic surface temperature variation for a semi-infinite solid: (a) boundary conditions and (b) instantaneous temperature profile at $t = t_1$. (Mills, 1992, pg. 161)

The following properties and temperatures were used for this test:

$$k = 52 \text{ W/m}\cdot\text{K}$$

$$\rho = 2050 \text{ kg/m}^3$$

$$C_p = 1840 \text{ J/kg}\cdot\text{K}$$

$$\alpha = 1.3786 \times 10^{-5} \text{ m}^2/\text{s}$$

$$T_0 = 20^\circ \text{ C}$$

$$T_s^* = 100^\circ \text{ C}$$

$$\omega = \pi \text{ rad/s}$$

The numerical code was validated against the analytical solution by comparing the temperature results at particular monitor points fixed in location. The temperature values were recorded at consecutive time steps. This comparison is shown in Figure 5.11. The values of temperature over time were taken at a distance of $y = 1.005 \times 10^{-4}$ m from the surface boundary. The figure shows that the numerical results match almost exactly to the analytical solution. Table 5.6 shows the percentage difference between the numerical results and the analytical solution. The error was calculated with each passing cycle of the numerical results to the analytical solution. As seen from the table the percentage difference values are under 1% for all cycles and remains under 0.3% after the third cycle. Other monitor points were also tested and gave similar results. In all cases the percentage difference was less than 1%.

Table 5.6 Monitor point percentage difference comparison at $y = 1.005 \times 10^{-4}$ m

Time, s	Percentage Difference, %
2	0.443
4	0.340
6	0.300
8	0.279
10	0.286
12	0.275
14	0.271
16	0.265

In addition, the numerical results were validated against the analytical solution by comparing the temperature results along a line from the surface to a depth of 0.02 m. Since the temperature follows a sinusoidal cycle has a period of 2 seconds, two different points in time were selected within the cycle for comparison. The temperature cycle has an amplitude of 80°C, where the maximum temperature is 100°C and the constant initial temperature is 20°C. The points selected for comparison within the cycle are at $\frac{1}{4}$ the cycle or at time $t = 0.5$ s and at the end of the cycle or time $t = 2.0$ s.

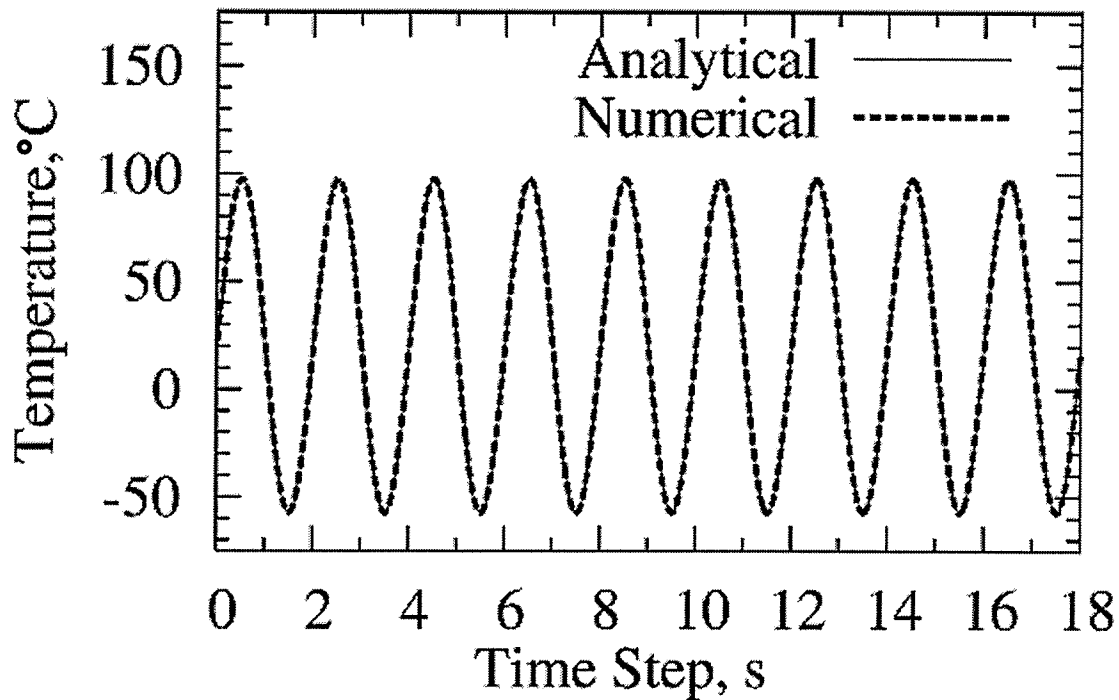


Figure 5.11 Numerical-monitor-point results comparison against the analytical solution for $y = 1.005 \times 10^{-4}$ m

Figure 5.12 shows the comparison between the numerical results and the analytical solution at $t = 0.5$ s. At $t = 0.5$ s the cycle is at its highest point. Therefore, the surface boundary is subjected to a temperature of $T = 100^\circ\text{C}$. Figure 5.12 shows that at $y = 0$, the temperature is 100°C . This temperature is sharply decreased within the first 0.005 m of distance and the effects of the boundary are very much dampened by $y = 0.02$ m. The figure shows that with each passing cycle the numerical results approximate more precisely the analytical solution. Table 5.7 shows the maximum calculated percentage error within the line section. The table shows how the error is decreased with each cycle, up to the point where the error is approximately 2%. Figure 5.12 demonstrates the numerical results to the first four cycles, which qualitatively shows its approximation to the true solution.

Similarly, Figure 5.13 shows the numerical results comparison for cycles 1 to 4 with the analytical solution for $t = 2.0$ s. As in the previous case, Table 5.8 shows the maximum

error for this comparison decreasing with each cycle to the point where the error is approximately 2.6 %. At $t = 2.0$ s the cycle is at its low-end point. Therefore, the surface boundary is at its initial temperature of $T = 20^{\circ}\text{C}$. The effects from the boundary are again, dampened within the first 0.02 m of the semi-infinite solid.

Table 5.7 Percentage difference comparison at $t = 0.5$ s

Cycle #	Time cycle [s]	Maximum Percentage Difference, %
1	0.5	67.147
2	2.5	18.063
3	4.5	10.002
4	6.5	6.661
5	8.5	4.801
6	10.5	3.805
7	12.5	3.180
8	14.5	2.760
9	16.5	2.470
10	18.5	2.264
11	20.5	2.120
12	22.5	2.022

Table 5.8 Percentage difference comparison at $t = 2.0$ s

Cycle #	Time cycle [s]	Maximum Percentage Difference, %
1	2.0	20.899
2	4.0	10.254
3	6.0	6.904
4	8.0	5.034
5	10.0	3.694
6	12.0	3.210
7	14.0	2.990
8	16.0	2.850
9	18.0	2.756
10	20.0	2.697
11	22.0	2.662
12	24.0	2.647

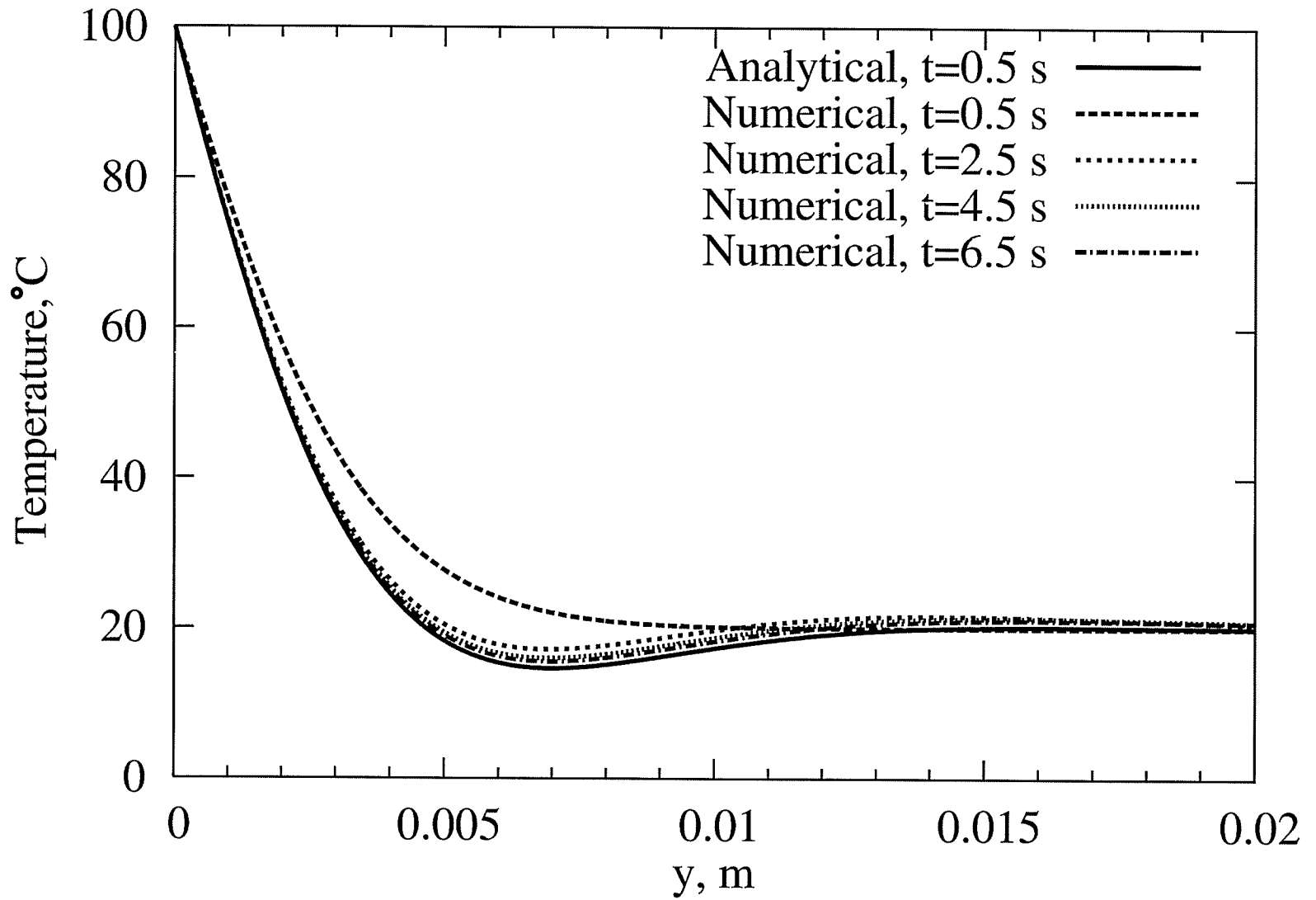


Figure 5.12 Numerical results comparison against analytical solution for $t = 0.5$ s

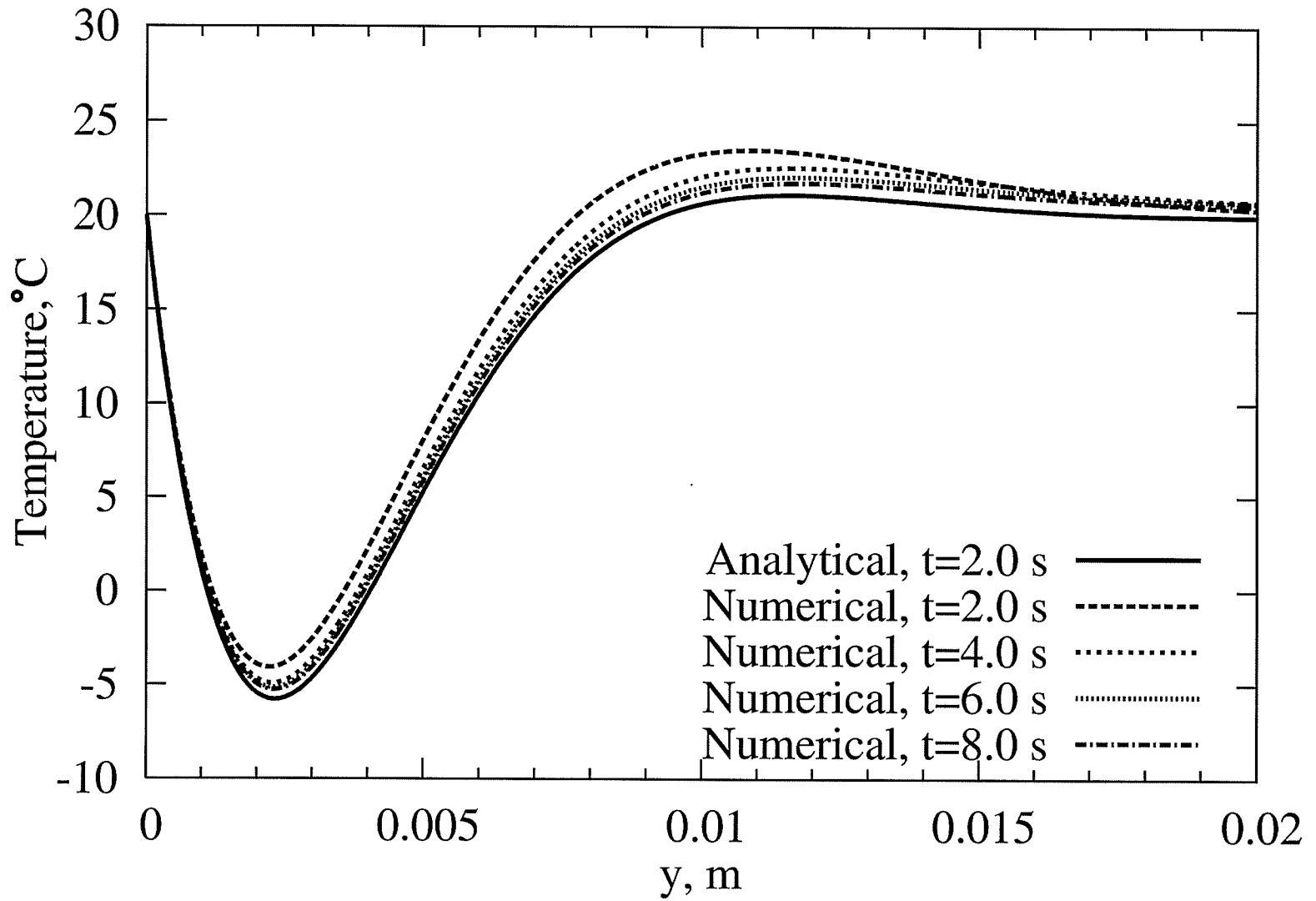


Figure 5.13 Numerical results comparison against analytical solution for t = 2.0 s

5.2.2 Composite Material Interface Balance

At the interface between two materials, in the absence of any interfacial resistance, the value of temperature and the heat flux are both continuous. For example, the temperature should be equal when changing between gravel and soil as illustrated in Figure 5.14. It is important to validate that CFX-5 is capable of handling a domain of composite materials accurately, as this is a major element of this research. Some computational fluid dynamics codes are not capable of handling composite solid domain as a result of the control volume method used. In these cases the control volume node is right at the interface of the two materials and the control volume is composed of the two materials. CFX-5 puts two control volume nodes on top of each other at the boundary of two adjoining regions. This allows maintaining the accuracy at each interface.

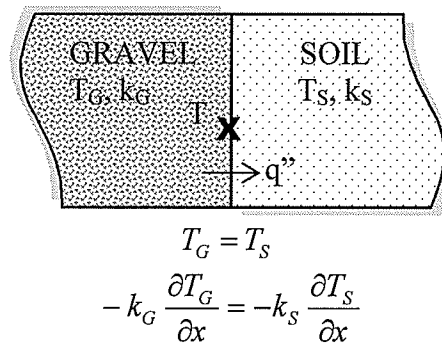


Figure 5.14 Example of thermal balance at a composite material interface

Many simple conductive heat transfer problems using composite domains were done to validate this condition. Two examples are included in this section as validation of this condition. The first case deals with a simple one dimensional conduction heat transfer problem, shown in Figure 5.15. The figure describes the domain and boundary conditions used for its solution. The thermal conductivity values were $k_a = 2 \text{ W/m}\cdot\text{K}$ and $k_b = 1 \text{ W/m}\cdot\text{K}$.

This problem can be easily solved analytically by hand, giving results of $T_1 = 85^\circ\text{C}$, $T_2 = 35^\circ\text{C}$ and $q = 30\text{W/m}$ depth. The results obtained in CFX-5 matched these values identically. Although this problem may seem simplistic, it was of key importance in quickly determining if the code was capable of handling composite domains. Fairly early in the research it was found that CFX-TASCflow was not able to handle composite domains correctly.

The second validation case was done with the two-dimensional heat transfer problem shown in Figure 5.16. For this case the thermal conductivity values were $k_b = 1\text{ W/m}\cdot\text{K}$ and $k_c = 10\text{ W/m}\cdot\text{K}$. The overall heat rate value was calculated and compared to the numerical solution obtained using the ANSYS finite element heat conduction code and using an 'in-house' code developed by Berg (2002). Comparing the result from CFX-5 to ANSYS resulted in a 0.117% difference. Meanwhile, comparing CFX-5 results against Berg resulted in a 0.163% difference.

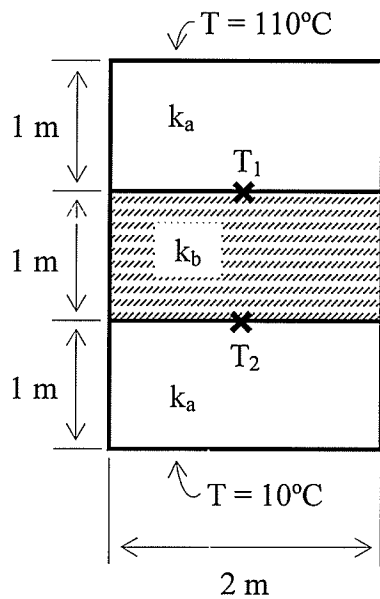


Figure 5.15 One-dimensional validation of a composite wall

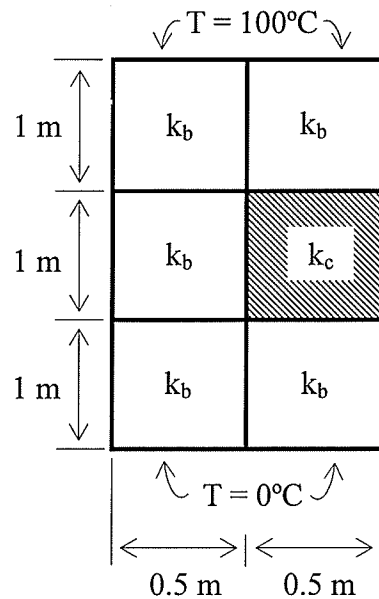


Figure 5.16 Two-dimensional validation of a composite wall

5.2.3 Validation Tests Against the Work of Krarti (1993b)

A validation test was done against the work of Krarti (1993b), which was summarized in Chapter 2, Section 2.3. Figure 2.2 shows a schematic of the domain modeled and boundary conditions used in the steady state heat transfer from a slab-on-grade floor with vertical insulation. As explained in Section 2.3, Krarti used the ITPE method which combines analytical and numerical techniques. A zero thickness was used for the vertical insulation in the Krarti analysis.

The results were validated using the same conditions and properties as given in Krarti's work. In order to compare accurately, the numerical results were obtained after reaching grid independence. Two main comparisons against Krarti are included in this section. The first comparison computes the local heat flux ($\Delta Q''$) at the left boundary using the temperature isotherms plotted at one degree Celsius intervals. For example, the distance between isotherms for 11°C and 12°C , denoted "11-12", was measured and the $\Delta Q''$ was

computed using $\Delta T/\Delta y$. Krarti published in his work a number of temperature isotherms for different conditions. The results for a slab without any vertical insulation were also compared.

The comparison of the interval change in heat flux is shown graphically in Figure 5.17. This figure shows that the numerical results obtained from CFX-5 closely approximate those of Krarti. Krarti's results are slightly higher for most points. The percentage deviation shown in Table 5.9 indicates that the maximum difference is 4.694%, which is within the error possible in digitizing the Krarti isotherms from the original article's figure.

Table 5.9 Summary of differential heat flux results comparison against Krarti

$\Delta T, ^\circ\text{C}$	$\Delta Q'', \text{W/m}^2$		Percentage Difference, %
	Krarti	CFX-5	
11-12	1.859	1.844	0.813
12-13	1.904	1.850	2.919
13-14	1.927	1.862	3.491
14-15	1.951	1.879	3.832
15-16	1.951	1.896	2.901
16-17	1.975	1.917	3.026
17-18	1.987	1.934	2.740
18-19	2.013	1.949	3.284
19-20	2.052	1.960	4.694

The second comparison with the work of Krarti focuses on his results on the effect of vertical insulation and its depth on the total slab heat losses. The total heat loss per unit depth (Q) was calculated as the integration of the slab heat flux values over the top area of the slab. The results published by Krarti gave Q for a range of vertical insulation depths. At each insulation depth, four types of insulation cases, each varying in conductance were tested by Krarti.

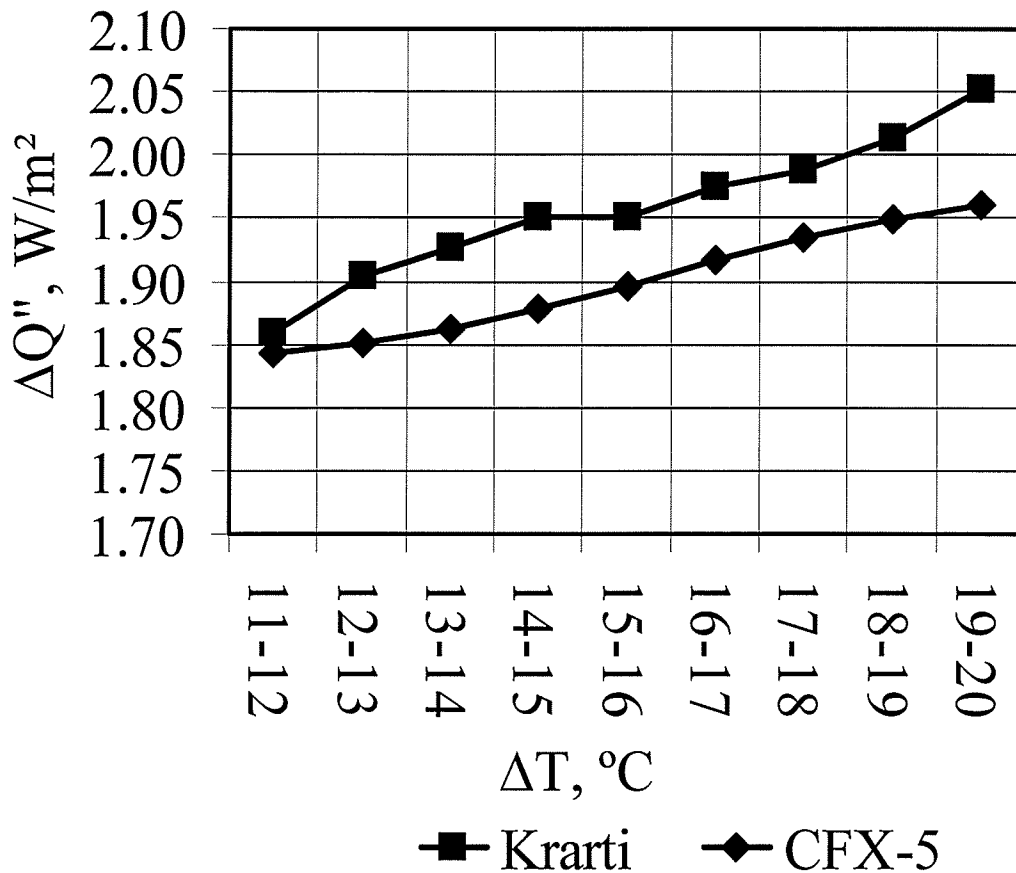


Figure 5.17 Validation against Krarti, differential heat flux results

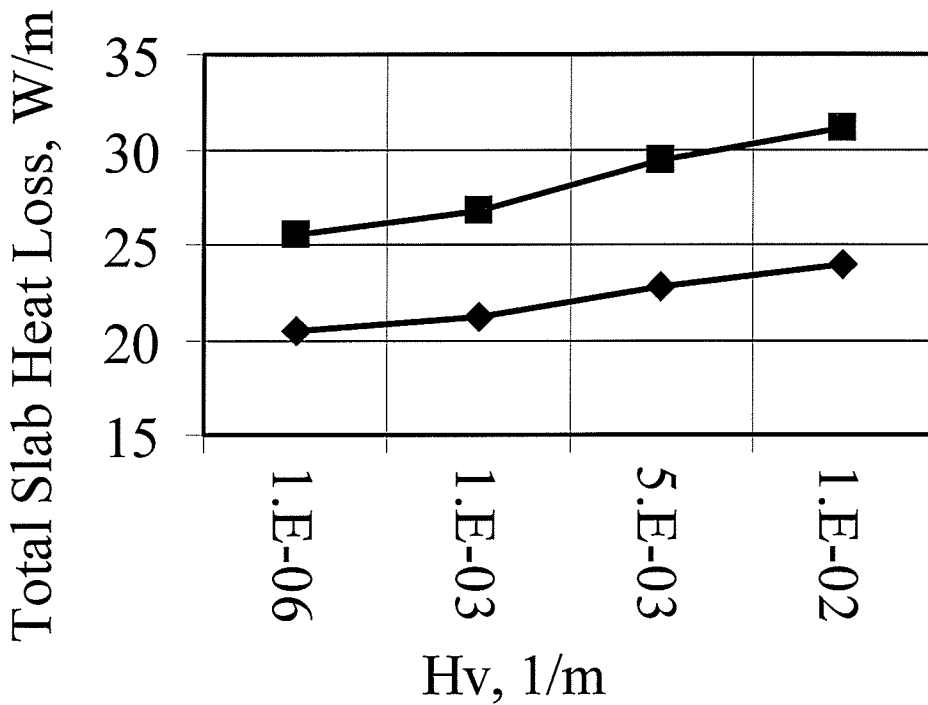
The case with an insulation depth of 2.0 m was analyzed in CFX-5 and is presented here. For this validation case, the domain and boundary conditions shown in Figure 2.2 were also used. The numerical results comparison are shown in Figure 5.18 and summarized in Table 5.10. Krarti designated H_v as the ratio of insulation to soil conductivities divided by the insulation thickness.

The results show that the values for Krarti are higher than those obtained in CFX-5. This difference results up to a 7.2% difference, which could be the result of digitizing the data points from the graphical format published in Krarti's article. Also deviation may be the result of a condition used by Krarti on the insulation that assigns a zero thickness; while in the numerical model used in CFX-5 a finite thickness of 0.01m was assigned to the

insulation. This would explain why the percentage difference between CFX-5 and Krarti is approximately the same for all points compared.

Table 5.10 Summary of total slab heat loss results

k_{insu} W/m·K	Q Krarti W/m	Q CFX-5 W/m	Percentage Difference, %
1.00×10^{-6}	25.5	20.505	5.0
1.00×10^{-3}	26.8	21.165	5.6
5.00×10^{-3}	29.4	22.814	6.6
1.00×10^{-2}	31.1	23.927	7.2



■ Krarti ◆ CFX-5

Figure 5.18 Validation of total slab heat loss results against Krarti

5.2.4 Other Verification Tests

5.2.4.1 Steady Periodic Results

The results were ensured to be steady periodic to obtain a trustworthy numerical solution. Steady periodic results are obtained when they are independent of initial conditions and a true steady behaviour is obtained after a number of iterations. In this model, a cycle or iteration is equivalent to a year. The results after 5 years were compared by calculating the error from two consecutive years. The procedure to check the yearly results is as follows: the temperature data along the line ($z = 2$ m) was obtained for the months of January and June. Various lines of data were compared, however, only this line ($z = 2$ m) is discussed. The results of the error comparison are found in Table 5.11.

Table 5.11 Steady periodic maximum percentage difference

Year	January	June
1		
2	-67.6269	-11.2764
3	-1.0683	-0.1978
4	0.0622	0.0458
5	0.0760	0.0468

Table 5.11 shows that the largest overall percentage difference was in the month of January. A criterion of a percentage difference of less than 1% was required to be considered steady periodic. The largest error occurs between years 1 and 2. From Table 5.11 the error is less than 0.065% after year 3, therefore, the results are steady periodic after year 3. For the remainder of the thesis, year 4 was selected to be steady periodic to ensure accuracy of the results.

Chapter 6

RESULTS AND DISCUSSION

6.1 Domain Definitions

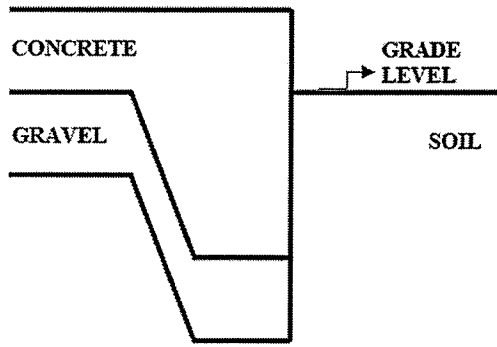
This chapter presents the results obtained from two types of simulations: steady state and transient. First, the steady state results will be presented and discussed, followed by the transient results for Winnipeg and Thompson. The climate and soil properties are different for the two locations, which gives rise to their own specific boundary conditions as discussed in Chapter 3. The results obtained in the simulation include heat transfer rates (heat loss) and the location of the zero-degree isotherm.

6.1.1 Insulation Configurations

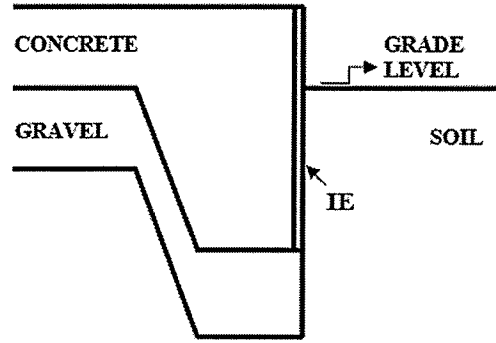
The results were obtained for a number of insulation configurations, which consist of insulation location placements with a variety of lengths and thicknesses. These tests have been performed on six specific insulation configuration cases which are presented in Figure 6.1. The variations of these insulation configurations cases, in terms of insulation lengths and thicknesses, are explained in Section 6.2.1 for the steady state simulations and in Section 6.3.1 for the transient simulations.

6.1.2 Geometries Studied

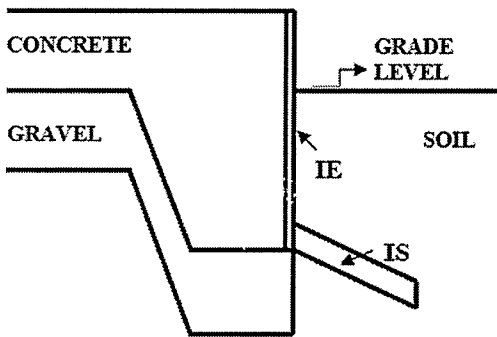
The modelled geometry is described by a number of horizontal, vertical, angular and depth parameters. These are illustrated in Figure 3.2 in Chapter 3. Some of these parameters are fixed while others are variable, depending on the case tested. The fixed parameters were obtained mainly from previous literature such as Labs *et al.* (1988), Robinsky and Bessflug (1973) and Goldberg (1999).



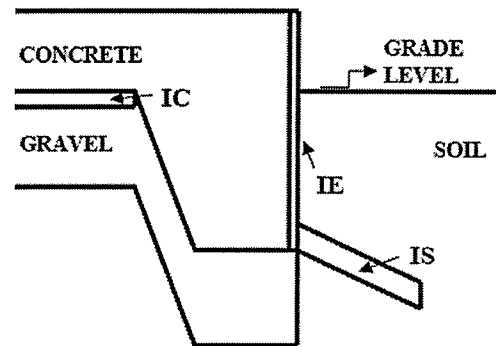
(a) Case A: No insulation



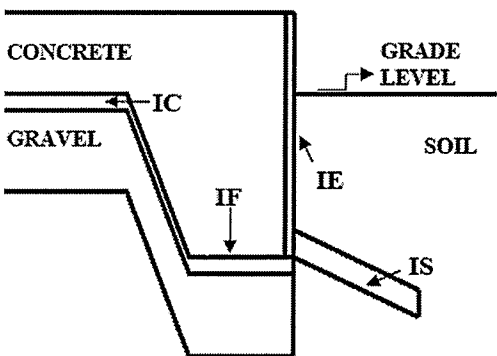
(b) Case B: IE only



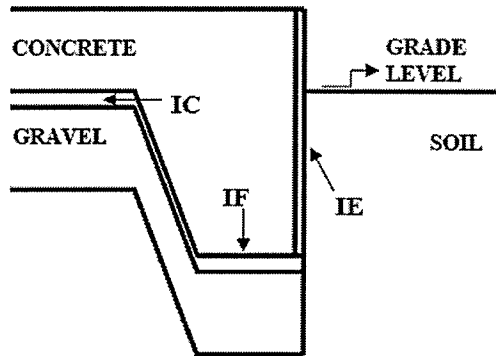
(c) Case C: IE and IS



(d) Case D: IE, IS and IC



(e) Case E: IE, IS, IC and IF



(f) Case F: IE, IC and IF

Figure 6.1 Diagrams of numerical cases studied

Due to the diversity of insulation configurations cases in thicknesses and placement, different grids were used to model the cases tested. Twenty grids were used to model the cases presented in this thesis for the steady state and transient analysis. Table 6.1 gives a summary of the fixed horizontal, vertical and angular parameters for these grids. Sixteen grids were used to model the cases of the steady state analysis. The variable horizontal and vertical parameters for the grids used in the steady state analysis are presented in Table 6.2 for grids 1 to 8, while Table 6.3 gives the values for grids 9 to 16. Also, Table 6.4 presents the variable horizontal and vertical parameters for grids used in the transient section. Many parameters were originally selected in English units, as these units are predominantly used in the construction market. Therefore, the above tables have been reproduced in English units and are presented in Appendix C.

As mentioned earlier in Section 5.1, a small fixed depth of 30 cm (11.81 in) and three nodes were placed in the Z direction. This was done to satisfy the three-dimensional requirement of CFX-5. The depth in the Z axis is fixed and no variation exist in this axis, consequently the problem was treated as a two-dimensional problem.

The results presented in the following sections consist of data reported for half of the TES foundation. Half the slab equals the length of the fixed parameter $L1 = 685.8$ cm (270 in) as illustrated in Figure 3.2. To obtain the values for the full slab, all data reported in this thesis must be multiplied by two.

Table 6.1 Horizontal, vertical and angular parameters fixed for all grids used (see Figure 3.2)

Parameters	[cm]	Parameters	[cm]	Parameters	[deg]
Px1	609.6	Py5	45.7	θ_1	45
Px2	30.5	Py6	15.2	θ_2	10
Px3	45.7	Py8	10.2		
Px4	15.2	Py11	15.2		
Py2	61.0	L1	685.8		
Py3	15.2	L2	714.2		

Table 6.2 Values of horizontal and vertical parameters varied in steady state simulation grids 1 to 8, in cm (see Figure 3.2)

Parameter	Grid 01	Grid 02	Grid 03	Grid 04	Grid 05	Grid 06	Grid 07	Grid 08
Px5	3.8	3.8	3.8	3.8	7.6	7.6	3.8	3.8
Px6	60.0	67.7	60.0	60.0	60.0	60.0	120.1	120.1
Px7	650.4	650.4	650.4	650.4	646.6	646.6	590.3	590.3
Py1	178.1	190.8	178.1	190.8	178.1	178.1	178.1	190.8
Py4	15.2	2.5	15.2	2.5	15.2	15.2	15.2	2.5
Py7	25.4	25.3	22.7	22.7	22.7	22.7	22.7	22.7
Py9	5.2	5.2	7.7	7.7	7.7	7.7	7.7	7.7
Py10	15.2	2.5	15.2	2.5	15.2	15.2	15.2	2.5
L3	300.0	300.0	300.0	300.0	300.0	300.0	300.0	300.0
L4	239.0	251.7	239.0	251.7	239.0	239.0	239.0	251.7
L5	315.2	315.2	315.2	315.2	315.2	315.2	315.2	315.2
L6	5.1	5.1	7.6	7.6	7.6	7.6	7.6	7.6
L7	61.0	61.0	61.0	61.0	61.0	61.0	121.9	121.9

Table 6.3 Values of horizontal and vertical parameters varied in steady state simulation grids 9 to 16, in cm (see Figure 3.2)

Parameter	Grid 09	Grid 10	Grid 11	Grid 12	Grid 13	Grid 14	Grid 15	Grid 16
Px5	7.6	7.6	7.6	7.6	7.6	7.6	7.6	7.6
Px6	60.0	60.0	60.0	60.0	120.1	120.1	120.1	120.1
Px7	646.6	646.6	646.6	646.6	586.5	586.5	586.5	586.5
Py1	178.1	190.8	178.1	190.8	178.1	190.8	178.1	190.8
Py4	15.2	2.5	15.2	2.5	15.2	2.5	15.2	2.5
Py7	25.3	25.3	22.7	22.7	25.3	25.3	22.7	22.7
Py9	5.2	5.2	7.7	7.7	5.2	5.2	7.7	7.7
Py10	15.2	2.5	15.2	2.5	15.2	2.5	15.2	2.5
L3	300.0	300.0	300.0	300.0	300.0	300.0	300.0	300.0
L4	239.0	251.7	239.0	251.7	239.0	251.7	239.0	251.7
L5	315.2	315.2	315.2	315.2	315.2	315.2	315.2	315.2
L6	5.1	5.1	7.6	7.6	5.1	5.1	7.6	7.6
L7	61.0	61.0	61.0	61.0	121.9	121.9	121.9	121.9

Table 6.4 Values of horizontal and vertical parameters varied in the transient simulation grids 17 to 20, in cm (see Figure 3.2)

Parameter	Grid 17	Grid 18	Grid 19	Grid 20
Px5	3.8	3.8	7.6	7.6
Px6	60.0	60.0	60.0	60.0
Px7	650.4	650.4	638.9	646.6
Py1	478.1	490.8	478.1	490.8
Py4	15.2	2.5	15.2	2.5
Py7	25.3	25.3	25.3	25.3
Py9	5.2	5.2	5.2	5.2
Py10	15.2	2.5	15.2	2.5
L3	600.0	600.0	600.0	600.0
L4	539.0	551.7	539.0	551.7
L5	615.2	615.2	615.2	615.2
L6	5.1	5.1	5.1	5.1
L7	61.0	61.0	61.0	61.0

6.2 Steady-State Results

6.2.1 Cases Studied

A total of twenty-nine cases are presented for the set of steady state simulations. These cases are summarized in Table 6.5. From Figure 6.1 it was seen that six main cases (A to F) describe the location of insulation placement. The cases listed in Table 6.5 are named with the first letter of the main case and then numbered according to the insulation configuration used. Different insulation configurations that study insulation length and thickness are summarized.

Each case has an “X” marked in the appropriate insulation configuration. Where insulation length and or thickness were varied, a separate column was assigned to the variable parameter. For example, IE1 and IE2 denote insulation placed at the edge. IE1

and IE2 correspond to an insulation thickness value of 3.8 cm (1.5 in) and 7.6 cm (2.0 in), respectively. The variable parameter describing the thickness of the edge insulation is Px5, as seen in Figure 3.2.

Columns IS1 to IS4 denote insulation placed in the skirt region. Each of these columns indicates the variable parameters used that describe the dimensions of the skirt as explained in Table 6.6. Column IC denotes that insulation was placed under the centre slab region, as indicated by parameter Px1 in Figure 3.2. Since Px1 is a fixed parameter for all grids used in this study, only one column is used. Similarly, column IF indicates insulation placed under the footing. A fixed value was used in this region, consequently one column is used to describe the insulation placed under the footing. Table 6.5 also reports the heat loss per unit depth through the slab, Q_i , as shown in Figure 5.7, for all the steady state cases. The following section explains in detail the results for both the zero temperature isotherms and heat transfer by comparing various cases.

6.2.2 Heat Loss and Zero Temperature Isotherms

Figure 6.2 gives an overview of the zero degree Celsius temperature contour for Cases A, B1 and B2. As a result of Case A having no insulation, the zero isotherm line passes through the side of the foundation. This causes a large amount of heat to escape from inside the house. The heat loss value for Case A corresponds to the highest heat loss in all the steady state cases studied. This value was calculated to be 66.6 W/m as given in Table 6.5.

The B cases have insulation along the vertical side edge. Cases B1 and B2 have a vertical edge insulation thickness of 3.8 cm (1.5 in) and 7.6 cm (3 in), respectively. Insulation added at the vertical edge next to the concrete results in the zero isotherm line moving outside the concrete into the vertical edge insulation, as seen in Figure 6.2. In addition, when doubling the vertical edge insulation thickness the zero isotherm line moves further away from the foundation while maintaining the same general path as shown by Case B2.

Table 6.5 Steady state heat loss values for TES foundation cases

Cases	IE1	IE2	IS1	IS2	IS3	IS4	IC	IF	Q _i [W/m]
A									66.6
B1	X								37.5
B2		X							34.2
C1	X		X						34.6
C2	X			X					34.0
C3	X				X				33.8
C4	X					X			33.0
C5		X	X						31.1
C6		X		X					30.6
C7		X			X				30.4
C8		X				X			29.6
D1	X		X				X		32.2
D2	X			X			X		31.7
D3	X				X		X		31.4
D4	X					X	X		30.7
D5		X	X				X		28.8
D6		X		X			X		28.3
D7		X			X		X		28.1
D8		X				X	X		27.3
E1	X		X				X	X	30.0
E2	X			X			X	X	29.5
E3	X				X		X	X	29.4
E4	X					X	X	X	28.9
E5		X	X				X	X	26.3
E6		X		X			X	X	25.9
E7		X			X		X	X	25.7
E8		X				X	X	X	25.2
F1	X						X	X	31.5
F2		X					X	X	28.0

Table 6.6 Dimensions of skirt insulation

	L6		L7	
	Thickness of Skirt		Length of Skirt	
	5.1 cm (2 in)	7.6 cm (3 in)	61.0 cm (24 in)	121.9 cm (48 in)
IS1	X		X	
IS2		X	X	
IS3	X			X
IS4		X		X

As a result of adding insulation the heat loss escaping from the house decreases when compared to the case with no insulation at all. The heat loss for Case B1 is 37.5 W/m while the heat loss for B2 decreases to 34.2 W/m. Consequently, as expected, adding more insulation results in lower heat loss.

Figure 6.3 shows the zero isotherm results for Cases C1, C2, C3 and C4. To give the reader a sense of the skirt dimensions Figure 6.3 shows the skirt insulation wire frame for Case C4 as it has the longest and thickest skirt configuration. All the other insulation configurations lie within the skirt region of Case C4. Table 6.6 shows the insulation amounts for Cases C1 to C4. Cases C1 and C2 have a skirt insulation length of 61.0 cm (24 in) and for Cases C3 and C4 the length is doubled to 121.9 cm (48 in). Between Cases C1 and C2 the thickness varies. Case C1 has a thickness of 5.1 cm (2 in) while Case C2 has a skirt thickness of 7.6 cm (3 in). The same occurs for Cases C3 and C4. Case C3 has the thinnest thickness of 5.1 cm (2 in) while C4 has a thickness of 7.6 cm (3 in).

It can be seen in Table 6.5 that the heat loss values among Cases C1 to C4 are very similar. Case C1 has a heat loss of 34.6 W/m. This value decreases to 34.0 W/m, 33.8 W/m and 33.0 W/m for cases C2, C3 and C4, respectively. These values indicate a slight change in heat loss among these cases. The total heat loss difference between Case C1 and Case C4 is at a maximum of 1.6 W/m or 4.55% relative to Case C1.

The results for the skirt insulation configuration shown in Figure 6.3 show the zero contour line for C1 closest to the foundation corner. The zero contour line furthest from the foundation corner belongs to Case C4. This shows that the skirt with the higher amount of insulation results in the furthest zero isotherm line. The zero line for Cases C2 and C3 are bounded by those of Cases C1 and C4. These two lines intersect the skirt insulation close to the same location. However, the lines do not follow the same path; the lines vary throughout the soil domain. The zero line for C3 follows a similar path for C4, while C2 has a similar path to Case C1.

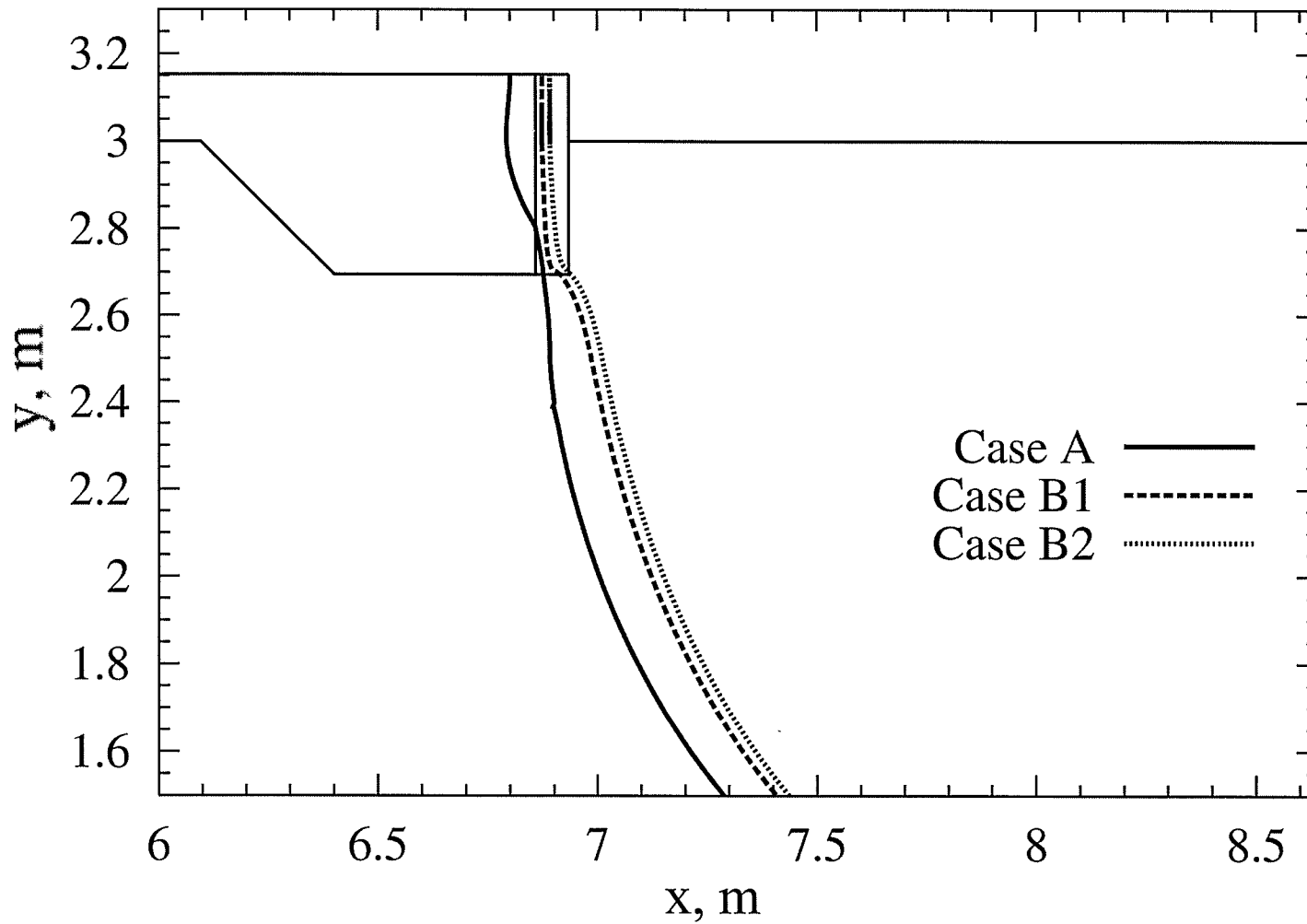


Figure 6.2 Steady state zero isotherm line results for Cases A, B1 and B2

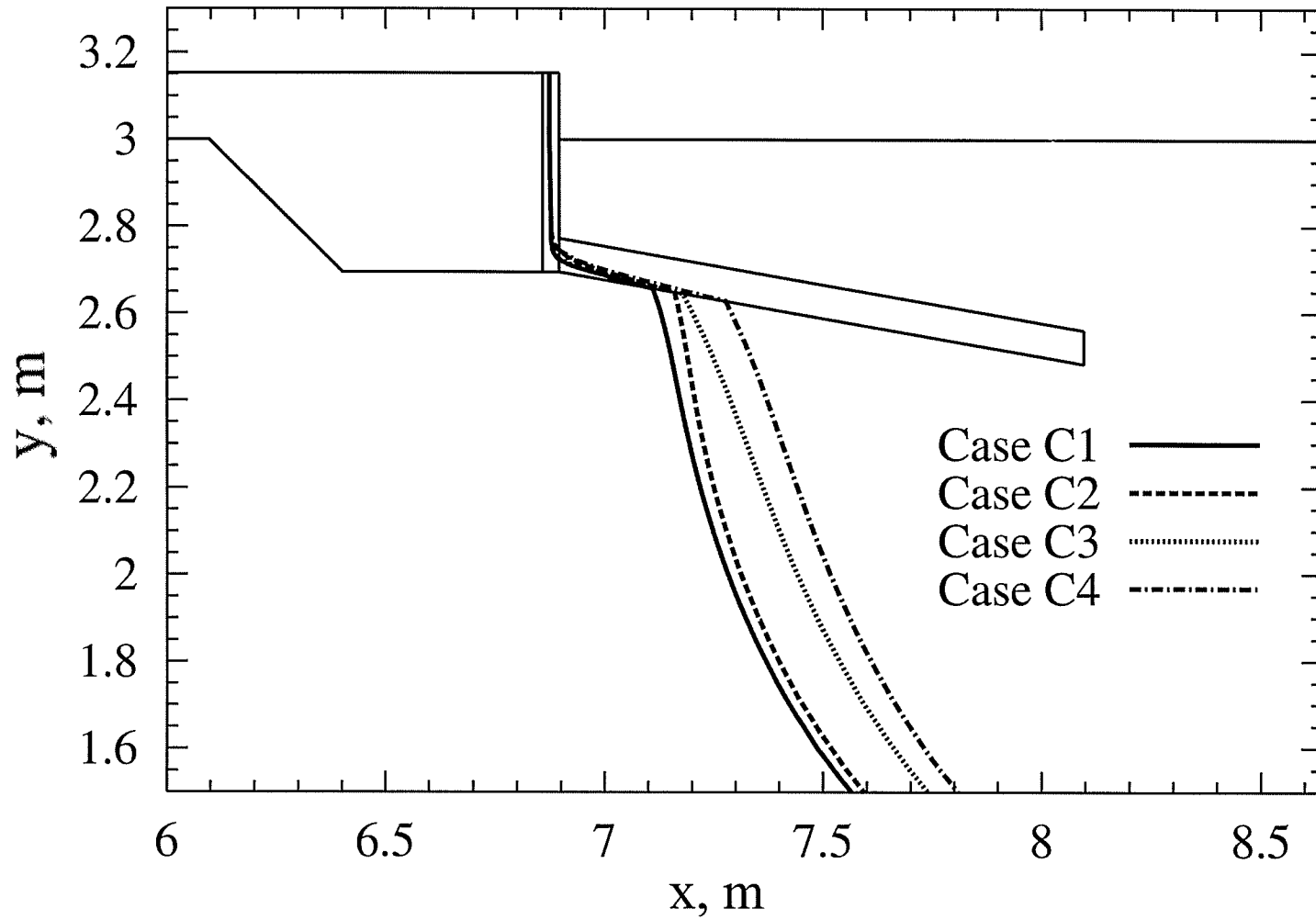


Figure 6.3 Steady state zero isotherm line results for Cases C1, C2, C3 and C4

Figure 6.4 shows the results for Cases C1, C2, C5 and C6. Cases C1 and C5 have the same skirt insulation configuration (length and thickness), likewise Cases C2 and C6. However, Cases C5 and C6 have the thicker vertical edge insulation of E2. The heat loss values for these cases are equal to 34.6, 34.0, 31.1, 30.6 W/m for cases C1, C2, C5 and C6, respectively. For Cases C5 and C6 the same paths of the zero isotherm lines are seen when compared to the paths of Cases C1 and C2. As a result of the thicker vertical edge insulation the zero contour lines for Cases C5 and C6 are seen to be shifted over to the right.

The results for Cases C3, C4, C7 and C8 are shown in Figure 6.5. Figure 6.5 shows results similar to those of Figure 6.4 with the exception that these results are for the longest skirt length insulation configuration. Cases C3 and C7 have the same skirt insulation configuration, as well as Cases C4 and C8 (except for having the thicker edge insulation of E2). The heat loss values are 33.8, 33.0, 30.4, 29.6 W/m for Cases C3, C4, C7 and C8, respectively. In a trend similar to that found in the previous figure, the zero contour lines for Cases C7 and C8 are shifted to the right as a result of the added edge insulation. Among all the cases studied for the skirt insulation configurations (i.e., C1 to C8), Case C8 has the thickest edge insulation and the longest skirt insulation which results in the zero contour line furthest from the foundation corner.

A comparison of insulation configurations for the C and D cases is shown in Figure 6.6 and Figure 6.7. Case C includes insulation regions at the vertical edge and skirt insulation. In addition to the regions of Case C, Case D includes an added region of insulation under the centre slab. Figure 6.6 depicts the zero contour lines for Cases C1, C2, D1 and D2. These cases all have the short skirt insulation length. Figure 6.7 shows the results for Cases C3, C4, D3 and D4. The cases depicted in Figure 6.7 have long skirt insulation length. In the two figures the trends are similar. The results of the D cases lie almost on top of the C cases with a very slight shift to the left with respect to their case C counterpart.

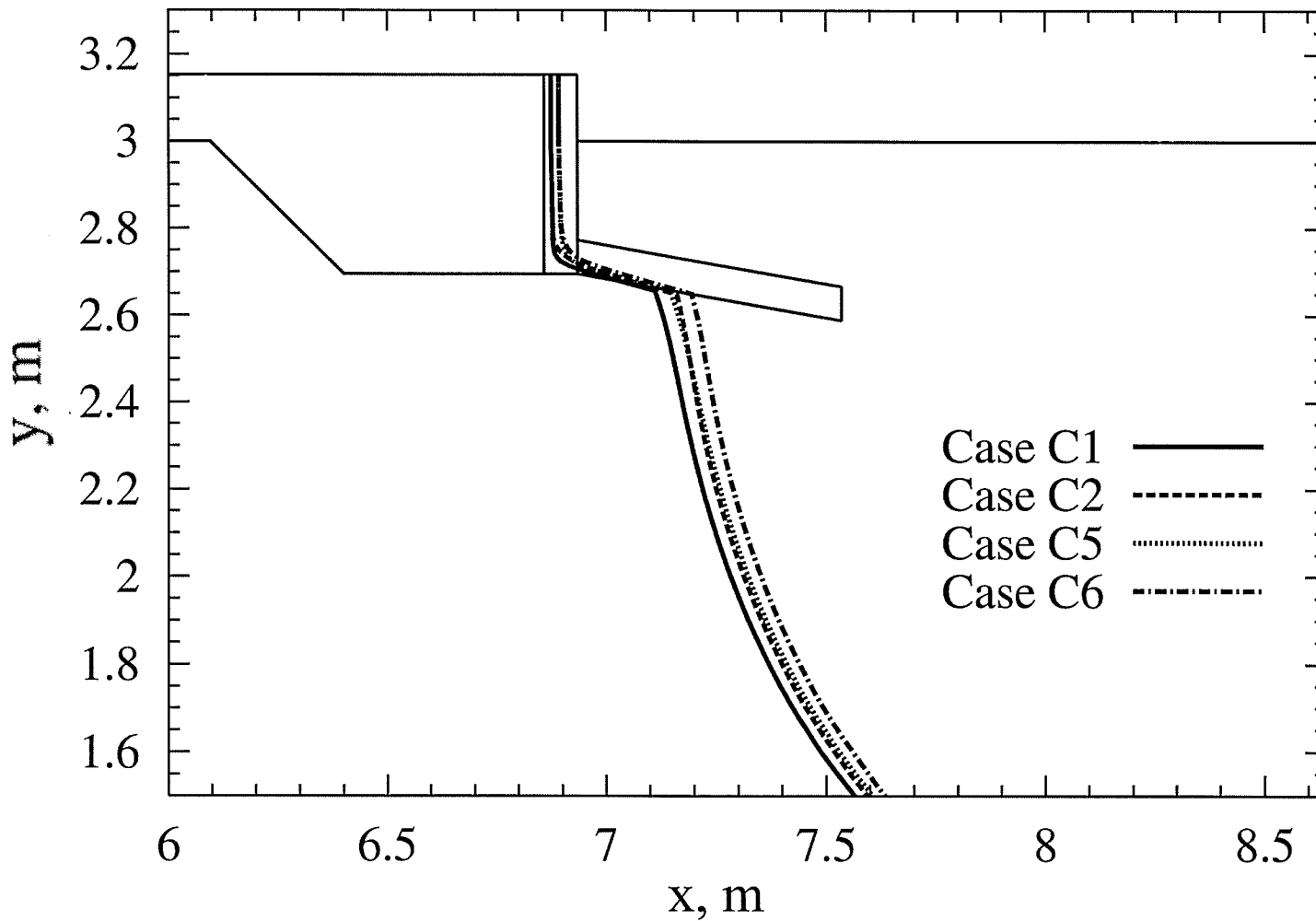


Figure 6.4 Steady condition zero isotherm line results for Cases C1, C2, C5 and C6

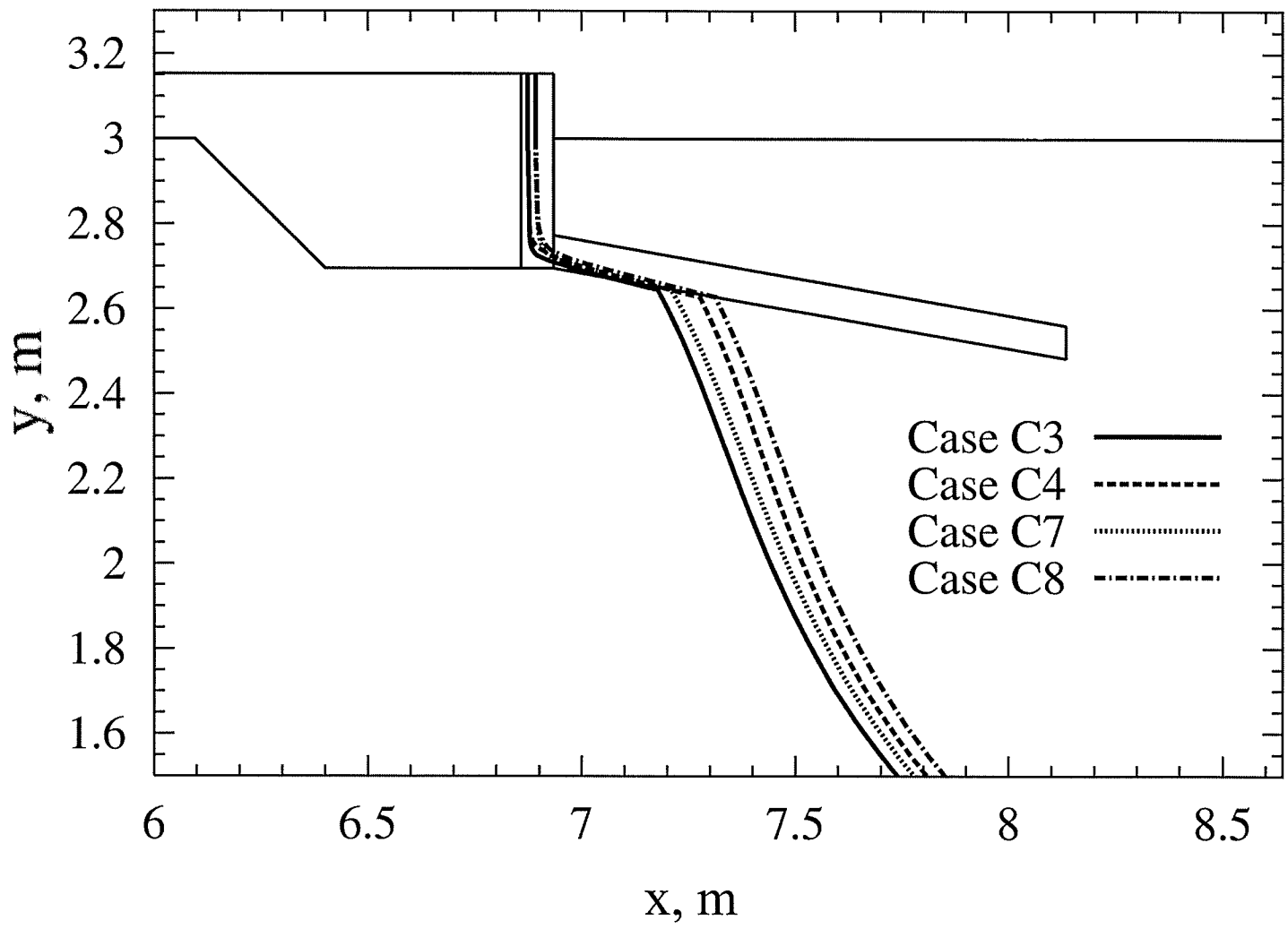


Figure 6.5 Steady state zero isotherm line results for Cases C3, C4, C7 and C8

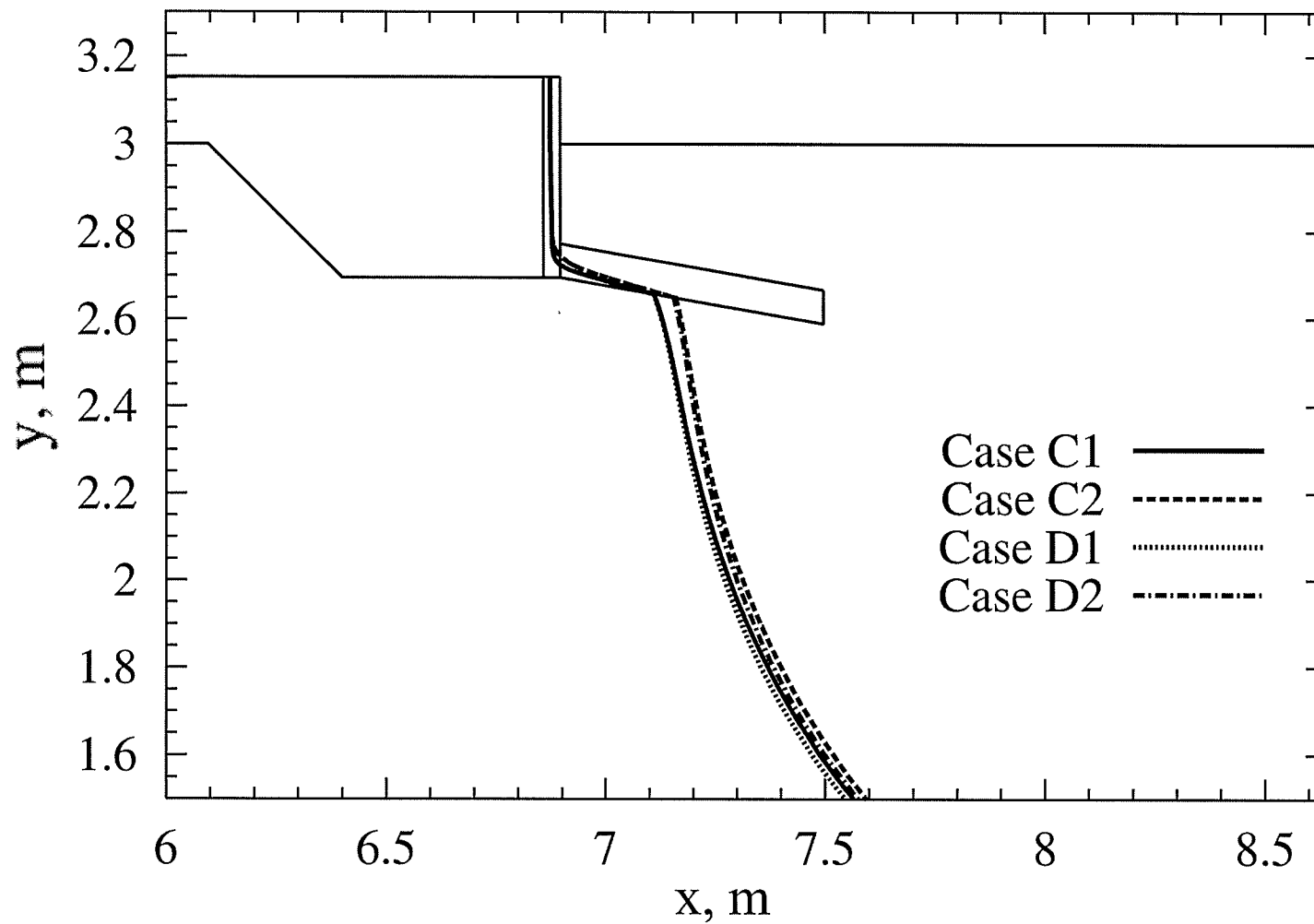


Figure 6.6 Steady state zero isotherm line results for Cases C1, C2, D1 and D2

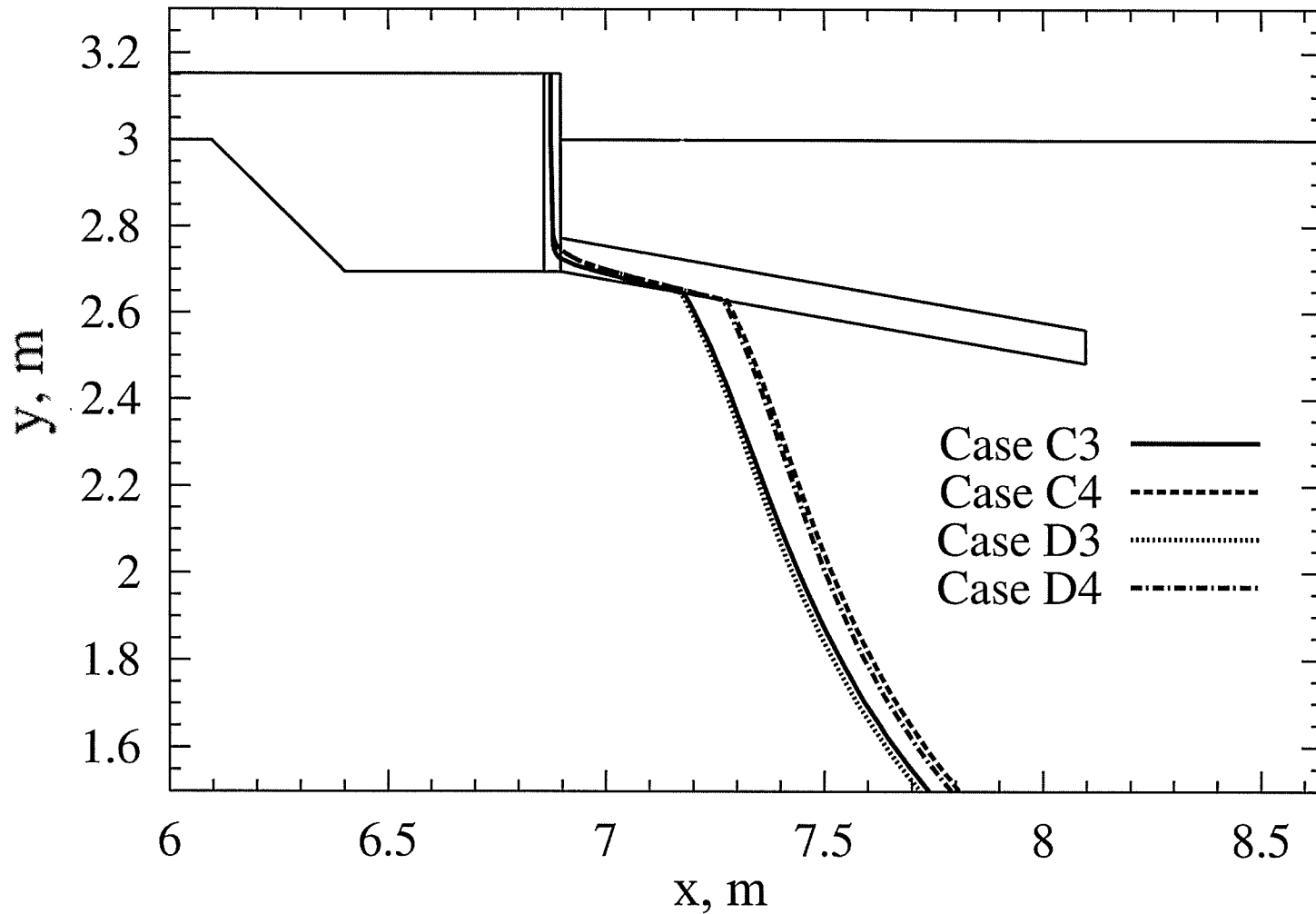


Figure 6.7 Steady state zero isotherm line results for Cases C3, C4, D3 and D4

It can be seen in Figure 6.6 that the intersection of the zero isotherm with the insulation is almost the same for cases C1 and D1. This trend also occurs for Cases C2 and D2, as well as in cases C3 and D3, and C4 and D4 as seen in Figure 6.7. Although, no significant change is seen in the zero contour lines between the C and D cases, adding an extra region of insulation under the centre slab as in the D cases, results in heat loss savings. The heat loss percentage difference between Cases C1 and D1 is about 7.441%. Similar percentage differences were calculated for the other cases in the above figures.

Figure 6.1 (d) and (e) shows a diagram of the location of the insulation for these cases. As seen from these figures, Case E is fully insulated. It has an extra region of insulation under the footing, which is the only region that is not a part of Case D. Figure 6.8 shows the zero contour lines for Cases D1, D2, E1 and E2, which have the short skirt insulation length. The long skirt insulation length is studied in Figure 6.9 for Cases D3, D4, E3 and E4. A comparison can be made between Cases D1 and E1, as they both have the same insulation configurations for the skirt, edge and under the centre slab. The only difference is that Case E1 has insulation under its footing.

Both Figure 6.8 and Figure 6.9 show similar trends. For cases E1 and E2, the zero isotherm lines are shifted over to the left making them lie closer to the foundation corner. The shift is more evident for Cases E3 and E4 in Figure 6.9 where the longer skirt is used. The heat loss is reduced with the addition of insulation. There is a 7.362% difference between Cases D1 and E1. Therefore, adding an extra region of insulation under the footing contributes to a decrease in heat loss. Although, a lower heat loss is obtained in the Case E configurations compared to corresponding Case D configurations, the addition of insulation under the footing is detrimental to the zero isotherm line position. Although the zero isotherm lines do not pose a threat (in terms of frost heave), even for case E, the objective is to obtain the zero contour line as far as possible from the foundation corner. The cases from Figure 6.9 provide a clear example that adding more insulation is not always optimal. In this case the zero isotherm moves back towards the foundation corner because of the addition of insulation under the footings.

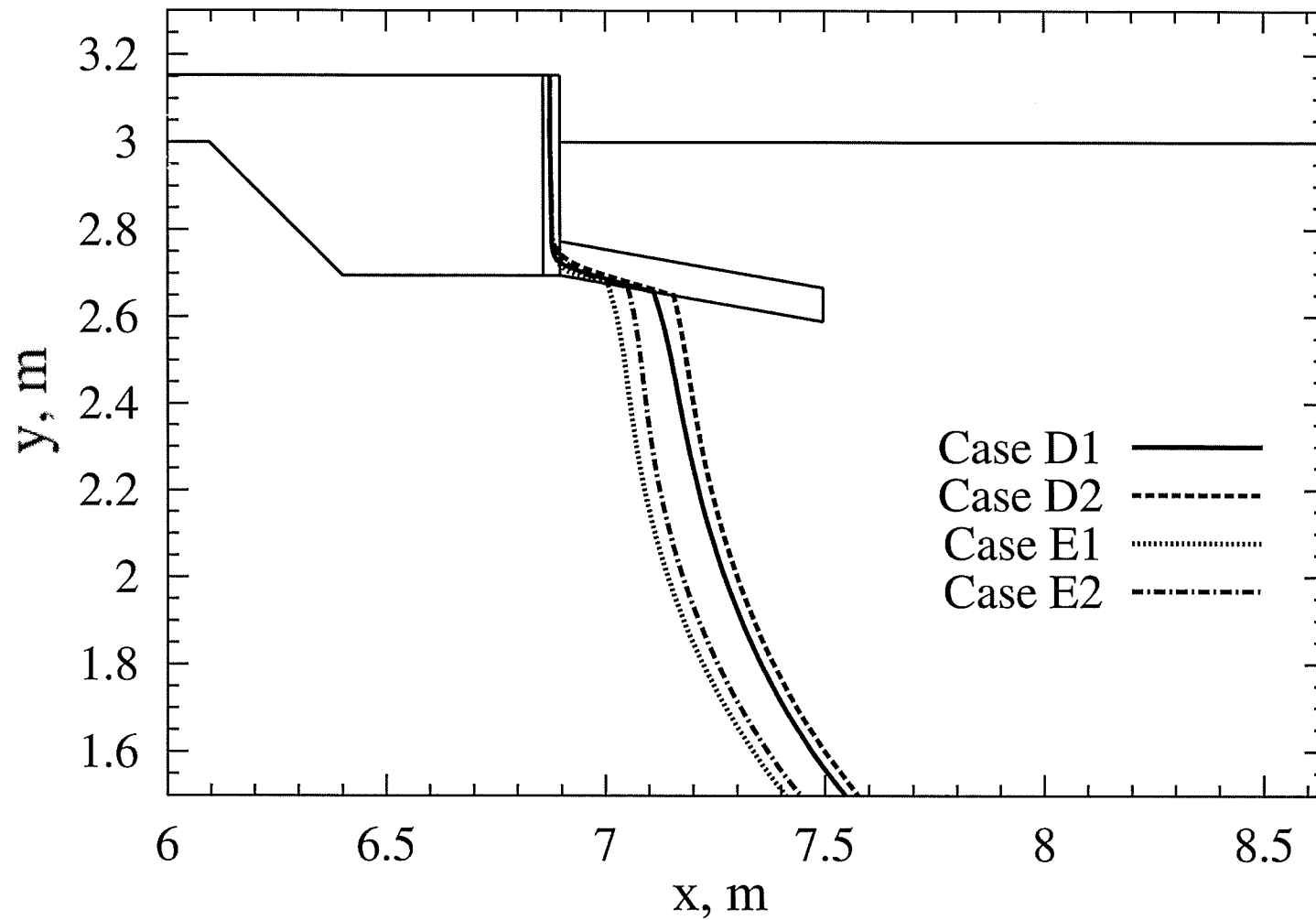


Figure 6.8 Steady state zero isotherm line results for Cases D1, D2, E1 and E2

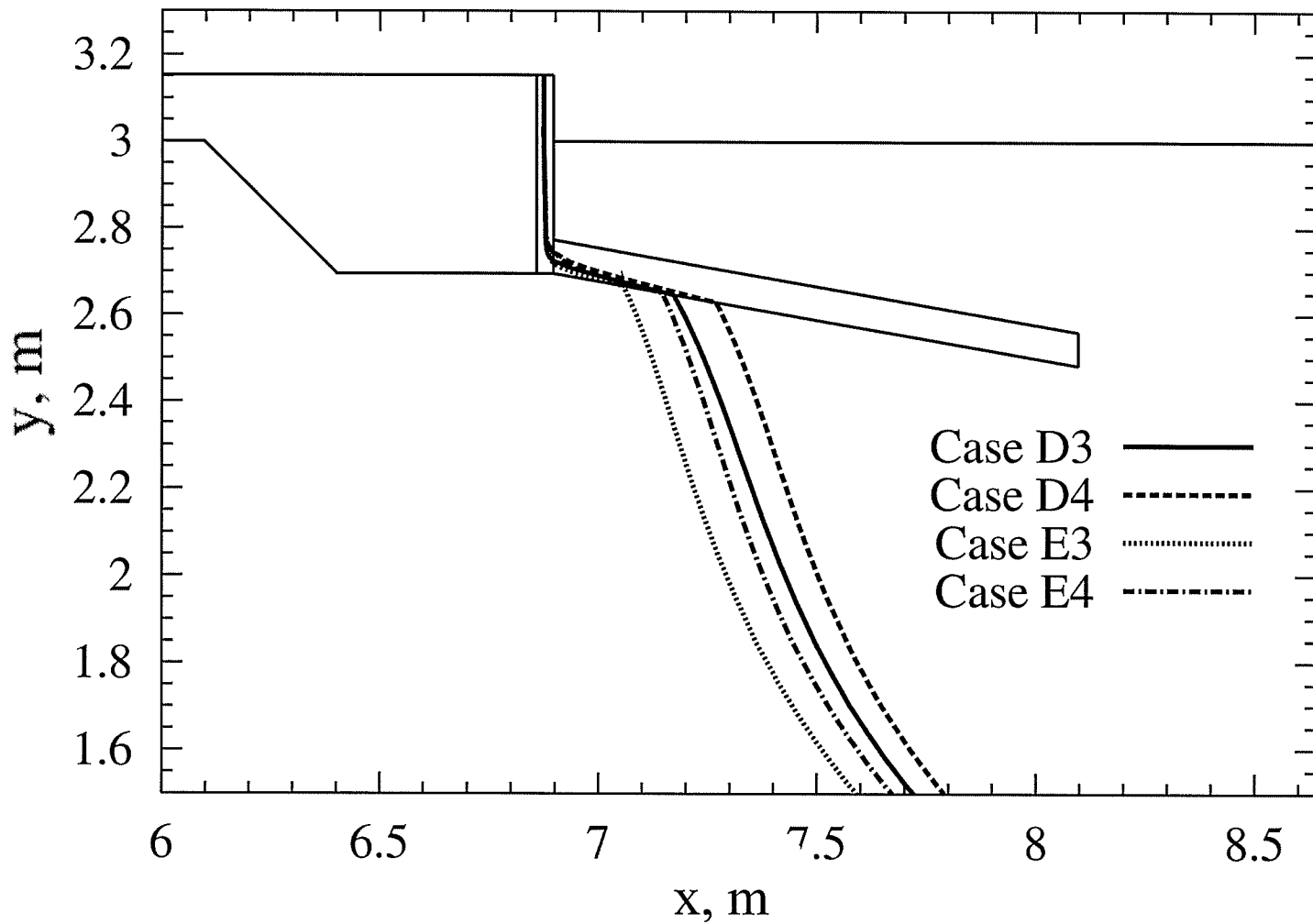


Figure 6.9 Steady state zero isotherm line results for Cases D3, D4, E3 and E4

6.2.3 Overall Trends

shows the zero isotherm lines of Cases A, B1 and F1. None of these cases contains skirt insulation. Case A has no insulation, Case B1 contains only edge insulation and Case F1 has insulation at the foundation edge, under the centre slab and under the footing. As mentioned earlier, in Case A the zero isotherm line passes through the foundation edge. This case also has the highest heat loss of 66.6 W/m, caused by the exposed slab side.

The exposed slab side is referred to as a cold bridge because it is a non-insulating material that is cold bridges directly exposed to outside temperature. Uninsulated or exposed concrete allows for higher amounts of heat from the house to “short circuit” to the cold air above ground instead of going into the ground under the footings where it keeps the ground from freezing (NAHB, 1996). Therefore, a higher potential for frost heave exists as the heat escapes to the air rather than heating the soil to prevent frost heave.

The results seen for Case A may give rise to adfreezing of the foundation. The strength of soil is greatly increased by the transformation of water (in the soil) to ice when the ground freezes. This strengthening process may also be responsible for the strong bond that may develop between a cold enough foundation edge and the soil. Adfreezing is the force transmitted by this bond to the foundation by the upward volume displacement of the frozen layer. The shearing stress experienced may displace the foundation unless the dead load of the building or other resisting forces exceeds the uplift force (Penner and Burn, 1970; Danyluk, 1997).

Adding edge insulation effectively forces the heat into the ground where it raises the soil temperature above freezing temperatures. That is the effect seen from Case B1. This trend has been recognized by many researchers such as NAHB (1996), Robinsky and Bessflug (1973), and Carmody *et al.* (1991). Case F1 shows the effect of adding too much insulation. In this case, not enough heat is allowed to flow to the soil, which causes the zero isotherm line to move very close to the foundation corner. The results show this

line moving almost underneath the foundation, which increases the risk of frost heave. Similar results are seen in Figure 6.11, where the edge insulation is doubled to 7.6 cm (3 in). The increased thickness displaces the zero isotherms slightly to the right.

Figure 6.12 shows a comparison of Cases C1, D1, E1 and F1. As shown in Figure 6.1 all cases have edge insulation; Cases C, D, and E have skirt insulation; Cases D, E and F have centre slab insulation and Cases E and F have footing insulation. As seen earlier, the cases with skirt insulation have their zero isotherm lines furthest away from the foundation corner. The cases with no skirt insulation region have the zero line almost next to the foundation corner, as seen by Case F1 and earlier by Cases A and B1 from .

The use of skirt insulation has been addressed by other researchers such as CMHC-SCHL (2000a and 2000b), NAHB (1996), and Danyluk (1997). The skirt insulation would be placed all around the three-dimensional slab. In this two-dimensional study, the effects of adding skirt insulation are clearly seen. Heat loss is reduced by adding the skirt insulation region. A reduction in heat loss is seen when comparing Cases B1 to any of the Cases C1 to C4 and when comparing Case B2 to any of the Cases C5 to C8. In addition, having a region of skirt insulation allows for the heat flow path to be extended. The temperature of the soil directly under the skirt increases from the heat flow coming from the house and the underlying geothermal heat. This is very beneficial as the risk of frost heave is minimized since the soil under the foundation has a higher temperature. Accordingly, the skirt insulation allows for the zero isotherm line to move away from the foundation corner. In short, the skirt insulation effectively conserves and redirects the heat coming from both the house and the underlying geothermal heat as well as moves the zero isotherm line away from the foundation corner which reduces the risk of frost heave.

Table 6.5 also indicates that the heat loss is reduced and redirected by adding insulation under the slab as shown by Case D1 and E1. In Figure 6.12, it is seen that the location of the zero isotherm line was not affected in Case D1 compared to C1. The heat loss, however, was decreased. The zero isotherm line for Case E1 moved closer to the

foundation corner. This happened because the heat flow was cut off from the slab footing. Therefore, leaving the slab footing clear of insulation allows for the heat to be directed more effectively toward the corner where it is needed.

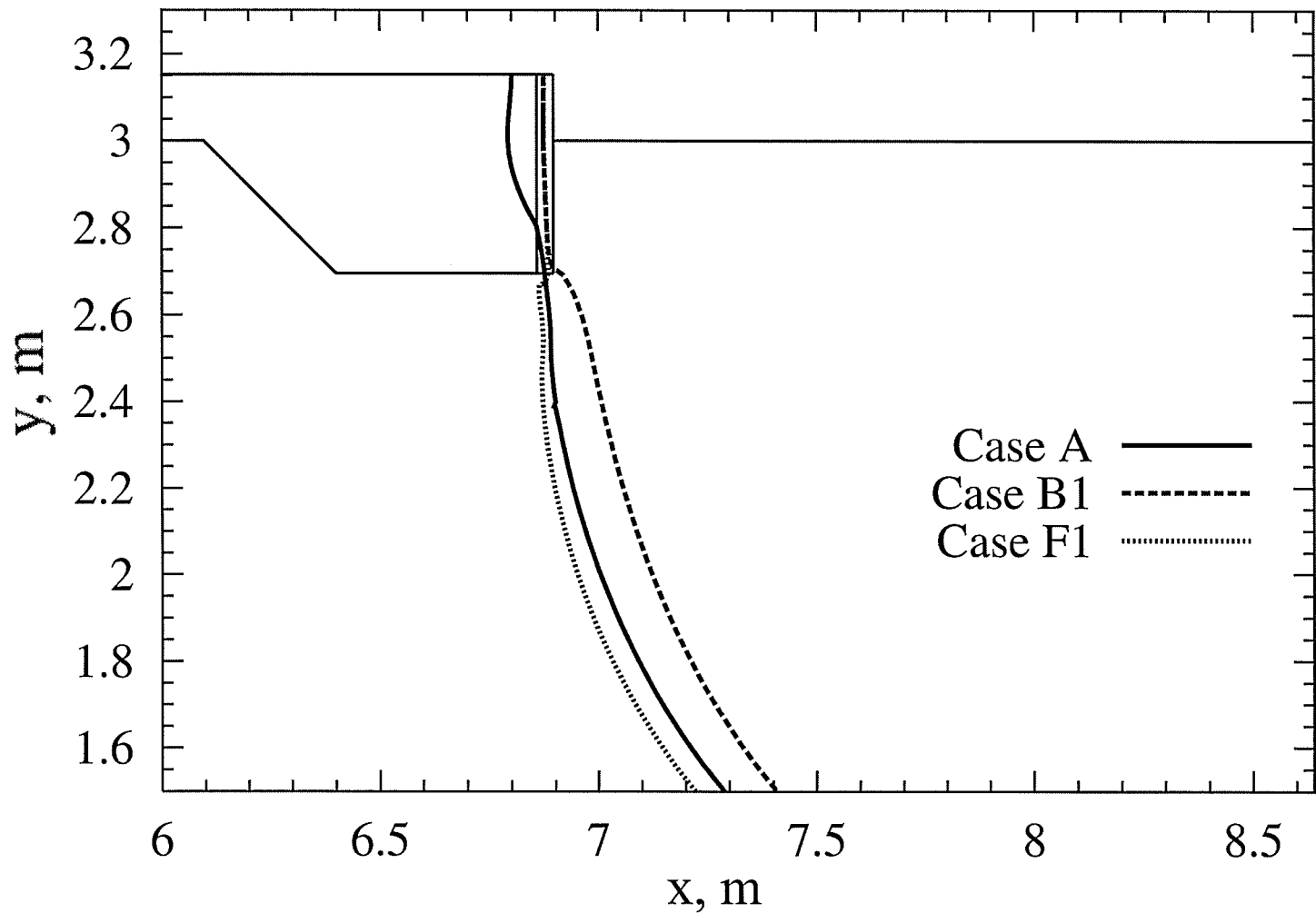


Figure 6.10 Steady state zero isotherm line results for Cases A, B1 and F1

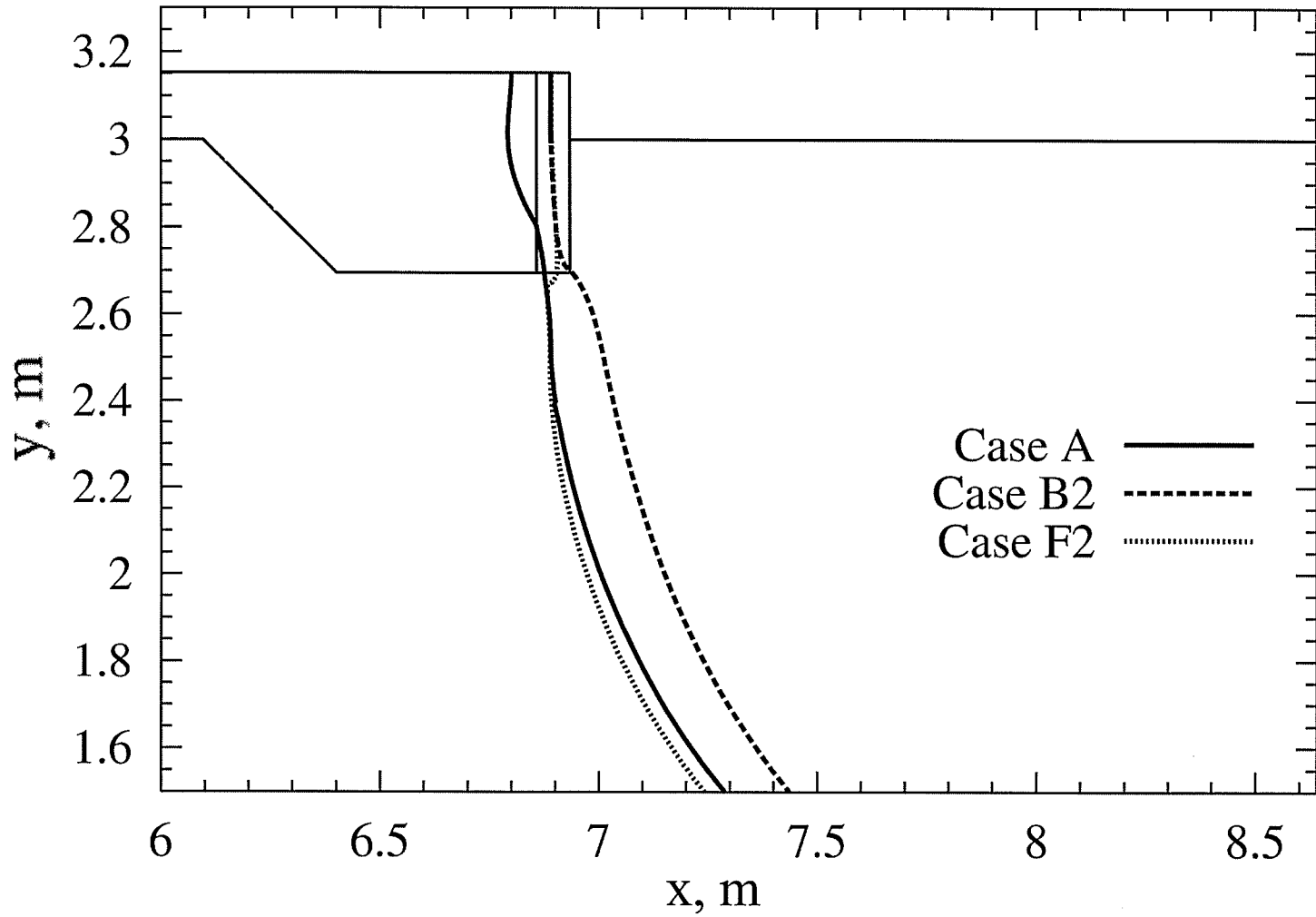


Figure 6.11 Steady state zero isotherm line results for Cases A, B2 and F2

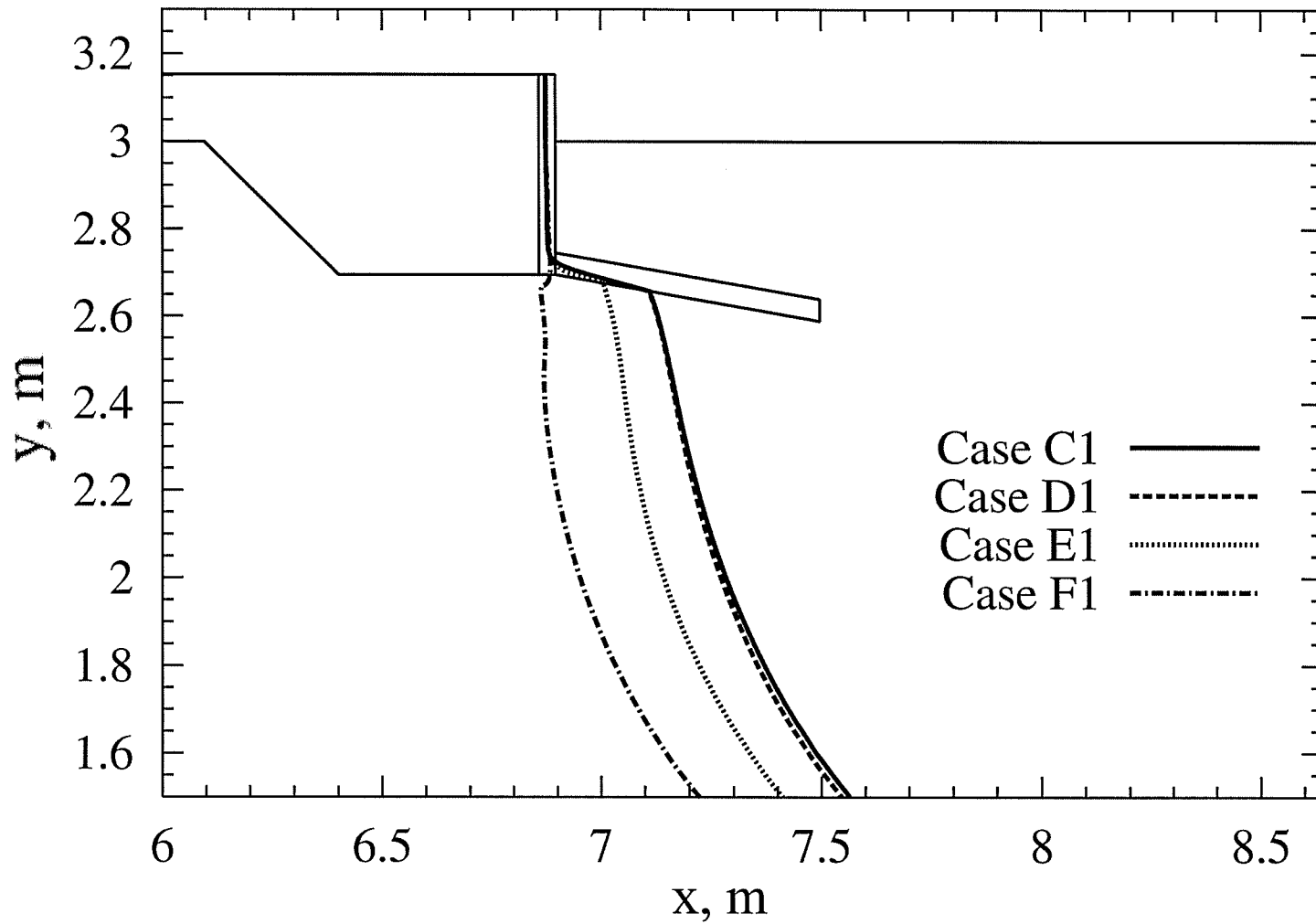


Figure 6.12 Steady state zero isotherm line results for Cases C1, D1, E1 and F1

6.3 Transient Results

6.3.1 Cases Studied

A subset of the steady state test matrix shown in Table 6.5 was used in the transient analysis. Key cases that showed significant results in the steady state analysis were selected for the transient analysis. Nine cases that study the major trends found in this research are shown in Table 6.7. Table 6.7 uses the same nomenclature as that explained in the steady state section for Table 6.5.

Table 6.7 Transient cases studied

	IE1	IE2	IS1	IS2	IS3	IS4	IC	IF
A								
B1	X							
B2		X						
C1	X		X					
C5		X	X					
D1	X		X				X	
E1	X		X				X	X
F1	X						X	X
F2		X					X	X

6.3.2 Grade Level Temperature Boundary Conditions

The results for the above cases were obtained with a transient boundary condition placed at the top ground surface. This transient boundary condition was obtained through a simple harmonic curve fit using the least squares method from soil temperature data at various depths. The resulting equation as shown in Section 3.3 gives cyclic monthly values through out a period of a year. The surface temperature results for Winnipeg and Thompson soil temperature data are plotted in Figure 6.13 and Table 6.8.

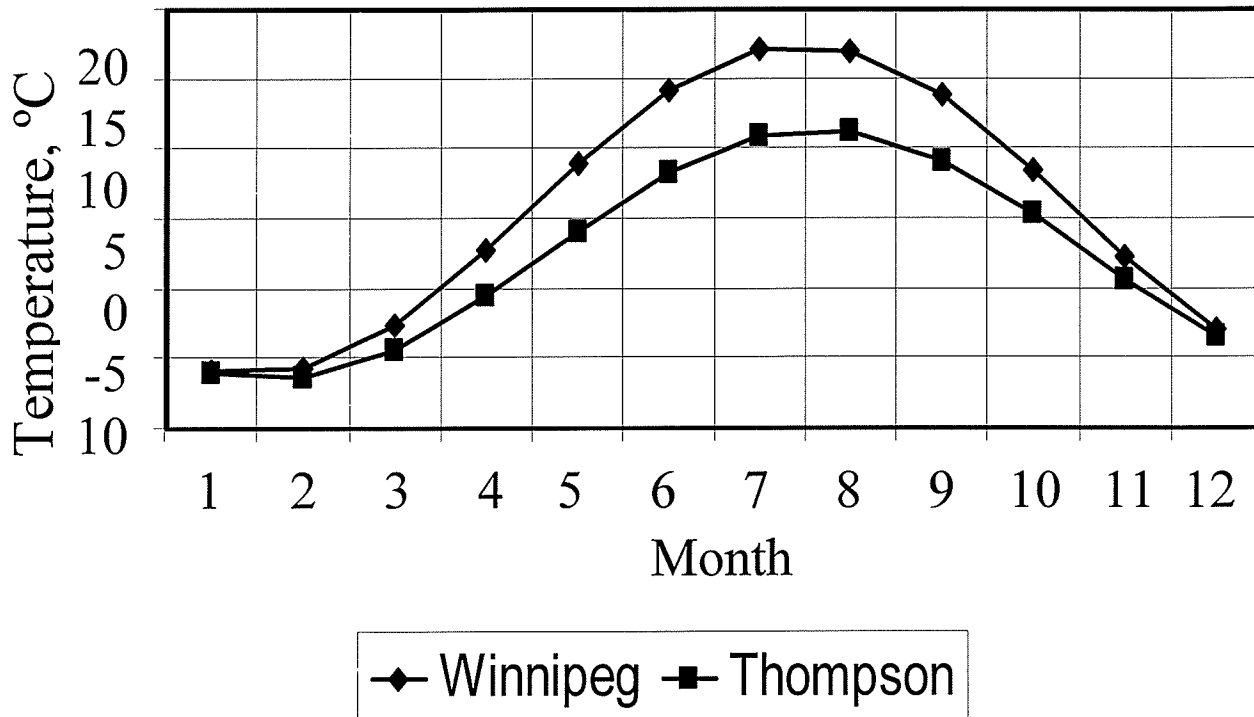


Figure 6.13 Surface soil temperature results for Winnipeg and Thompson

Table 6.8 Surface soil temperature for Winnipeg and Thompson

Month	Winnipeg °C	Thompson °C
(1) Jan	-5.94	-6.11
(2) Feb	-5.80	-6.42
(3) Mar	-2.61	-4.38
(4) Apr	2.78	-0.53
(5) May	8.91	4.09
(6) Jun	14.16	8.25
(7) Jul	17.10	10.83
(8) Aug	16.96	11.14
(9) Sep	13.77	9.10
(10) Oct	8.39	5.25
(11) Nov	2.25	0.63
(12) Dec	-2.99	-3.53

6.3.3 Domain and Solution Approach

The transient analysis was performed with a domain six metres in height. Figure 3.2 shows the dimension L3. This dimension was set to $L3 = 6.0$ m for grids used in the transient analysis. At 6-m depth the time variations of the outside boundary condition has negligible effect on the soil temperature. The percentage difference between the temperature at this depth and the average annual temperature is less than one percent. Using a grid with a depth of six metres allows the use of a constant soil temperature at the bottom boundary condition. In all the work presented here, steady periodic results were obtained in the fourth year of cyclic simulation. A time step of one month (2.592×10^6 seconds) was used.

6.3.4 Zero Temperature Isotherms

The zero degree Celsius temperature isotherms are very important in determining the location and the amount of frost penetration. Assessing the isotherm location is very important because an objective of foundation design and insulation placement is to avoid frost heave. Figure 6.14 to Figure 6.22 show the time variation of the zero isotherms to enable tracking the change of the zero temperature isotherms for Winnipeg throughout one complete cycle (equivalent of one year). Monthly results are obtained for the zero temperature isotherms, since monthly time steps were taken in the numerical simulation. The results shown in Figure 6.14 to Figure 6.19 will be discussed first, followed by a discussion of heat loss. The results from Figure 6.20 to Figure 6.22 will be discussed after that. The equivalent results for Thompson are described in a later section.

From Figure 6.14, one can see that the zero isotherms pass through part of the foundation for Winnipeg's Case A. This is better seen in Figure 6.14(b). Because Case A has no insulation, the foundation is exposed to very cold temperatures (under 0°C) all around its edge. This causes the foundation to experience large heat losses. However, the results show that none of the zero isotherms penetrate under the foundation corner. Although

this is true, Case A is not a desirable case because of the large heat transfer losses that occur.

In the analysis performed for Winnipeg, only the months of January, February, March and December have zero-degree isotherms. The soil is frozen in the region above the zero isotherm line. For example, in Figure 6.14, the soil first has a frozen region in December. The depth of this frozen region is about 40 cm at the right boundary. At the right boundary the effects of the slab on the soil temperature distribution are almost negligible. This is the direct result of placing the right boundary condition far enough where the soil behaves like a semi-infinite medium.

Also, Figure 6.14 shows that in January, the depth of frozen soil has increased to approximately 90 cm at the right boundary. The deepest penetration occurs in February where the depth of frozen soil is predicted to be greater than 1.2 m. The soil starts to warm in March. In this month the depth of frost is still the same as in February but the zero degree line starts to move upwards showing less frozen ground near the foundation. By April all the soil is above zero degrees Celsius. Figure 6.14(b) shows the zero isotherm lines pass through part of the slab.

Figure 6.15, shows the zero temperature isotherms for Case B1 for Winnipeg. Case B1 has insulation only on the vertical side edge. The figure shows that the zero isotherms do not pass through any part of the foundation. The isotherms meet the edge insulation along the side edge of the foundation and go straight up as seen in Figure 6.15 (b). The edge insulation prevents the zero or lower degree temperature isotherms from passing through the side of the foundation and moves them outside of the concrete. Because the foundation is protected from cold temperatures, lower heat losses occur, as discussed shortly.

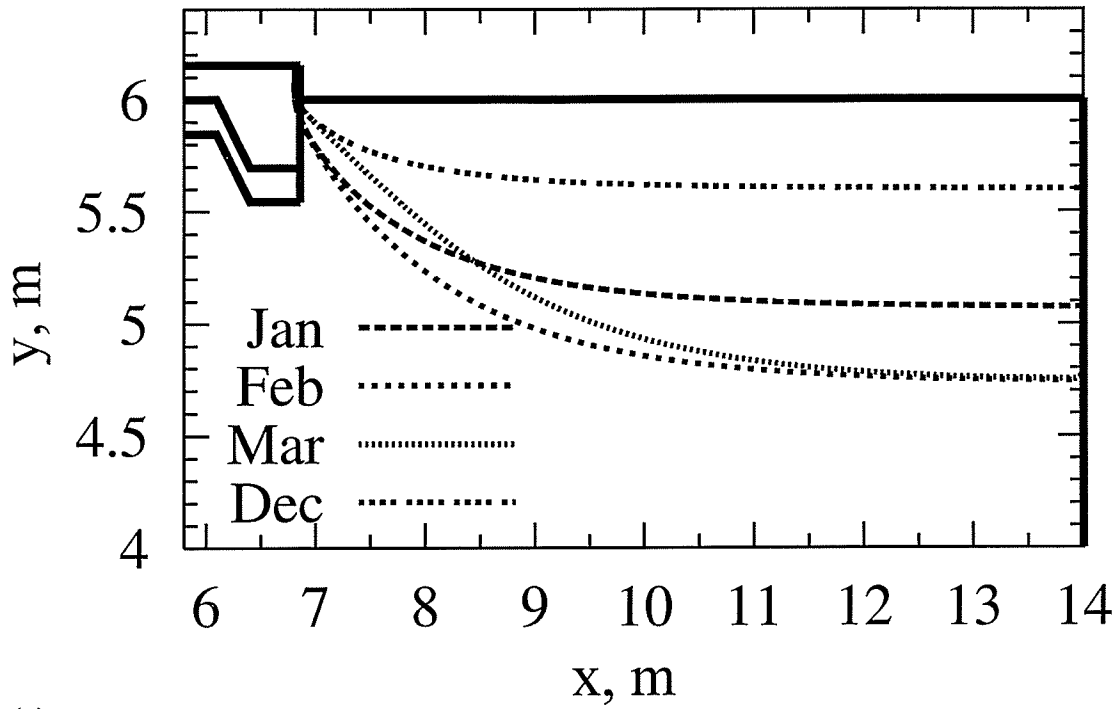
It is also noted from Figure 6.15 (b) that the zero isotherms meet the side edge of the foundation near the base of the thickened-edge. Although these zero isotherms are close to the foundation corner, it seems unlikely that they would go under the foundation,

except for the case of a rare, extremely lengthy cold period. Also noted are the frozen depths seen on the vertical axis at the right boundary. The depth of frozen soil in each month, are always constant for all cases that the Winnipeg boundary condition was applied. This is further evidence that the soil far away from the foundation is unaffected.

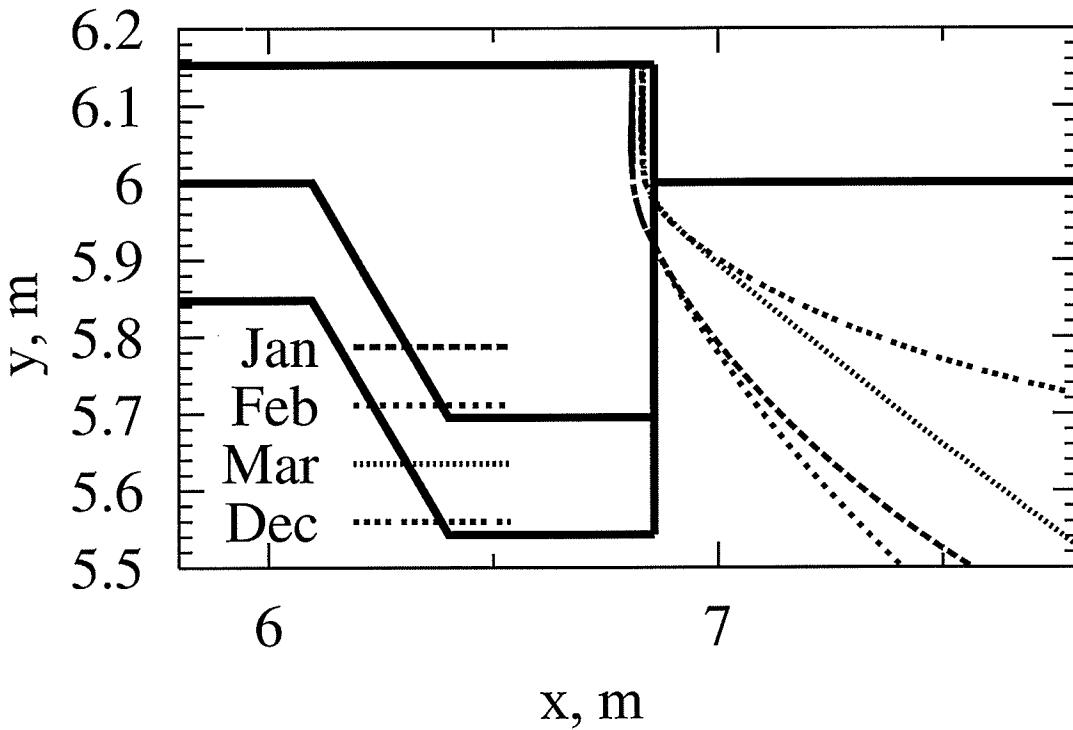
Case C1 zero isotherm results are presented in Figure 6.16. The figure shows that the foundation is protected with edge and skirt insulation. The skirt insulation acts as a guide for the zero isotherms to run through. All zero isotherm lines (December to March) join the skirt insulation at its end or through its upper surface, as seen from Figure 6.16 (b). The zero isotherms follow a path that goes through the skirt insulation and up the vertical side edge. If the skirt insulation were positioned higher, the zero isotherms would be even further from the insulation corner. The skirt insulation must be placed to ensure that it has a layer of soil above it for protection against the elements. In addition, it will give the home owner the ability to plant small root plants next to the wall for aesthetic reasons.

The zero isotherm lines for Cases D1 and E1 in Figure 6.17 and Figure 6.18 look very similar to that of Case C1. No significant difference is seen qualitatively. The difference in these cases will be seen in the heat losses measured. These will be discussed shortly.

Figure 6.19, shows the zero isotherms for Case F1. In this case, the foundation is insulated on the side edge, under the center slab and under the footing. Since the skirt insulation is not present, the zero isotherms join along the edge insulation. The same effect was seen in Case B1. However, the zero isotherms have a deeper penetration than those observed for Case B1. That is, there is a higher threat that the zero isotherms could go under the foundation corner in the case of a very cold winter.

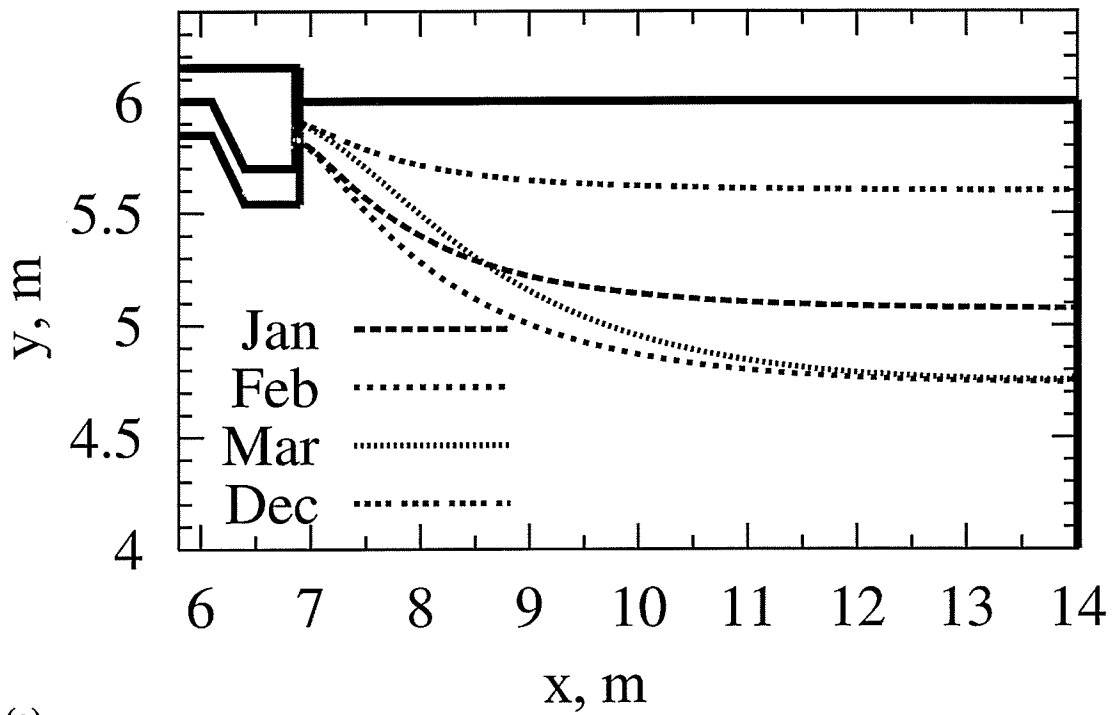


(a)

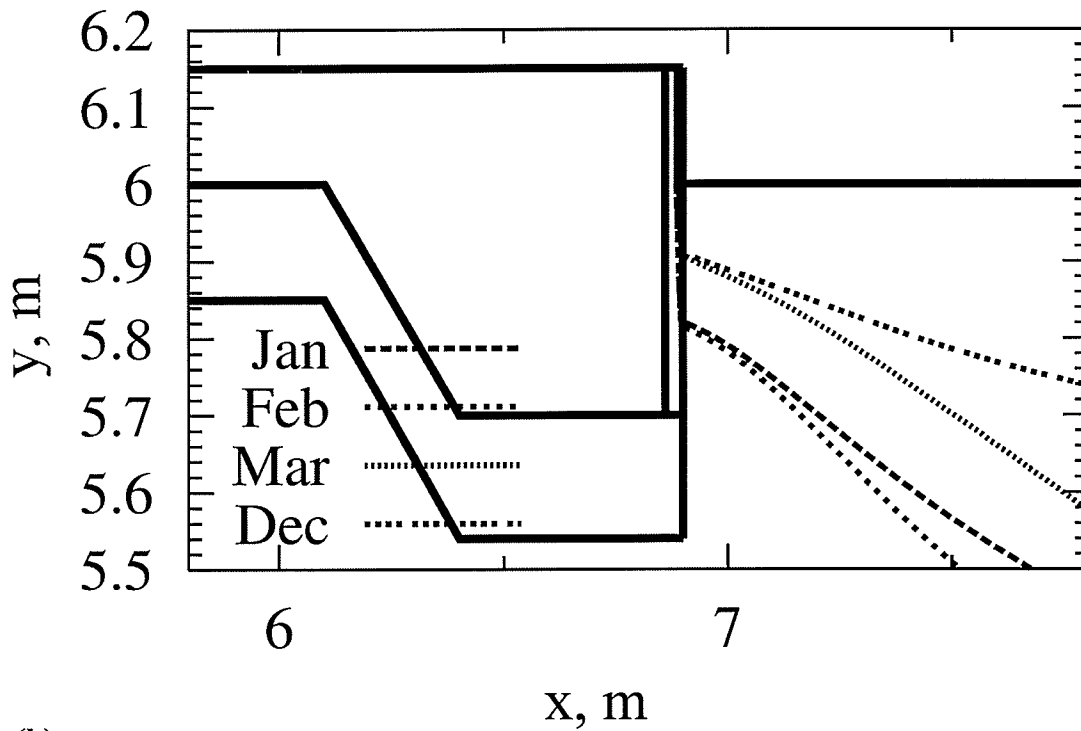


(b)

Figure 6.14 Winnipeg zero temperature isotherms for Case A, (a) full domain, (b) detailed view of foundation corner



(a)



(b)

Figure 6.15 Winnipeg zero temperature isotherms for Case B1, (a) full domain, (b) detailed view of foundation corner

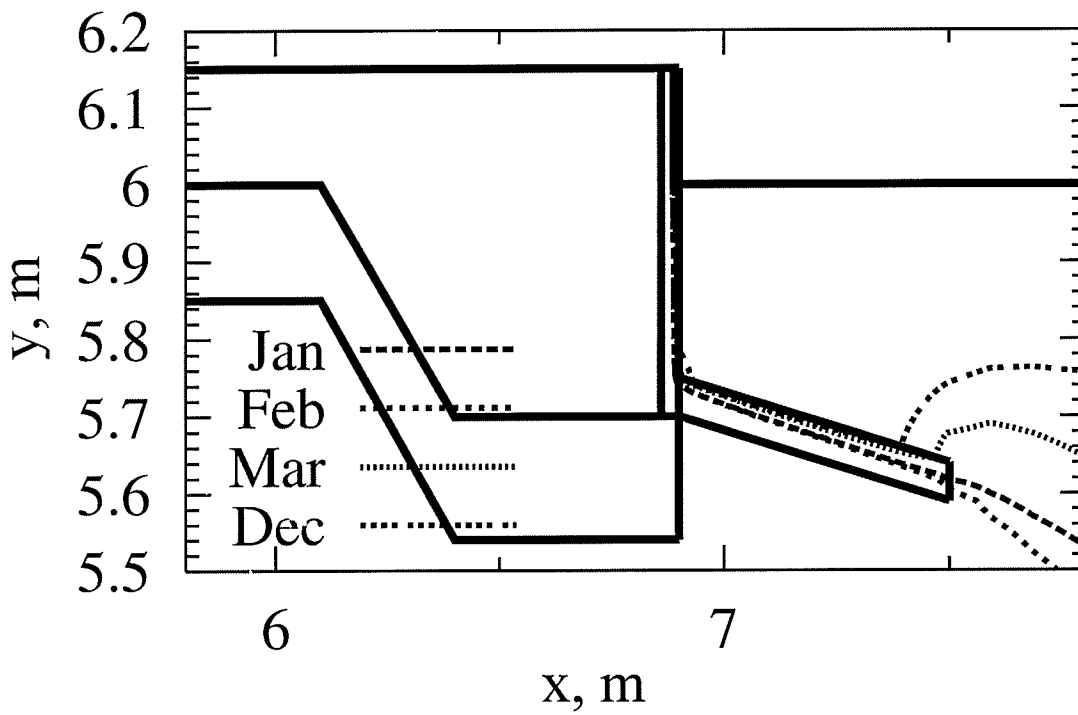
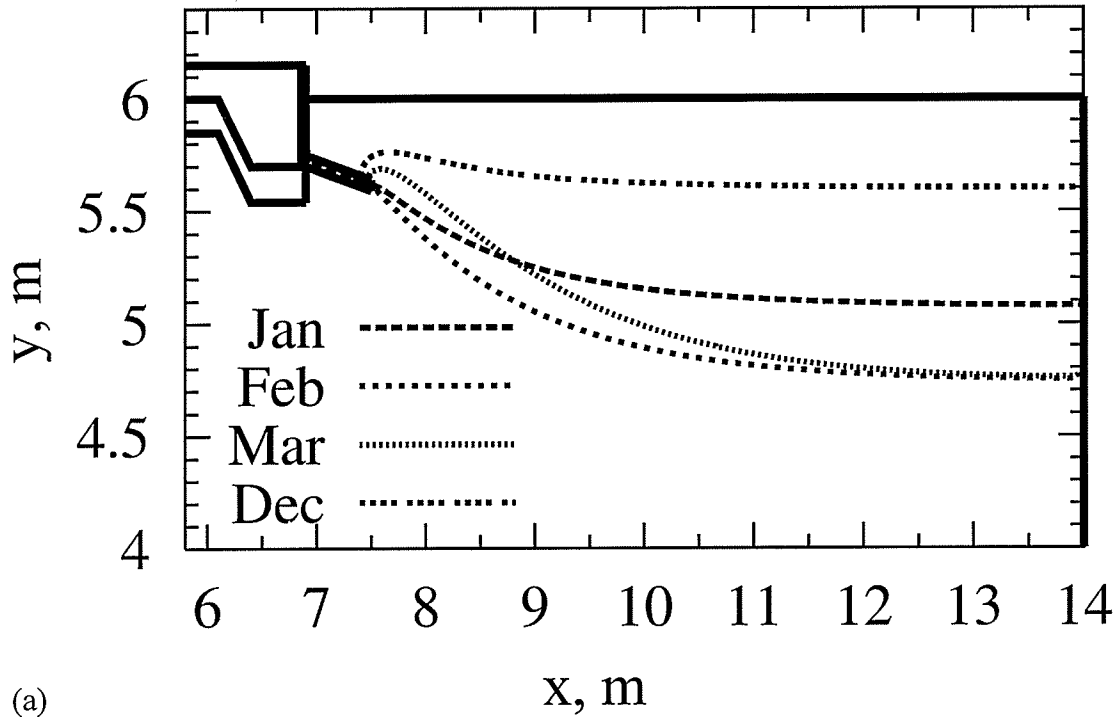
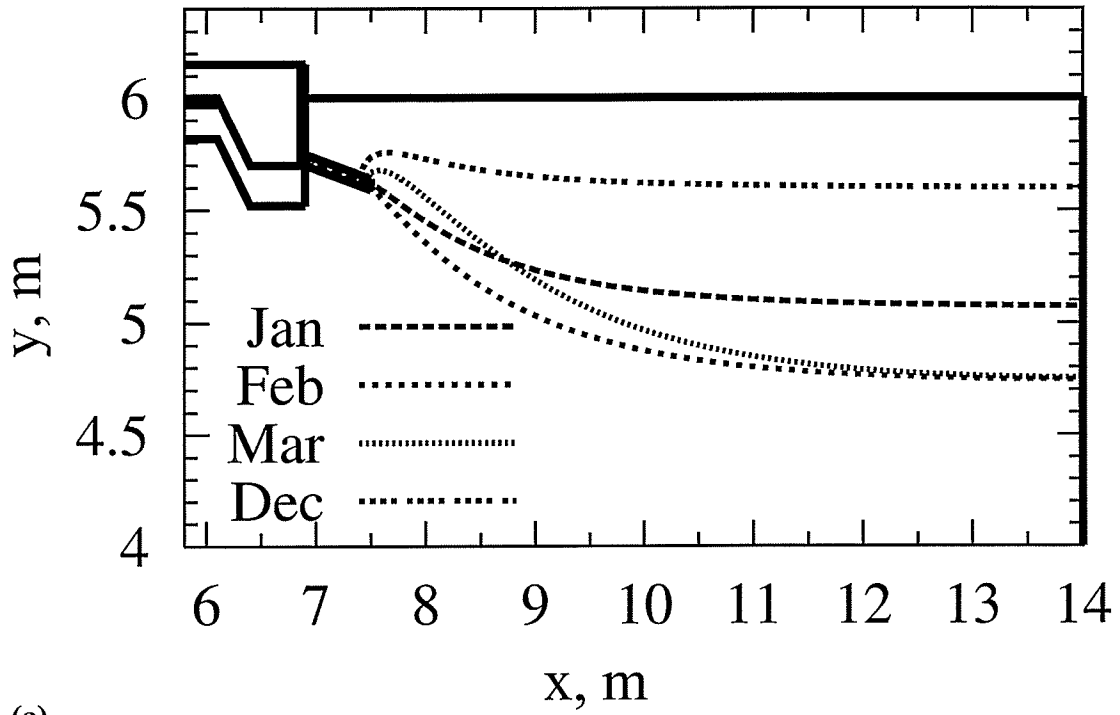
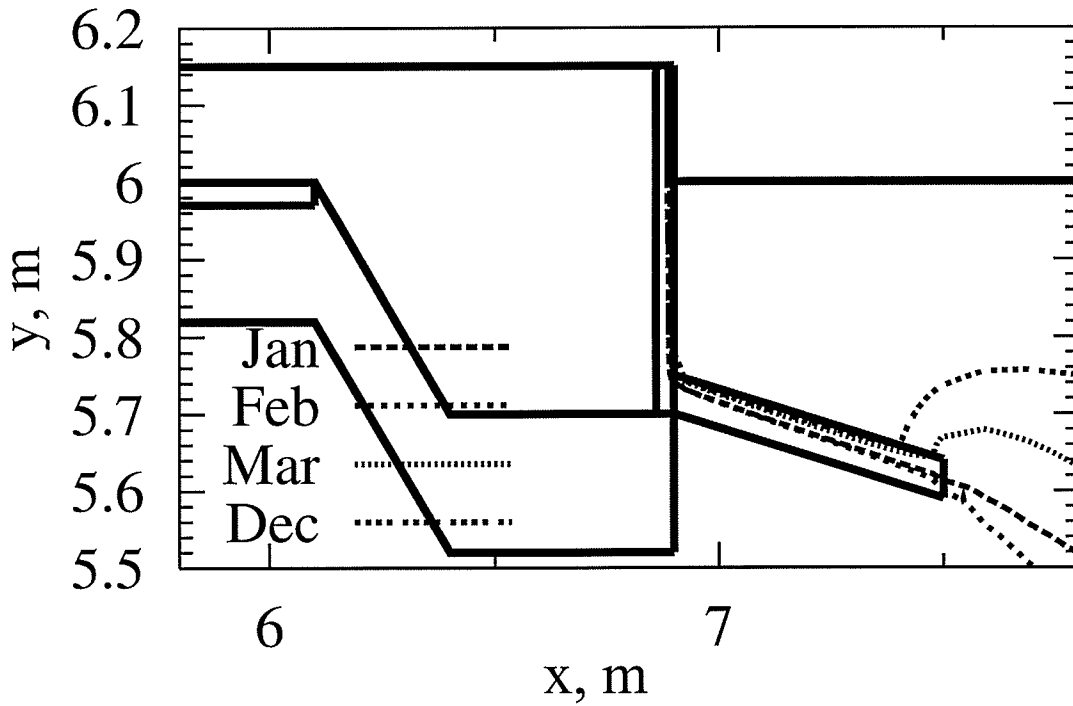


Figure 6.16 Winnipeg zero temperature isotherms for Case C1, (a) full domain, (b) detailed view of foundation corner

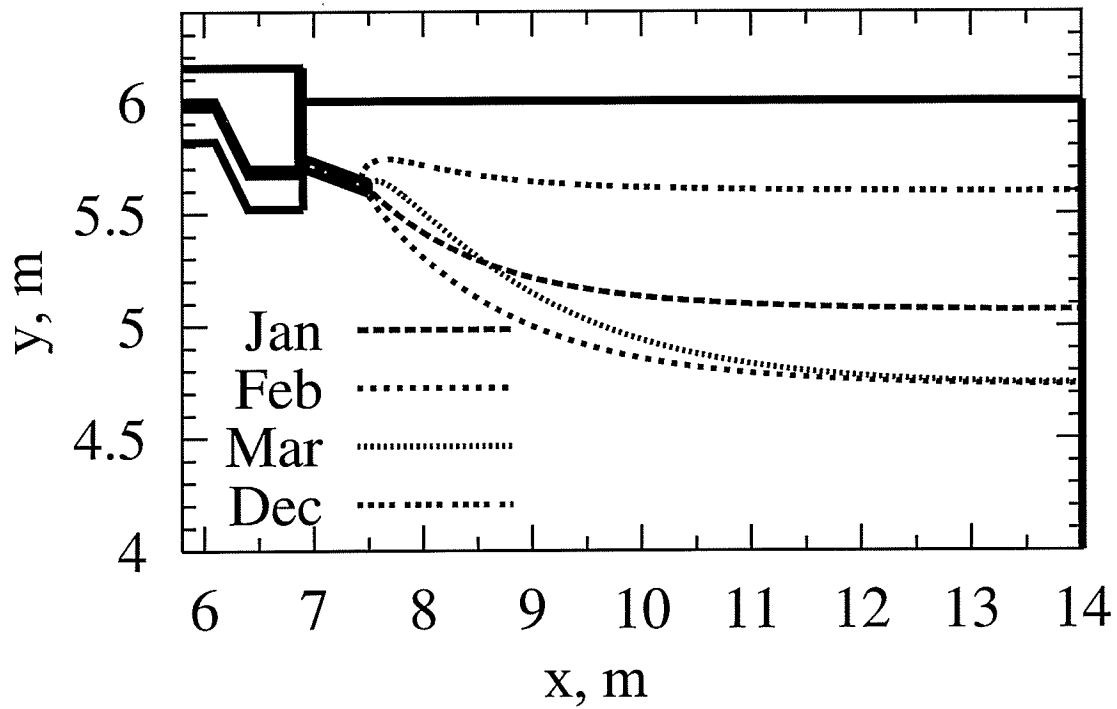


(a)

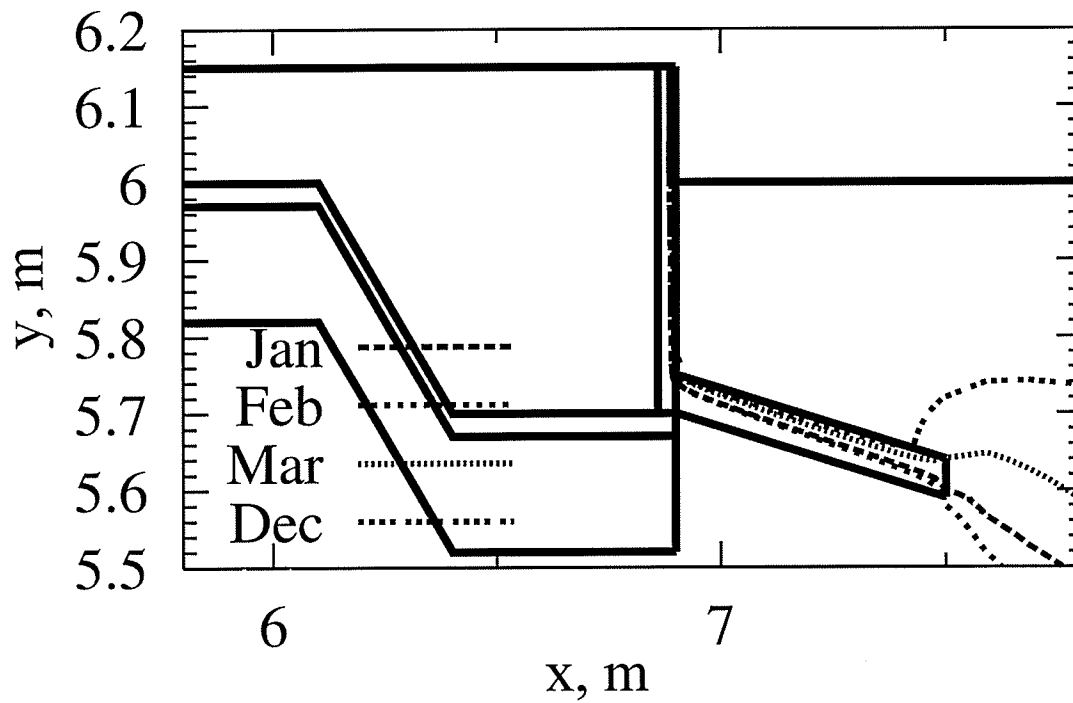


(b)

Figure 6.17 Winnipeg zero temperature isotherms for Case D1, (a) full domain, (b) detailed view of foundation corner

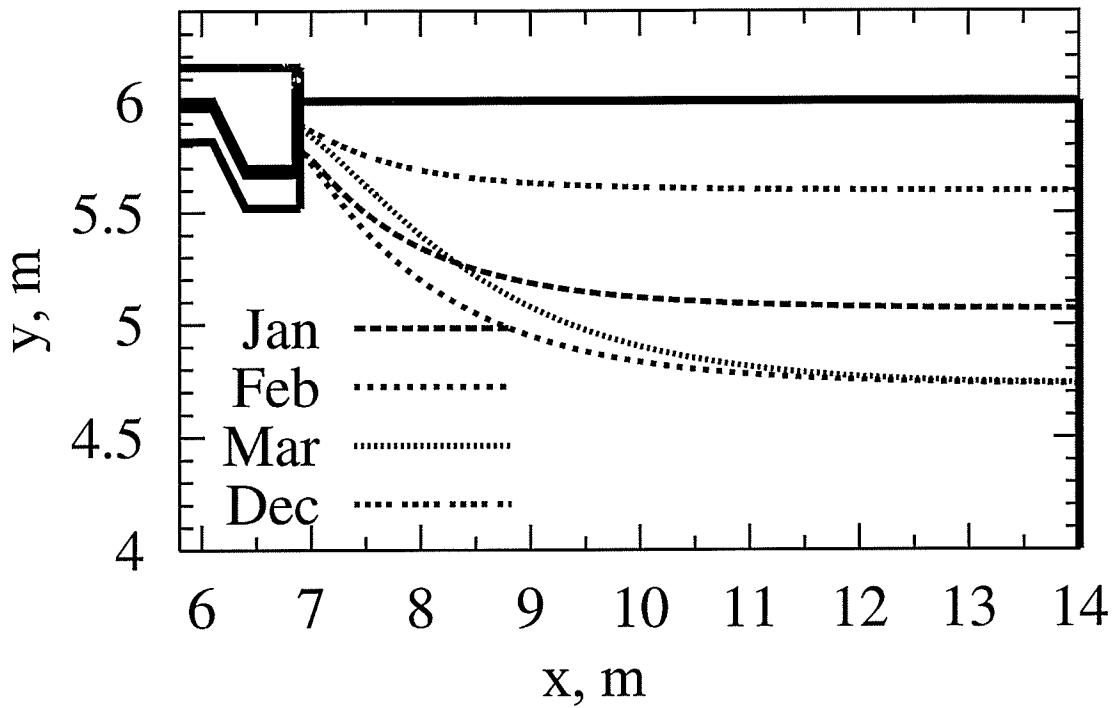


(a)

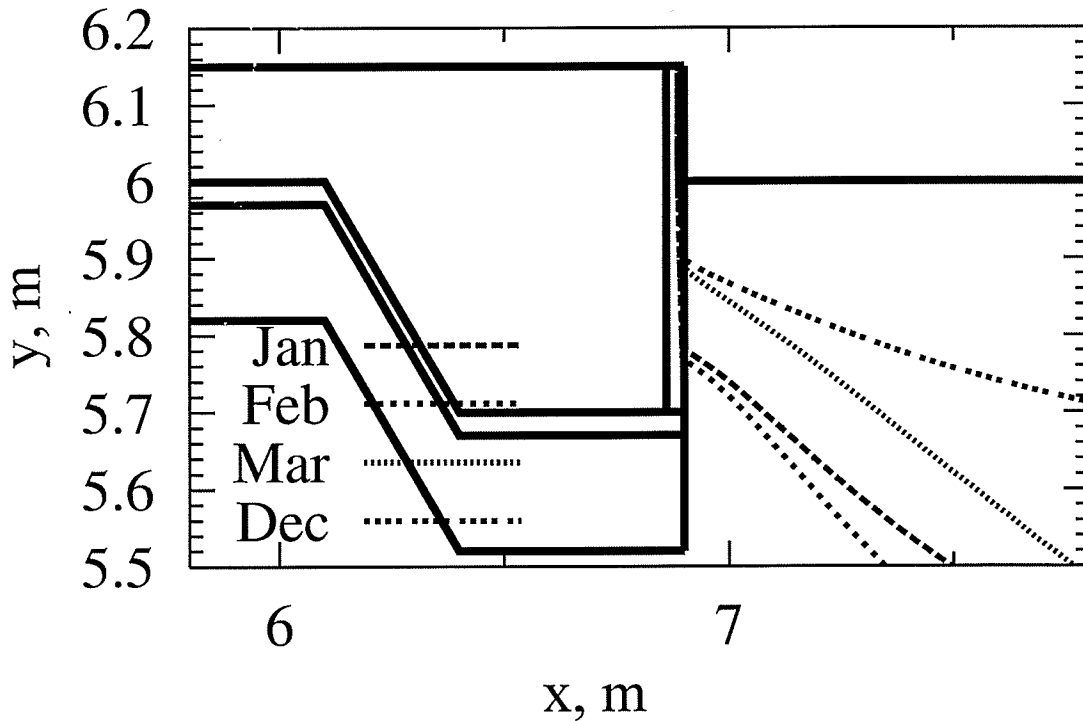


(b)

Figure 6.18 Winnipeg zero temperature isotherms for Case E1, (a) full domain, (b) detailed view of foundation corner



(a)



(b)

Figure 6.19 Winnipeg zero temperature isotherms for Case F1, (a) full domain, (b) detailed view of foundation corner

6.3.5 Summary of Transient Analysis Heat Loss

The energy loss per unit depth in kWh values from the top slab surface (Q_i) in the domain shown in Figure 1.2 are calculated for Winnipeg and summarized in Table 6.9 and Table 6.10. The values obtained for Thompson are summarized in Table 6.11 and Table 6.12. Note that the values are for the domain simulated which is for half the slab. The tables display the results for the different test cases for Winnipeg and Thompson. The values shown include the monthly and annual per unit depth heat loss values. One can see that throughout all the months of the year the heat transfer is positive. This means that in every month the house experiences heat losses through the foundation.

In looking at the annual heat transfer loss from the tables, one can see that, in general, increasing the amount of insulation decreases the heat loss from the house, especially when looking from Cases A through to Case F1. Although a certain amount of heat loss from the house is beneficial to maintain the zero isotherms as far as possible, the objective is to find the most minimal amount of heat loss that achieves this. It is for this reason that various cases were simulated. Cases A and B1 through F1 demonstrate the variation in insulation placement. Cases B2, C5 and F2 demonstrate the variation in the amount of insulation.

Note that the values of heat loss for Table 6.9 through Table 6.12 are for half the slab which is the domain simulated. To obtain the heat loss for the full two-dimensional slab, values need to be multiplied by two.

Table 6.9 Monthly and annual heat loss for Winnipeg, Cases A, B1, C1, D1, E1 and F1

Winnipeg		Q _i [kWh/m]				
Case	A	B1	C1	D1	E1	F1
Jan	49.09	28.68	25.85	22.90	20.77	21.95
Feb	50.04	29.64	26.71	23.65	21.33	22.66
Mar	47.15	29.20	26.51	23.43	21.09	22.33
Apr	41.11	27.45	25.35	22.28	20.17	21.12
May	33.65	24.87	23.53	20.60	18.74	19.39
Jun	26.73	22.15	21.50	18.74	17.23	17.55
Jul	22.14	20.02	19.85	17.29	16.01	16.08
Aug	21.17	19.07	18.96	16.54	15.47	15.41
Sep	24.11	19.54	19.18	16.79	15.72	15.73
Oct	30.12	21.26	20.33	17.85	16.60	16.85
Nov	37.62	23.85	22.17	19.57	18.03	18.63
Dec	44.53	26.53	24.18	21.39	19.56	20.45
Annual	427.47	292.25	274.10	241.03	220.72	228.16

Table 6.10 Monthly and annual heat loss for Winnipeg, Cases B2, C5 and F2

Winnipeg		Q _i [kWh/m]	
Case	B2	C5	F2
Jan	26.99	24.16	20.16
Feb	27.94	25.01	20.84
Mar	27.66	25.02	20.70
Apr	26.27	24.18	19.87
May	24.14	22.78	18.58
Jun	21.80	21.11	17.08
Jul	19.89	19.68	15.91
Aug	18.91	18.84	15.23
Sep	19.17	18.87	15.33
Oct	20.57	19.68	16.12
Nov	22.72	21.05	17.44
Dec	25.08	22.74	18.90
Annual	281.12	263.12	216.17

Table 6.11 Monthly and annual heat loss for Thompson, Cases A, B1, C1, D1, E1 and F1

Thompson		Q _i [kWh/m]				
Case	A	B1	C1	D1	E1	F1
Jan	38.74	18.05	16.65	16.04	15.08	15.76
Feb	39.48	18.44	16.99	16.34	15.33	16.04
Mar	37.74	18.25	16.85	16.17	15.12	15.85
Apr	33.91	17.47	16.23	15.56	14.54	15.21
May	29.06	16.31	15.31	14.65	13.70	14.24
Jun	24.52	15.09	14.31	13.66	12.83	13.22
Jul	21.40	14.09	13.52	12.91	12.17	12.48
Aug	20.59	13.58	13.16	12.51	11.83	12.09
Sep	22.29	13.75	13.23	12.63	11.98	12.23
Oct	26.05	14.49	13.75	13.21	12.55	12.84
Nov	30.85	15.63	14.66	14.04	13.33	13.76
Dec	35.42	16.83	15.62	14.96	14.13	14.70
Annual	360.05	192.00	180.28	172.68	162.56	168.43

Table 6.12 Monthly and annual heat loss for Thompson, Cases B2, C5 and F2

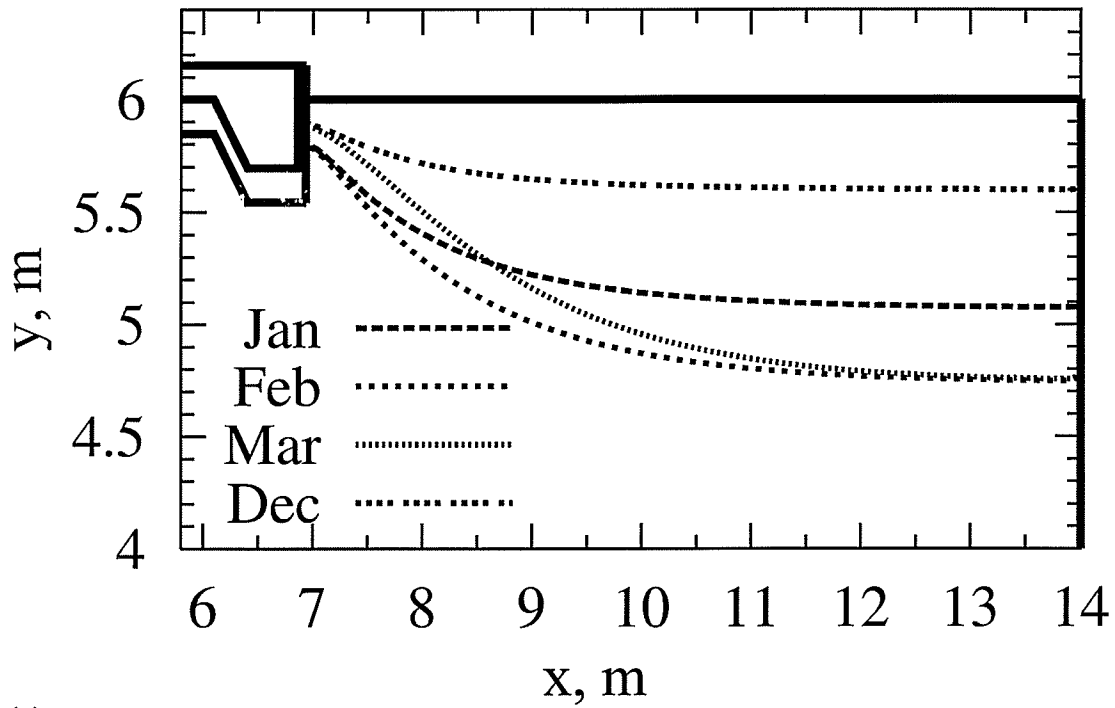
Thompson		Q _i [kWh/m]	
Case	B2	C5	F2
Jan	16.54	15.07	14.07
Feb	16.94	15.37	14.31
Mar	16.85	15.31	14.28
Apr	16.26	14.96	13.87
May	15.38	14.28	13.20
Jun	14.38	13.57	12.47
Jul	13.56	12.92	11.87
Aug	13.10	12.57	11.55
Sep	13.16	12.59	11.59
Oct	13.66	12.92	11.91
Nov	14.51	13.51	12.53
Dec	15.47	14.22	13.24
Annual	179.80	167.30	154.89

6.3.6 Effect of Edge Insulation

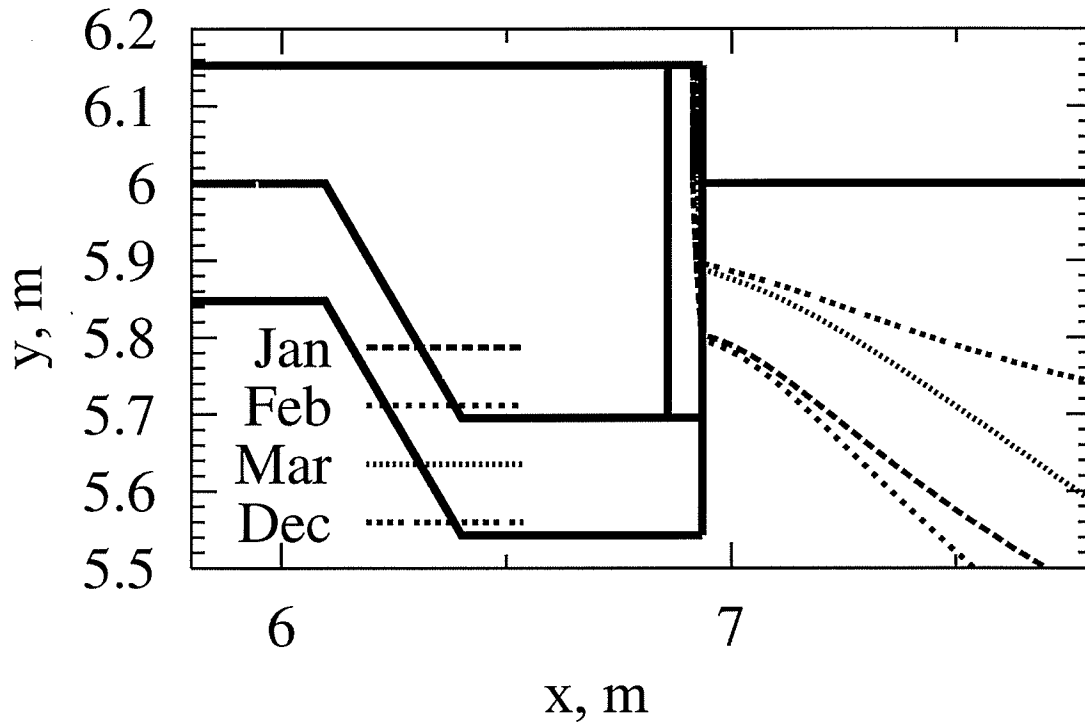
The edge thickness was increased and its effect was investigated from the pair of Cases B1 and B2, C1 and C5 as well as F1 and F2 as shown in Table 6.7. These pairs of cases have everything in common except for the thicker edge. The zero isotherms plots for Cases B2, C5 and F2 are found in Figure 6.20 through Figure 6.22, respectively. These plots show the domain wire frame with a thicker insulation edge. The domain wire frame of the foundation is plotted to scale in the figures. The insulation edge increased to E2 corresponds to 7.6 cm (3 in) in insulation thickness. The previous cases with a side edge of E1 have only 3.8 cm (1.5 in) in thickness.

Doubling the edge insulation thickness made very little difference in the zero isotherm plots when comparing both Cases B1 and B2 (Figure 6.15 and Figure 6.20), and Cases C1 and C5 (Figure 6.16 and Figure 6.21). The vertical location of the isotherm lines is unchanged. Horizontally, the lines are displaced to the edge of the extra 3.8 cm (1.5 in) of insulation. To compare among these pairs of cases the zero isotherm plots were simply placed one on top of the other and aligning them to the edge of the vertical insulation. When doing so, very minimal displacement was noticed. Looking at Table 6.9 and Table 6.10, the results among these two pair of cases show a small decrease in the heat loss. Between Cases B1 and B2 there is a 3.96% reduction. Between Cases C1 and C5 there is a 4.17% reduction.

Some difference is seen in the zero isotherm line plots for Cases F1 and F2 shown in Figure 6.19 and Figure 6.22. When comparing these plots, the difference noted was in the location where the zero isotherms touch the side edge. The zero isotherms touch lower for Case F2 than those of Case F1. Comparing results in Table 6.9 and Table 6.10 indicates that doubling the edge insulation to E2 had a 5.55% decrease in the heat loss experienced. The decrease in heat loss in Case F2 forced the zero isotherm lines to move closer to the foundation corner, posing a higher threat to permit frost to form closer to the foundation corner.



(a)



(b)

Figure 6.20 Winnipeg zero temperature isotherms for Case B2, (a) full domain, (b) detailed view of foundation corner

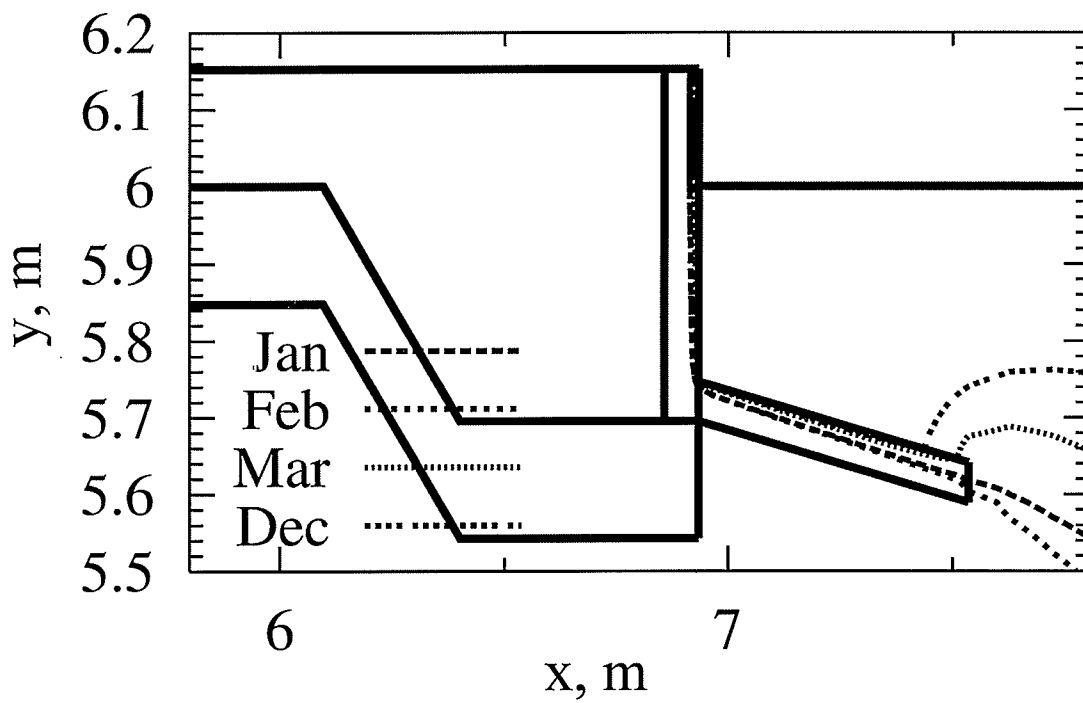
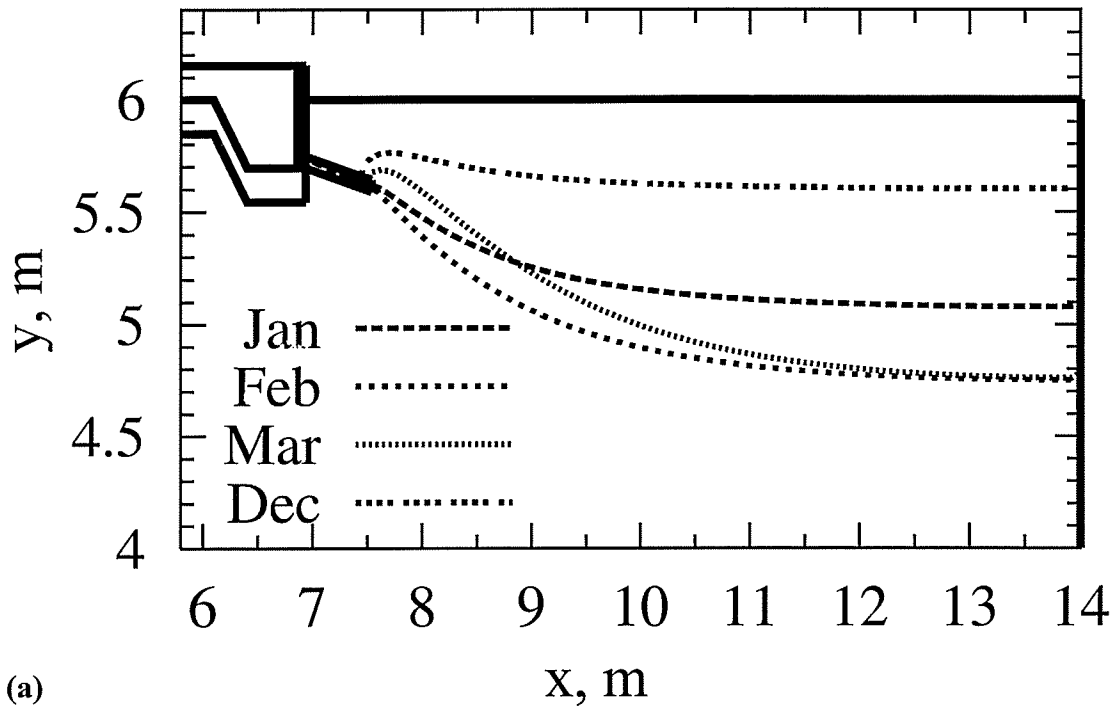


Figure 6.21 Winnipeg zero temperature isotherms for Case C5, (a) full domain, (b) detailed view of foundation

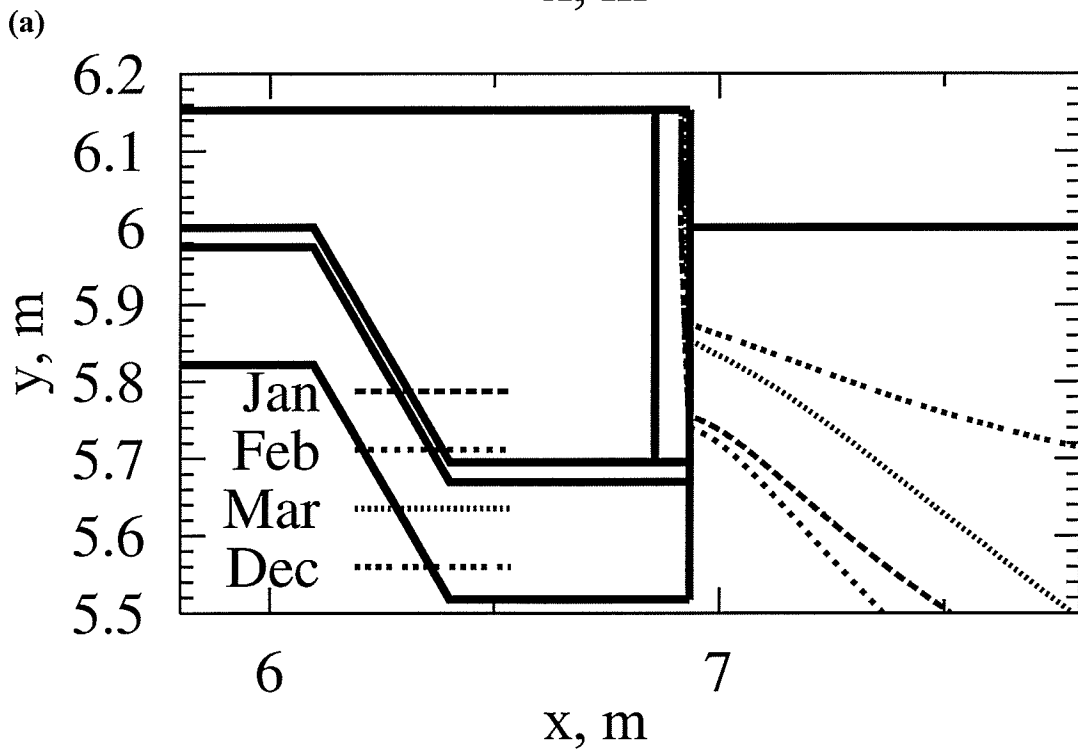
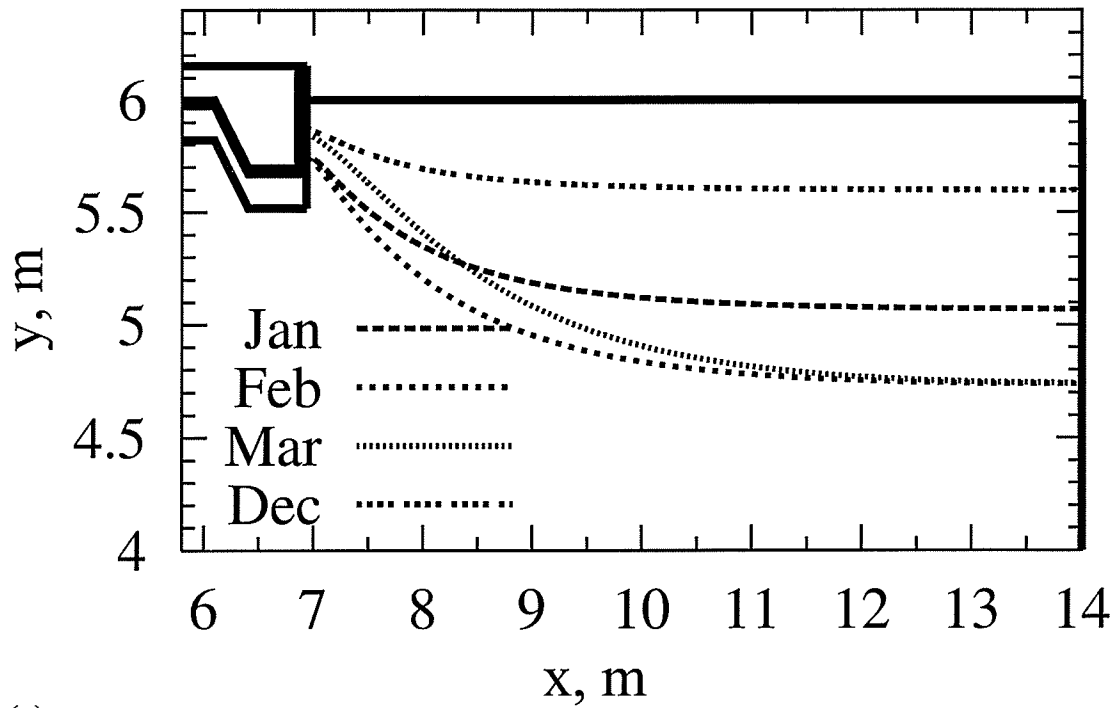


Figure 6.22 Winnipeg zero temperature isotherms for Case F2, (a) full domain, (b) detailed view of foundation corner

6.3.7 Zero Temperature Isotherms for Thompson

Figure 6.23 shows the zero isotherms obtained for Thompson for Case A. As in Case A for Winnipeg (Figure 6.14), the zero isotherms for Thompson pass through the foundation side edge. These results indicate that the foundation side is exposed to sub-zero temperatures and therefore large heat losses are experienced from the house. The large heat losses coming from the house, warm up the soil around the foundation. Consequently, in this case, none of the zero isotherms go under the foundation corner.

Figure 6.23 shows that in the analysis performed for Thompson, the winter months of January, February, March, April and December have zero-degree Celsius isotherms. The freezing season starts in December and achieves its deepest penetration in March. The soil starts to warm in April, where the depth of frost is still the same as in March but the freezing line starts to move upwards showing less frozen ground near the foundation.

Some trends are seen from this figure when comparing against Case A for Winnipeg in Figure 6.14. Thompson's soil remains frozen for a longer period of time than Winnipeg's, since no zero isotherms exist in April for Winnipeg. Thompson's soil not only remains frozen for a longer period of time, but the frost penetrates more slowly than for the same case in Winnipeg. These findings are consistent with the lower thermal diffusivity for Thompson. As seen from Table 3.2 the thermal diffusivity (α) for Winnipeg and Thompson are 4.0016×10^{-7} and 1.3786×10^{-7} m^2/s , respectively. The thermal diffusivities, as explained in more detail in Appendix A, were obtained from a curve fit of various under ground depths soil temperatures. The thermal diffusivity "measures the ability of a material to conduct thermal energy relative to its ability to store thermal energy" (Incropera and DeWitt, 1996). Therefore, Winnipeg's soil with larger soil α , responds quickly to changes in its environment, while Thompson's soil with a smaller soil α , responds more sluggishly, taking longer to reach a new equilibrium condition.

Figure 6.23 shows shallower frost penetration depths for the months January and February. Since frost penetration is slower in Thompson, the deepest frost penetration occurs in March as opposed to the month of February for Winnipeg. However, the overall frost penetration for the freezing season is slightly deeper in Thompson, to slightly over 1.3 meters. This is the result of the lower outside air temperatures experienced in Thompson.

Figure 6.24 shows the zero temperature isotherms for Case B1 for Thompson. Case B1 has insulation only on the vertical side edge of the foundation. The figure shows that the zero isotherms do not pass through any part of the foundation. The isotherms intersect the edge insulation along the side edge of the foundation and go straight up as seen in Figure 6.24 (b). The edge insulation prevents zero degree temperature isotherms or isotherms of lower temperatures to pass through the side of the foundation. This will result in heat savings from the house as the heat flow is prevented to simply flow to the outside air. Also, energy is directed downward to avoid the freezing isotherm underneath the footing.

It is noted from Figure 6.24 (b) that the zero isotherms meet the side edge of the foundation near the base of the thickened-edge. This result was also seen in Case B1 for Winnipeg in Figure 6.15. As was argued for the Winnipeg's case, although the zero isotherms are close to the foundation corner, it seems unlikely that they would go under the foundation, except for the case of a rare, extremely lengthy cold period. In comparing Thompson freezing lines location to those of Winnipeg, one can notice that the lines lie higher than those of Winnipeg's for Case B1. Although the far right boundary the freezing depth is lower than Winnipeg's, at the foundation side edge the freezing lines do not penetrate as much as in the case for Winnipeg.

Case C1 zero isotherm results, presented in Figure 6.25, shows the foundation protected with edge and skirt insulation. The zero isotherms pass through the skirt insulation and up the vertical side edge. In the same way as Winnipeg's Case C1 in Figure 6.16, the skirt insulation acts as a guide for the zero isotherms to run through. In the discussion for

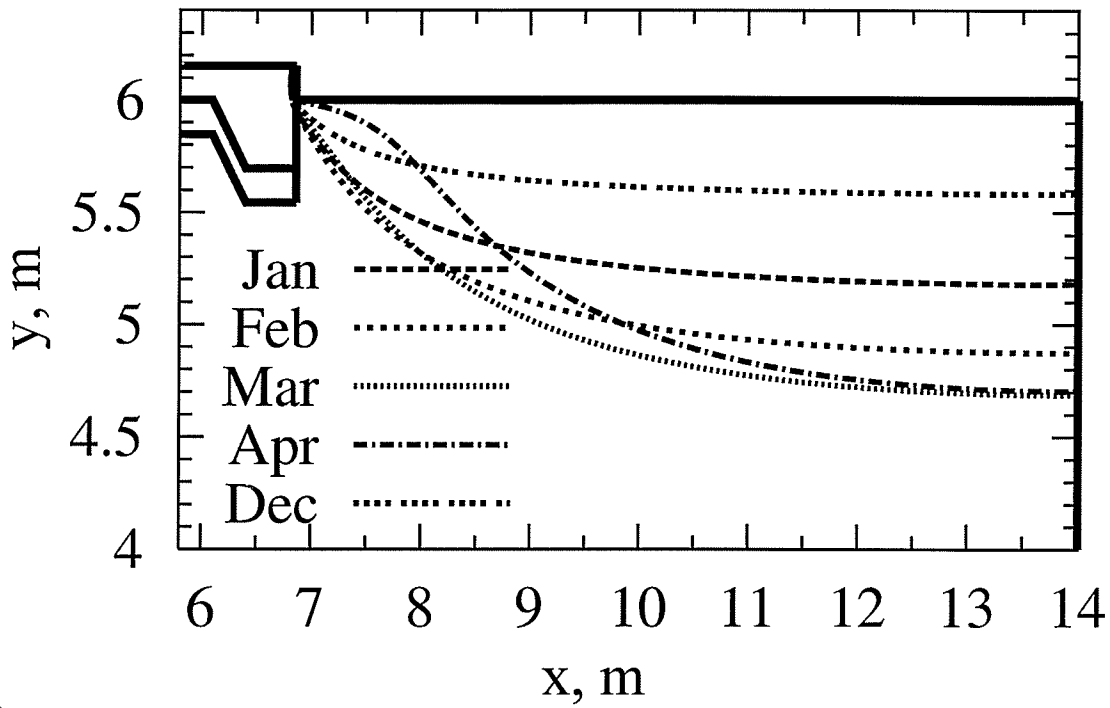
Winnipeg's Case C1 it was mentioned that if the skirt insulation were positioned higher, the zero isotherms would be even further from the insulation corner. However, the skirt insulation was positioned to allow for a protective layer of soil above it.

One main difference noted in Figure 6.25 the depth penetration of the freezing lines on the corner of the edge and skirt insulation. In this case, the freezing line does not penetrate as much, remaining away from the foundation corner. This is specially seen more intensely in the month of December when the freezing season starts. In this month the freezing line has not penetrated as much as it did in the Winnipeg's Case C1.

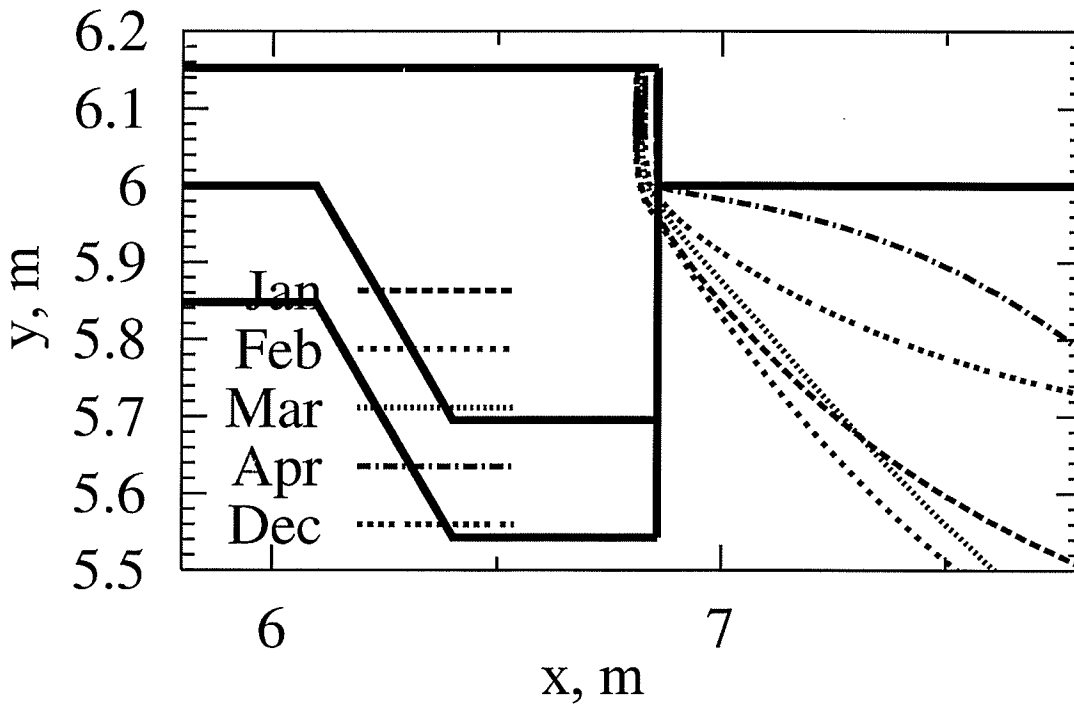
The zero isotherm lines for Thompson's Case D1 in Figure 6.26 look very similar to those of Case C1 in Figure 6.25. Insignificant differences are seen qualitatively in the isotherms. The insulation under the centre slab added in Case D1 reduced the heat loss by 4.2%.

The zero isotherms lines for Case E1 in Figure 6.27 display differences when compared to those of Case D1. The isotherm lines have penetrated deeper into the soil next to the foundation corner. This is attributed to the fact that the heat flow path directed towards the foundation corner in Case E1 is prevented from flowing through the footing due to insulation under the footing. This result in colder temperatures near the foundation corner, what may be considered an unacceptable risk of frost heave.

Figure 6.28 shows the zero isotherms for Case F1. In this case, the foundation is insulated on the side edge, under the center slab and under the footing. Since the skirt insulation is not present, the zero isotherms intersect along the edge insulation. The same effect was seen in Case B1. However, the zero isotherms have a deeper penetration than those observed for Case B1, as the heat flow path through the footing has been prevented through the placement of insulation under the footing. As was the case for Winnipeg, this case represents an undesirable potential for frost heave under the foundation corner, as the heat flow from the footing region into the soil is reduced significantly.

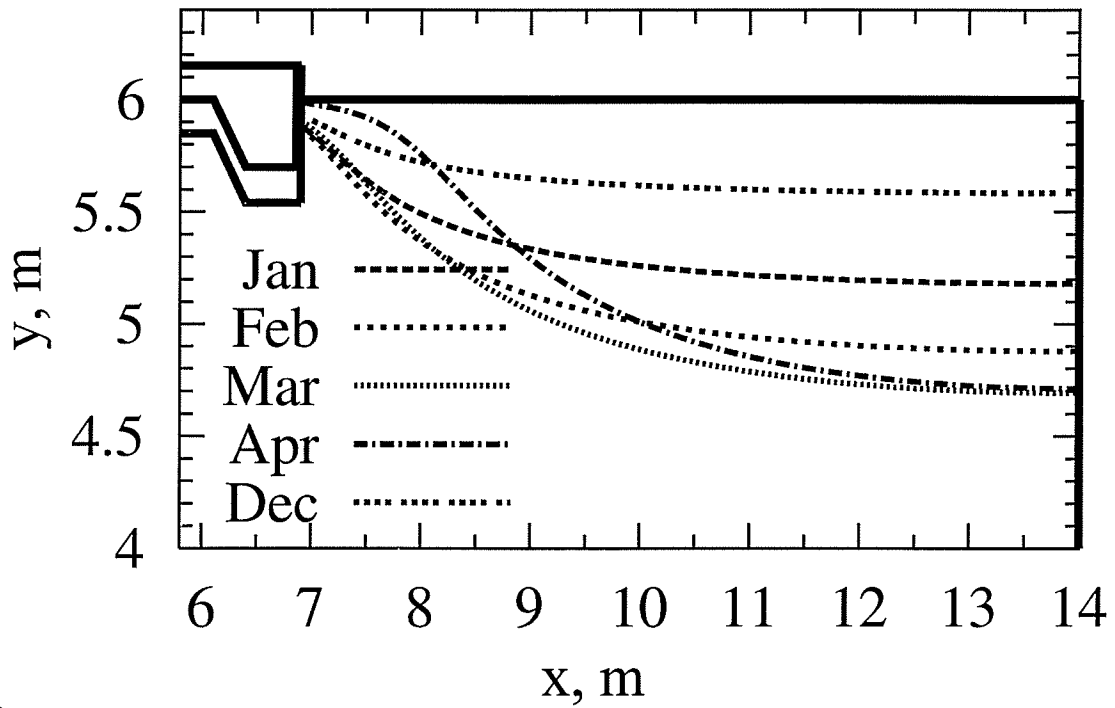


(a)

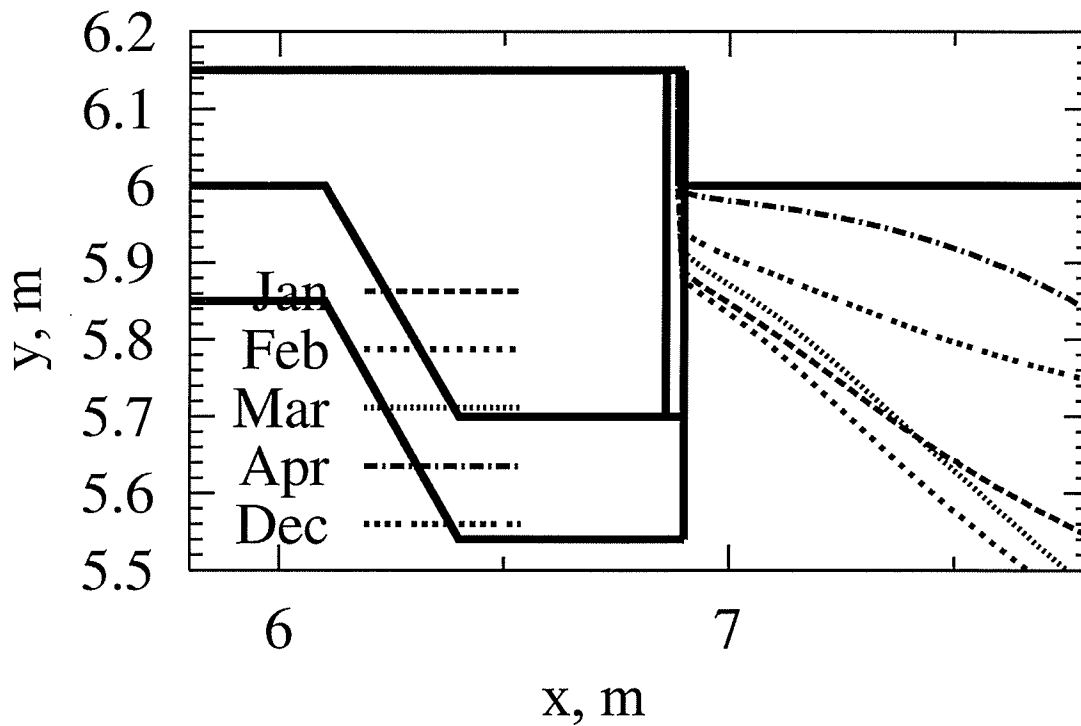


(b)

Figure 6.23 Thompson zero temperature isotherms for Case A, (a) full domain, (b) detailed view of foundation corner

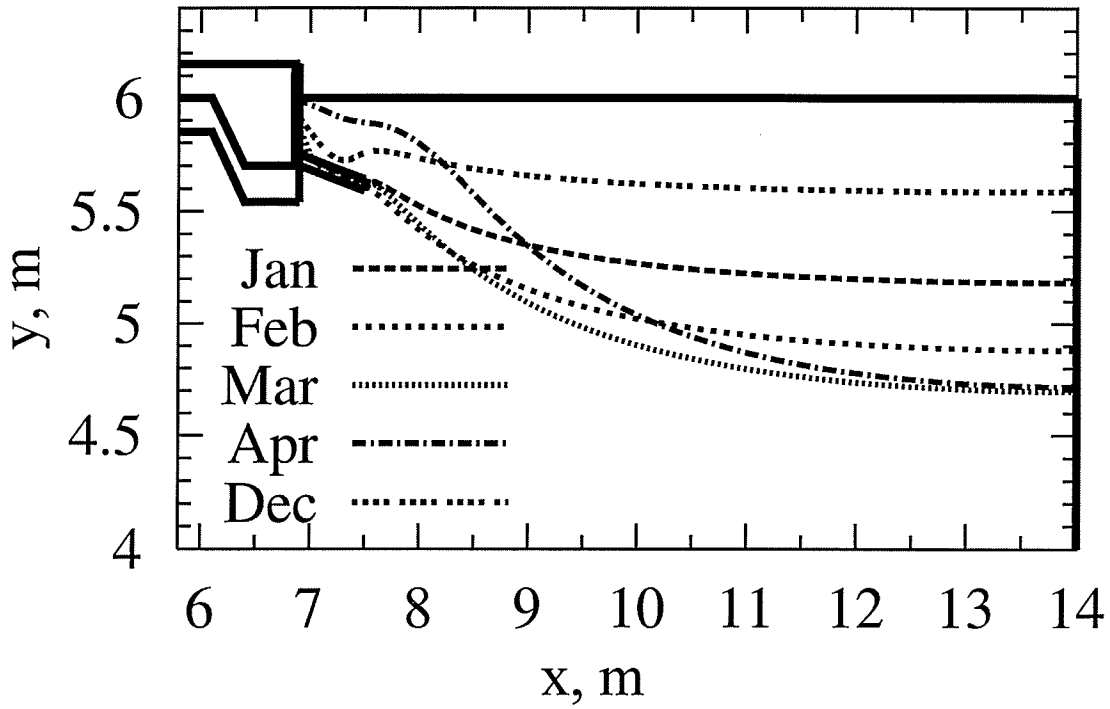


(a)

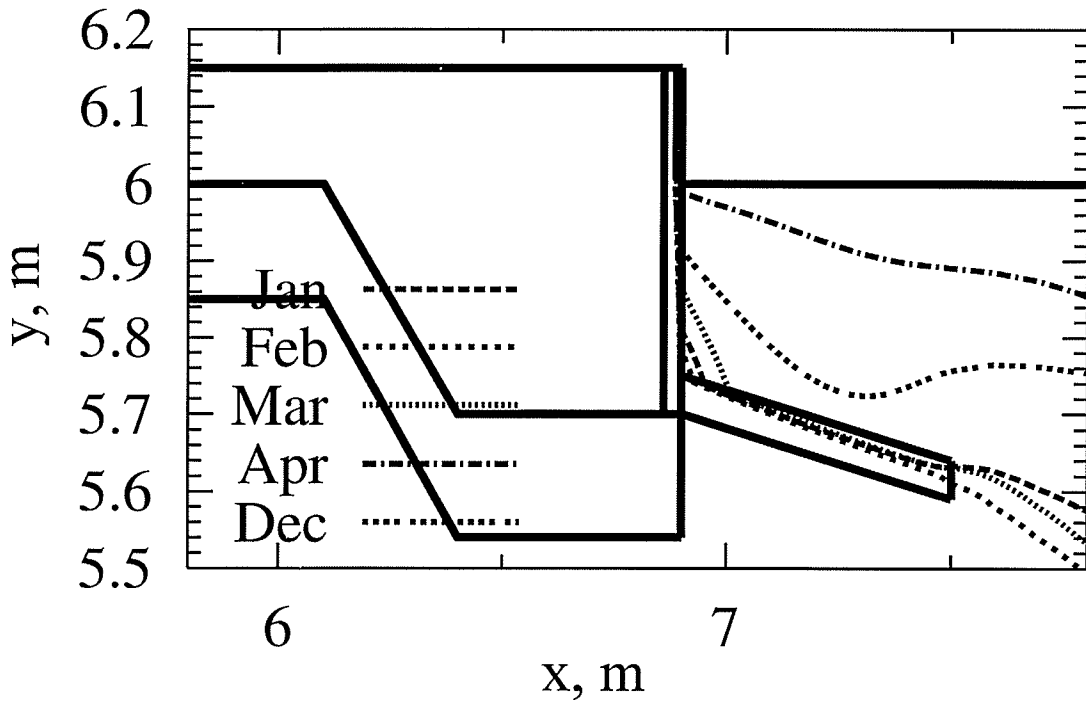


(b)

Figure 6.24 Thompson zero temperature isotherms for Case B1, (a) full domain, (b) detailed view of foundation corner

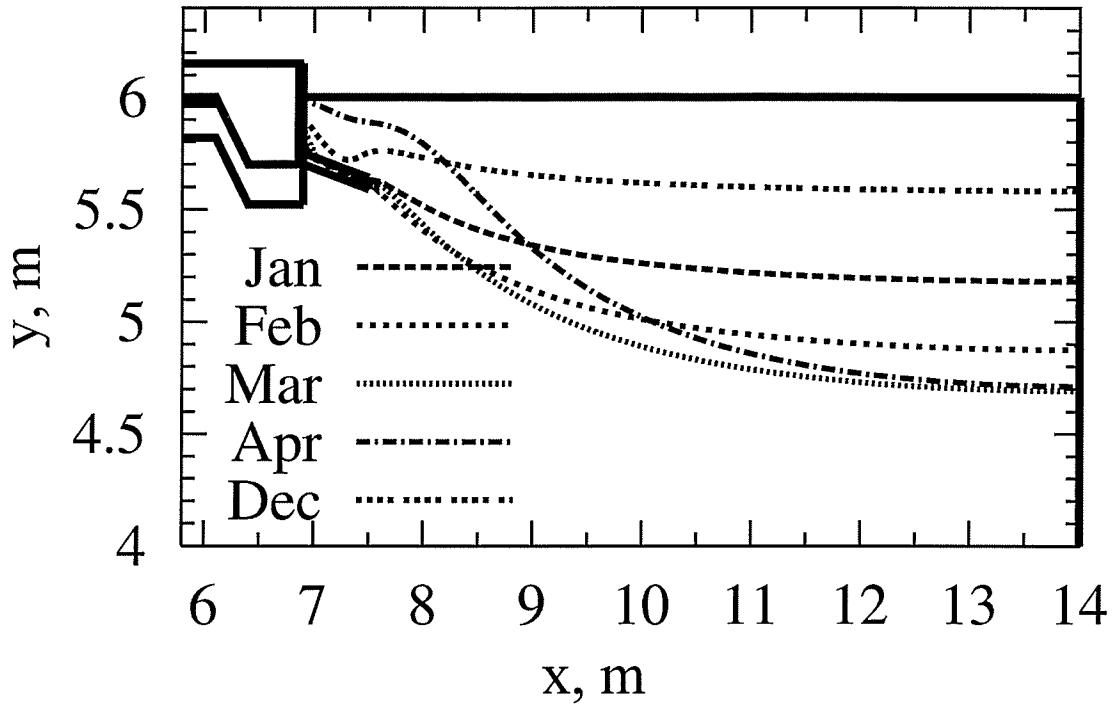


(a)

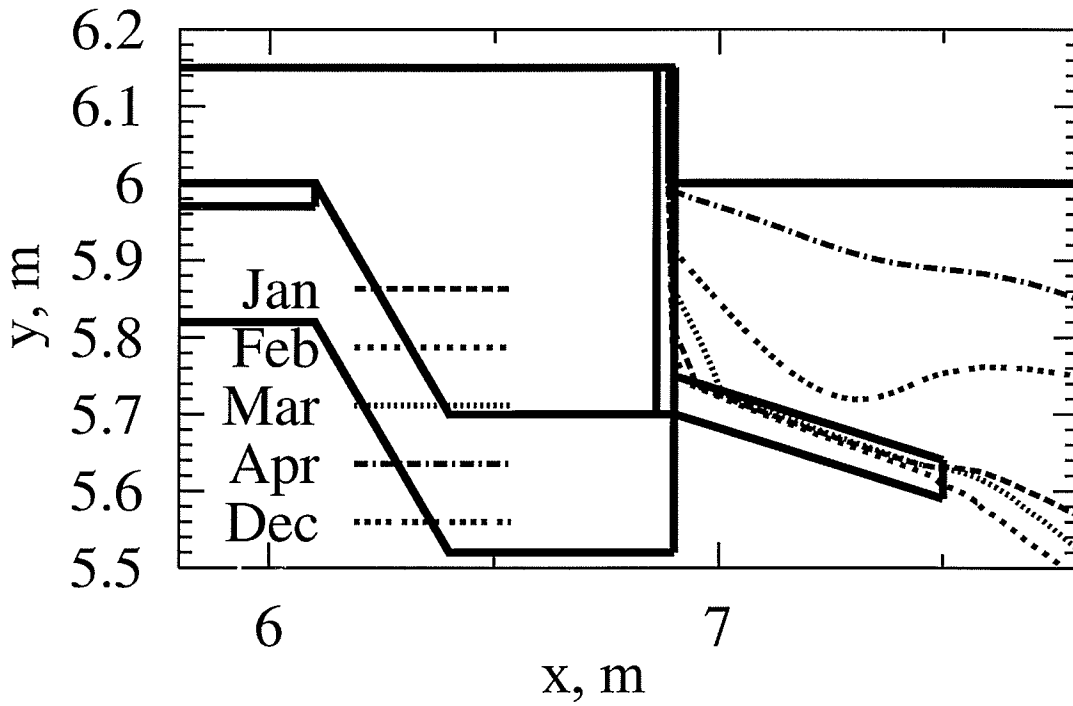


(b)

Figure 6.25 Thompson zero temperature isotherms for Case C1, (a) full domain, (b) detailed view of foundation corner

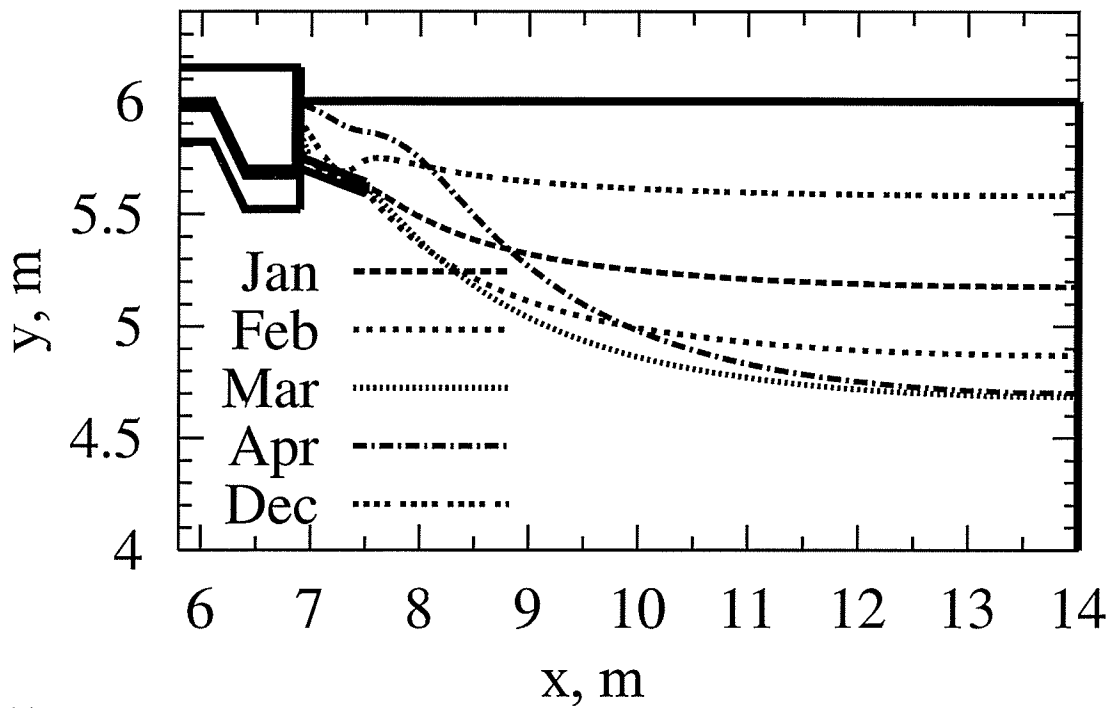


(a)

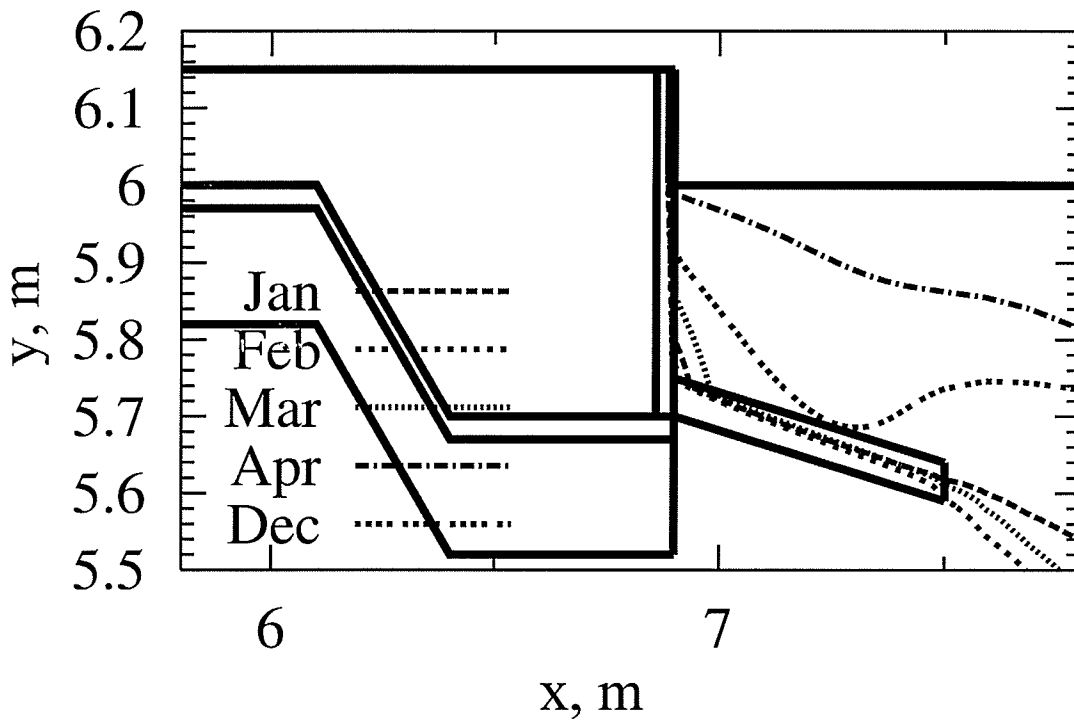


(b)

Figure 6.26 Thompson zero temperature isotherms for Case D1, (a) full domain, (b) detailed view of foundation corner

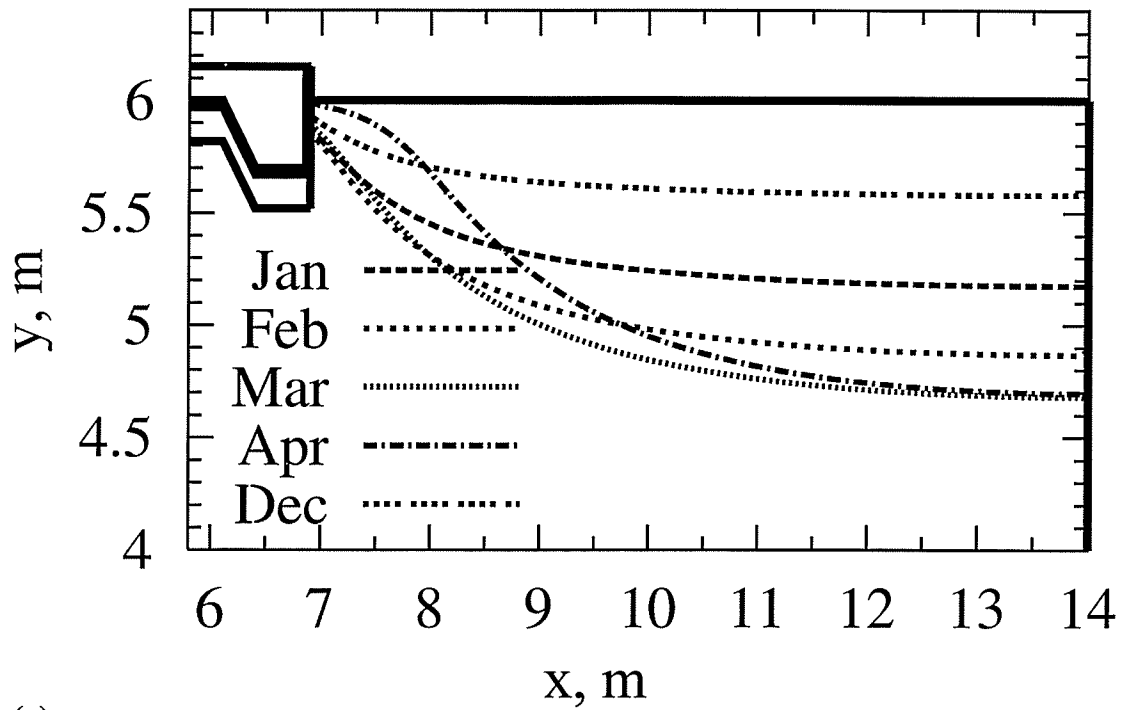


(a)

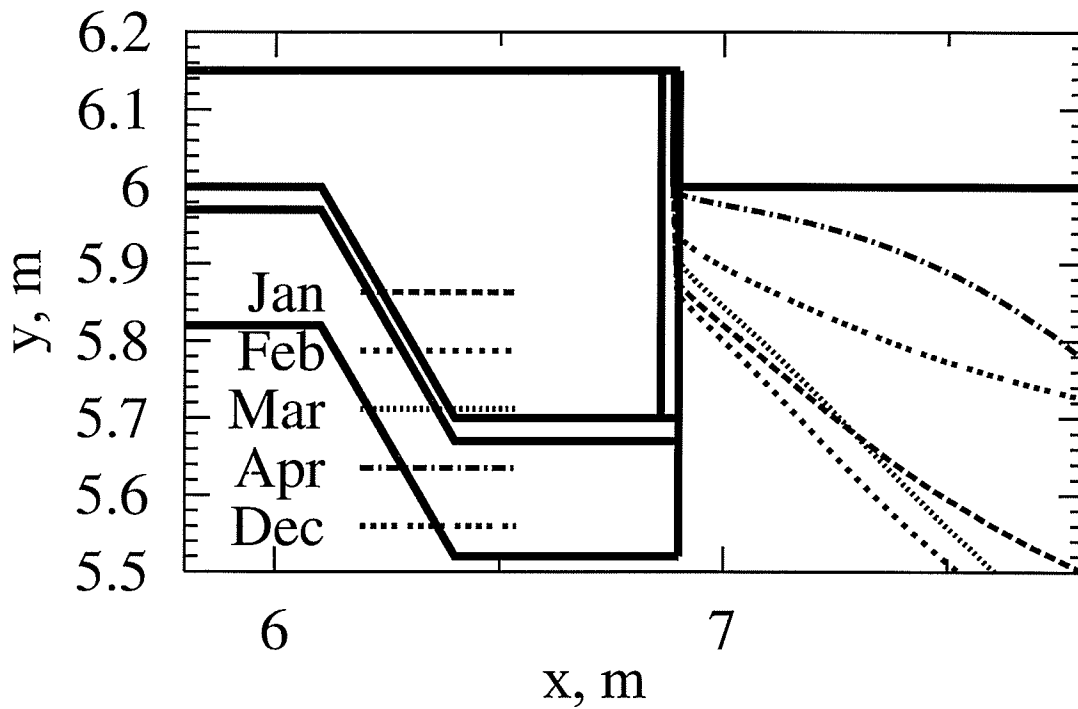


(b)

Figure 6.27 (a) Thompson zero temperature isotherms for Case E1, (a) full domain, (b) detailed view of foundation corner



(a)



(b)

Figure 6.28 Thompson zero temperature isotherms for Case F1, (a) full domain, (b) detailed view of foundation corner

6.3.8 Relative Benefit of Insulation Placement

Looking at the initial investment of insulation is also an important factor in analyzing the results of this work. One measure of the benefit of insulation is to determine the amount of heat loss reduction relative to the cost of insulation to the cost of insulation added. It is important to find out which out of all the cases is the most efficient in reducing the heat loss, while maintaining the most economical investment of insulation. Figure 6.29 is a plot of Q_{annual} (annual heat loss per unit depth in kWh/m) in the left vertical scale and the insulation volume per unit depth (in cm^3/m) on the right vertical scale.

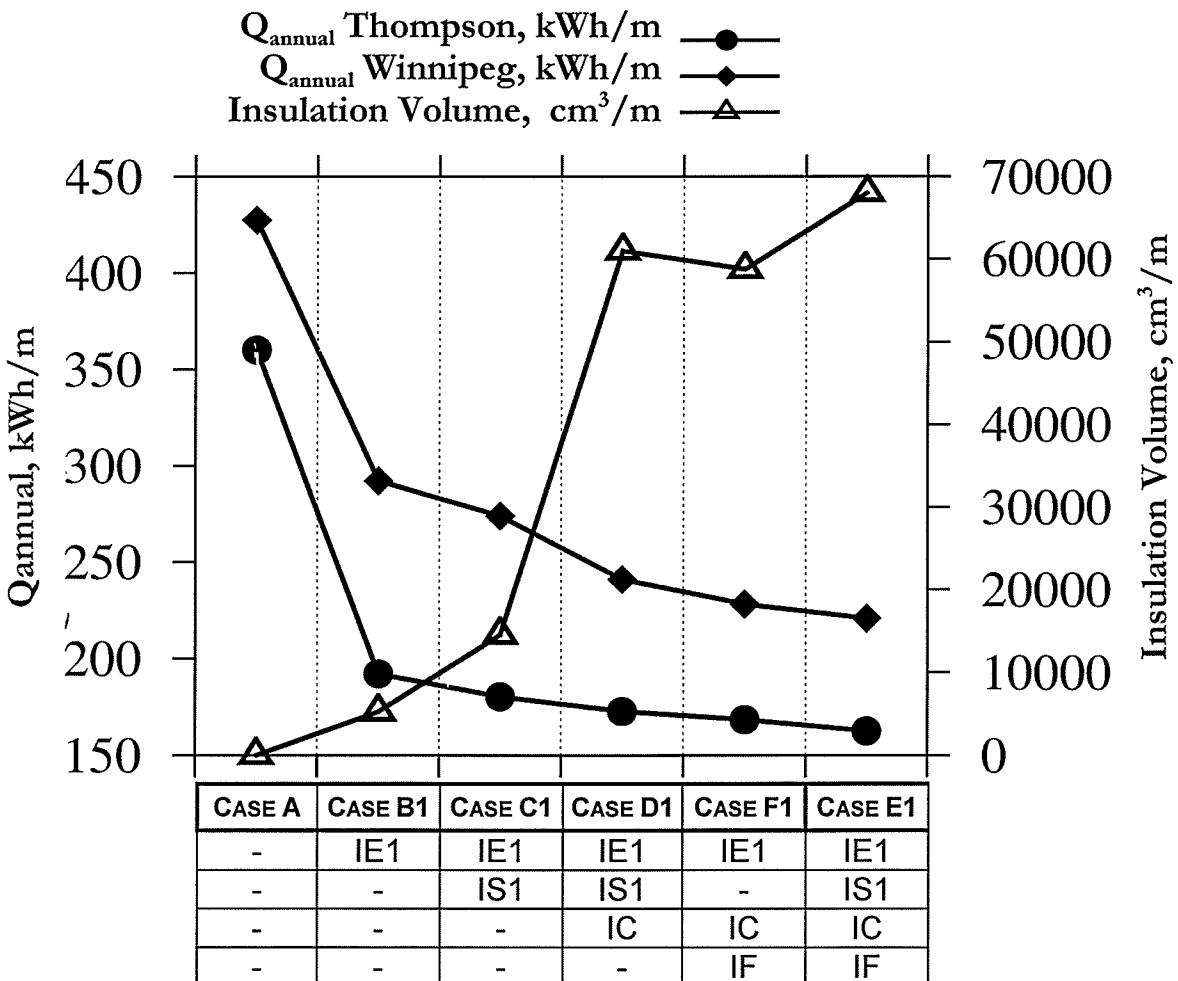


Figure 6.29 Summary of location of insulation cases versus amount of insulation for Winnipeg and Thompson

In Figure 6.29 the line with the filled circles and diamonds correspond to the annual heat losses for Thompson and Winnipeg, respectively for various insulation cases. The line with the triangles represents the amount of insulation need for each particular case. In the bottom horizontal axis are the cases compared. They have been positioned in columns. In this way one can see in one column the information for each case. For example, for Case C1 its column shows a heat loss of 180 and 270 kWh/m for Thompson and Winnipeg, respectively; this case has an insulation of approximately 14500 cm³/m. Going from Case A to Case E1 the annual heat loss is reduced. There is a 197.49 kWh/m difference between the annual heat losses from Case A to Case E1 for Thompson. For Winnipeg, the difference between Case A and Case E1 is 206.75 kWh/m.

Figure 6.29 also shows that the annual heat losses for all of the cases are overall lower for Thompson. Therefore a house in Winnipeg will experience more heat losses from the foundation than one in Thompson. Generally, Thompson atmospheric temperatures are lower than Winnipeg and since Thompson is considerably north of Winnipeg these results were unexpected. However, these results are directly related to the less conductive and lower thermal diffusive soil properties, which hinder and retard the temperature outside conditions penetrating into the soil depth. These results, shed light in opting for the construction of TES foundation in this part of Manitoba, as this type of foundation will be even more economical in that region.

Although the overall annual heat losses for Thompson are lower, the general trend followed among the cases is maintained in both Thompson and Winnipeg. That is, the heat losses all decrease when moving from Case A to Case E1. There is a significant difference in heat loss reduction between Cases A to Case B1. Subtle differences between Cases B1, C1 and D1 and minimal changes are seen between Cases D1, F1 and E1. Since this trend was shown by the results from both Thompson and Winnipeg, a similar trend is expected for other cities and towns in Manitoba. Details of the trade-off between heat loss and amount of insulation are now discussed. Table 6.13 shows the actual values plotted in Figure 6.29 and the relative increase in insulation and the percentage changes in annual heat loss per unit depth.

Table 6.13 Quantitative summary of annual heat loss versus amount of insulation

CASE	Insulation [cm ³ /m]	Net Increase in Insulation	THOMPSON		WINNIPEG	
			Q _{annual} [kWh/m]	Percentage Reduction in Q _{annual}	Q _{annual} [kWh/m]	Percentage Reduction in Q _{annual}
A	0.00		360.05		427.47	
B1	5225.80	5225.80	192.00	85.095	292.25	65.404
C1	14516.10	9290.30	180.27	5.935	274.10	8.779
D1	60967.62	46451.52	172.68	3.846	241.03	15.991
F1	58736.12	-2231.50	168.43	2.151	228.15	6.230
E1	68026.42	9290.30	162.56	2.971	220.72	3.594

As mentioned earlier, the insulation line in Figure 6.29 shows that moving from Case A to E1 the volume of insulation increases. More insulation regions are placed with each case with the exception of Case F1 where insulation is reduced because the skirt insulation was excluded from this case. Going from Case A to Case B1 there is a 5,225.80 cm³/m increase in insulation as shown in Table 6.13. The increase in insulation results in a 65.4% and 85.1% decrease in heat loss for Winnipeg and Thompson, respectively. These are substantial savings for a relatively small amount of insulation. The percentage difference presented in Table 6.13 is calculated as the difference between any two consecutive cases and divided by the overall difference between Cases A and E1 which is of 206.75 and 197.49 kWh/m for Winnipeg and Thompson, respectively.

Going from Case B1 to Case C1 there is a 9,290.30 cm³/m increase in insulation which is equivalent to 8.7% and 5.9% savings in heat loss for both Winnipeg and Thompson, respectively. However, going from Case C1 to Case D1 there is a significant increase in insulation volume of 46,451.52 cm³/m which contributes to only 16.0% and 3.8% savings in heat loss for both Winnipeg and Thompson. Here the investment is large compared to the percentage of heat loss saved.

Case E1 has insulation in all the possible insulation regions with a total of 68,026.42 cm³/m. Due to all the insulation placement, this case has the lowest overall heat loss of

all cases. However, a small marginal benefit in heat loss savings is obtained from the extra amount of insulation which probably does not financially justify the benefit of this Case E1.

In case F1 insulation is placed all around the foundation except in the skirt insulation region. From Figure 6.29 one can easily see that the total amount of insulation of Case F1 is slightly smaller than those of Cases D1 and E1. The annual heat loss incurred by Case F1 is lower than that of Case D1 even though Case D1 has more insulation. In that regard Case F1 is considered more energy efficient than Case D1. Case D1 has insulation everywhere except under the slab footing.

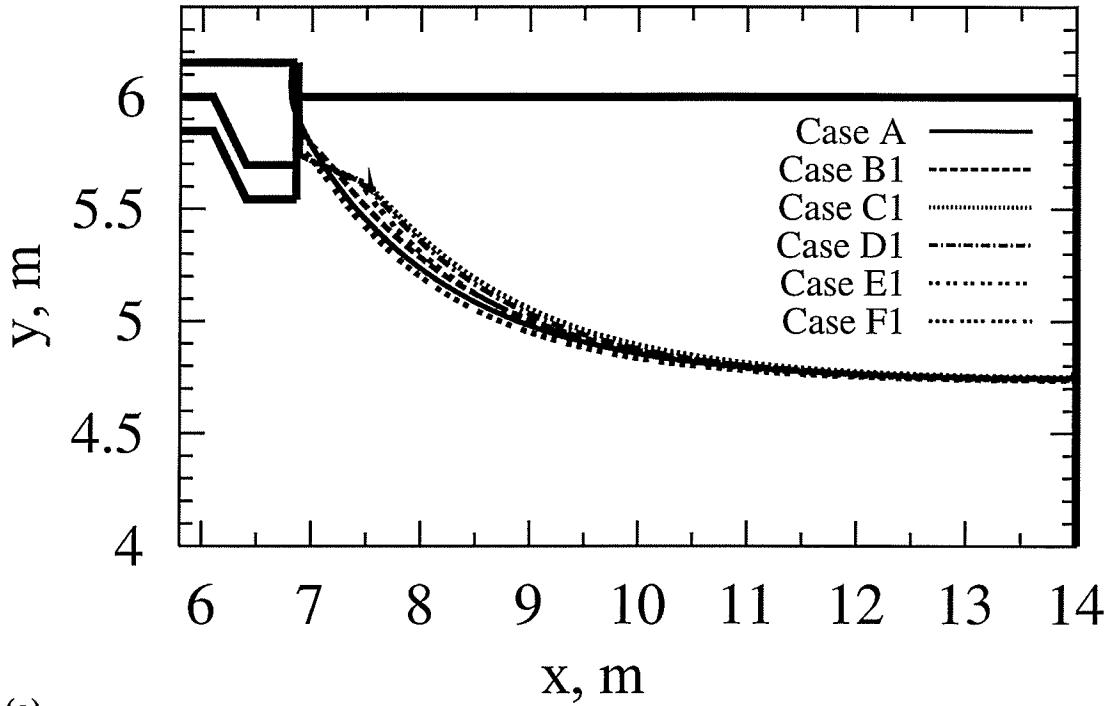
6.3.9 Overall Trends for Isotherms

A comparison of the zero temperature isotherms in the deepest frost penetration month of February is shown in Figure 6.30 for Winnipeg and in Figure 6.31 for Thompson. For all the cases with skirt insulation, the zero isotherms pass through the skirt region but the skirt region is omitted for clarity. In Figure 6.30 and Figure 6.31 the zero contour lines are guided for the cases that have skirt insulation that is, Cases C1, D1 and E1. Those cases which do not have skirt insulation (A, B1 and F1) their zero temperature lines come in contact with the side edge along the side edge.

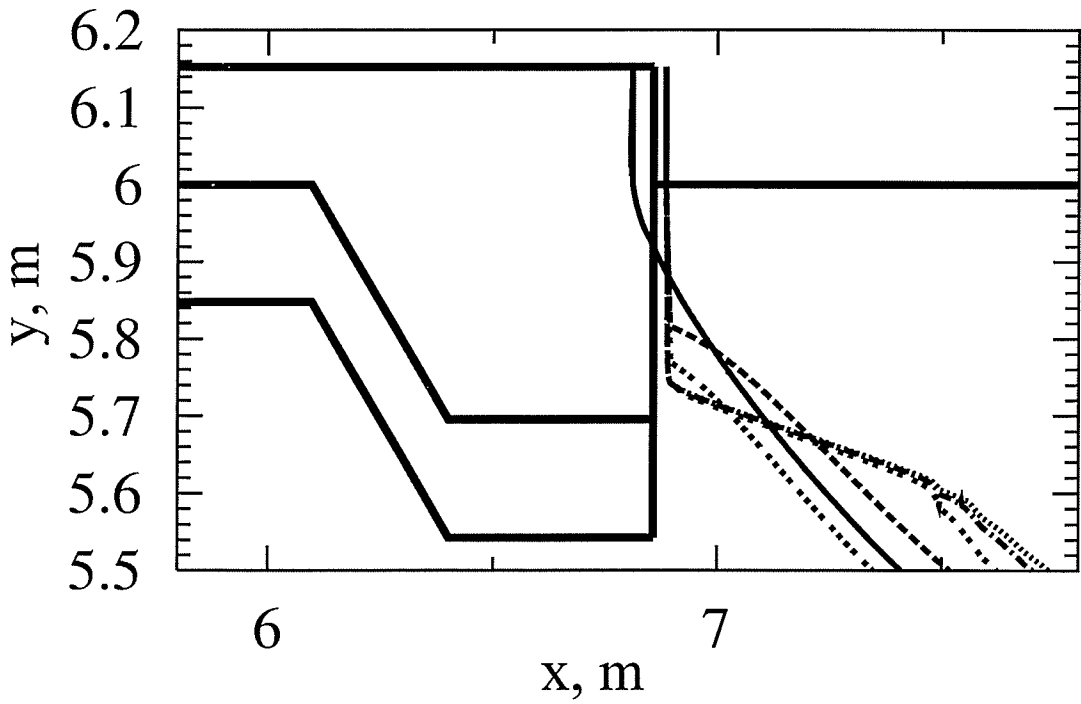
The skirt insulation acts as a barrier to frost penetration near the foundation corner. The skirt can be placed anywhere along the side of the foundation not necessarily at the bottom corner as shown in Figure 6.30. If the skirt insulation were placed higher, the zero contour lines will be further from the foundation corner avoiding potential frost heaving conditions. The limitation on this is the need for soil above the skirt to act as a protection barrier against the elements. Skirt insulation is then beneficial in guiding the zero isotherm line. This will ensure the path of the zero isotherm line away from the foundation corner thereby, eliminating the risk of frost heave.

Figure 6.30 (b) as well as Figure 6.31 (b) show that the zero contour line for Cases B1 and F1 intersects the vertical edge insulation along the side of the foundation because of the lack of skirt insulation. The risk exists that during an extremely cold winter, the zero isotherm line for these cases would intercept at a lower point along the edge. This is undesirable, especially for Case F1 which has insulation under the foot, resulting in a colder region around the foundation corner. Consequently, the zero isotherm touches lower along the insulation edge. It is important to remember that the outside boundary condition of this study is based on average soil temperatures at different underground depths. For example, Winnipeg data was obtained from Environment Canada, which averages the data points over many years of readings.

In summary, Figure 6.29 and Table 6.13 give a concise representation of the trade off between heat loss and the amount and location of insulation. From the economical stand point it seems that the insulation amount of Case B1 would be the absolute minimum in order to minimize heat losses. When considering the location of the zero isotherm line it is important to guide the isotherm through the skirt insulation region, thereby making Case C1 the most rational choice.

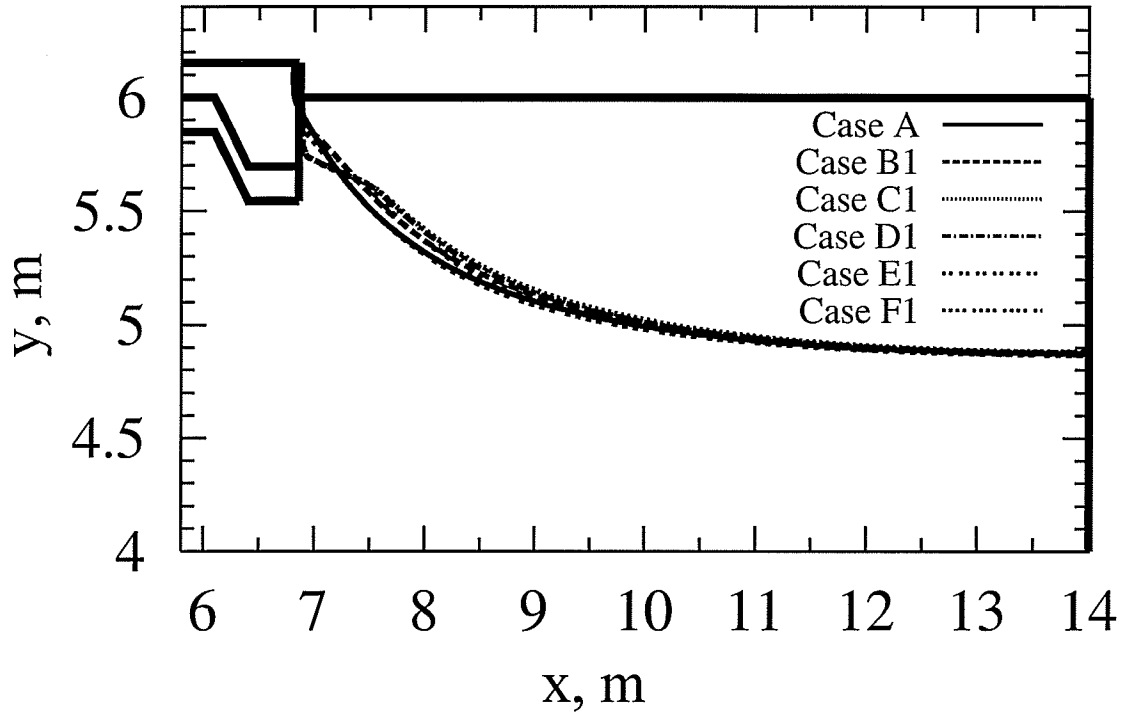


(a)

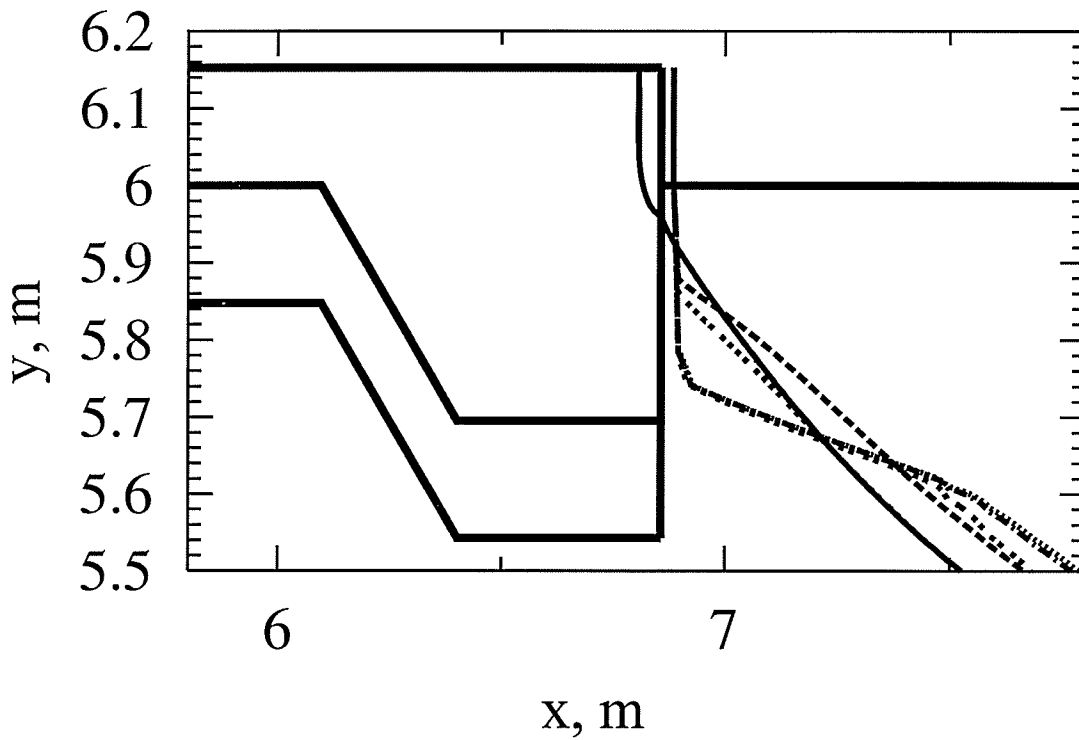


(b)

Figure 6.30 Winnipeg zero temperature isotherm for the month of February (deepest frost penetration), Cases A, B1, C1, D1, E1 and F1 (a) full domain (b) detailed view of foundation corner



(a)



(b)

Figure 6.31 Thompson zero temperature isotherm for the month of February (deepest frost penetration), Cases A, B1, C1, D1, E1 and F1 (a) full domain, (b) detailed view of foundation corner

Chapter 7

SUMMARY, CONCLUSIONS AND RECOMMENDATIONS

7.1 Summary

The thickened-edge slab-on-grade foundation is a shallow foundation of an integral casting of a flat slab with thickened footings. This foundation has been deemed a Power Smart application by Manitoba Hydro. It is cost effective because its construction, excavation, labour and material costs are much lower than traditional foundations. This foundation also requires less construction time. Energy savings are expected when compared to the traditional full basement foundation as the heating of the additional air space is avoided. The thickened-edge slab-on-grade foundation is a good alternative in cases when the considerable investment needed to make a basement a comfortable living space is absent.

In the present study, the foundation is placed at 30.5 cm (12 in) under the soil grade level. Because of its shallow depth the foundation needs to be protected against frost heave damage. Enough heat needs to be present to ensure that the soil temperature is above freezing under and around the foundation. However, the optimal amount of heat needs to be obtained in order to ensure heat loss effectiveness. Insulation needs to be placed strategically around the outside of the foundation. The purpose of insulation is to reduce heat loss and redirect the building's heat loss. The frost line can be raised and move away from the foundation by the proper location of insulation while reducing the heat loss.

The heat loss from TES foundation occur primarily through the foundation edge to the outdoor air and to the soil under layers. Insulating the slab not only reduces the heat loss but it also allows for the heat to be directed strategically to raise the soil temperature especially to the footing of the foundation. The footing is the crucial area in which to raise the soil temperature as it is the location most prone to frost heave. The use of skirt

insulation conserves geothermal energy and protects the foundation lower edges from frost. The edge insulation was found to significantly reduce the heat loss to the outdoor air. The skirt insulation region was added in addition to the edge insulation. In other words, no cases were tried where the skirt insulation was the only insulation region placed. Approximations in steady state and transient were done. Their results are summarized in the following sections.

7.2 Conclusions Based on the Steady State Analyses

Case A, which has no insulation, results in its zero degree Celsius temperature isotherm passing through the foundation footing. This results in a thermal bridge to the outside air where a large amount of heat is lost. For the configuration studied, the heat loss was calculated to be 66.6 W/m. Not only a thermal bridge is formed in this case but there is also the potential of adfreezing. Adfreezing is the force transmitted through a bond formed between the rising frozen soil and a cold enough foundation wall.

Adding insulation to the edge of the foundation reduced the heat loss. Two thicknesses were studied: 3.8 cm (1.5 in) and 7.6 cm (3 in). The heat loss was reduced to 37.5 and 34.2 W/m, respectively. The benefit of adding insulation is seen in the zero temperature isotherm line. This line no longer passed through the foundation but passed through the foundation edge. Doubling the thickness at the edge resulted in about 10% of savings in heat loss.

The addition of skirt insulation further reduced the heat loss to a lowest value of 29.6 W/m. However, its main benefit is seen in the shifting away of the zero temperature isotherm from the foundation corner. In all the Case C insulation configurations studied, the zero temperature isotherm lines passed through the skirt insulation and into the vertical edge insulation. This made the zero isotherm line lie well away from the foundation corner.

Although only a range of savings in heat loss of 5 W/m was obtained among all the skirt configurations cases done, the location where the zero isotherm line lies is largely affected. The longer, thicker skirt insulation (IS4), resulted in the zero isotherm line furthest away from the foundation corner. The zero isotherm line lies at the same position when comparing between skirts IS2 and IS3. Therefore skirt IS2, which is the thickest shortest out of the two is the most practical to use in a real life construction.

The D cases where insulation was added under the slab showed negligible benefit in terms of the location of the zero isotherm line. Also, small benefit was obtained in the reduction of heat loss. Case D8 heat loss was of 27.3 W/m, which results in a decrease of 8% from the equivalent C8 Case.

The study of the E cases, in which insulation is added under the footing proved to be detrimental to the location of the zero temperature isotherm line. Although savings in heat loss were obtained, these were minimal to the effect that adding this region of insulation had on the zero isotherm line. A heat loss of 25.2 W/m was calculated for case E8 which results in 8% savings compared to case D8.

With no skirt insulation, Case F proved the importance of having skirt insulation. This insulation must be placed to guide the zero isotherms away from the foundation corner. For this case, the zero isotherms lied very close to the foundation corner, which may introduce the potential for frost heave. This was a result of having insulation under the foundation foot. The heat escaping from the foundation foot warms up the soil around the foundation corner.

7.3 Conclusions Based on the Transient Analyses

The transient results performed for Winnipeg show below freezing soil temperatures for the months of January, February, March and December. The deepest frost penetration occurs in February where the depth of frozen soil is calculated to be 1.2 m from the soil

surface. The depth of frost penetration is of an undisturbed soil where the heat from the house has no effect.

The transient results for Winnipeg's Case A indicate that the zero isotherm lines pass through the foundation footing. The foundation experiences large heat losses as a result of very cold temperatures around its edge. Placing edge insulation prevents the zero temperature isotherm line to pass through the side of the foundation as seen from Case B. The lines meet the edge insulation near the lower portion of the foot side.

Case C showed the zero isotherm line go through the skirt and up the vertical side edge insulation. The skirt insulation acts as a guide for the zero isotherms to run through. Therefore, positioning the skirt higher would raise the depth of the freezing line. However, the skirt insulation must be protected with a layer of soil.

Cases D and E showed insignificant differences in their zero temperature isotherm when compared to Case C. Case F results of the zero temperature isotherm posed more of a threat as they could go under the foundation.

In studying the effect of the vertical edge insulation it was found that doubling the thickness had a small effect in both the location of the zero temperature isotherm and the amount of heat loss. Isotherm plots were qualitatively compared by aligning them to the outside edge of the vertical insulation and placing them on top of each other. The heat loss was reduced by up to 5.55%. Case F2 was an exception in that having a thicker insulation edge was detrimental to the zero isotherm lines as they moved closer to the bottom corner of the foundation where they pose a higher threat.

The transient results for Thompson also showed a freezing isotherm line for the same months as Winnipeg, in addition to the month of April. Although the frost penetration was slower than Winnipeg's, Thompson's freezing depth reached lower to slightly over 1.3 metres, which peaked in the month of March. This is thought to be the results of the colder air temperatures experienced in Thompson. Similar behaviour to the cases

explained above for Winnipeg took place for Thompson, with the exception of Case E. The zero isotherms for Case E penetrated deeper as a result of cutting the heat flow supply to the soil next to the foundation corner through the footing.

Comparing the overall results for Winnipeg and Thompson, the annual heat losses of all the cases are overall lower for Thompson. Although, atmospheric temperatures are lower at Thompson, its soil has a lower thermal conductivity and thermal diffusivity than Winnipeg, which allows for a slower response to the cold winter temperatures. This explains the slower freezing penetration depth as well as the longer melting time frame seen in the results.

7.4 Recommendations

The objective of this research is to study the optimal amount and location of insulation in order to minimize the amount of heat loss while effectively avoiding the threat of frost heave. For a practical solution the optimization of the economical investment to the marginal benefit is also relevant. Case C is thought to be the most balanced option. It gave a large benefit in heat savings to the cost associated with its amount of insulation. In addition, its skirt insulation region guided the zero isotherm line away from the foundation corner. The location of the freezing line and the marginal benefit in savings of heat loss are best addressed by Case C when compared to its amount of insulation.

The present study is based on a two dimensional approximation. According to Robinsky and Bessflug (1973) the heat loss from slab foundations is greatest at the corners. The scope of this work includes only a two-dimensional model. Therefore, further studies of three dimensional approximations will be needed to address the significance of heat loss from the slab corners as part of a future research work. Other recommendations include further research on the effects of other cities climate and soil properties. As well as the transient simulation of a coldest winter. Of particular importance would be a scenario simulation of loss of heating during January.

REFERENCES

Ackerman, M. and Dale, J.D., "Measurement and Prediction of Insulated and Uninsulated Basement Wall Heat Losses in a Heating Climate", ASHRAE Transactions, Vol. 93, Pt. 1, pp. 897-908, 1987.

Adjali, M.H., Davies, M. and Littler, J., "Earth-Contact Heat Flows: Review and Application of Design Guidance Predictions", Building Services Engineering Research and Technology, Vol. 19, No. 3, pp. 111-121, 1998.

Adjali, M.H., Davies, M. and Littler, J., "A Numerical Simulation of Measured Transient Temperatures in the Walls, Floor and Surrounding Soil of a Buried Structure", International Journal of Numerical Methods for Heat and Fluid Flow, Vol. 9, No. 4, pp. 405-422, 1999.

Akridge, J.M. and Poulos, J.F.J., "The Decremental Average Ground Temperature Method for Predicting the Thermal Performance of Underground Walls", ASHRAE Transactions, Vol. 89, Part 2A, 1983.

ANSYS CFX, "CFX-5.7 Discretisation and Solution Theory Manual", ANSYS CFX, pp. 227-250, 2004

Bahnfleth, W.P. and Pedersen, C.O., "A Three-Dimensional Numerical Study of Slab-on-Grade Heat Transfer", ASHRAE Transactions, Vol. 96, Pt. 2, pp. 61-72, 1990.

Berg, J. "Conduction in Composite Walls with Series-Parallel Configurations"
Bachelor of Science (Mechanical Engineering) Thesis, University of Manitoba, 2002

Bullock, P.R., "Manitoba Agriculture Northern Soil Temperatures", Department of Soil Science, University of Manitoba, 2003

Burn, K.N., "CBD-182 Frost Action and Foundations", Canadian Building Digest, 1976

Carmody, J., Christian, J. and Labs, K., "Builder's Foundation Handbook", Oak Ridge National Laboratory, 1991.

Carson, J.E., "Analysis of soil and air temperatures by Fourier Techniques", Journal of Geophysical Research, Vol. 68, pp. 2217-2232, 1963

Christian, J.E., Strzepek, W.R., "Procedure for Determining the Optimum Foundation Insulation Levels for New, Low-Rise Residential Buildings", ASHRAE Transactions, Vol. 93, Pt. 1, pp. 909-938, 1987.

Chuangchid, P. and Krarti, M., "Foundation Heat Loss from Heated Concrete Slab-on-Grade Floors", Building and Environment, Vol. 36, pp. 637-655, 2001a.

Chuangchid, P. and Krarti, M., "Steady-State Component of Three-Dimensional Slab-on-Grade Foundation Heat Transfer", Transaction of the ASME, Vol. 23, pp. 18-29, 2001b.

CMHC-SCHL, "Home Care – A guide to Repair and Maintenance", Canadian Mortgage and Housing Corporation CMHC-SCHL publication, 1982.

CMHC-SCHL, "Research Report – Insulated Slab-on-Grade Foundations: A Design Guide for Rural, Northern and First Nations Housing", Canadian Mortgage and Housing Corporation CMHC-SCHL publication, 2000a.

CMHC-SCHL, "Research Highlights – Slab-on-Grade Construction ", Canadian Mortgage and Housing Corporation CMHC-SCHL publication, Technical Series 00-127, 2000b.

Crandell, J., "Insulating Building Foundations for Frost Protection, Energy Conservation, and Affordability", The 1994 EEBA Conference: Excellence in Housing, Dallas, TX, February 23, pp. A106-22, 1994.

Danyluk, L.S., "Shallow Insulated Foundation at Galena, Alaska – A case Study", CRREL Special Report 97-7, U.S. Army Corps of Engineers Cold Regions Research and Engineering Laboratory, 1997.

Deru, M., Judkoff, R. and Neymark, J., "Whole-Building Energy Simulation with a Three-Dimensional Ground-Coupled Heat Transfer Model", ASHRAE Winter Meeting Conference, Chicago, Illinois, Jan 25-29, 2003.

Environment Canada, "2002 CDCD West CD" Environment Canada, Government of Canada, 2002

Eyolfson, E.M., Manitoba Hydro, Personal Communication, 2002.

Ferziger, J.H. and Peric, M., "Computational Methods for Fluid Dynamics", Springer, Berlin, 1999

Goldberg, L.F., "Frost Protected Shallow Foundation Design Specifications", College of Architecture and Landscape Architecture, Building Research Group, 1999.

Huang, Y.J., Shen, L.S., Bull, J.C. and Goldberg, L.F., "Whole House Simulation of Foundation Heat Flows Using the DOE-2.1C Program", ASHRAE Transactions, Vol. 94, 1988.

Incropera, F.P. and DeWitt, D.P., "Fundamentals of Heat and Mass Transfer", Fourth Edition, John Wiley and Sons, Inc., 1996.

Ingersoll, J.G., "Analytical Determination of Soil Thermal Conductivity and Diffusivity", Transactions of the ASME, Vol. 110, pp. 306-312, 1988.

Khalifa, A.N., "Heat Loss from Below Ground Basements: Validation of Some Available Methods", Energy Conversion and Management, Vol. 40, No. 18, pp.1963-1977, 1999.

Krarti, M., "Steady-State Heat Transfer Beneath Partially Insulated Slab-on-Grade Floor", International Journal of Heat and Mass Transfer, Vol. 32, No. 5, pp. 961-969, 1989.

Krarti, M., "Steady-State Heat Transfer from Horizontally Insulated Slabs", International Journal of Heat and Mass Transfer, Vol. 36, No. 8, pp. 2135-2145, 1993a.

Krarti, M., "Steady-State Heat Transfer from Slab-on-Grade Floors with Vertical Insulation", International Journal of Heat and Mass Transfer, Vol. 36, No. 8, pp. 2147-2155, 1993b.

Krarti, M., "Time-Varying Heat Transfer from Partially Insulated Basements", International Journal of Heat and Mass Transfer, Vol. 37, No.11, pp.1657-1671, 1994a.

Krarti, M., "Time-Varying Heat Transfer from Horizontally Insulated Slab-on-Grade Floors", Building and Environment, Vol. 29, No.1, pp. 63-71, 1994b.

Krarti, M., "Time-Varying Heat Transfer from Slab-on-Grade Floors with Vertical Insulation", Building and Environment, Vol.29, No. 1, pp. 55-61, 1994c.

Krarti, M. and Choi, S., "Heat Transfer for Slab-on-Grade Floor with Stepped Ground", Energy Conversion Management, Vol. 39, No. 7, pp. 691-701, 1998.

Krarti, M. and Claridge, D.E., "Two-Dimensional Heat Transfer from Earth-Sheltered Buildings", *Journal of Solar Energy Engineering*, Vol. 112, pp. 43-50, 1990.

Krarti, M. and Piot, O., "Steady-State Heat Transfer from Adjacent Slab-on-Grade Floors", *Transactions of the ASME*, Vol. 117, pp. 60-63, 1995.

Krarti, M., Claridge, D.E. and Kreider, J.F., "ITPE Technique Applications to Time-Varying Two-Dimensional Ground-Coupling Problems", *International Journal of Heat and Mass Transfer*, Vol. 31, No. 9, pp. 1899-1911, 1988a.

Krarti, M., Claridge, D.E. and Kreider, J.F., "The ITPE Technique Applied to Steady-state Ground-coupling Problems", *International Journal of Heat and Mass Transfer*, Vol. 31, No. 9, pp. 1885-1898, 1988b.

Krarti, M., Claridge, D.E. and Kreider, J.F., "ITPE Technique Applications to Time-Varying Three-Dimensional Ground-Coupling Problems", *Journal of Heat Transfer*, Vol. 112, pp. 849-856, 1990.

Krarti, M., Claridge, D.E. and Kreider, J.F., "A Foundation Heat Transfer Algorithm for Detailed Building Energy Programs", *ASHRAE Transactions*, Vol. 100, No. 2, 1994.

Krarti, M., Lopez-Alonzo, C., Claridge, D.E. and Kreider, J.F., "Analytical Model to Predict Annual Soil Surface Temperature Variation", *Journal of Solar Energy Engineering*, Vol. 117, pp. 91-99, 1995.

Kusuda, T., "Engineering and Instrumentation", *Journal of Research of the National Bureau of Standards*, Vol. 71c, no. 1, pp. 43-50, 1966.

Kusuda, T. and Achenbach, P. R., "Earth Temperature and Thermal Diffusivity at Selected Stations in the United States", no. 1914, pp. 61-75, 1965.

Labs, K., Carmody, J.C., Sterling, R.L., Shen L.S., Huang, Y.J. and Parker, D.S., "Building Foundaiton Design Handbook", Oak Ridge, TN: Oak Ridge National Laboratory, ORNL/Sub/86-72143/1, 1988.

Latta, J.K. and Boileau, G.G., "Calculation of Basement Heat Losses", National Research Council of Canada, Division of Building Research Report, NRC 10477, 1968.

Latta, J.K. and Boileau, G.G., "Heat Losses from House Basements", National Research Council of Canada, Vol. XIX, No. 10, pp. 39-42, 1969.

Legget, R.F., "CBD-3 Soil and Buildings", Canadian Building Digest, 1960.

MacDonald, G.R., Claridge, D.E., and Oatman, P.A., "A Comparison of Seven Basement Heat Loss Calculation Methods Suitable for Variable-Base Degree-Day Calculations", ASHRAE Transactions, Vol. 91, Pt. 1B, pp. 916-933, 1985.

Maref, W., Swinton, M.C., Kumaran, M.K. and Bomberg, M.T., "Three-Dimensional Analysis of Thermal Resistance of Exterior Basement Insulation Systems (EIBS)", Building and Environment, Vol. 36, No. 4, pp. 407-419, 2001.

Mills, A. F., "Heat transfer", Richard D. Irwin Inc., 1992.

Mitalas, G.P., "Calculation of Basement Heat Loss", ASHRAE Transactions, Vol. 89, Pt. 1, pp. 420-437, 1983.

Mitalas, G.P., "Calculation of Below-Grade Residential Heat Loss: Low-Rise Residential Building", ASHRAE Transactions, Vol. 93, Pt. 1, pp. 743-783, 1987.

NAHB Research Center, "Energy-Efficient Resource-Efficient Frost-Protected Shallow Foundations", NAHB Research Center, 1999.

http://www.nahbrc.org/docs/subsystemnav/foundations/3808_nahb_fpsf.pdf

NAHB Research Center, "Design Guide for Frost-Protected Shallow Foundations"
Second Edition, NAHB Research Center, 1996.

Patankar, S.V., "Numerical Heat Transfer and Fluid Flow", McGraw-Hill, New York,
1980

Parker, D.S., "F-Factor Correlations for Determining Earth Contact Heat Loads",
ASHRAE Transactions, Vol. 89, Pt. 1B, pp. 784-790, 1987.

Parker, D.S. and Carmody, J.C., "Optimization of Foundation Insulation Levels",
ASHRAE Transactions, Vol. 94, 1988.

Penner, E., "CBD-26 Ground Freezing and Frost Heaving", Canadian Building Digest,
1962.

Penner, E. and Burn, K.N., "CBD-128 Adfreezing and Frost Heaving of Foundations",
Canadian Building Digest, 1970.

Robinsky, E.I. and Bessflug, K.E., "Design of Insulated Foundations", Journal of the Soil
Mechanics and Foundation Division, ASCE, Vol. 99, No. SM9, pp. 649-667, 1973.

Shen, L.S. and Ramsey, J.W., "An Investigation of Transient, Two-Dimensional Coupled
Heat and Moisture Flow in the Soil Surrounding a Basement Wall", International Journal
of Heat and Mass Transfer, Vol. 31, No. 7, pp. 1517-1527, 1988.

Shen, L.S., Poliako Va, J. and Huang, Y.J., "Calculation of Building Foundation Heat
Loss Using Superposition and Numerical Scaling", ASHRAE Transactions, Vol. 94, Pt.
2, pp. 917-935, 1988.

Shipp, P.H., "The Thermal Characteristics of Large Earth-Sheltered Structures", Ph. D.

dissertation, Department of Mechanical Engineering, University of Minnesota, Minneapolis, 1979.

Shipp, P.H., "Basement, Crawl Space and Slab-On-Grade Thermal Performance", ASHRAE SP 38 Thermal Performance of the Exterior Envelopes of Buildings II, American Society of Heating, Refrigeration and Air-Conditioning Engineers, 1983.

Shul'gin, A.M., "The Temperature Regime of Soils", Gimiz Gidrometeorologicheskoe Izdatel'stvo, Leningrad (1957), Translated from Russian, Israel Program for Scientific Translations, Jerusalem, 1965

Sobotka, P., Yoshino, H. and Matsumoto, S., "Thermal Performance of Three Deep Basements: A comparison of Measurements with ASHRAE Fundamentals and the Mitalas Method, the European Standard and the Two-Dimensional FEM Program", Energy and Buildings, Vol. 21, No. 1, pp. 23-34, 1994.

Swinton, M.C. and Platts, R.E., "Engineering Method for Estimating Annual Basement Heat Loss and Insulation Performance", ASHRAE Transactions, Vol. 87, Pt. 2, pp. 343-358, 1981.

Wang, F.S., "Mathematical Modeling and Computer Simulation of Insulation Systems in Below Grade Applications", ASHRAE/DOE Conference on Thermal Performance of the Exterior Envelopes of Buildings, Orlando, FL, pp. 456-471, 1979.

Yard, D.C., Gibson, M. and Mitchell, J.W., "Simplified Relations for Heat Loss from Basements", ASHRAE Transactions, Vol. 89, pt. 2A, 1984.

Appendix A
DETERMINATION OF GRADE LEVEL PERIODIC TEMPERATURE
BOUNDARY CONDITION

A.1 Introduction

During the summer months the main sources of heat entering the ground are provided by solar radiation and convection from the outside air. The heat absorbed by the ground surface will be transferred by conduction to lower soil layers. During the winter months the ground will experience heat losses to the outside. Depending on the latitude, the top layers of the ground will freeze for a number of days or even months. The longer sub-zero temperatures are experienced, the deeper the frost penetration into the soil and the longer the soil will be frozen.

However, deep underground the soil will maintain a constant average temperature. Since the ground is a very large object, it can be treated as a semi-infinite solid. In a semi-infinite solid only a finite depth is affected by surface conditions. The effects from the surface are dampened with depth penetration. There is a point in depth that, when reached, the rest of the solid remains unchanged at the mean annual temperature.

The ground surface is very much influenced by random and systematic climatic conditions that affect its temperature. Random conditions are quick climatic disturbances such as cloudiness, precipitation, winds, El Niño effects, snow, evaporation of water, etc. Systematic conditions are those occurring daily due to radiation during the day and night. As well as seasonal conditions occurring yearly, such as summer and winter temperatures.

Environment Canada is the main Canadian agency that has measured and recorded temperatures of air and soil for different depths over several years and for many cities in Canada. In this research only seasonal or systematic conditions are taken into

consideration. All random conditions are not be accounted for. In fact, Environment Canada data is taken over such a large period of time, over many decades that such effects have been averaged out and do not represent large discrepancies.

The top ground layer is very active in transferring energy to lower layers as a result of its exposure to these conditions. Greater temperature differences between the soil surface and deeper layer will result in greater amounts of heat entering and leaving the soil. Since the ground surface temperature is always changing, it would be convenient to capture its change with an equation that predicts this temperature as a function of time.

In this appendix an equation that calculates a suitable prediction of soil temperature at the surface is obtained. To accurately account for the variation of temperature throughout the year, the equation is derived as a function of time which accounts for its periodic behaviour. The following are three options to obtain such an equation:

1. Use grade level temperature data and create a function that represents the data.
2. Use air temperature data and create a function to represent the data.
3. Use soil temperature data from various depths to obtain a soil behaviour that will allow extrapolating to the grade level, thereby obtaining a function that represents the soil temperature variation.

Option 1 sounds to be the most reasonable and straight forward. That is to get a function from the temperature data at the ground. However, it is very difficult to obtain reliable temperature data at the surface. Mostly, because the Earth's surface is difficult to define with respect to elevation and also because soil temperature at the surface have considerable deviations as a consequence of random conditions (cloudiness, precipitation, winds evaporation of water), Shul'gin (1965) and Kusuda (1966). Most likely, it is for that reason that Environment Canada does not report temperature data at the surface.

Although air temperatures are readily available, the overall average air temperature is much lower than the deep soil average temperature. Therefore, Option 2 is too

conservative. Also, either a relationship of the degree days at each location would have to be included, or the assumption that the air convection coefficient equals infinity must be made. Figure A.1 illustrates this assumption.

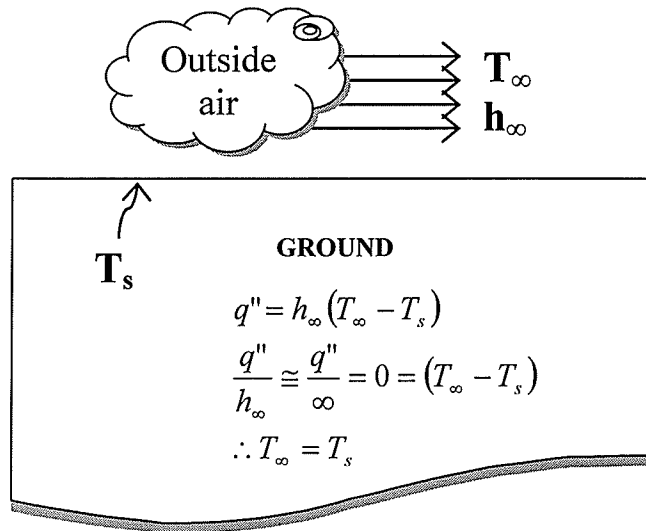


Figure A.1 Assumption of convection coefficient equals infinity

Option 3 is the most feasible because data at various soil depths are available and are less prone to deviation from outside random conditions as compared to the surface. Also, the general behaviour of soil underneath, such as the dependency of its properties, will be inherited and carried in the extrapolation of its temperature. As well, the constant average temperature of soil is obtained, which is typical of the particular latitude location. Due to its feasibility this option was selected to obtain the equation that describes the surface soil temperature. The equation is entered in CFX-5 as the top soil surface transient boundary condition. However, one must expect that error is introduced by the extrapolation from experimental data at various depths, as well as the errors introduced when creating the function using curve fitting.

Option 3 was selected and is explained in detail in this appendix. An equation is derived to obtain the soil temperature at grade level and use as input to the transient boundary condition used in this research. This equation curve fits the data available at different soil depths and then extrapolates to the grade level or zero depth. The soil temperature measurements at various depths are utilized based on one very important assumption already mentioned. That is, the thermal behaviour of soil is that of a semi-infinite solid that is subject to systematic and periodic temperature changes. This is explained in more detail in section A.2.

In this appendix the following will be discussed:

- The simple harmonic function that is used for a least square fitting of soil data observed for two locations in Manitoba: Winnipeg and Thompson
- The methods for obtaining annual average temperature, annual amplitude, and phase angle of the temperature cycle from the curve fit function.
- Determination of thermal diffusivity used for the calculation of soil thermal properties in Appendix B.
- Comparison of observed data to calculated soil temperatures using the Separate Method and the Two-Dimensional Method.
- Calculation of soil surface temperatures for Winnipeg and Thompson.

A.2 Assumed Behaviour of Soil

The ground surface is subject to a time periodic temperature variation from the outdoor air. As it is well known, the outdoor temperature is governed by a periodic cycle of a year in which four seasons take place, each with its own air temperature range. The change in temperature at the surface is transferred to lower soil layers by conduction. Deep underground the outside temperature effects are damped and reduced to zero where a mean temperature prevails. The main assumption used here is that the soil behaves like a homogeneous semi-infinite solid, with a periodic temperature variation applied at its exposed surface.

The theory of the semi-infinite solid with a periodic temperature variation is explained in detail in Sections 5.2.1 and Sections 5.2.1.2. In these sections, validations of the numerical code were done against the analytical solution for this theory. Shown in Equation (5.6) is the Temperature boundary condition at the surface. The periodic behaviour is represented by a sinusoidal in the function. The general solution equation is included in Equation (5.7) and the solution to the surface temperature is found in Equation (5.8). Figure 5.10 is a sketch of the analytical solution to these equations. From this figure one can see that the amplitude of the sinusoidal is attenuated with depth (along the y axis). The term $(T_s^* - T_0)$ in Equations (5.7) and (5.8) represents the amplitude. The exponential part of the equation gives the decay for the amplitude attenuation. The equation used for the top outside transient boundary condition in this research uses the format of this equation.

Two equations are derived for two locations for the province of Manitoba, the city of Winnipeg and the town of Thompson. The latter is the highest populated town in northern Manitoba. The temperature data for different soil depths has been obtained from Environment Canada for Winnipeg and Agriculture Manitoba for Thompson. The program GNUPLOT was used to curve fit the equations which uses a non-linear least squares curve fit method.

The data have been curve fitted using two methods, the Separate Method (explained in detail in Section A.3.1) and the Two-Dimensional Method (explained in Section A.3.2). The Separate Method curve fits each soil temperature data set for each depth separately. In the Two-dimensional Method all the depths are curve fitted at once. The resulting equation is a two-dimensional function of depth and time. The Separate Method results are used to validate those obtained from the Two-dimensional Method.

A.3 Curve Fitting Procedure

The use of cyclic soil temperatures to curve fit an equation has been done in the past by Kusuda and Achenbach (1965), Kusuda (1966), Carson (1963). In most cases the investigation was for the purposes of obtaining the thermal diffusivity of soil. Kusuda and Achenbach (1965) began with the basis that earth temperature cycles follow a simple harmonic mode. They used a least square curve fit technique and monthly average soil temperatures to form annual cycles, which is very similar to the analysis done in this research. Other investigators have used the Fourier series technique as an alternative to the least square method for curve fitting.

According to Kusuda “the Fourier series technique is applicable only to a single complete cycle where data points consist of a unique set of temperatures for equally incremented time coordinates”. The use of a simple harmonic function and the least square method were deemed the most appropriate in this research. Since the number of data points, the time interval for the temperature observations and the number of data for a given time is not restricted as they are in a Fourier analysis. This is especially useful in dealing with the Thompson data as they are not available at a specific time interval.

The least squares technique fits a sinusoidal curve to the observed data in such a manner that the variance calculated from the residual deviations of the observed temperature from the fitted curve is a minimum. GNU PLOT was the program used to obtain the curve fit.

The function representing periodic soil temperatures has four parameters: the thermal diffusivity (which will be explained in more detail in the Two-dimensional section), average temperature, annual amplitude, and the phase angle of the temperature cycle.

A3.1 Separate Method

Equations (A.1) and (A.2) are the functions used for the cyclic temperature equation at a given depth in the Separate method.

$$T(t) = T_0 - (T_s^* - T_0) \cos [\omega(t - 0.5\Delta.) - \Theta] \quad (\text{A.1})$$

$$T(t) = a_0 - a_1 \cos [\omega(t - 0.5\Delta.) - a_2] \quad (\text{A.2})$$

where:

T Soil temperature, °C

$\omega = \frac{2\pi}{n \cdot \Delta t}$ Frequency of the temperature cycle, rad/s

$n = 12$ $\Delta t = 2.592 \times 10^6$ s (Winnipeg)

$n = 360$ $\Delta t = 8.640 \times 10^4$ s (Thompson)

$a_0 = T_0$ Annual average soil temperature, °C

$a_1 = (T_s^* - T_0)$ Annual amplitude of temperature cycle, °C

$a_2 = \Theta$ Phase angle of soil cycle, rad

The raw data of soil temperature versus time for a given depth are used with Equation (A.1) and (A.2) to determine the above parameters.

A.3.2 Two-Dimensional Method

In the Two-Dimensional method, the annual periodic cyclic temperature is not only fitted with time as in the Separate Method but it is also fitted with depth. Therefore, all the

temperatures at each depth are fitted simultaneously. The resulting equation is a function of two dimensions, time and depth “y”.

$$T(y, t) = T_0 - (T_s^* - T_0) \cdot \exp\left(-y \sqrt{\frac{\omega}{2\alpha}}\right) \cdot \cos\left[\omega(t - 0.5\Delta t) - y \sqrt{\frac{\omega}{2\alpha}} - \Theta\right] \quad (\text{A.3})$$

$$T = g_0 - g_1 \cdot \exp(-y \cdot g_2) \cdot \cos[\omega(t - 0.5\Delta t) - y \cdot g_2 - g_3] \quad (\text{A.4})$$

where

T	Soil temperature, °C
y	Depth distance from ground surface, m
$\omega = \frac{2\pi}{n \cdot \Delta t}$	Frequency of the temperature cycle, rad/s
n = 12	$\Delta t = 2.592 \times 10^6$ s (Winnipeg)
n = 360	$\Delta t = 8.640 \times 10^4$ s (Thompson)
$g_0 = T_0$	Annual average soil temperature, °C
$g_1 = (T_s^* - T_0)$	Annual amplitude of temperature cycle, °C
$g_2 = \sqrt{\frac{\omega}{2\alpha}}$	
$g_3 = \Theta$	Phase angle of soil cycle, rad

The temperature decay in depth seen earlier is approximated by the exponential function in the Two-Dimensional method. The phase angle explains the point of the temperature sinusoidal curve at which the analysis commences. The starting point is the first day of January. The thermal diffusivity is calculated from the resulting value of g_2 . Therefore, only one thermal diffusivity α is calculated, as explained shortly.

To test the accuracy of the curve fit, higher orders of harmonic terms were added to Equation (A.4). However, the results obtained show that higher harmonic terms end up cancelling each other out, thereby making no additional contribution.

The results from the curve fit equations from the Separate Method and the Two-Dimensional Method are plotted along with the original soil temperature data. These plots give an easy appreciation of the accuracy of both methods, especially of the Two-Dimensional Method which was the equation used in this research. Figure A.2 through Figure A.8 correspond to the soil depths of 5, 10, 20, 50, 100, 150 and 300 cm for Winnipeg. Figure A.9 through Figure A.14 correspond to the soil depth of 5, 10, 20, 50, 100 and 150 cm for Thompson.

As seen from the temperature plots in Figure A.2 through Figure A.8 for Winnipeg and Figure A.9 through Figure A.14 for Thompson the annual amplitude of soil temperatures decreases with increasing depth distance. From Table A.2 and Table A.5 one can see that the annual average temperature (a_0) at each depth remains relatively the same. Some irregularities were noticed near the surface especially in the data analysis of Thompson. The Thompson data contains another set of temperature depth at 2.5cm from the surface. When analyzing this data set, large irregularities were noticed when compared to the rest of the other depth data sets. It was therefore, agreed to exclude the temperature data set at 2.5cm as they introduced too large of a discrepancy. Such irregularities near the ground surface have also been experienced by researchers Kusuda and Achenbach (1965), which they attributed to climatic conditions and soil near the surface not being entirely homogeneous. For instance, soil density and water content are most likely to vary near the surface. The average RMS (Root Mean Square) error for the curve fit functions compared to the actual soil data are 0.86125 and 2.23343 for Winnipeg for Thompson, respectively.

From the results of the coefficients the thermal diffusivity was calculated. This value is used in determining the thermal properties that were used in this research which is explained in detail in Appendix B. Yet, the Separate Method has the disadvantage of yielding two possibly different thermal diffusivities for a given set of temperature data. The diffusivities were calculated from:

- a) The difference of logarithmic amplitudes
- b) The difference of phase angles.

This disagreement of the results was also experienced by Kusuda (1966). According to Kusuda the diffusivities calculated did not agree, differing by a factor of two in some instances. Also, even when employing a consistent method to compute the diffusivities at two different depth levels for the same station, two different estimates of the diffusivities were obtained. As is Kusuda's case, two different diffusivities were also obtained in this research. The problem was overcome by the use of the Two-Dimensional method. From this method, a single thermal diffusivity is obtained from Equation (A.5).

The Thermal diffusivities are calculated from the values of g_2 in Tables A.3 and A.6 for Winnipeg and Thompson, respectively.

$$g_2 = \sqrt{\frac{\omega}{2\alpha}} \quad (\text{A.5})$$

As found in the previous section the soil annual temperature averages at different depths are all the same. This indicates that by extrapolating this average the surface will also have the same average. The Two-Dimensional method equation is then ideal to use for the ultimate objective, which is to find an equation that will predict the transient soil temperature at the surface. The equation can be easily extended to the surface by having $y = 0$ [m] as follows:

$$T_s = g_0 - g_1 \cos [\omega (t - 0.5 \Delta t) - g_3] \quad (\text{A.6})$$

$$T_s = T_0 - (T_s^* - T_0) \cos [\omega (t - 0.5 \Delta t) - g_3] \quad (\text{A.7})$$

Winnipeg $g_2 = 0.5072$ $\alpha = 3.9267 \times 10^{-7}$ [m²/s]

Thompson $g_2 = 0.8858$ $\alpha = 1.2871 \times 10^{-7}$ [m²/s]

Where: $\omega = 2.0201 \times 10^{-7}$ [rad/s]

The surface temperature results from Equation (A.6) for Winnipeg and Thompson soil temperature data were plotted and summarized in Section 6.3.2. The coefficients obtained from the Separate Method and Two-Dimensional Method curve fit are summarize for each soil depth in Tables A.2 and A.3 for Winnipeg and Tables A.5 and A.6 for Thompson.

A.4 Soil Temperature Data

The soil temperature data were chosen for two locations in the province of Manitoba: the city of Winnipeg and the town of Thompson. These two locations were studied to calculate the transient surface soil temperature equation. For the city of Winnipeg the soil temperature data came from Environment Canada. Environment Canada takes readings at specified depths from undisturbed open flat fields with possible grass cover. Environment Canada (Environment Canada, 2002) has been taking readings for numerous years. For instance, Winnipeg's soil temperature readings have been taken since 1938 to 1993. The readings are taken constantly over daily intervals and in some cases hourly intervals. The readings are then averaged over that many years to produce monthly readings. The soil temperature values at the different depths are tabulated in Table A.3.

Soil temperature data in less populated regions are not taken by Environment Canada. However, Agriculture Manitoba has soil temperature data collected at many isolated regions and less populated northern towns. These readings are often taken at places where Environment Canada has no available soil temperature information. The data used for Thompson were taken from this agency (Bullock, 2003).

The way in which these data are collected is not as consistent as that of Environment Canada. The readings have been taken over a period of eight years. During the year, random readings are taken. Consequently, the readings are published as sole daily readings with their date noted. In order to be used as input to the curve fit procedure, the

data were recalculated and plotted over a 360-day year as opposed to a normal 365-day year. This was done to maintain consistency in the period of time with the other curve fit equation for Winnipeg and with the time intervals in the numerical analysis, which is also of 360-day years. The data were analyzed and some data point readings were excluded. The data points excluded were those which seem like anomalies with respect to the majority of the data points. Although, the data from Agriculture Manitoba are not as consistent as the long-term average values for Environment Canada, they are a still valid source of data for the soil temperature variation near Thompson. The soil temperature values for Thompson are included in Table A.6.

According to Kusuda and Achenbach (1965), many parameters affect the temperature of the soil. Surface condition such as snow, grass covered or bare with a concrete surface will affect the soil temperature. Other parameters such as climatic conditions, soil thermal properties such as density, moisture content etc. will also affect the temperature of the soil. It is therefore almost unattainable to exactly predict future soil temperature at any given location and time, especially close to the surface where these effects are likely to influence more extensively the soil temperature. The soil temperature predictions are of a statistical nature and some deviation from the true value is expected to take place.

Table A.1 Winnipeg coefficients for the separate method

Separate Method			
Depth Below Surface [cm]	Average (a_0)	Amplitude (a_1)	Phase Angle (a_2)
5	4.9250	11.3015	0.4897
10	5.3750	11.1252	0.5417
20	5.6333	10.6400	0.6070
50	5.7333	9.2881	0.7765
100	5.7750	7.3814	1.0462
150	5.7583	6.0630	1.2806
300	5.8750	2.6337	2.1429

Table A.2 Winnipeg coefficients for the two-dimensional method

2-D Method	
g0	5.5821
g1	11.8550
g2	0.5072
g3	0.5007

Table A.3 Observed monthly average earth temperatures

Source: Canadian Climate Data 9 ©1994 Environment Canada
 Location: Winnipeg International Airport, Manitoba (49°54'N 97°14'W, 239m, 1938 to 1993)
 ID: 5023222, User Calculated Means For (1961-1990)

Depth Below Surface [cm]	Month of Year											
	1	2	3	4	5	6	7	8	9	10	11	12
5	-5.2	-5.0	-2.5	1.1	7.1	13.5	17.1	16.5	12.4	6.5	1.0	-3.4
10	-4.4	-4.5	-2.3	1.0	6.9	13.4	17.2	17.0	13.2	7.5	1.9	-2.4
20	-3.6	-3.8	-2.0	0.7	6.2	12.8	16.8	17.0	13.6	8.3	2.9	-1.3
50	-1.6	-2.4	-1.5	-0.1	4.2	10.6	15.0	16.0	13.8	9.4	4.7	0.7
100	0.9	-0.2	-0.4	0.0	2.1	7.4	11.9	13.9	13.3	10.4	6.8	3.2
150	2.5	1.3	0.7	0.6	1.5	5.2	9.4	12.0	12.4	10.7	7.9	4.9
300	6.4	5.3	4.4	3.7	3.3	3.5	4.8	6.6	7.9	8.6	8.4	7.6

Table A.4 Thompson coefficients for the separate method

Separate Method			
Depth Below Surface [cm]	Average (a_0)	Amplitude (a_1)	Phase Angle (a_2)
5	2.62476	9.49471	0.596501
10	2.37669	7.88059	0.661836
20	1.61734	7.16958	0.803857
50	2.39844	5.68074	1.12721
100	2.38408	3.77029	1.45188
150	2.59871	2.5674	1.79451

Table A.5 Thompson coefficients for the two-dimensional method

2-D Method	
g0	2.35946
g1	8.94906
g2	0.885839
g3	0.590835

Table A.6 Observed daily average earth temperatures for Thompson at different depths

Day #	Depth (cm)					
	5	10	20	50	100	150
29.5	-3.2	-2.7	X	-0.3	1.1	2.7
61.5	-4.5	-3.8	-3.2	-2.1	0.5	0.9
78.5	-2.8	-2.8	-2.8	-1.1	0	0.6
84.5	0.1	0.2	0.2	0.5	1.3	2
98.5	1.3	1.3	1.1	-0.1	-0.2	-0.3
104.5	2.3	2	3	2.7	X	X
126.5	0.6	0.6	0	0	0	0.6
126.5	-2.8	X	-2.8	0	0	2.8
130.5	-0.4	-0.4	-0.4	-0.7	-0.5	-0.2
134.5	0	0	0	0	0	0
145.5	7.8	4.4	2.2	1.7	1.7	1.7
146.5	6.8	3.8	0.4	-0.6	-0.5	-0.1
149.5	0.2	0.2	-0.2	-0.1	0.1	0.2
155.5	9.3	6.4	2.9	1.2	0.9	1.5
156.5	4.4	2.8	-0.2	-0.2	2.2	2.2
157.5	1.7	0.6	0	-0.6	-0.6	-0.6
158.5	10	8.3	7.8	2.8	2.8	3.3
163.5	7.2	4.4	2.8	-0.8	2.8	2.8
166.5	8.3	6.1	2.2	2.2	0	-0.6
168.5	8.8	6.8	5.1	2.2	0.1	0.5
170.5	9.4	8.3	6.1	2.8	2.8	2.2
172.5	11.1	8.3	6.1	3.9	1.1	1.1
174.5	11.1	8.3	6.1	2.8	1.1	1.1
177.5	12.2	7.8	3.9	1.7	1.7	1.7
178.5	14.4	10.6	7.8	4.4	2.2	2.2
182.5	X	11.7	10.6	6.7	2.2	2.2
183.5	12.2	8.9	5.6	2.2	0	-0.6
187.5	7.8	7.8	7.8	5.6	2.2	1.1
190.5	14.4	11.1	7.8	3.3	1.7	1.7
197.5	11.1	8.9	6.1	3.9	0.6	0.6
199.5	13.3	11.7	9.4	7.8	4.4	2.8
204.5	13.9	11.7	8.9	8.3	6.1	4.4
207.5	13.3	11.1	8.9	7.8	3.3	0

Day #	Depth (cm)					
	5	10	20	50	100	150
208.5	11.7	9.4	6.1	X	2.2	1.1
214.5	17.2	15	X	11.1	7.2	4.4
216.5	14.4	13.3	11.7	10.6	7.8	5
218.5	13.3	12.2	11.1	10.6	8.3	6.1
221.5	17.8	14.4	11.7	10	7.8	5.6
225.5	X	X	12.2	7.8	3.9	1.7
226.5	X	X	X	12.8	X	X
228.5	15.6	14.4	X	11.1	7.8	5.1
235.5	10.6	9.4	10	9.4	7.8	5.6
235.5	11.1	11.1	10.6	8.9	7.2	6.1
237.5	6.3	7.2	8.8	8.4	6.8	X
241.5	8.9	8.3	7.8	6.7	5.6	3.9
241.5	X	X	X	12.8	X	X
245.5	X	7.2	8.2	8.4	7.2	5.7
249.5	8.9	8.9	8.3	8.3	7.8	6.1
253.5	7.1	6.3	6.7	6.8	5.4	4.2
255.5	11.7	11.1	11.1	11.1	X	X
255.5	9.1	8.3	8.4	8.3	7.9	6.8
256.5	10.6	8.9	7.8	6.7	5	3.9
258.5	7.1	6.2	5.7	5.3	4.3	3.6
259.5	6.7	7	7.3	7.3	6.3	5.1
260.5	11.7	8.9	7.2	6.7	5.6	4.4
261.5	6.5	6.6	6.8	7.4	6.8	5.7
263.5	X	7.8	7.8	7.8	6.1	5
279.5	X	1.7	2.8	3.9	4.4	4.4
280.5	6.7	6.7	7.2	7.8	7.8	7.2
288.5	6.1	7.8	8.3	8.3	7.8	7.8
291.5	7.8	6.1	4.4	4.4	5.6	6.1
304.5	0.9	1.2	2	2.3	3.1	3.9
310.5	-0.6	0	1.7	2.8	3.3	3.9
314.5	-1.7	0.6	0	1.7	2.8	3.3
338.5	-4.8	-3.5	-7.7	1.1	2.1	2.9
345.5	-2.2	-1.9	-1.5	-0.4	0.3	1

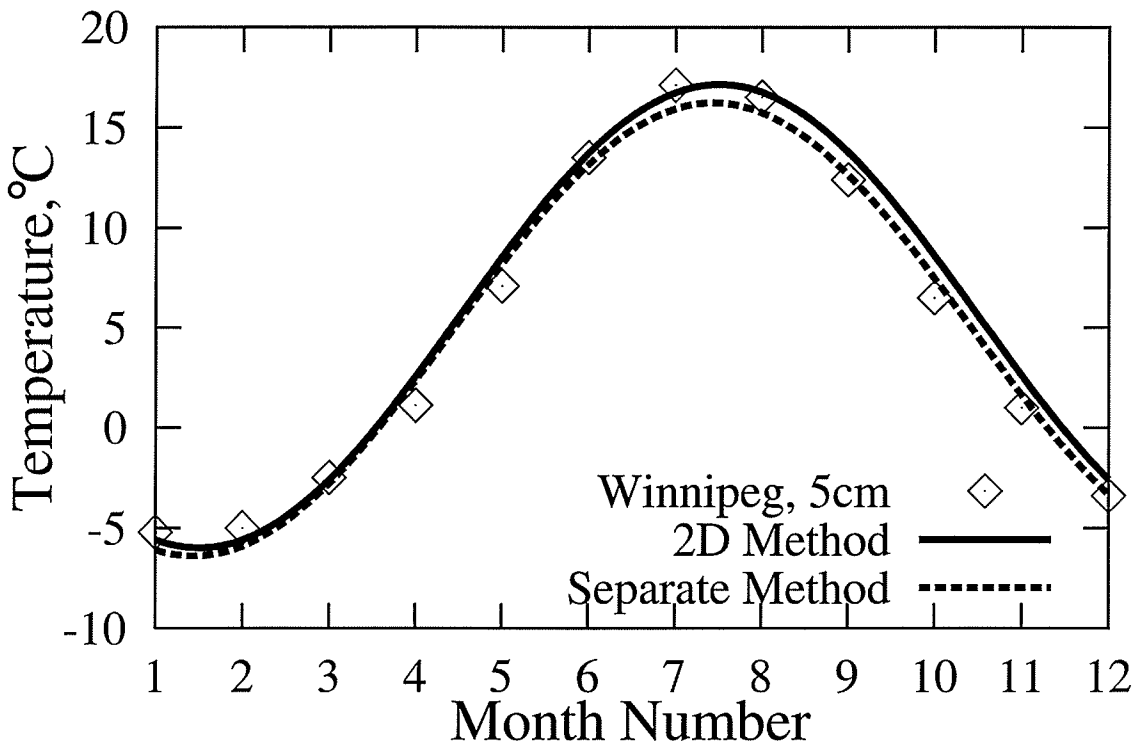


Figure A.2 Temperature versus month for Winnipeg, 5 cm

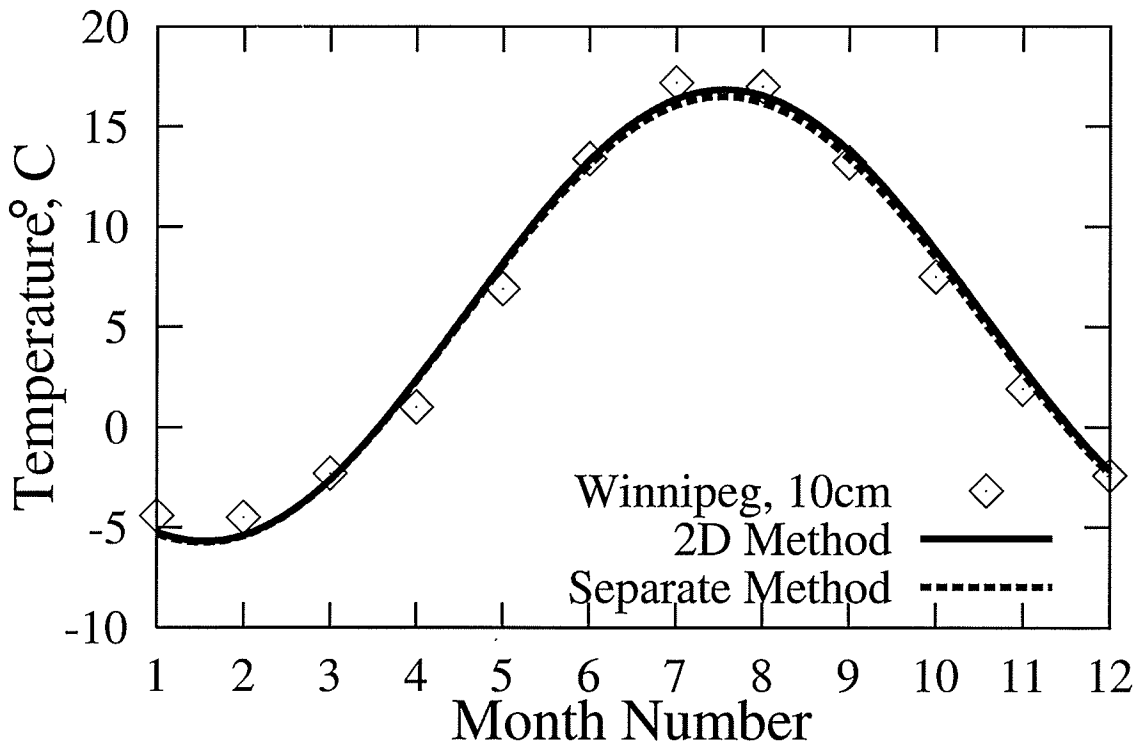


Figure A.3 Temperature versus month for Winnipeg, 10 cm

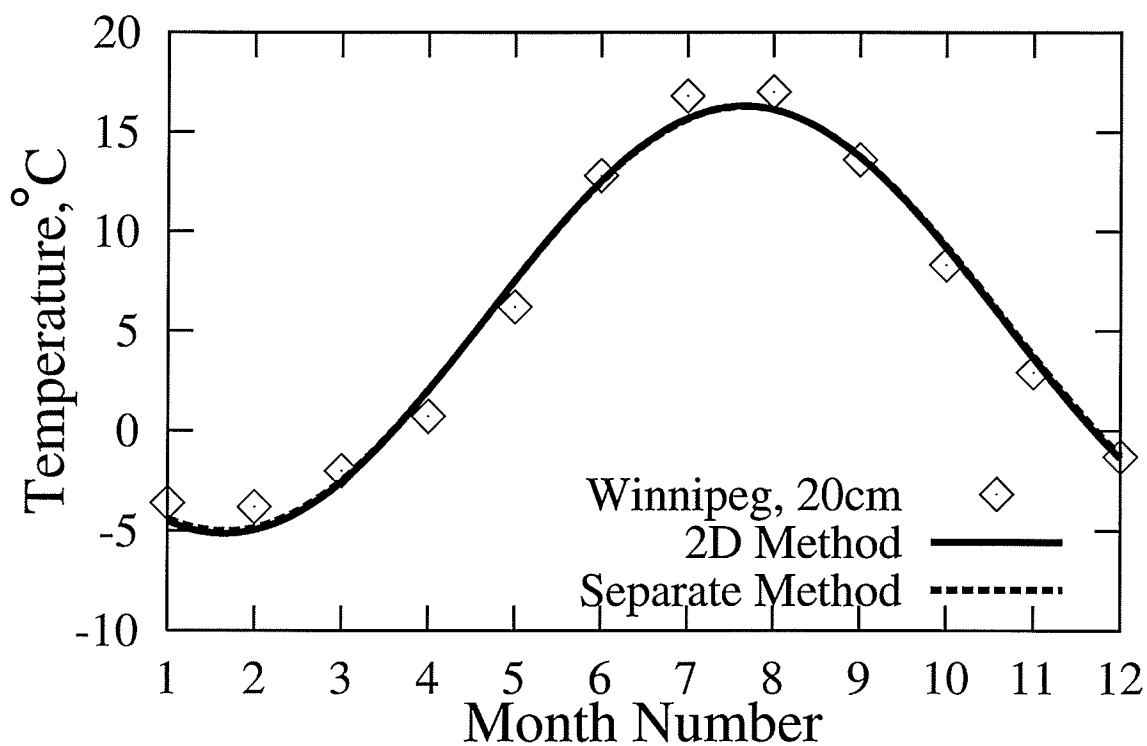


Figure A.4 Temperature versus month for Winnipeg, 20 cm

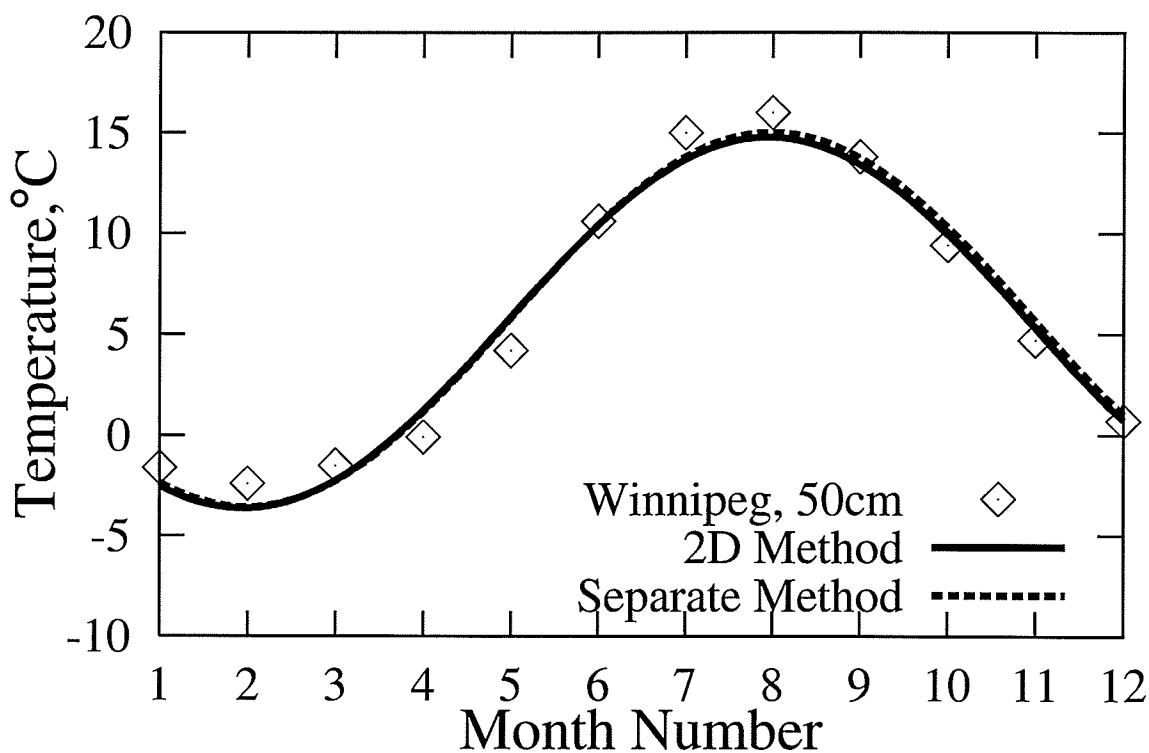


Figure A.5 Temperature versus month for Winnipeg, 50 cm

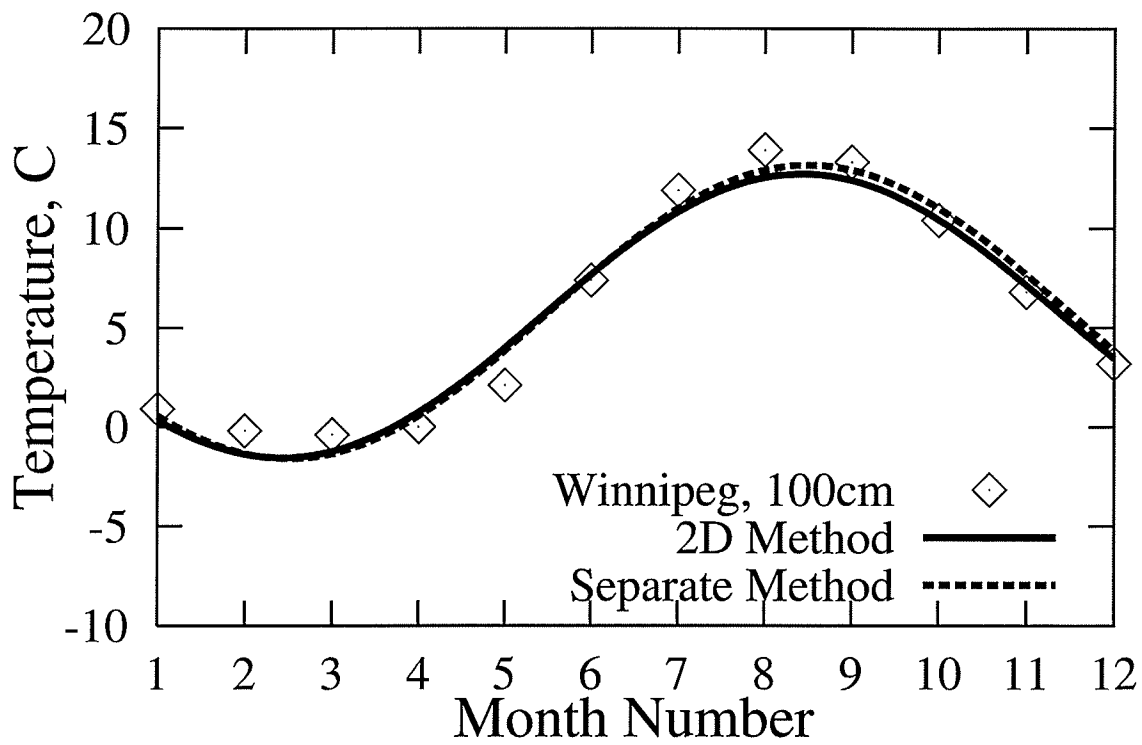


Figure A.6 Temperature versus month for Winnipeg, 100 cm

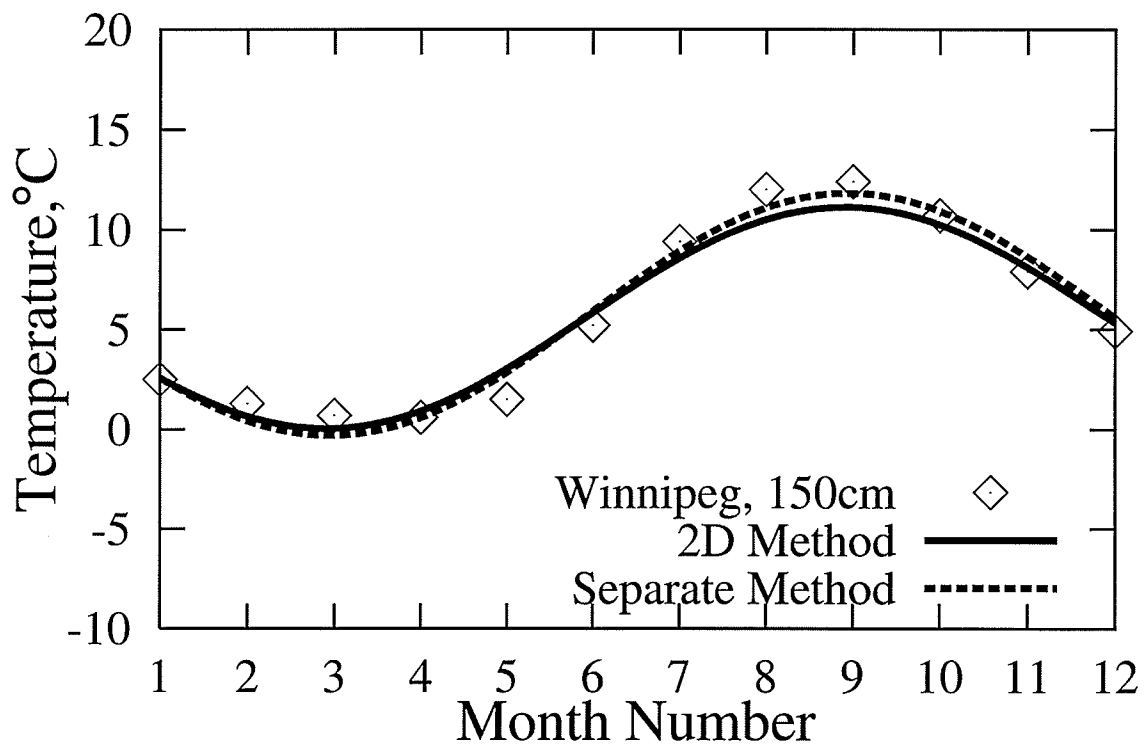


Figure A.7 Temperature versus month for Winnipeg, 150 cm

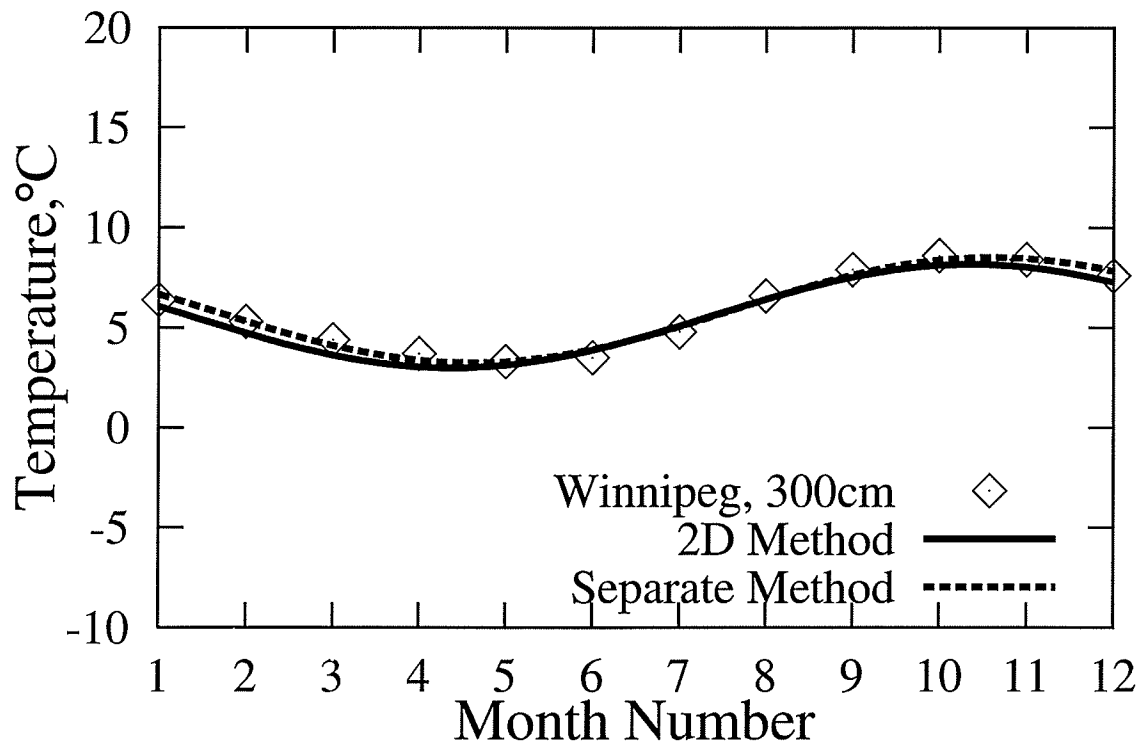


Figure A.8 Temperature versus month for Winnipeg, 300 cm

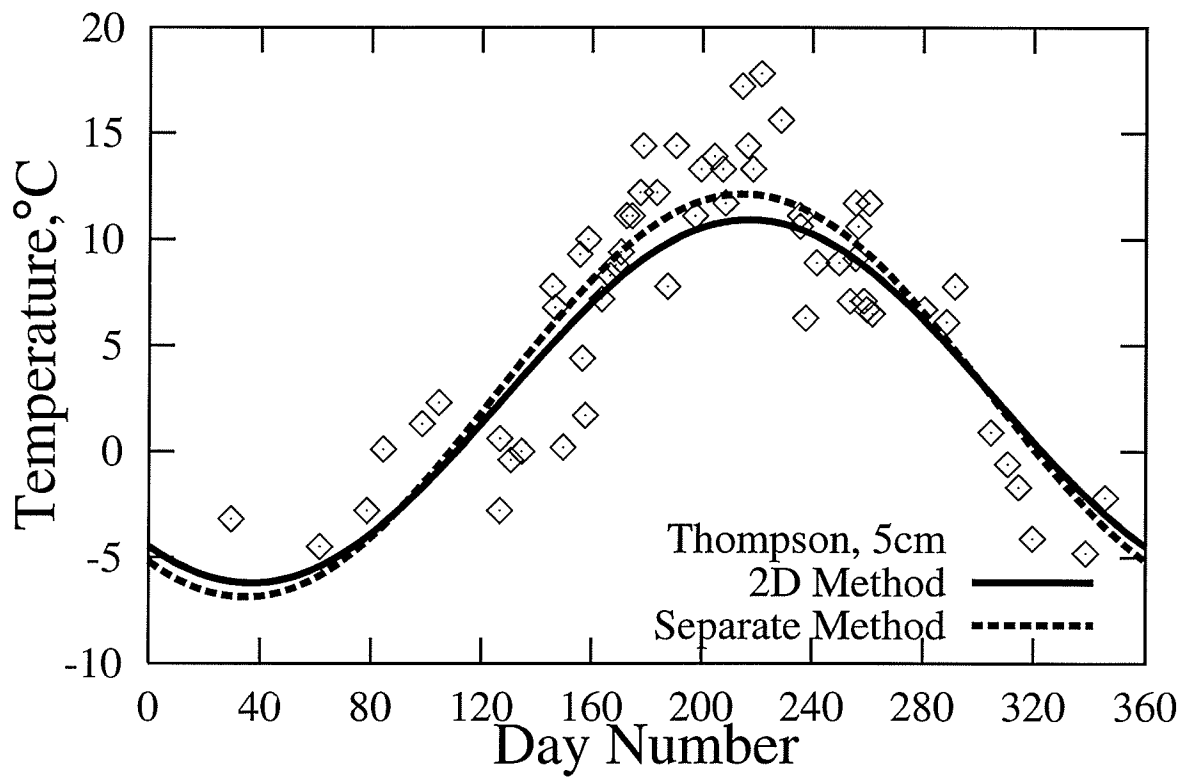


Figure A.9 Temperature versus month for Thompson, 5 cm

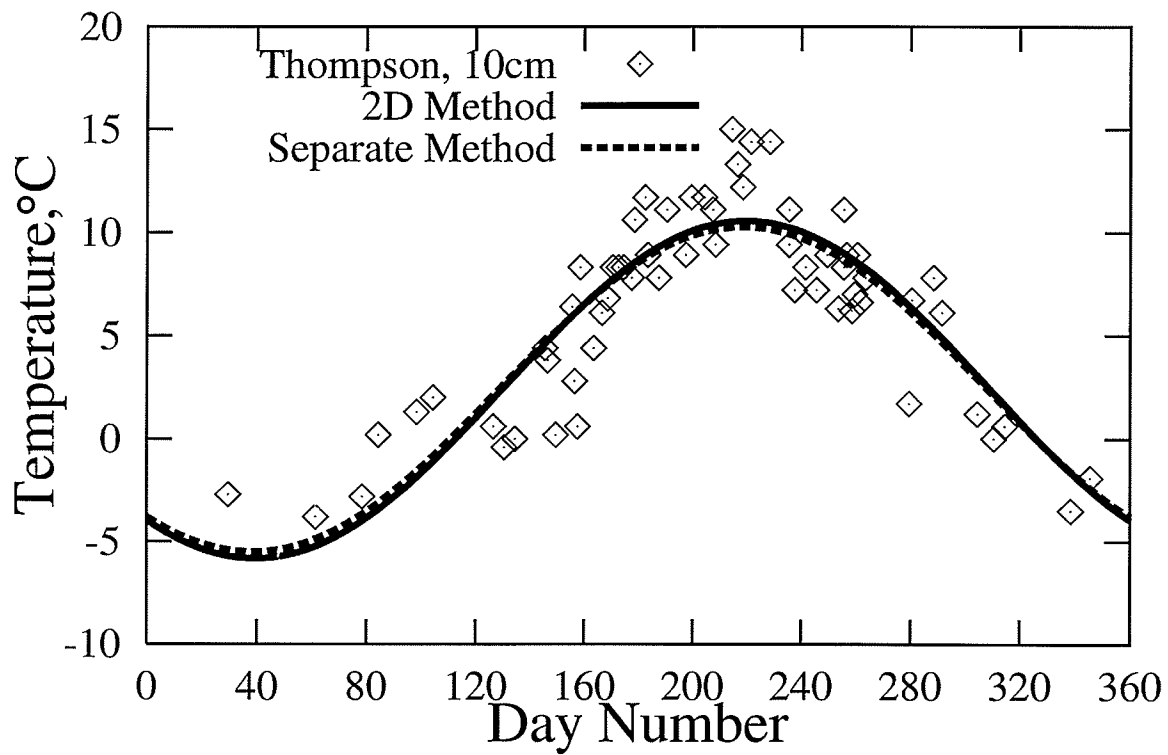


Figure A.10 Temperature versus month for Thompson, 10 cm

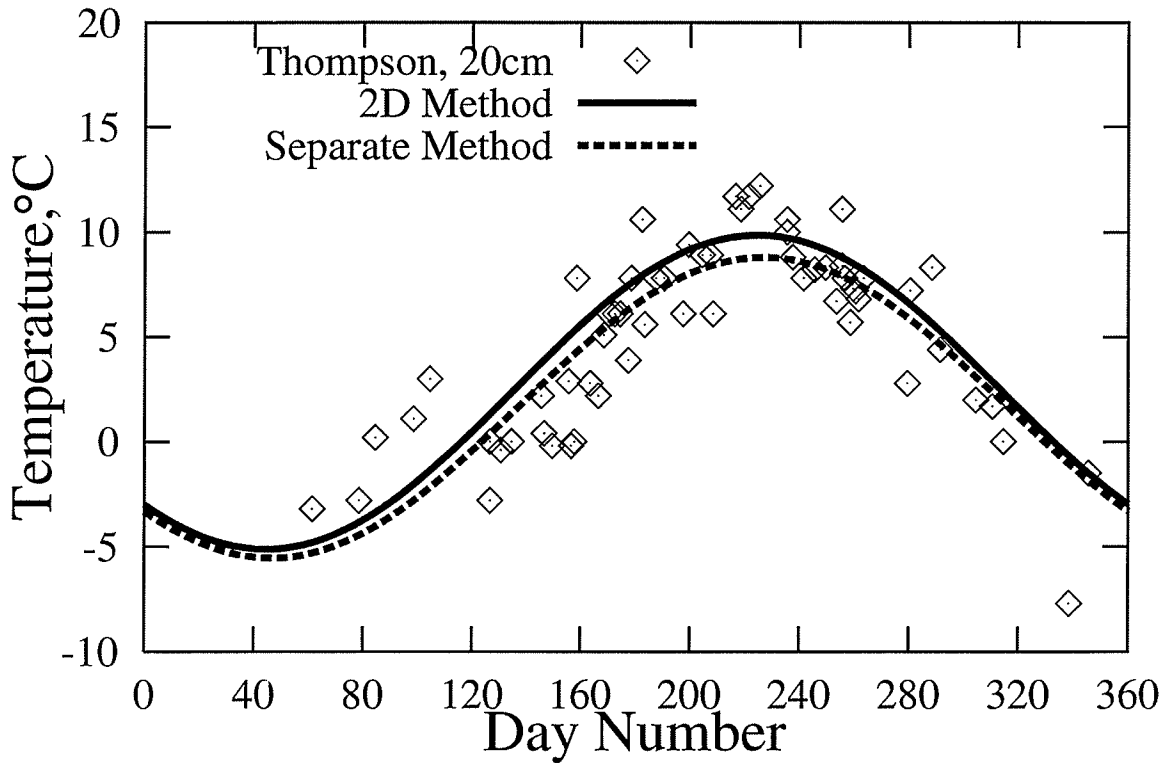


Figure A.11 Temperature versus month for Thompson, 20 cm

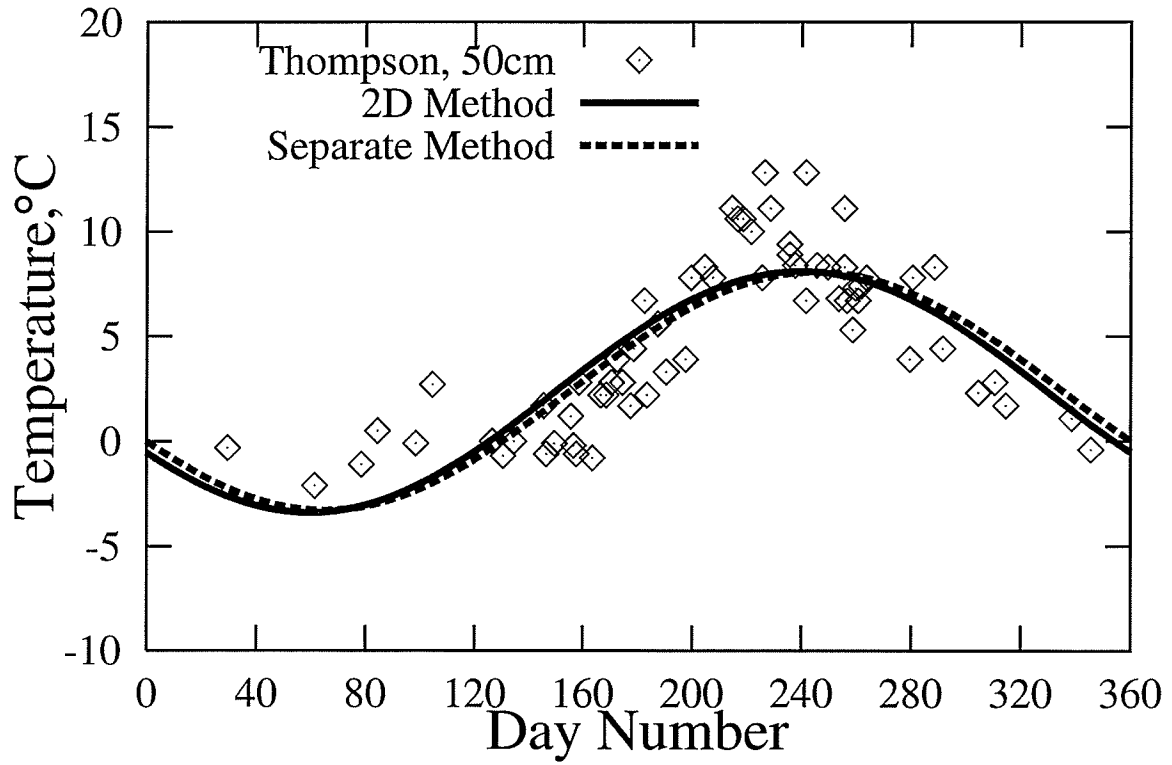


Figure A.12 Temperature versus month for Thompson, 50 cm

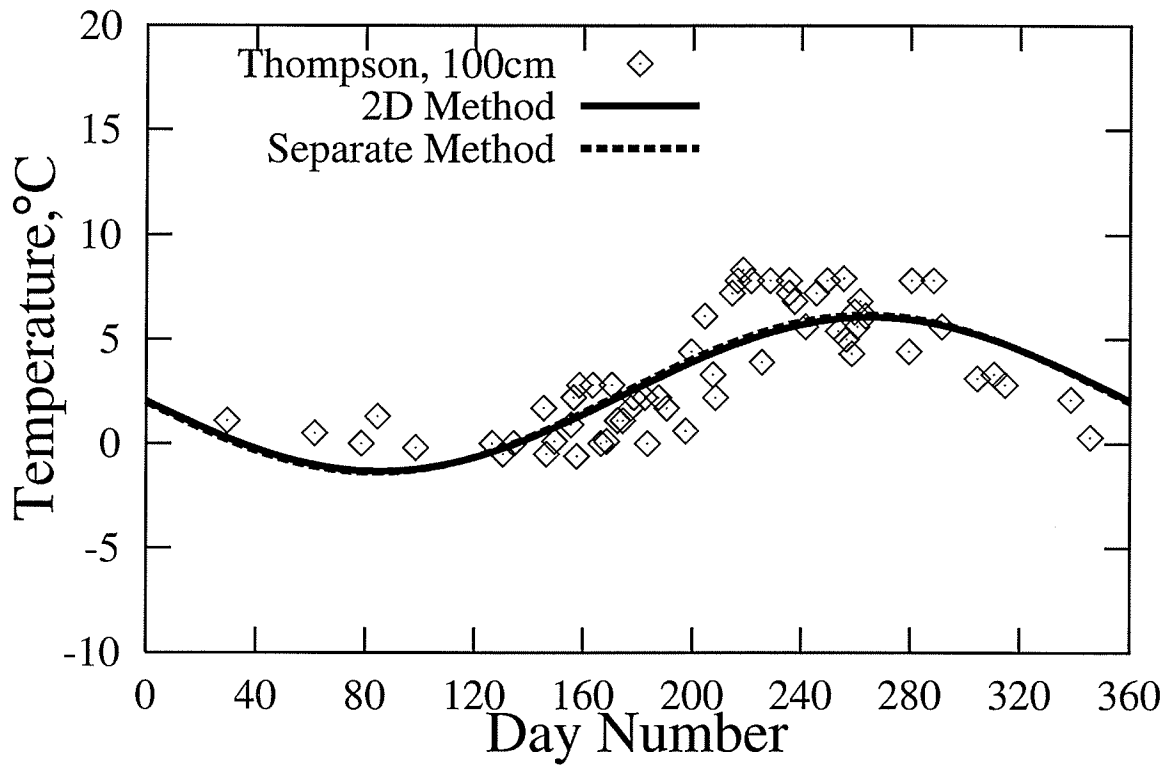


Figure A.13 Temperature versus month for Thompson, 100 cm

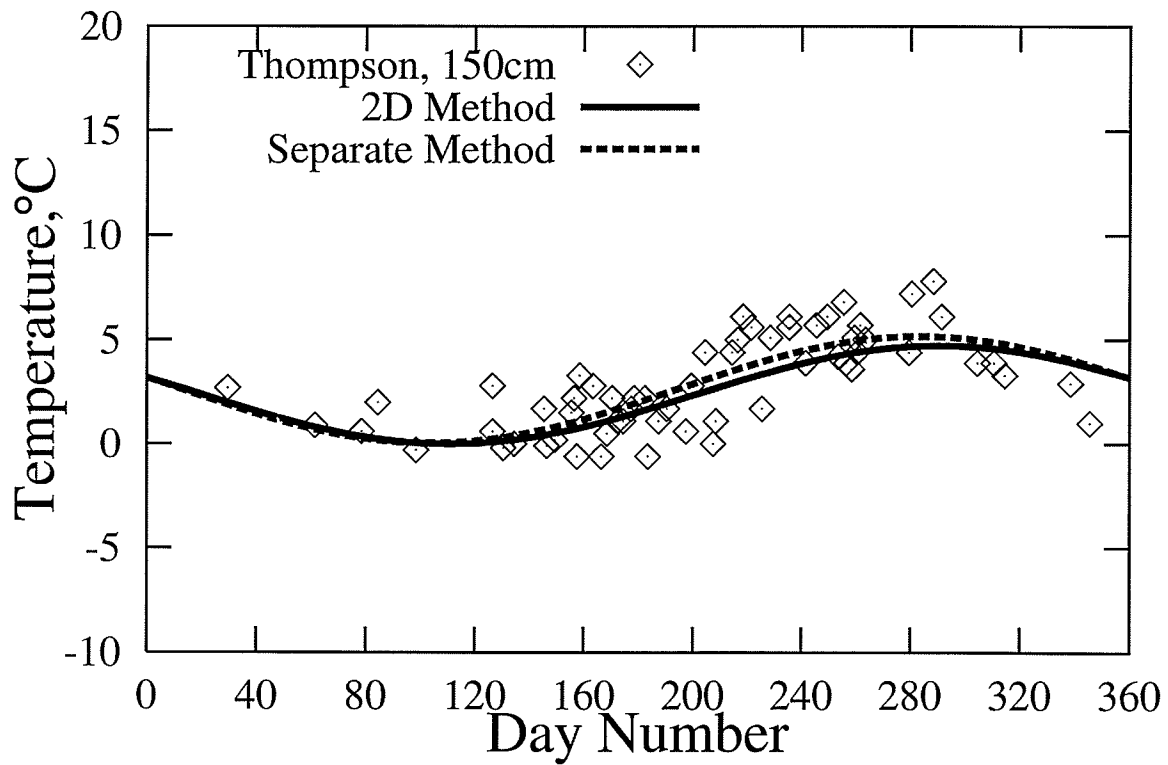


Figure A.14 Temperature versus month for Thompson, 150 cm

Appendix B

MATERIAL PROPERTIES

This appendix includes the properties for the materials used in the numerical simulation. These include soil, gravel, insulation and concrete. Among these, the soil properties are by far the most difficult to estimate. The following subsections discuss the properties for each material.

B.1 Soil

Soil is denoted as all the unconsolidated material in the crust of the earth. Soil is present at every construction site as it envelops and supports building foundations. Soil consist of particles of different sizes, all derived from solid rock (Legget, 1960). Soil particle composition determines the type of soil, such as sand, silts and clays. In nature there are soils composed of mixtures of this particles.

Canada's soil varies in composition in different regions due to its diverse geography. According to Legget (1960), various geological processes have transported soil particles from their original location. Particles transported by wind (aerolian soils) exist in notable deposits in western Canada. All over Canada are found deposits of glacial till, a mixture of gravel, sand, silt and clay, which were transported as glaciers receded. Also, well graded deposits of sand, silt or clay washed down from glaciers, were sorted by the action of water. On the Prairies and in river valleys such as the St. Lawrence valley are great deposits of clay that steamed from glacial lakes. Winnipeg's soil consists of a large percentage of clay, the remains of Lake Agassiz. Marine glacial deposits and clay are found in Ottawa and Montreal. Toronto soil is a mixture of glacial till, fresh water clays and sand deposits.

The type of soil not only has different physical characteristics but also denotes slight differences in its thermal characteristics. In Appendix A the thermal diffusivity for

Winnipeg and Thompson was derived from a curve fit of soil temperatures at different depths. The temperature data readings were taken throughout a year. From the curve fit the thermal diffusivity values were calculated to be:

$$\text{Winnipeg} \quad \alpha = 3.9267 \times 10^{-7} \text{ [m}^2\text{/s]}$$

$$\text{Thompson} \quad \alpha = 1.2871 \times 10^{-7} \text{ [m}^2\text{/s]}$$

The thermal properties were obtained by approximating the thermal diffusivity to the thermal properties of the type of soil that exist at Winnipeg and Thompson. For Winnipeg a mixture of moist soil and clay is assumed. For Thompson a dry soil is assumed. The thermal properties were obtained from an extensive search of soil thermal properties in literature as summarized in Table B.1.

From the overall properties from Table B.1, Winnipeg's representative soil properties were chosen to be:

$$k = 1.2 \text{ [W/m}\cdot\text{K]}$$

$$\rho = 1800 \text{ [kg/m}^3\text{]}$$

$$C_p = 1666 \text{ [J/kg}\cdot\text{K]}$$

$$\alpha = 4.0016 \times 10^{-7} \text{ [m}^2\text{/s]}$$

For Thompson the representative soil properties were chosen to be:

$$k = 0.52 \text{ [W/m}\cdot\text{K]}$$

$$\rho = 2050 \text{ [kg/m}^3\text{]}$$

$$C_p = 1840 \text{ [J/kg}\cdot\text{K]}$$

$$\alpha = 1.3786 \times 10^{-7} \text{ [m}^2\text{/s]}$$

The thermal diffusivity obtained from the thermal properties chosen was approximated as close as possible to those calculated from Appendix A.

B.2 Insulation

Among the insulation materials, there are those that resist water absorption less effectively than others. It is widely recognized in the scientific community that water absorption in insulation results in thermal degradation. According to Danuluk (1997), “extruded polystyrene is usually recommended when the insulation is to be buried. Its closed-cell design inhibits moisture absorption, thus enabling its thermal resistance to remain high. Expanded polystyrene may be used if precautions are taken to limit its exposure to moisture”. Crandell *et al.* (1994), mentions that in cases where bearing structural loads from footings is required, higher density polystyrenes for the required compressive strengths may be used. In the Galena, Alaska study, Danuluk (1997) chose extruded polystyrene for the insulation requirements. Danuluk used extruded Polystyrene for edge and skirt insulation as well as under the slab in compressive loading. As a result, extruded Polystyrene was determined to be the best representative insulation for this study.

Extruded Polystyrene thermal properties obtained from Incropera and DeWitt (1996) are as follows:

$$k = 0.027 \text{ [W/m}\cdot\text{K]}$$

$$\rho = 55 \text{ [kg/m}^3\text{]}$$

$$C_p = 1210 \text{ [J/kg}\cdot\text{K]}$$

$$\alpha = 4.0571 \times 10^{-7} \text{ [m}^2\text{/s]}$$

B.3 Gravel

In the regions where gravel was used, the thermal properties for Sand/Gravel Aggregate (dried) from Mills (1992) were used.

$$k = 1.296 \text{ [W/m}\cdot\text{K]}$$

$$\rho = 2240 \text{ [kg/m}^3\text{]}$$

$$C_p = 920 \text{ [J/kg}\cdot\text{K]}$$

$$\alpha = 6.2888 \times 10^{-7} \text{ [m}^2\text{/s]}$$

B.4 Concrete

Thermal properties from Incropera and DeWitt (1996) for concrete (stone mix) are used in this study. These are as follows:

$$k = 1.4 \text{ [W/m}\cdot\text{K]}$$

$$\rho = 2300 \text{ [kg/m}^3\text{]}$$

$$C_p = 880 \text{ [J/kg}\cdot\text{K]}$$

$$\alpha = 6.9170 \times 10^{-7} \text{ [m}^2\text{/s]}$$

Table B.1 Soil thermal properties found in literature

Soil Description	Literature Source	k [W/m·K]	ρ [kg/m ³]	Cp [J/kg·K]	α [m ² /s]
Soil, Low (Upper) Thermal Characteristic	Mitalas (1987)	0.80	-	-	-
Soil, Low (Lower) Thermal Characteristic	Mitalas (1987)	0.90	-	-	-
Soil, Medium (Upper) Thermal Characteristic	Mitalas (1987)	1.20	-	-	-
Soil, Medium (Lower) Thermal Characteristic	Mitalas (1987)	1.35	-	-	-
Soil, High (Upper) Thermal Characteristic	Mitalas (1987)	1.80	-	-	-
Soil, High (Lower) Thermal Characteristic	Mitalas (1987)	2.00	-	-	-
Soil, Dry	Ingersoll (1988)	0.35	1682	-	-
Soil, 15%Moisture	Ingersoll (1988)	1.38	-	-	-
Soil, 30%Moisture	Ingersoll (1988)	1.90	-	-	-
Soil, Dry W.C. 0 %, P. 40 %	Ingersoll (1988)	0.35	-	-	2.8000X10 ⁻⁷
Soil, Dry W.C. 0 %, P. 20 %	Ingersoll (1988)	0.62	-	-	3.7000X10 ⁻⁷
Soil, Arid W.C. 1 %, P. 40 %	Ingersoll (1988)	0.46	-	-	3.5000X10 ⁻⁷
Soil, Arid W.C. 2 %, P. 40 %	Ingersoll (1988)	0.57	-	-	4.3000X10 ⁻⁷
Soil, Humid W.C. 9 %, P. 20 %	Ingersoll (1988)	2.17	-	-	1.0600X10 ⁻⁶
Soil, Moist W.C. 15 %, P. 40 %	Ingersoll (1988)	1.38	-	-	7.3000X10 ⁻⁷
Soil, Moist W.C. 25 %, P. 40 %	Ingersoll (1988)	1.75	-	-	7.6000X10 ⁻⁷
Soil, Moist W.C. 30 %, P. 40 %	Ingersoll (1988)	1.90	-	-	7.6000X10 ⁻⁷
Soil, Moist W.C. 15 %, P. 20 %	Ingersoll (1988)	2.50	-	-	1.0900X10 ⁻⁶
Soil, Wet W.C. 35 %, P. 40 %	Ingersoll (1988)	2.04	-	-	7.5000X10 ⁻⁷
Soil, Wet W.C. 20 %, P. 25 %	Ingersoll (1988)	2.39	-	-	9.9000X10 ⁻⁷
Soil, Wet W.C. 18 %, P. 20 %	Ingersoll (1988)	2.62	-	-	1.0800X10 ⁻⁶
Soil, Saturated W.C. 40 %, P. 40 %	Ingersoll (1988)	2.16	-	-	7.4000X10 ⁻⁷
Soil, Saturated W.C. 20 %, P. 20 %	Ingersoll (1988)	2.68	-	-	1.0700X10 ⁻⁶

Table B.1 (Continued)

Soil Description	Literature Source	k [W/m·K]	ρ [kg/m ³]	Cp [J/kg·K]	α [m ² /s]
Soil, Property Groups Base Case	Bahnfleth and Pedersen (1990)	1.00	1200	1200	6.9444X10 ⁻⁷
Soil, Property Groups Case A	Bahnfleth and Pedersen (1990)	2.00	1700	1700	6.9204X10 ⁻⁷
Soil, Property Groups Case B	Bahnfleth and Pedersen (1990)	1.00	1700	1700	3.4602X10 ⁻⁷
Soil, Property Groups Case C	Bahnfleth and Pedersen (1990)	0.50	1200	1200	3.4722X10 ⁻⁷
Soil, Property Groups Case D	Bahnfleth and Pedersen (1990)	2.00	1500	1500	8.8889X10 ⁻⁷
Soil, Basement A, Run 1	Sobotka <i>et al.</i> (1994)	0.88(0.8-0.9)	-	-	3.3500X10 ⁻⁷
Soil, Basement A, Run 2	Sobotka <i>et al.</i> (1994)	0.88(0.8-0.9)	-	-	3.5500X10 ⁻⁷
Soil, Basement A, Run 3	Sobotka <i>et al.</i> (1994)	1.275(1.2-1.35)	-	-	4.2500X10 ⁻⁷
Soil, Basement A, Run 4	Sobotka <i>et al.</i> (1994)	1.90(1.8-2.0)	-	-	8.6400X10 ⁻⁷
Soil, Room C and D, Run 1	Sobotka <i>et al.</i> (1994)	0.85(0.8-0.9)	-	-	3.7000X10 ⁻⁷
Soil, Room C and D, Run 2	Sobotka <i>et al.</i> (1994)	0.85(0.8-0.9)	-	-	3.7000X10 ⁻⁷
Soil, Room C and D, Run 3	Sobotka <i>et al.</i> (1994)	1.275(1.2-1.35)	-	-	4.2500X10 ⁻⁷
Soil, Room C and D, Run 4	Sobotka <i>et al.</i> (1994)	1.90(1.8-2.0)	-	-	8.6400X10 ⁻⁷
Soil, Base Case	Krarti <i>et al.</i> (1995)	1.00	-	-	6.4500X10 ⁻⁷
Soil, Dry	Mills (1992)	1.00	1500	1900	3.5088X10 ⁻⁷
Soil, Wet	Mills (1992)	2.00	1900	2200	4.7847X10 ⁻⁷
Soil, Temperature Ref. 300K	Incropera and DeWitt (1996)	0.52	2050	1840	1.3786X10 ⁻⁷
Soil Undisturbed, Depth : 0-0.45 m	Adjali <i>et al.</i> (1998)	1.14	1611	2322	3.0475X10 ⁻⁷
Soil Undisturbed, Depth : -0.76 m	Adjali <i>et al.</i> (1998)	0.96	1506	1990	3.2033X10 ⁻⁷
Soil Undisturbed, Depth : -1.06 m	Adjali <i>et al.</i> (1998)	1.15	1810	1722	3.6897X10 ⁻⁷
Soil Undisturbed, Depth : -1.73 m	Adjali <i>et al.</i> (1998)	0.97	1836	1638	3.2254X10 ⁻⁷
Soil Undisturbed, Depth : -1.67 m	Adjali <i>et al.</i> (1998)	0.88	1863	1615	2.9248X10 ⁻⁷
Soil Undisturbed, Depth : -1.98 m	Adjali <i>et al.</i> (1998)	1.83	2014	1970	4.6124X10 ⁻⁷

Table B.1 (Continued)

Soil Description	Literature Source	k [W/m·K]	ρ [kg/m ³]	Cp [J/kg·K]	α [m ² /s]
Soil Undisturbed, Depth : Deep ground	Adjali <i>et al.</i> (1998)	1.09	1906	1682	3.4000X10 ⁻⁷
Soil, Solid Matter	Ingersoll (1988)	3.1(2.1-4.1)	2600	800	-
Quartz	Ingersoll (1988)	8.90	-	-	-
Sand (Average)	Ingersoll (1988)	3.50	-	-	-
Sand, Dry	Ingersoll (1988)	0.35	1522	-	-
Sand, 10%Moisture	Ingersoll (1988)	1.04	1602	-	-
Sand, Dry	Krarti <i>et al.</i> (1995)	-	-	-	2.3330X10 ⁻⁷
Sand, Wet	Krarti <i>et al.</i> (1995)	-	-	-	7.4290X10 ⁻⁷
Clay Minerals	Ingersoll (1988)	2.70	-	-	-
Clay, Dry	Ingersoll (1988)	0.52	2002	-	-
Clay, 30%Moisture	Ingersoll (1988)	2.42	2002	-	-
Clay, Dry	Krarti <i>et al.</i> (1995)	-	-	-	2.0000X10 ⁻⁷
Clay, Wet	Krarti <i>et al.</i> (1995)	-	-	-	5.4290X10 ⁻⁷
Organic Matter	Ingersoll (1988)	0.30	-	-	-
Peat, Dry	Krarti <i>et al.</i> (1995)	-	-	-	4.0000X10 ⁻⁸
Peat, Wet	Krarti <i>et al.</i> (1995)	-	-	-	1.0430X10 ⁻⁷

Appendix C
GEOMETRY PARAMETERS IN ENGLISH UNITS

The following tables give a summary of the horizontal and vertical parameters for each of the grid used in the cases simulated in this thesis. These tables give all values in English Units. Tables in SI Units were included as part of Section 6.1.2 ‘Geometries Studied’.

Table C.1 Horizontal and vertical parameters fixed for all grids used (see Figure 3.2)

Parameter	[in]
Px1	240.00
Px2	12.00
Px3	18.00
Px4	6.00
Py2	24.00
Py3	6.00
Py5	18.00
Py6	6.00
Py8	4.00
Py11	6.00
L1	270.00
L2	281.18

Table C.2 Values of horizontal and vertical parameters varied in steady state simulation grids 1 to 8, in inches (see Figure 3.2)

Parameter	Grid 01	Grid 02	Grid 03	Grid 04	Grid 05	Grid 06	Grid 07	Grid 08
Px5	1.500	1.500	1.500	1.500	3.000	3.000	1.500	1.500
Px6	23.635	26.635	23.635	23.635	23.635	23.635	47.271	47.271
Px7	256.050	256.050	256.050	256.050	254.550	254.550	232.410	232.410
Py1	70.110	75.110	70.110	75.110	70.110	70.110	70.110	75.110
Py4	6.000	1.000	6.000	1.000	6.000	6.000	6.000	1.000
Py7	10.000	9.969	8.954	8.954	8.954	8.954	8.954	8.954
Py9	2.031	2.031	3.046	3.046	3.046	3.046	3.046	3.046
Py10	6.000	1.000	6.000	1.000	6.000	6.000	6.000	1.000
L3	118.110	118.110	118.110	118.110	118.110	118.110	118.110	118.110
L4	94.110	99.110	94.110	99.110	94.110	94.110	94.110	99.110
L5	124.110	124.110	124.110	124.110	124.110	124.110	124.110	124.110
L6	2.000	2.000	3.000	3.000	3.000	3.000	3.000	3.000
L7	24.000	24.000	24.000	24.000	24.000	24.000	48.000	48.000

Table C.3 Values of horizontal and vertical parameters varied in steady state simulation grids 9 to 16, in inches (see Figure 3.2)

Parameter	Grid 09	Grid 10	Grid 11	Grid 12	Grid 13	Grid 14	Grid 15	Grid 16
Px5	3.000	3.000	3.000	3.000	3.000	3.000	3.000	3.000
Px6	23.635	23.635	23.635	23.635	47.271	47.271	47.271	47.271
Px7	254.550	254.550	254.550	254.550	230.910	230.910	230.910	230.910
Py1	70.110	75.110	70.110	75.110	70.110	75.110	70.110	75.110
Py4	6.000	1.000	6.000	1.000	6.000	1.000	6.000	1.000
Py7	9.969	9.969	8.954	8.954	9.969	9.969	8.954	8.954
Py9	2.031	2.031	3.046	3.046	2.031	2.031	3.046	3.046
Py10	6.000	1.000	6.000	1.000	6.000	1.000	6.000	1.000
L3	118.110	118.110	118.110	118.110	118.110	118.110	118.110	118.110
L4	94.110	99.110	94.110	99.110	94.110	99.110	94.110	99.110
L5	124.110	124.110	124.110	124.110	124.110	124.110	124.110	124.110
L6	2.000	2.000	3.000	3.000	2.000	2.000	3.000	3.000
L7	24.000	24.000	24.000	24.000	48.000	48.000	48.000	48.000

Table C.4 Values of horizontal and vertical parameters varied in the transient simulations grid 17 to 20, in inches (see Figure 3.2)

Parameter	Grid 01	Grid 02	Grid 09	Grid 10
Px5	1.500	1.500	3.000	3.000
Px6	23.635	23.640	23.635	23.635
Px7	256.046	256.050	251.550	254.550
Py1	188.221	193.220	188.220	193.220
Py4	6.000	1.000	6.000	1.000
Py7	9.969	9.970	9.969	9.969
Py9	2.031	2.030	2.031	2.031
Py10	6.000	1.000	6.000	1.000
L3	236.221	236.220	236.220	236.220
L4	212.220	217.220	212.220	217.220
L5	242.221	242.220	242.220	242.220
L6	2.000	2.000	2.000	2.000
L7	24.000	24.000	24.000	24.000